UNIVERSITY OF
LIVERPOOL

Synthesis and Structure-Metabolism Relationships of Halogenated Carbamazepine Analogues

Thesis submitted in accordance with the requirements of the University of Liverpool for the degree of Doctor in Philosophy

By

Emma-Claire Elliott

30th September 2011

Acknowledgements

I would like to begin by thanking my supervisors, Dr. Andrew V. Stachulski and Prof. B. Kevin Park, for giving me the opportunity to study with them. I am also indebted to Prof. Rick Cosstick for all his assistance, support, and encouragement in the final years of the PhD.

I also express gratitude to Dr. Sophie L. Regan and Dr. James L. Maggs of the MRC Centre for Drug Safety Science for their close collaboration with the structure-metabolism work, and for their assistance in determining the purity of the carbamazepine analogues.

Thanks go to the members of the Stachulski group, both past and present, and to the members of the Aspinall and Greeves group for their excellent company in the lab and for making Liverpool a thoroughly enjoyable place to work for the past for years. Special thanks go to Laura, Helen, Xiao Li, and Chandra for all their help, friendly discussions and camaraderie

To all my friends, old and new, in no particular order: Jacqui, Ev, Oliver, Matt, Neil, Lyndsey, Ste, Robin and Michelle for always being on hand with a cup of tea or a pint on a Friday night.

I am extremely thankful to my family, to whom I dedicate this thesis. My parents Alex and Jean, and my brother Adam, for not disowning me. For their love, support, inspiration and encouragement through good times and bad. Finally I thank Tom for always going the extra mile and especially for his forbearance over the late nights, early starts, and long weekends.

Abstract

Adverse drug reactions are a significant burden on industry and healthcare providers. They account for approximately 5 % of hospital admissions and are a considerable cause of morbidity and mortality in patients. While it is widely considered that an individual's susceptibility to idiosyncratic reactions is caused by a variety of factors; ADRs are thought to be linked to the formation and accumulation of reactive drug metabolites rather than the parent drug.

Of the patients administered carbamazepine 30-50 % are subject to the development of some form of adverse drug reaction. Carbamazepine is metabolized extensively *in vivo* and hypersensitivity reactions have been hypothetically linked to the formation of chemically reactive arene oxide or iminoquinone metabolites. In order to understand the mechanisms behind such ADRs it is important to synthesize a variety of chemical probes to observe changes in pharmacokinetic and pharmacodynamic properties of the compounds.

The overall theme of this thesis is the synthesis and the examination of the structure-metabolism relationships for halogenated analogues of carbamazepine. It is divided into three main sections; a general introduction introduces the reader to the basics of drug metabolism from how drugs are metabolized to the implications of halogen substitution on the metabolism of drugs. It next covers the synthetic strategies employed in the formation of halogenated carbamazepine analogues before ending on a discussion of the key findings of the structure-metabolism relationships that may be derived from *in vitro* investigations

Publications

Elliott, E.-C.; Bowkett, E. R.; Maggs, J. L.; Bacsa, J.; Park, B. K.; Regan, S. L.; O'Neill, P. M.; Stachulski, A. V., Convenient Syntheses of Benzo-Fluorinated Dibenz[b,f]azepines: Rearrangements of Isatins, Acridines, and Indoles. *Organic Letters* **2011**. *Paper in press*

Emma-Claire Elliott, Sophie L. Regan, James L. Maggs, Elizabeth R. Bowkett, Laura Parry, Dominic P. Williams, B. Kevin Park, and Andrew V. Stachulski: Haloarene derivatives of carbamazepine with reduced bioactivation liabilities: 2-monohalo and 2,8-dihalo derivatives. *Manuscript in Preparation*
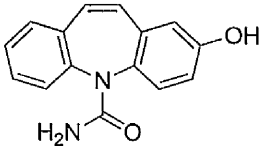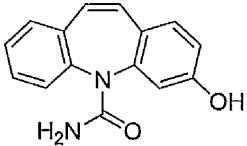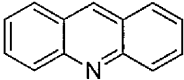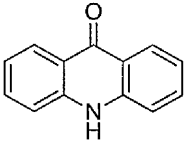
Abbreviations
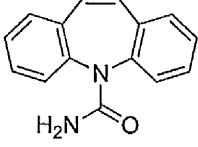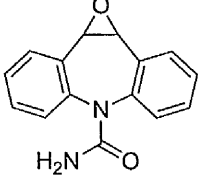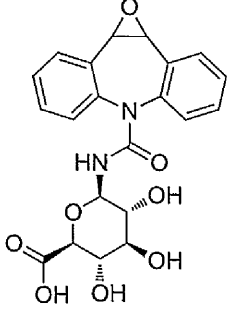
9-AC	9-Acridine carbaldehyde
ABT	1-Aminobenzotriazole
Ac$_2$O	Acetic anhydride
ACBN	1,1'-Azobis(cyclohexanecarbonitrile)
AcCl	Acetyl chloride
Acetone-d_6	Deuterated acetone
ADR	Adverse Drug Reaction
AI	Acridine
AO	Acridone
ATR-IR	Attenuated Total Reflection Infrared Spectroscopy
br. s.	Broad singlet
CBZ	Carbamazepine
CBZ-2,8-Br	2,8-DiBromo carbamazepine
CBZ-2,8-Br E	2,8-DiBromo carbamazepine-10,11-epoxide
CBZ-2,8-Br -N-gluc	2,8-DiBromo carbamazepine-N-glucuronide
CBZ-2,8-BrE-N-gluc	2,8-DiBromo carbamazepine-10,11-epoxide-N-glucuronide
CBZ-2,8-Cl	2,8-DiChloro carbamazepine
CBZ-2,8-Cl E	2,8-DiChloro carbamazepine-10,11-epoxide
CBZ-2,8-Cl E-N-gluc	2,8-DiChloro carbamazepine-10,11-epoxide-N-glucuronide
CBZ-2,8-Cl -N-gluc	2,8-DiChloro carbamazepine-N-glucuronide
CBZ-2,8-F	2,8-DiFluoro carbamazepine
CBZ-2,8-F -N-gluc	2,8-DiFluoro carbamazepine-N-glucuronide
CBZ-2,8-FE	2,8-DiFluoro carbamazepine-10,11-epoxide
CBZ-2,8-FE-N-gluc	2,8-DiFluoro carbamazepine-10,11-epoxide-N-glucuronide
CBZ-2-Br	2-Bromo carbamazepine
CBZ-2-BrE	2-Bromo carbamazepine-10,11-epoxide
CBZ-2BrE-N-gluc	2-Bromo carbamazepine-10,11-epoxide-N-glucuronide
CBZ-2-Br-N-gluc	2-Bromo carbamazepine-N-glucuronide
CBZ-2-Cl	2-Chloro carbamazepine
CBZ-2-ClE	2-Chloro carbamazepine-10,11-epoxide
CBZ-2-ClE-N-gluc	2-Chloro carbamazepine-10,11-epoxide-N-glucuronide
CBZ-2-Cl-N-gluc	2-Chloro carbamazepine-N-glucuronide
CBZ-2-F	2-Fluoro carbamazepine
CBZ-2-F E	2-Fluoro carbamazepine-10,11-epoxide
CBZ-2-F E-N-gluc	2-Fluoro carbamazepine-10,11-epoxide-N-glucuronide

CBZ-2-F -*N*-gluc	2-Fluoro carbamazepine-*N*-glucuronide
CBZ-2-F.OSO$_3$	2-Fluoro carabamazepine *O*-sulfonate
CBZ-2-OH	2-Hydroxy carbamazepine
CBZ-3-OH	3-Hydroxy carbamazepine
CBZDHD	Carbamazepine-10,11-dihydrodiol
CBZE	Carbamazepine-10,11-epoxide
CBZ-*N*-Gluc	Carbamazepine-*N*-glucuronide
CBZ-SG	Carbamazepine-glutathione conjugate
CCl$_4$	Carbon tetrachloride
CDCl$_3$	Deuterated chloroform
CF$_3$SO$_3$H	Trifluromethyl sulfonic acid
CH$_2$Cl$_2$	Dichloromethane (methylene chloride)
CHCl$_3$	Chloroform
CI	Chemical Ionisation
d	Doublet
dd	Doublet of doublets
ddd	Doublet of doublets of doublets
DHD	Di-hydrodiol
DHOH	Dihydroxylated
DMAP	Dimethyl amino pyridine
DMSO	Dimethylsulfoxide
DMSO-*d$_6$*	Deuterated dimethylsulfoxide
dt	Doublet of triplets
EI	Electron Ionisation
eq	Equivalents
Et$_2$O	Diethyl ether
EtOAc	Ethyl acetate
EtOH	Ethanol
GSH	Glutathione
GST	Glutathione-*S*-transferase
h	Hours
HBr	Hydrogen bromide
HCl	Hydrochloric Acid
HLM	Human Liver Microsomes
HPLC	High-Pressure Liquid Chromatography
I$_2$	Iodine

IDB	Iminodibenzyl
IR	Infra-Red spectroscopy
ISB	Iminostilbene
ISB-2-OH	2-Hydroxy iminostilbene
K₂CO₃	Potassium carbonate
KOCN	Potassium isocyanate
KOH	Potassium Hydroxide
LC-MS	High Pressure Liquid Chromatography-Mass Spectrometry
LC-UV	High Pressure Liquid Chromatography (with UV detection)
m	(NMR) multiplet; (IR) medium
MeCN	Acetonitrile
min	Minutes
mp	Melting Point
MPO	Myeloperoxidase
Na₂SO₄	Sodium sulfate
NaOCN	Sodium isocyanate
NaOH	Sodium Hydroxide
NAPQI	*N*-acetyl para-benzo quinoneimine
NBS	*N*-bromo succinimide
NCS	*N*-chloro succinimide
NEt₃	Triethylamine
NH₄Cl	Ammonium chloride
NIH	National Institutes of Health
NMR	Nuclear Magnetic Resonance
P450	Cytochrome P450
PEG 400	Polyethylene glycol (molecular weight = 400)
PhCF₃	Trifluoromethyl toluene
pKₐ	acid dissociation constant
PPA	Polyphosphoric acid
P*t*-Bu₃	Tri-*tert*-butyl phosphine
q	Quartet
s	(NMR) singlet (IR) strong
SAR	Structure-Activity Relationship
SiO₂	Silica Gel
SKF	Proadifen hydrochloride
t	Triplet

TFA	Trifluoroacetic acid
THF	Tetrahydro furan
TIC	Total Ion Current
TLC	Thin layer chromatography
w	Weak
w/v	Weight to volume
WHO	World Health Organisation
XIC	Extracted Ion Current

Structural Abbreviations

Abbreviation	Structure
CBZ-2-OH	
CBZ-3-OH	
AI	
AO	
CBZ	
CBZE	
CBZE-*N*-gluc	

CBZ-*N*-gluc

Glucuronic acid

COOH
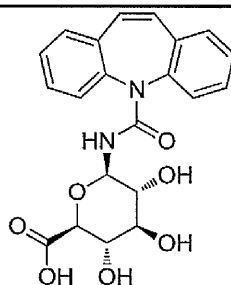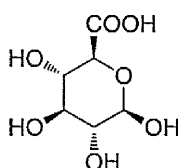
GSH (glutathione)

Contents

General Introduction

Chapter 1

This general introduction is aimed at a reader with a degree in chemistry. Its aim is to provide the reader with the fundamentals of how drugs are metabolised to the metabolic implications of halogen incorporation and how this could apply to metabolism of halogenated carbamazepine analogues.

Contents

1. General Introduction

1.1 Drug metabolism

Once a xenobiotic, such as a drug, is administered to an animal or man it is subject to transformation by a diverse range of enzymes. Primarily the role of these enzymes is to degrade or modify both exogenous and endogenous compounds so they are less toxic and more easily excreted. As a result most xenobiotics undergo such reactions forming new compounds known as metabolites.[1]

Metabolism is typically divided into two stages; Phase 1 (functionalisation) and Phase 2 (conjugation) and the common reactions associated with each stage are summarized in **table 1.1**. Most phase 1 and 2 reactions occur in the liver although some occur in plasma (suxamethonium); lungs (prostanoids); or the gut (salbutamol).[2] The majority of hepatic drug-metabolizing enzymes (including cytochrome p450) are located in the smooth-endoplasmic reticulum. To reach their pharmacological target and to be successfully transformed by these enzymes xenobiotics must first cross several membranes. Except where specific transporter systems exist (such as for dapsone), non-polar drugs cross membranes faster than polar drugs, thus hepatic metabolism is less important for polar drugs, which are rapidly excreted in urine due to their water solubility, than for non-polar which must be transformed to a more water soluble compound first or they remain in the blood and tissues of the host and maintain pharmacological effects for extended periods of time.[2]

Phase 1 metabolism consists of oxidation, reduction and hydrolysis reactions, although some other reactions are outlined in **table 1.1** their role is to functionalise

the drug; by either revealing or introducing a chemically reactive functional group into the molecule where phase 2 metabolism can occur. These metabolites often lose the pharmacological activity of the parent compound. However their reactivity is also increased and so, paradoxically, a metabolite can be more toxic or carcinogenic than the parent compound.[1, 3]

Table 1.1: Summary of common Phase I and phase II metabolism processes.

Phase 1 metabolism	Phase 2 metabolism
Oxidation	Glucuronidation
Reduction	Sulfation
Hydration	Methylation
Hydrolysis	Acetylation
Isomeriszation	Amino Acid Conjugation
Dethioacetylation	Glutathione Conjugation

Phase 2 metabolism is the major detoxicating pathway and these metabolites account for the majority of the excreted, inactive products of the drug. Phase 2 metabolism occurs mainly in the liver, where water-soluble sugars, amino acids and salts are attached at the polar functional group that was introduced or revealed during phase 1 metabolism. Many of the reactions of phase 1 and phase 2 may occur numerous times on the same substrate and so there is the possibility of interaction between various metabolic routes by competition for the same substrate. It is worth noting that although the term phase 2 implies that a phase 1 reaction must first occur, it is not necessarily the case and many pharmaceuticals are known to be able to undergo phase II conjugations directly (minoxidil).[2, 3]

Metabolites themselves may fall into several different categories. Often transformation of the parent compound results in the formation of inactive

3

metabolites, where the metabolite has lost the activity of the parent compound and has no effect on biological systems, such as the hydrolysis of procaine to the inactive metabolites *p*-aminobenzoic acid and diethyethanolamine as shown in **figure 1.1(a)**.[4]
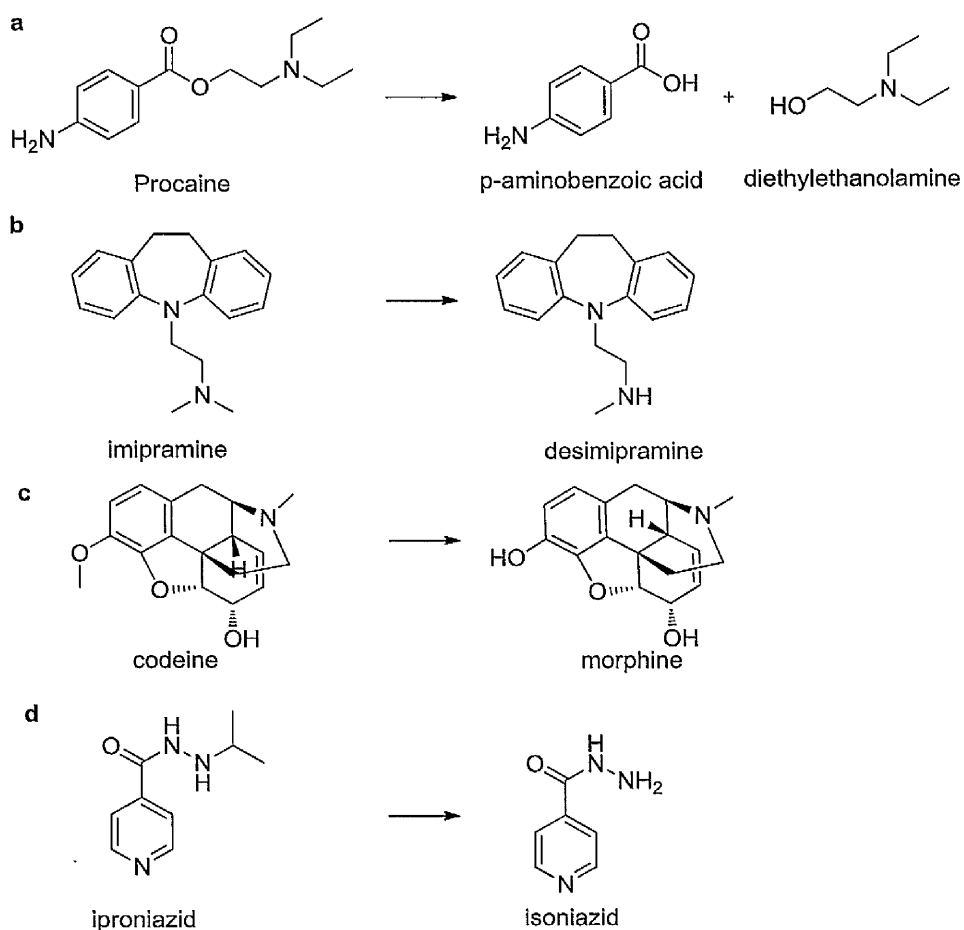
Figure 1.1: Some metabolites have profoundly different properties to their parent compound.

Some metabolites are able to retain similar activity to the parent drug, for example the demethylation of imipramine yields desimipramine **(figure 1.1(b))** which is an equally active antidepressant.[5] Occasionally a metabolite may be more potent than the parent drug, such as the demethylation of codeine to morphine **(figure 1.1(c))**.[6] Interestingly metabolites may have entirely different pharmacological activity to the

4

parent drug such as the anti-depressant iproniazid which is dealkylated to form the antitubercular agent isoniazid (**figure 1.1(d)**).[7]

1.1.1 Cytochrome P450 and oxidative metabolism

Mixed function-oxidases are found in microsomes (smooth endoplasmic reticulum) of many cells, in particular in the liver, kidney, lungs and intestine. They perform a large range of functionalisations, and are major catalysts in the detoxication of endogenous and exogenous compounds.[2] Cytochrome P450s are capable of reductions but their primary function is the insertion of a single oxygen atom into a relatively unreactive substrate, although there are exemptions to the rule.[8] The overall general reaction catalyzed by P450s is that of mixed-function oxidation with the general formula below:[9]

$$NADPH + H^+ + O_2 + R \rightarrow NADP^+ + H_2O + RO$$
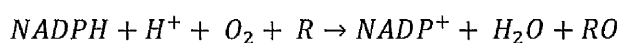
While the main goal of mixed function oxygenases is the detoxication of endogenous and exogenous compounds, this only occurs if the formed metabolite is intrinsically less reactive than the parent compound. A metabolite of a compound that has direct toxicity, or is capable of interacting with a receptor to elicit a toxic effect, will only have reduced toxicity if the metabolite is less intrinsically toxic than the parent.[9] For example, over 90 % of a therapeutic dose of paracetmol is metabolised *in vivo* to glucuronide and sulfate conjugates, a further 2-3 % remains unchanged. The remaining drug is converted to *N*-acetyl-p-benzo-quinoneimine (NAPQI) shown in **figure 1.2**.[10] Despite its presence as a minor metabolite NAPQI is significant; it is toxic and contributes to paracetamol hepatotoxicity. At therapeutic doses, paracetamol is rapidly transformed to unreactive glutathione or sulfate conjugates. NAPQI is also subject to glutathione conjugation and is thus excreted as a non-toxic

conjugate (**figure 1.2**). However in overdose, although the relative quantities of the

metabolites remain similar, there is much more NAPQI formed. In time this depletes

glutathione in the body and NAPQI instead binds to cysteine residues of cellular

macromolecules resulting in hepatotoxicity.[3, 10]
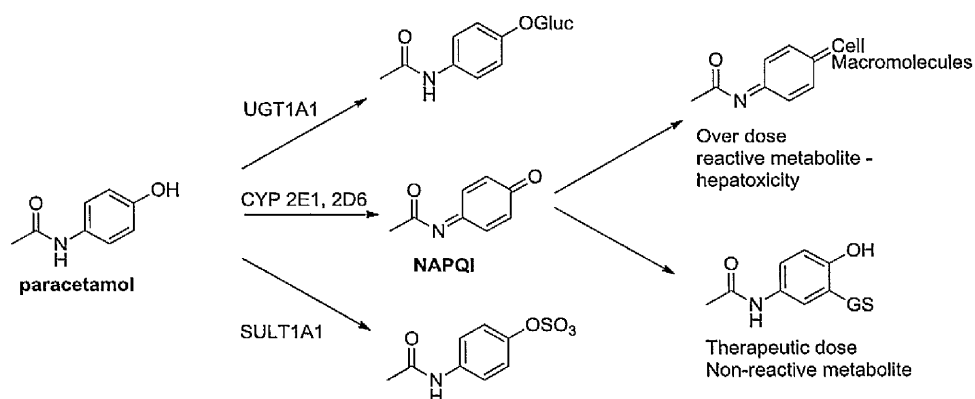
Figure 1.2: Metabolism of paracetamol at therapeutic and overdose situation resulting in either detoxication or toxicity.

Other mechanisms of metabolite derived chemical toxicity exist, such as

transformation of a xenobiotic to a highly reactive intermediate capable of binding

with macromolecules. For example the metabolism of hexane to 2,5-hexanedione,

which can react with lysine residues of proteins to form pyrroles.[9, 11] Alternatively

these highly reactive intermediates may interact with a target to induce toxicity.

Hydroxylation of trimethylpentane forms an alcohol that is able to strongly bind to

microglobulins to produce droplets in kidneys of male rats which develop into

tumours.[12]

1.1.2 Cytochrome P450 Catalytic cycle

The structural aspects and catalytic cycle of P450s are still not fully understood but is

the subject of numerous reviews.[13, 14] What follows is a brief discussion of the

important stages of the P450 catalytic cycle which are covered more extensively elsewhere, as regards oxygen insertion into X-H.[15, 16]

The core of all cytochrome P450s is the haem structure Ferriprotoporphyrin-9 (F-9) and is shown in figure **1.3(a)**.[1, 17] It is the area where iron catalyses the oxidation of the xenobiotic. The iron is bound by a five bond attachment to two other molecules; in the horizontal plane, four pyrrole nitrogens of haem, and the fifth group sulfur from a cysteine residue. This is known as the high-spin "pentacoordinate" state and is often described as the resting state of the enzyme prior to interaction with a substrate.
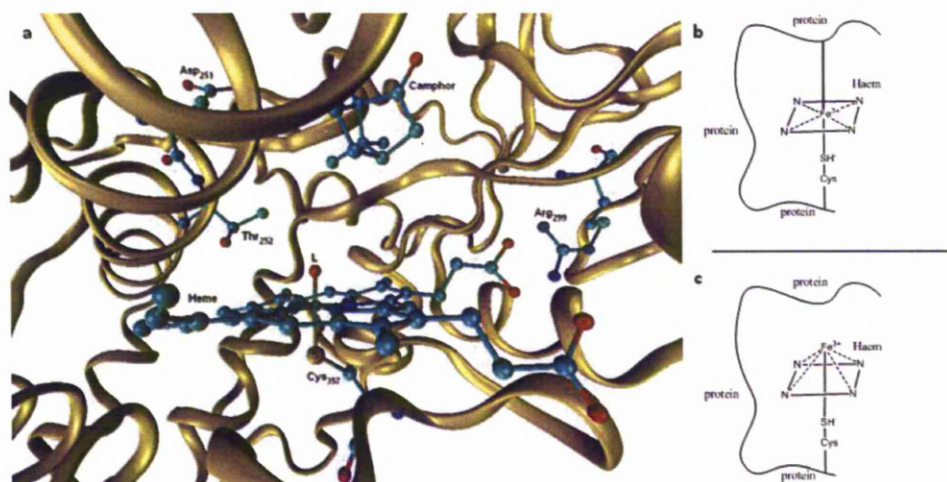
Figure 1.3: **(a)** Close-up of the active site of P450cam, for P450 camphor (CYP101), taken from the X-ray structure (pdb code: 1DZ9) of Schlichting *et al*[17] with key residues highlighted.[16] Showing the activated oxygen species 7 of **figure 1.4**. **(b)** schematic representation of the hexaco-ordinated, low spin P450 with the iron lying in the plane of haem **(c)** penta co-ordinated high spin P450 with iron sitting out of plane (typically by ~ 0.3 Å for P450cam).[17]

Prior to interaction with substrates, the haem iron is in equilibrium between its high- and low-spin states (**Figure 1.3b** and **1.3c** respectively).[18] Approach of a substrate disrupts this equilibrium, and although there are exceptions,[19] cytochrome P450s predominantly bind the substrate in stage **1** (**figure 1.4**) with the iron in its low-spin state.[1, 20] Binding of the substrate occurs on the protein section in such a manner that

the most susceptible part of the molecule is exposed allowing rapid modification of the substrate with minimum energy expenditure.[21] Once bound, a one-electron reduction, transferred from NADPH by NADPH cytochrome P450 reductase (stage 2),[22, 23] reduces the iron to its ferrous state (Fe^{2+}). This complex is highly unstable but it has been observed in some microsomal P450s.[9] Once reduced, ferrous ion then binds molecular oxygen from the lungs (stage **3**), this complex is highly unstable and generates ferric iron and the superoxide O_2^-. Fe^{2+}-O_2 complexes have been observed in some microsomal P450s[23] but the characterization of intermediates beyond this stage are much less certain and the likeliest pathway has been determined with consideration to what is possible and what has happened in terms of products which have been characterized: some inferences come from peroxidases and biomimetic metalloporphyrin models.[20]
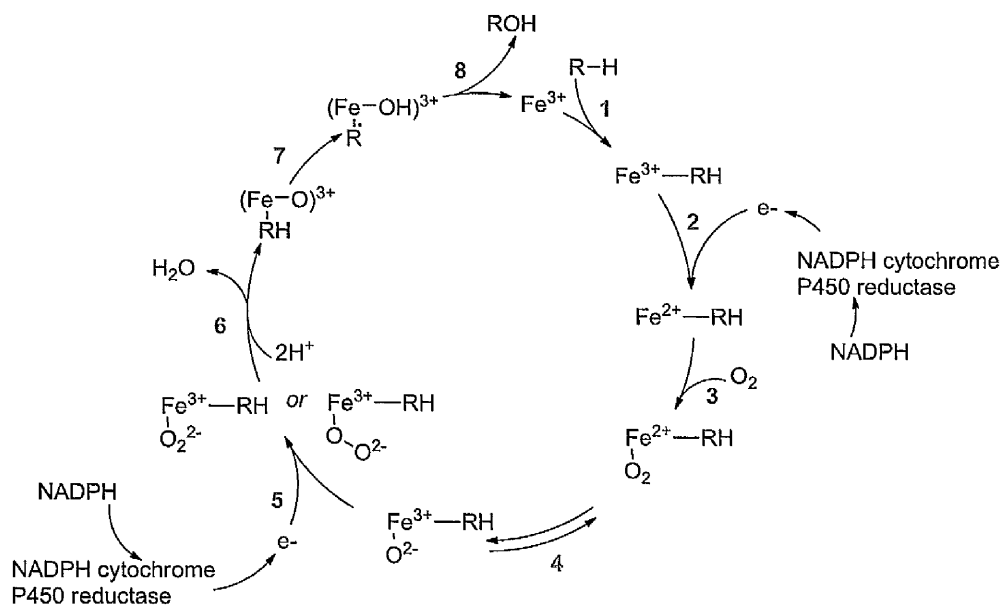

Figure 1.4: Catalytic cycle of cytochrome P450s.

Scission of oxygen at step **4** is a high energy process and is thought to initially involve the slow transfer of an electron from the ferrous ion to oxygen forming O_2^-, and is the rate limiting step of the cycle.[24] Step **5** is the key to whether or not a substrate is oxidized. A second electron enters the system, forming the highly reactive $Fe^{2+}O_2^{2-}$ species. This electron can be supplied by NADPH via NADPH cytochrome P450 reductase, but other enzymes are also capable of supplying this electron in other systems.[25] This reactive species rapidly picks up two protons during step **6** cleaving the oxygen-oxygen bond, generating one molecule of water and a high valent complex often described as FeO^{3+}. Such perferryl complexes are thought to be the main insertion route by P450s and are able to activate the substrate by proton abstraction or addition of an electron (supplied by a nitrogen atom) from the substrate in step **7**. The hydrogen removed will be closest to the carbon to be oxidised, the abstracted proton then becomes bound to the perferryl complex, leaving the compound with a spare electron, and the subsequent radical is now much more likely to react with the hydroxyl group. Step **8** is the subsequent reaction between the formed carbon radical and the OH of the perferryl forming an alcohol ('rebound' mechanism). The compound has now changed both structurally and electronically such that it is no longer a good substrate for the enzyme and the product leaves the active site.[1, 3, 9]

1.1.3 Other forms of oxidative metabolism
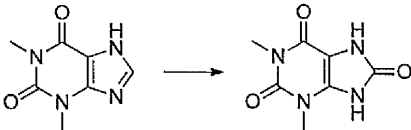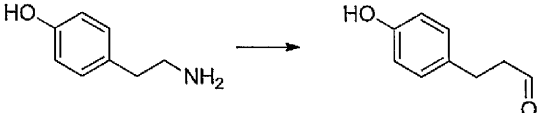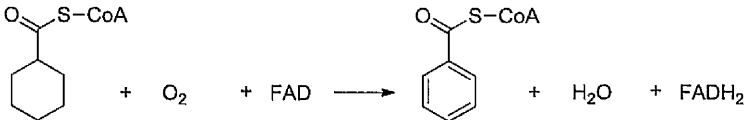
Not all oxidations of xenobiotics are performed by cytochrome P450: others are outlined in table 2.[26] Many of these enzymes are more closely concerned with the metabolism of a variety of endogenous compounds, and will not be discussed in

detail here. Nonetheless some of these enzymes have been demonstrated to metabolise some drugs to potentially reactive metabolites.[26]

Of particular interest in this study is the amine oxidase family of enzymes. They may be divided into two classes: monoamine oxidases are responsible for metabolism of catecholamines and diamine oxidases which are able to deaminate endogenous diamines like histamine.[1] Monoamine oxidase in particular metabolises exogenous amines obtained from diet, such as tyramine which is found in cheese, to the corresponding aldehyde as shown in **table 1.2**[1].

Table 1.2: Oxidative enzymes other than cytochrome P450.[1]

Enzyme	Example
Alcohol dehydrogenase	
Aldehyde dehydrogenase	
Xanthine oxidase	
Amine oxidases	
Aromatases	

Diamine oxidases are almost exclusively involved in metabolism of endogenous materials, but *N*-oxidases are of great significance in the metabolism of drugs like imipramine as shown in **figure 1.5**.[27] While these enzymes seem to require NADPH and molecular oxygen to function they are not mixed-function oxidases like cytochrome P450s – they are flavoproteins.

10
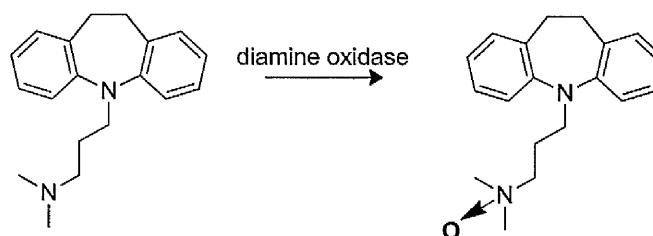
Figure 1.5: *N*-oxidation of imipramine by diamine oxidase.

Myeloperoxidases, a type of heme peroxidase-cyclooxygenase that are found in neutrophils (and in monocytes and macrophages)[28] have also been theoretically linked to the formation of active drug metabolites of carbamazepine.[29] Neutrophils are found in the blood stream of mammals, and are the most abundant of the white blood cells forming an essential part of the immune system.[28] Myeloperoxidases are released by neutrophils during immunological response and they release several oxidising enzymes and compounds. The unique activity of myeloperoxidase is its ability to utilise chloride ions as a co-substrate with hydrogen peroxide to form the powerful oxidant hypochlorous acid, which is a potent antimicrobial agent.[30] This strongly oxidising system is potentially capable of oxidizing drugs to chemically reactive intermediates.[31] For example, the widely prescribed antiarrhythmic procainamide is subject to very high incidences of drug-induced lupus and aganulocytosis. It has been demonstrated that procainamide is metabolised *in vivo* to a nitroso- intermediate derived from a hydroxylamine intermediate,[32] as shown in **figure 1.6**, that is capable of covalently binding to microsomal proteins.[33]

Although cytochrome p450 enzymes have been shown to activate amines to hydroxylamine compounds,[34] it may be argued that reactive metabolites generated by leukocytes and myeloperoxidase in the blood stream are more likely to give rise to immunological responses than those generated in the liver. This is because

11

hydroxylamines formed in the liver are rapidly removed from circulation by

erythrocytes, which have been shown to preferentially take up hydroxylamines and

hence protect white blood cells from toxicity *in vitro*.[32]
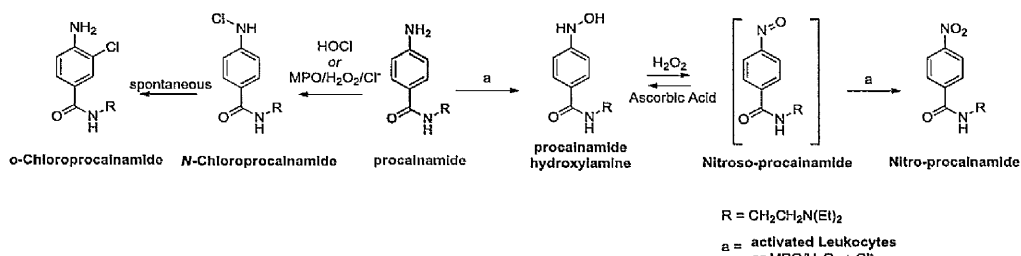
Figure 1.6: Metabolism of procainamide by a myeloperoxidase system.[33]

When exposed to activated leukocytes procainamide is oxidised to nitro-

procainamide as shown in **figure 1.6**. Although there was no direct observation of

nitro-procainamide in the system, addition of ascorbate did increase the quantitiy of

procainamide hydroxylamine.[35] Model studies demonstrated the hydrogen peroxide

was able to oxidize procainamide hydroxylamine to nitroso-procainamide and then

nitro-procainaimide and that exposure of myeloperoxidase to hydrogen peroxide was

also able to oxidize procainamide to the same three metabolites.[35]

When chloride is added to the incubations the rate of oxidation vastly increased. The

major metabolite observed was *N*-chloroprocainamide. This compound was

relatively stable but on standing spontaneously isomerizes to *o*-chloroprocainaimde.

However, although the purified *N*-chloroprocainamide isomerized it is possible that

direct chlorination of the aromatic ring formed some of the metabolite. Reaction of

procainamide with dilute hypochlorous acid was also able to produce the same

chlorinated metabolites.[36] Incubation of [^{14}C] radiolabelled procainamide with

activated cells or the myeloperoxidase system did show binding to exogenous protein

but although the chlorinated procainamides were reactive, their major mechanism of

action was chlorination of the protein rather than alkylation indicating that the hydroxylamine pathway is more efficient at protein binding.[33]

1.2 Carbamazepine

Carbamazepine (CBZ) is a first line drug in treatment of partial and *grand mal* epileptic seizures and trigeminal neuralgia. Additionally, it is becoming much more widely used in the treatment of bipolar depression.[37-39] It is also widely prescribed "off-label" for a variety of other indications[40] including; attention-deficit hyperactivity disorder (ADHD),[41] schizophrenia,[42-44] phantom limb syndrome,[45] and post-traumatic stress disorder.[46] However, its clinical use is associated with a wide variety of adverse drug reactions (ADRs) from common and relatively mild reactions such as somnolence, nausea, dizziness, and rash,[47] to more severe events such as blood dyscrasia,[48, 49] hyponotraemia,[50, 51] hepatotoxicity,[52, 53] and the rare but potentially fatal anticonvulsant hypersensitivity syndrome (AHS).[54]

Adverse drug reactions (ADRs), as defined by the world health organization (WHO), are harmful, unintended reactions to medicines that occur at normally therapeutic doses.[55] As a result of evidence of toxicity, 16 of 548 (2.9 %) of new chemicals that were approved for the US market between 1975 and 1999 were withdrawn from the market and 56 out of 548 (10.2 %) were given a black box warning (a warning that appears on patient information leaflets that indicates the potential for ADRs).[56] They are a significant burden on industry and health care providers as such reactions are difficult to diagnose early as their pathophysiology and molecular basis remain largely unelucidated.[57] They have been reported to account for 5 % of hospital admissions, and are a considerable cause of morbidity and mortality in patients.[58-60] In the case of sensitivity to anti-epileptics it has been shown that ADRs account for

approximately half all recorded treatment failures.[55] Such reactions are difficult for physicians to diagnose as they do not have a predictable pattern of progression and often mimic the pathology of common ailments;[61] they also have low reaction rates (1:1000 to 1:10,000 exposures), have variable latency periods, and are not dose-dependent.[62]

It is widely considered that an individual's susceptibility to idiosyncratic reactions may be caused by several factors such as: race,[63, 64] genetics,[64, 65] age, and gender.[66] However, the cause of many ADRs has been linked to the formation and accumulation of *reactive drug metabolites* rather than the parent drug.[67, 68] Between 30-50 % of patients administered carbamazepine are subject to the development of ADRs.[67] Furthermore cross-reactivity among the major anticonvulsants is not uncommon and pre-existing sensitization to carbamazepine will often result in more severe reactions upon subsequent exposures.[69]

1.2.1 Carbamazepine Metabolism

Whether after repeated administration or a [70]single dose, carbamazepine is almost completely removed by metabolism as less than 5 % of the dose is excreted unchanged in urine. Frigero *et al* identified the first metabolite in 1972 and since then over 30 metabolites have been identified in man.[71] **Figure 1.7** summarizes the main metabolic pathways for CBZ. In particular CBZ is known to form the 10,11-epoxide (**CBZE**), 10,11-dihydrodiol (**CBZDHD**), N-glucuronide (**CBZ-*N*-glucuronide**), glutathione conjugates (**CBZSG-1 and -2**) and 2- and 3-hydroxy derivatives (**CBZ-2-OH** and **CBZ-3-OH**) respectively. Hypersensitivity reactions have been linked hypothetically to chemically reactive intermediates the structures of which are inferred from the products such as the arene oxide (**iii**)[72] and iminoquinone (**iv**).[70, 73]
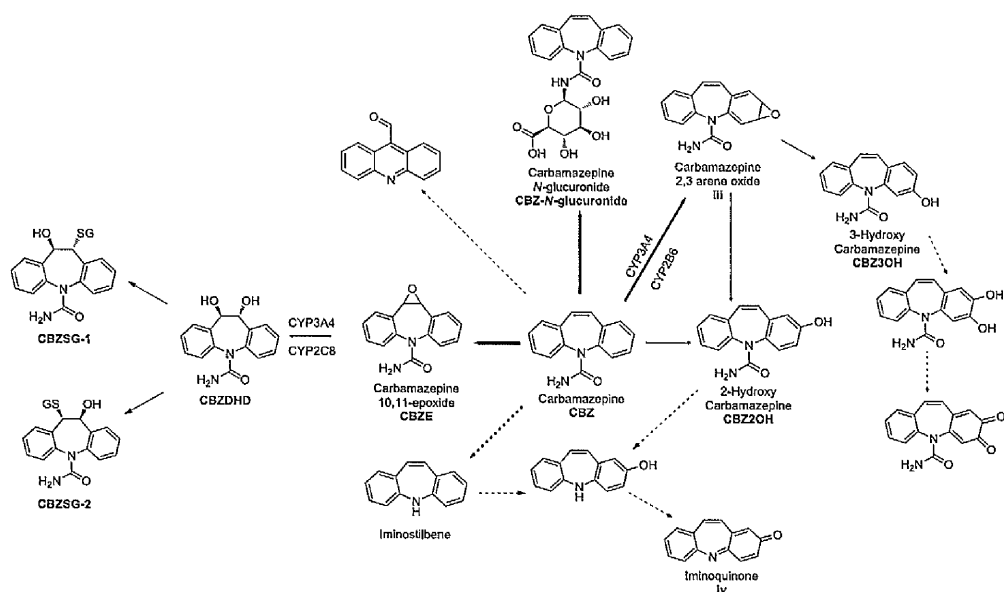
Figure 1.7: Paths of formation of common carbamazepine metabolites.[74]

The highly stable CBZE is particularly important as it retains enough activity of the parent to be pharmacologically active and although interactions between CBZE and lamotrigine were known[75, 76] it was, until recently, thought that CBZE was unreactive. Studies have shown that CBZE may be chemically reactive, as incubations of CBZE with glutathione in the absence of biological matrices and cofactors, formed two glutathione conjugates, CBZE-SG1 and CBZE-SG2, with retention times of ~27.5 and ~30 min respectively as shown in **figure 1.8**.[77] Each peak showed m/z 560, which is consistent with a direct CBZE-glutathionyl adduct.[77] Incubation of CBZ and glutathione in HLM incubations, also yielded two compounds with MH$^+$ ions at m/z 560, indicating that the doublet observed in the HLM-CBZ incubation may be similar in nature to the chemical reaction of CBZE.[77]
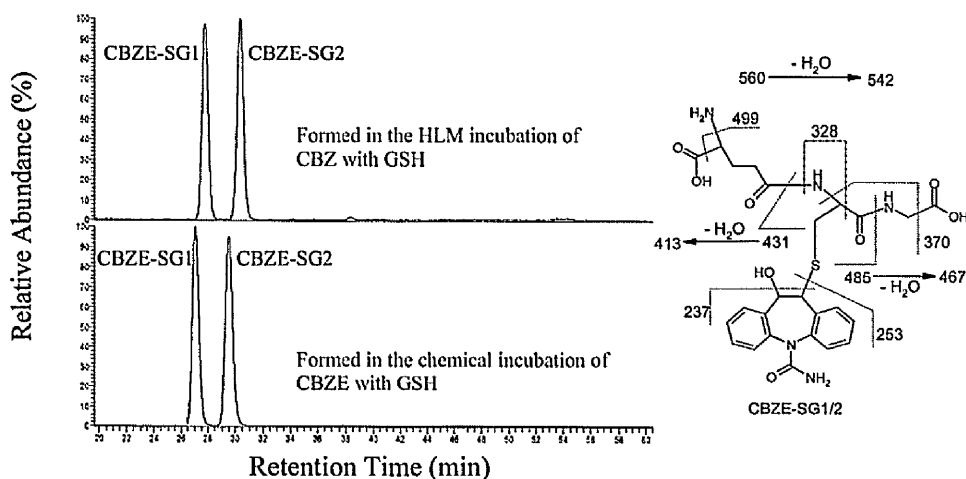
Figure 1.8: LC-MS traces showing the two glutathione conjugates formed in HLM incubations of CBZ and GSH and of CBZE with GSH and the proposed fragmentation pathway of the conjugate.[77]

Based on the conjugation mechanism of epoxides with GSH and considering the symmetry of CBZE it is not surprising that incubations of CBZE formed two diastereomeric products, (S,S)-CBZE-SG and (R,R)-CBZE-SG in a 1:1 ratio in the absence of glutathione-*S*-transferases (GST) as highlighted in **figure 1.8**. GST however, are stereoselective in catalyzing GSH conjugation[1, 3] and therefore one of two CBZE-SG conjugates should be formed preferentially if CBZE is converted by GST to any extent. However the formation of the two adducts in the presence of Human liver microsomes (HLMs) was maintained in a 1:1 ratio when CBZ or CBZE was incubated suggesting that these conjugations were not appreciably mediated by GST.[77]

Epoxidation may also occur on the aromatic rings although the high instability of the intermediates means that they are not easily observed. Instead the structure of these arene oxides is inferred from the structure of the hydroxylated metabolites. 2-hydroxy carbamazepine (CBZ-2-OH) and 3-hydroxy carbamazepine (CBZ-3-OH) are the two main ring-hydroxylated carbamazepine metabolites and are thought to

16

derive from a common 2,3-arene oxide intermediate as shown in **figure 1.5**. However formation of hydroxylated metabolites is not necessarily proof of formation of an arene oxide. Instead formation of di-hydrodiols (DHD) or dihydroxylated (DHOH) metabolites are more indicative of arene oxide formation.[72] Madden *et al* demonstrated that carbamazepine was able to undergo activation to three glutathione adducts with *m/z* 560 which is the expected molecular ion of a dihydroxy carbamazepine glutathione adduct. At high cone voltages dehydration of these adducts was observed, with subsequent fragmentation of the tripeptide and carbamazepine residues.[72]

CBZ-2-OH has further been implicated in toxicity by formation of a highly reactive iminoquinone intermediate.[78] Both 2-hydroxy iminostilbene (ISB-2-OH) and CBZ-2-OH have been detected in the urine of patients taking carbamazepine and it has been hypothesized that CBZ-2-OH can be oxidised to the iminoquinone intermediate as described in **figure 1.9**.[78]
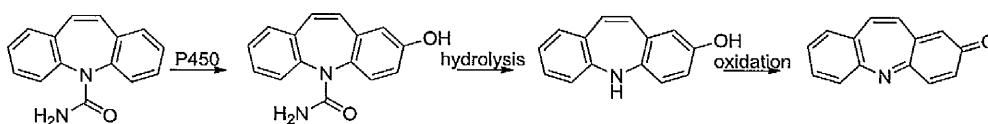
Figure 1.9: Proposed metabolic pathway resulting in the highly reactive iminoquinone metabolite.[78]

They demonstrated that when exposed to HOCl or H_2O_2, ISB-2-OH was oxidised readily to iminoquinone although at a much slower rate for H_2O_2. The formed iminoquinone was shown to be highly reactive, e. g. with GSH.[78]

Glucuronidation is the next major detoxicating pathway and is important, as CBZ-*N*-glucuronide and glucuronides of the hydroxylated metabolites comprise a significant proportion of urinary metabolites. To date there has been no study that implicates a

glucuronide metabolite as a cause of ADRs.[79] The major glucuronidated CBZ metabolite is the *N*-glucuronide (**figure 1.5**) although *O*-glucuronides have been identified for all 13 hydroxylated metabolites of CBZ as highlighted in **figure 1.10**.[80]
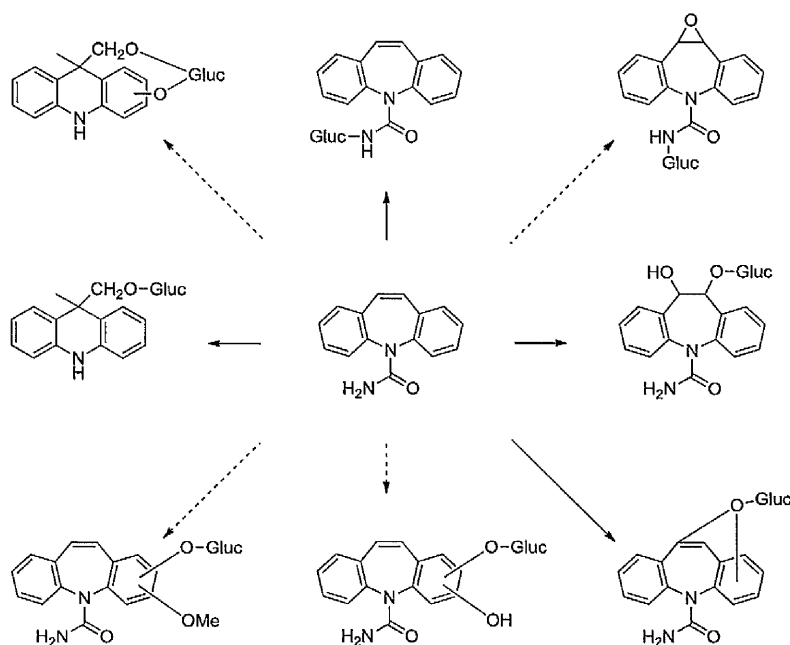
Figure 1.10: Glucuronide metabolites found in human urine. Arrows and broken arrows indicate major and minor metabolites respectively.[80]

Activated neutrophils have been implicated in the formation of reactive metabolites of carbamazepine. Furst *et al* demonstrated that carbamazepine was converted by either $MPO/H_2O_2/Cl^-$ or HOCl to an intermediate aldehyde, acridine, acridone, and chloroacridone as illustrated in **figure 1.11**.[81] 9-Acridine carboxaldehyde was oxidised by HOCl to acridine and acridone. Acridine itself may be further oxidised by HOCl to acridone and the mono- and di-chloroacridone metabolites. Incubations with carbamazepine where concentrations of HOCl were increased resulted in formation of two closely eluting chloroacridones (retention times of 8 and 10 min) as well as di-chloroacridones at later retention times of 21, 25, and 26 min.

18

Carbamazepine was also metabolised to a lesser extent to acridine but no other metabolites were detected.
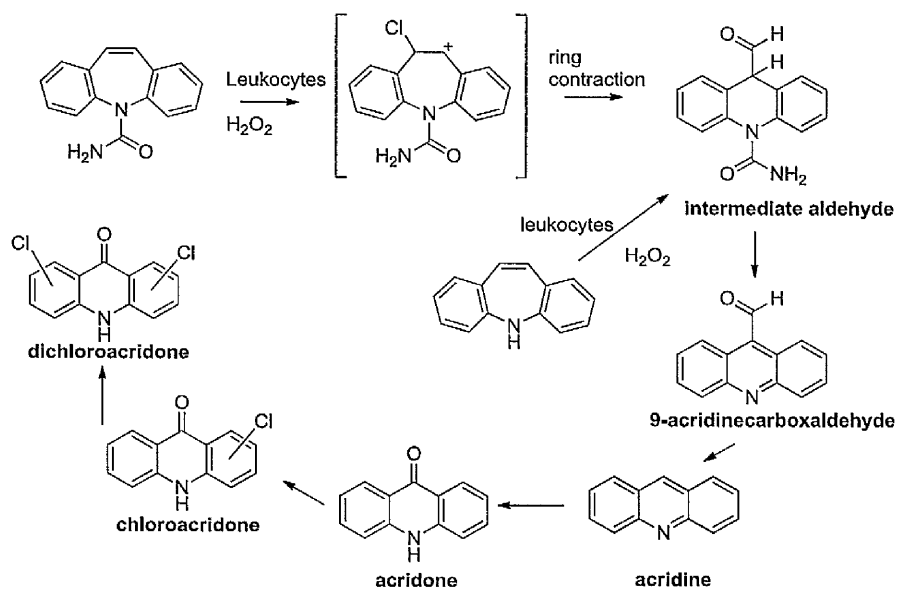
Figure 1.11: Proposed metabolic pathway of sequential bioactivation of carbamazepine and iminostilbene by MPO/H$_2$O$_2$/Cl$^-$ and HOCl.

In contrast to carbamazepine, iminostilbene (which is a potential metabolite) was more extensively oxidised by activated neutrophils. Observed metabolites were similar to those derived from carbamazepine metabolism. Incubation of iminostilbene with HOCl or the MPO/H$_2$O$_2$/Cl$^-$ system also formed the same metabolites.

However, the discovery that acridones and acridine may be formed outside of the liver in leukocytes was never confirmed or investigated *in vivo*. Formation of acridone from carbamazepine has been observed in wastewater treatment plants,[82, 83] and Mathieu and co-workers investigated the minor metabolites in the blood of patients prescribed CBZ.[84]

They found that the major metabolites observed, despite the differences in age, sex, and weight of the patients studied, were CBZE and its dihydroxydiol. CBZ-3-OH was observed more frequently than CBZ-2-OH in accordance with the observations of other groups[70, 84] and levels of acridine and acridone were of similar magnitude to those of CBZ-2-OH and CBZ-3-OH their magnitude was again in accordance with other researchers.[70] Therefore acridine and acridone may be considered normal, minor, metabolites of CBZ in man.[84]

1.3   Implications of Halogen Substitution1.3.1   Physicochemical properties of Carbon-Halogen bonds

The dependence of structure, electronics, and other physicochemical properties on CBZ metabolism is not understood. It is turned over by metabolic enzymes to a number of highly reactive metabolites which are postulated to cause ADRs yet the exact identity of any metabolite causing an ADR has not currently been identified. Chemical modification of CBZ resulting in a decrease in oxidative metabolism could therefore be very informative in the assessment of associated ADRs with pathways of bioactivation.

Halogens are routinely incorporated into a variety of drug molecules and drug candidates typically to exploit the steric effects of Cl, Br and I, by virtue of their ability to occupy specific binding sites of a particular molecular target.[85] Yet they have effects on processes beyond their steric influences alone. For instance, halogen bonding in ligand-target complexes is recognized as a significant intermolecular interaction that contributes to the stability of protein-ligand complexes.[86] Often halogens, in particular fluorine,[87-89] are incorporated into drugs as they impart other properties such as increased lipophilicity, stability, and resistance to metabolism. Yet

despite their properties, inclusion of these molecules into lead candidates is somewhat under-exploited as most structure-activity relationship (SAR) discussions only pertain to the steric influences of the heavier halogens.[85]
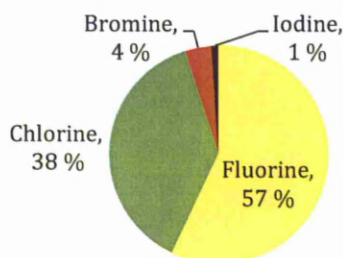
Figure 1.12: Graph showing the percentages of halogenated drugs approved by the FDA between 1988 and 2006. Salts and metallic complexes were not included in the research.[85]

Analysis of the drugs approved by the FDA between 1988 and 2006 (**figure 1.12**)[85] demonstrates the importance of fluorine in pharmaceutical agents: fluoro analogues make up over half of all approved halogenated drugs. Chlorine is the second most frequently incorporated atom. It has an intermediate position in the halogen series with respect to its steric influence shown schematically in **figure 1.13**, and as highlighted in **table 1.3** intermediate with respect to its electronegativity. Unlike fluorine, chlorine is able to interact as a modest halogen bond acceptor. Replacing hydrogen with chlorine confers substantial influence on both size and shape of the molecule, and compounds containing chlorine may be able to enhance binding in deep, hydrophobic pockets of target proteins.[85]

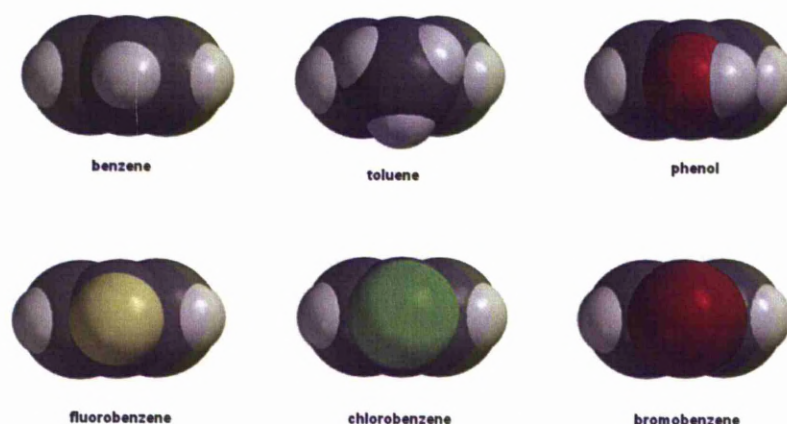**Figure 1.13:** Space filling model of substituted benzenes where white represents hydrogen; grey, carbon, red, oxygen; yellow, fluorine; green, chlorine; and brown, bromine.

Bromine and iodine are the least incorporated into drug molecules: the only iodine compound released during this time was the thyroid hormone thyroxine.[85] Iodine compounds are relatively unstable, which may be rationalized by the high polarizability and low bond strength of the C-I bond, and as such, synthetic methods to make such compounds are often multistep and avoided by the pharmaceutical industry as the cost of producing such a drug would be prohibitive. In contrast the chemical procedures for producing brominated, chlorinated and fluorinated pharmaceuticals are well established in industrial scale production and the products are stable and cheaper to produce.

Table 1.3: Physicochemical properties of the carbon-halogen bond.[88]

Element	H	C	O	F	Cl	Br
Electronegativity	2.20	2.55	3.44	3.98	3.16	2.96
van der Waals radius (Å)[90]	1.20	1.70	1.52	1.47	1.75	1.85
Bond Length (Å) (H_3C-X)	1.087	1.535	1.425	1.382	1.785	1.933
Bond dissociation energy (kcal/mol)	103.1	88.0	90.2	108.1	81.1	67.9
Ionization potential (kcal/mol)	313.9	259.9	314.3	402.2	299.3	272.7
Electron affinity (kcal/mol)	17.42	29.16	3.73	78.52	83.40	77.63

The van der Waals radius of fluorine is particularly interesting as it is considered to cause minimal steric effects at receptor sites and to be a good substitute for hydrogen. However, as is seen in **table 1.3** the van der Waals radius of fluorine (1.47 Å) lies between that of oxygen (1.52 Å) and hydrogen (1.09 Å). Regardless of its larger size relative to hydrogen there are several studies indicating the minimal steric demand at receptor sites of fluorine and its ability as a hydrogen mimic.[87, 89, 91] Chlorine and bromine have much larger van der Waals radii (1.75 Å and 1.85 Å) respectively and assert a greater steric demand at receptor sites. However, the appropriate attachment of such large atoms or groups could occupy a large proportion of the active site of a molecular target, including the deeper binding pockets as shown for the adenosine deaminase inhibitors in **figure 1.14** where incorporation of the bulky CF_3 substituent greatly enhanced binding.[92]
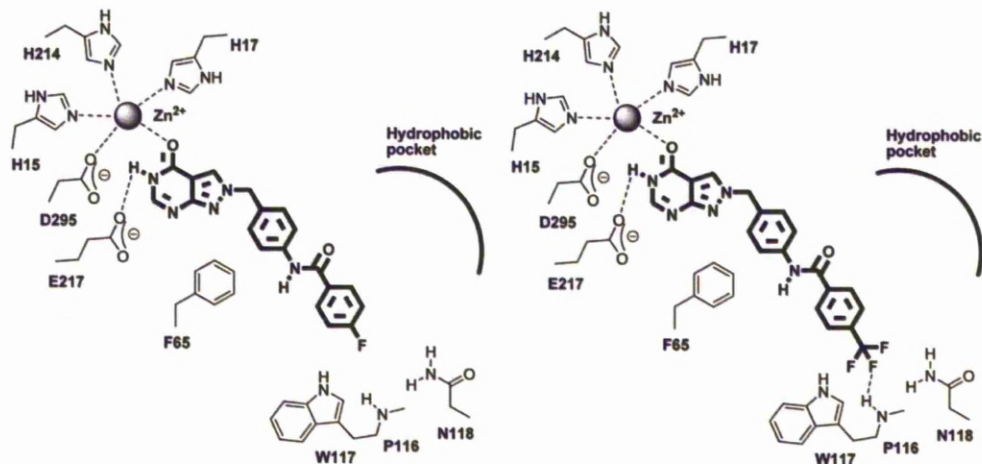
Figure 1.14: Binding mode of two adenosine deaminase (ADA) inhibitors into the ADA binding cavity. Incorportion of the bulky CF_3 group allows interactioin with amino acid residues deeper in the protein.[92]

Halogen atoms are capable of short contact binding modes similar to hydrogen bonds. A large number of structural surveys and *ab initio* molecular orbital calculations have established that the interaction is essentially electrostatic, with contributions from polarization, dispersion and charge transfer.[93]

As halogen bonding is an electrostatic interaction, the electrostatic potential surrounding the halogen is important. **Figure 1.15** shows the electrostatic potential of methyl fluoride (**a**), methyl chloride (**b**), and methyl bromide (**c**): it can be clearly seen that there is the expected anisotropic distribution of charge with the carbon being more positive in character and halogen being more negative in character across the series. Observation of the molecule along the carbon-halogen axis reveals that the negative charge is unevenly distributed across the surface of the larger halogens. Fluorine remains almost entirely electronegative (red) but chlorine and bromine show increasing amounts of electropositive potential at the top of the atom (green). This anisotropic distribution of the electron density across the halogen atom has been termed the positive cap[94] or as a sigma hole.[95]
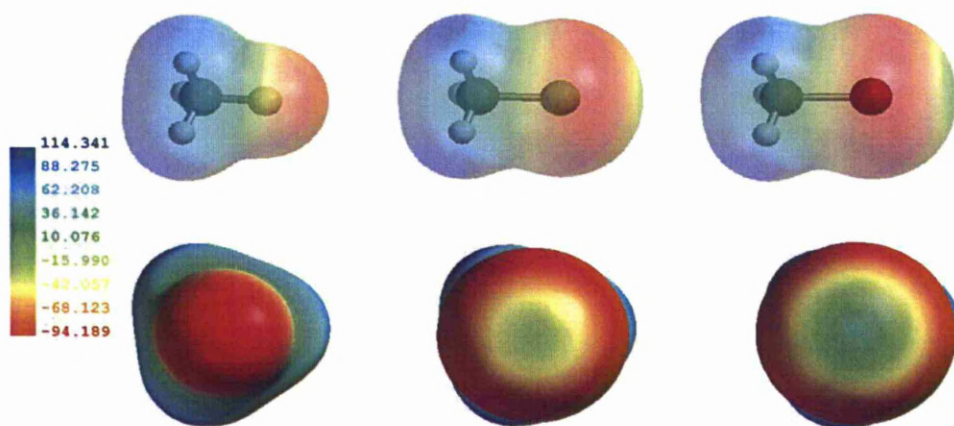

Figure 1.15: *Ab initio* calculations of methyl fluoride (a), methyl chloride (b), and methyl bromide (b) to compare induced negative (red), neutral (green) and positive (blue) electrostatic potential around the halogen surface. The energy potentials range from -175 to 114 kJ/mol. The geometry was optimised at the Hartree-Fock/6-31G level and the surface generated by mapping the electrostatic potential onto the surface using Spartan '08 v1.2.0 build 132.

It is worthy of note that generally, for any given halogen, carbon-halogen bond strength increases with the electron withdrawing nature of the carbon it is covalently bound to. Typically, this gives rise to the trend $C(sp)-X > C(sp^2)-X > C(sp^3)-X$ and the more electron withdrawing an attached carbon is in character the more

electropositive potential is developed at the halogen surface.[96] This is illustrated in **figure 1.16**, where increasing amounts of positive charge (blue) may be seen appearing at the apex of the bromine atom as the attached carbon moves from sp hybridization to sp^3. Moreover, as shown in **table 1.3**, bond strength decrease down the series (F > Cl > Br), and the size of the electropositive cap increases with the opposite trend (Br > Cl > F) with the increasing electropositive potential increasing in-line with the size and polarizability of the halogen. This further suggests that bromine (and iodine) will have the strongest halogen bonding interactions. In contrast, by virtue of its lack of electropositive potential, fluorine is much more likely to act as a hydrogen bond acceptor.[97]
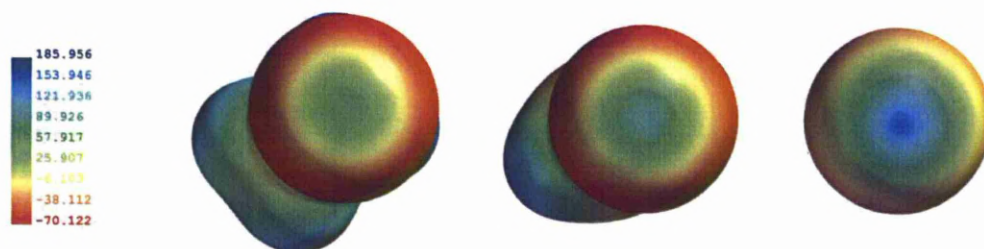

Figure 1.16: *Ab initio* calculations of bromoethane, bromoethene, and bromoethyne, observed along a C-X axis, to compare the induced negative (red), neutral (green) and electropositive (blue) electrostatic potential across the halogen surface. The energy potential ranges from -70 to +186 kJ/mol. The geometry was optimized at the hartree-fock_6-31G level and the surface generated by mapping the electrostatic potential onto the surface using Spartan '08 v1.2.0 build 132.

As alluded to earlier, when considering their interactions with biological targets, halogen atoms in bioactive compounds are usually understood to be involved in non-directional hydrophobic interactions, or to occupy relatively empty cavities, deep in binding pockets, without being involved in major stabilizing contacts.[96] However, the complexity of biological systems, and the abundance of electron rich functional groups on amino acid residues (π-systems, oxygen, nitrogen, sulfur, etc) allow opportunity for halogen bonding with surrounding amino acids, stabilizing molecule-protein substrates.[96]

This effect was well illustrated by Hardegga *et al*[86] where a wide range of novel human Cathepsin L inhibitors (hCatL) were investigated as a comprehensive investigation of the importance of halogen bonding in biological environments.[86] **Figure 1.17** depicts the substrate under investigation in the binding site of hCatL where the atom highlighted in green (x) is the atom that is most likely to participate in halogen bonding. The IC_{50} values remain largely unchanged upon switching H (IC_{50} 0.29 μM) to F (0.34 μM) as shown in **table 1.4**. This is largely attributable to inability of fluorine to participate in halogen binding due to the lack of σ-hole (as shown in **figure 1.15**)
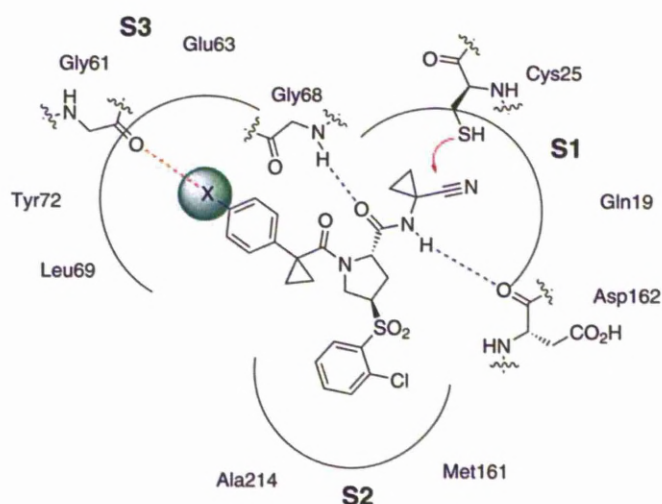

Figure 1.17: Binding mode of covalent inhibitors at the active site of hCatL (a lysosomal cysteine protease) with its three pockets. The substituent which is capable of participation in halogen bonding (indicated by a dashed red line) is highlighted in green.[86]

The half-maximal inhibitory concentration (IC_{50}) values also decreased down the series. Thus the iodine-substituted compound, which has the most polarisable atom, is the most active inhibitor within that particular class of substrates. Moreover, incorporation of a methyl substituent did not substantially enhance the binding affinity of the substrate in hCatL. As methyl substituents (1.70 Å) are most similar in

size to chlorine atoms (1.75 Å) this observation further highlights the importance of halogen bonding in the inhibition of hCatL, as the steric influence alone was not enough to enhance the binding interaction.[86]

Table 1.4: Pharmacological properties of hCatL inhibitors.

	H	Me	F	Cl	Br	I
IC$_{50}$ (μM)	0.29	0.13	0.34	0.022	0.012	0.0065
log$D$	2.11	2.57	2.36	2.73	2.96	3.23

1.3.2 Metabolic dehalogenation

Studies on the dehalogenation of aliphatic-halogenated hydrocarbons demonstrated that the order of halogen elimination decreased in the order I > Br > Cl > F.[98] This is concordant with the strength of carbon halogen bonds (table 1.3) which decreases from fluorine to iodine. By virtue of its greater bond-strength fluorine is routinely incorporated into drugs and drug-like molecules to block bioactivation or metabolism.[87] However, fluorine is an excellent nucleofuge, so much so that despite the relative strength of the carbon-fluorine bond, metabolic defluorination can readily occur during biotransformation by virtue of the formation of the stable fluoride ion.[87] If a molecule is sufficiently electrophilic to undergo direct reaction with nucleophilic groups present in proteins and amino acids (such as the amino group in lysine) defluorination may spontaneously occur.[99] Such compounds are often highly toxic, with the type of toxicity being dependent on the target macromolecues.[100] This potent leaving group ability is exploited in the treatment of advanced pancreatic cancer by gemcitabine (2'-deoxy-2',2'difluorocytidine). Gemcitabine is a pro-drug that is 5'-phosphorylated *in vivo*. The triphosphate is an efficient DNA polymerase chain

terminator, where the diphosphate is a suicide substrate for ribonucleotide reductase.[101]

Generation of fluoride during biological oxidation has been observed for a variety of drugs; such as the metabolism of 3,5-difluoro-4-hydroxybenzoic acid to fluorobenzoquinone-5-carboxylic acid and fluoride ion **figure 1.18a**.[87] Similarly for the metabolism of the novel quinoxaline antiviral (S)-2-ethyl-7-fluoro-3-oxo-2,3-dihydro-2H-quinoxaline-carboxylic acid isopropyl ester (GW420867X) by CYP 1A2 yielding its hydroxylated metabolite as shown in **figure 1.18b**.[102]
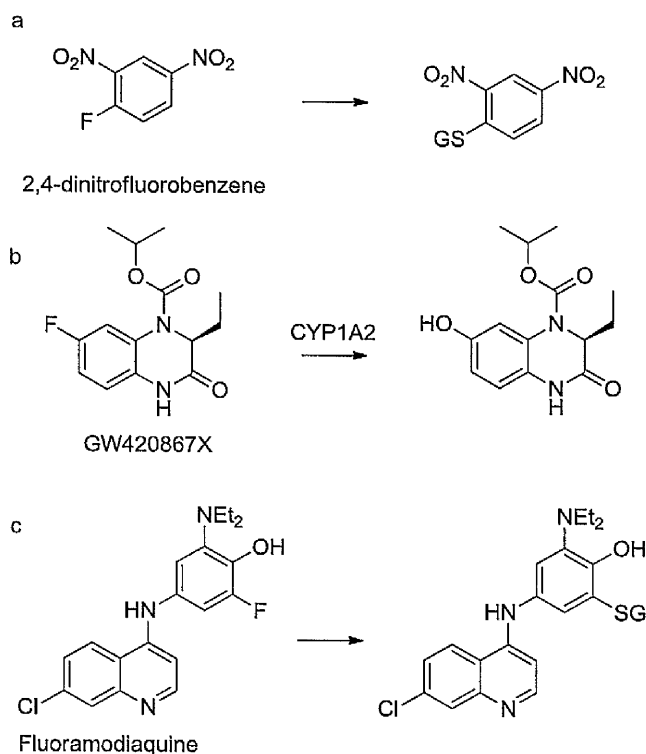

Figure 1.18: Examples of metabolic dehalogenation.

The antimalarial drug amodiaquine **(figure 1.18c)** undergoes extensive biotransformation *in vivo* to give a quinoneimine metabolite, excreted in bile as the

5-glutathionyl metabolite. Attempts to block this biotransformation with fluorine substitution at the 5 position[103] instead only formed 5-glutathionyl amodiaquine. Here the fluoride elimination was caused by oxidation to a quinoneimine; followed by subsequent Michael addition of glutathione, and then subsequent elimination of hydrofluoric acid to restore the aromatic system.[87]

Not all dehalogenation reactions are the result of oxidative-type metabolism. The volatile anaesthetic halothane is subject to a number of idiosyncratic reactions, the most prevalent being hepatotoxicity.[104, 105] It is metabolised *in vivo* by both oxidative and reductive pathways.[106] It is widely regarded that the oxidative metabolic pathway is the major detoxicating route[107] for halothane but the reductive metabolism has been implicated as the cause of hepatotoxicity of this drug.[108]

As in oxidative P450 metabolism, halothane is reductively metabolised by two consecutive dehalogenation steps (de-bromination then de-fluorination). It has been shown that this type of metabolism is stimulated by enzyme induction with Phenobarbital which implies a central role of the P450s in the reductive dehalogenation of halothane and the proposed mechanistic route is shown in **figure 1.19**.[109]
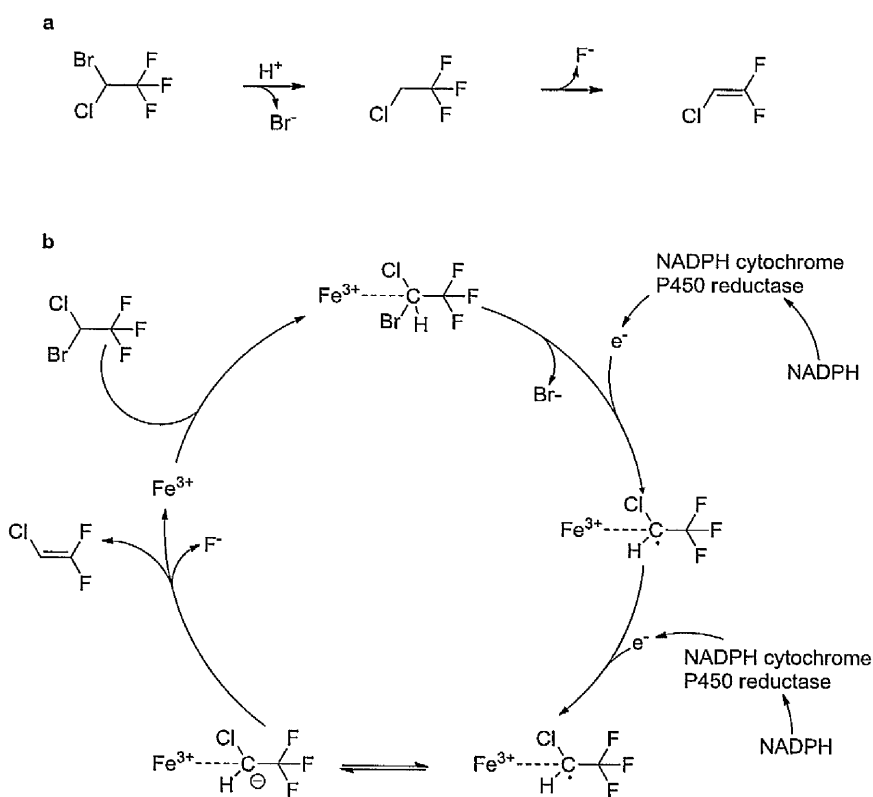
Figure 1.19: Reductive dehalogenation of halothane by cytochrome P450. **(a)** General mechanistic pathway forming 2-chloro-1,1,1-trifluoroethane and 2-chloro-1,1-ethylene. **(b)** Proposed catalytic pathway for cytochrome P450 in the dehalogenation of halothane.[98]

The proposed mechanistic route[98] in **figure 1.19** has several features in common with the oxidative catalytic cycle of P450s (**figure 1.4**). Both schemes incorporate substrate binding and two successive single electron transfers. However, in anaerobic metabolism there is no requirement for oxygen and the reducing electrons are utilized in the formation of radical and carbanion complexes of halothane rather than oxygen scission and activation.

Considering the high affinity of cytochrome P450 for oxygen, and that oxygen could actively compete for the reducing equivalents in the catalytic cycle, the lack of oxygen in the cycle is perhaps surprising. Yet certain cells in tissues, particularly the centre of liver lobules, are perfused poorly with oxygen and thus have relatively low

oxygen tensions. It is plausible then, that under these almost anaerobic conditions, Cyp P450 would act in a reductive mode.

1.3.3 Halogens and the National Institutes of Health (NIH) shift

In higher organisms aromatic compounds, such as carbamazepine, are transformed to phenols, *trans*-dihydrodiols, glutathione conjugates and pre-mercapturic acids from postulated arene-oxide intermediates.[110] Stability of epoxides varies greatly yet is mostly dependent on the electron density of the double bond being oxidised with those with high electron densities being the most stable; such as CBZ-E. It is in this way that several epoxides with varying stabilities are formed by the same molecule. The distribution and nature of arene oxide derived metabolites is dependent on several factors:[110]

- The intrinsic stability of the oxide with regards to isomerisation to phenols

- Susceptibility to conversion to *trans*-dihydrodiols by epoxide hydrolase enzymes

- Susceptibility to phase 2 metabolism (glutathione conjugation) and

- Affinity of the metabolite for nucleophilic groups of macromolecules

The isolation and identification of naphthalene-1,2-oxide in 1968 as the key intermediate in the hepatic metabolism of naphthalene, ended years of speculation over the role such unstable arene oxides played in the metabolism of aromatic compounds.[110]
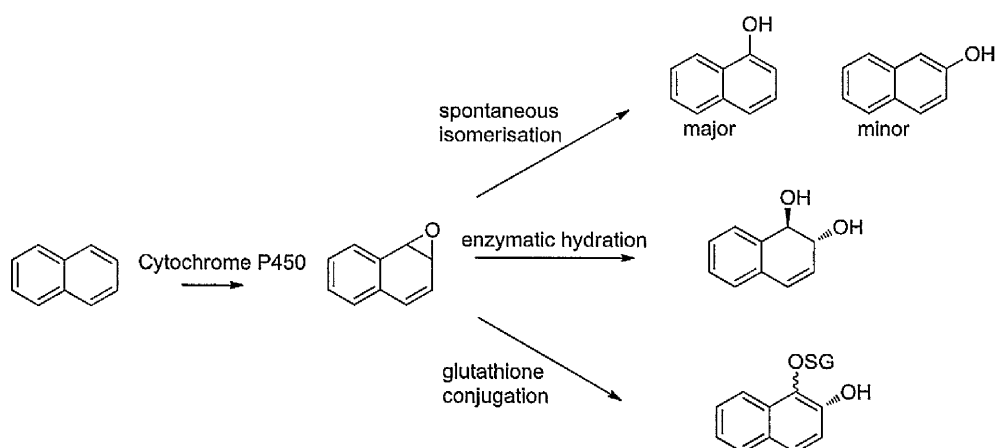
Figure 1.20: Pathways of naphthalene metabolism.

Hepatic MFOs were shown to convert naphthalene to naphthalene-1,2-oxide as shown in **figure 1.20**. This intermediate can spontaneously isomerize or undergo further biotransformation to *trans*-dihydrodiols by epoxide hydrolase. It may also undergo conjugation reactions with glutathione by glutathione *S*-transferase as shown in **figure 1.20**. However, spontaneous isomerisation of deuterio-labelled naphthalene-1,2-oxide is accompanied by deuterium migration from the 1 to the 2 position.[110] This phenomenon became widely known as the NIH shift, named for the U.S. National Institutes of Health where the phenomenon was first observed and is illustrated in **figure 1.21**.
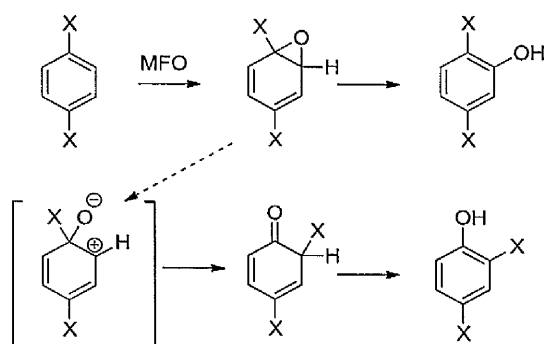

Figure 1.21: The NIH shift in a 1,2-disubstituted benzene.[87]

The NIH shift has been reported for a wide variety of substituents since its initial discovery including; deuterium, tritium, alkyl, and halogens. The extent to which these substituents are able to migrate have also been shown to be dependent upon the nature of the substituent itself, and the nature of other substituents present.[111]

The importance of the NIH shift in the metabolism of halogenated materials is still less well documented than for deuterated and tritiated compounds.[112] In the study of a range of *para*-substituted phenylalanines to their *para*-hydroxylated metabolites by the enzyme phenylalanine hydroxylase shown in **figure 1.22**; bromine and chlorine substituents were observed to migrate, whereas iodine and fluorine substituents were preferentially lost from the molecule.[113, 114] Up until 1998 the NIH shift was virtually undocumented for fluorine and iodine substituents, *in vitro* studies of 4-fluoroaniline, 4-fluoroacetanilide and 4-iodoanisole reported that, analogous to phenylalanine hydroxylase reactions, fluorine or iodine was lost from the molecule in preference to the halogen shift.[115] However, the apparent inability of fluorine to give rise to an NIH shift in P450-catalysed oxidations had only been reported for 4-fluoroaniline and 4-fluoroacetanilide.[114-116] As NIH shifting had already been shown to be dependent upon the type and placement of other substituents on the ring, it was unclear if fluorine was generally resistant to NIH shifting or if an electron donating substituent *para* to fluorine artificially enhanced the ability of fluorine to undergo elimination.
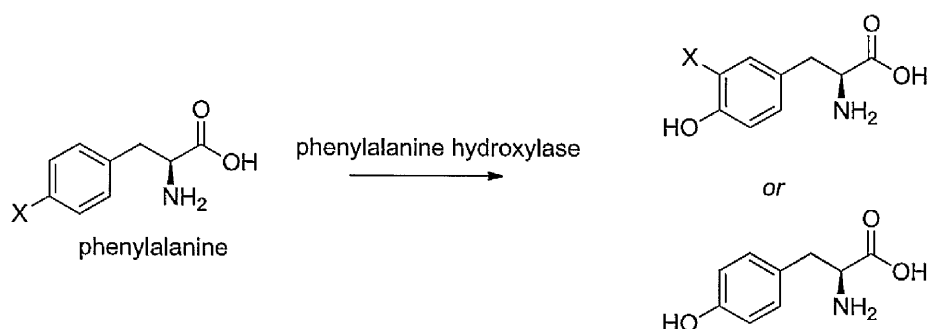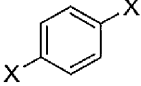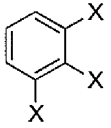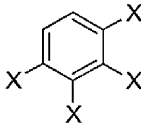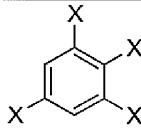
Figure 1.22: Chemical probes used to probe NIH shifting and metabolic defluorination. When X is fluorine or iodine, the halogen is displaced from the molecule. When X is bromine or chlorine it is observed to shift around the ring.[114-116]

Studies by Koerts *et al* compared the extent of NIH shifting of a range of di-, tri-, and tetra-substituted benzenes as outlined in **table 1.5**.[114] It is clearly seen that the percentage of NIH shifted metabolites for the fluorinated analogues is significantly lower than the values for chlorinated analogues. This suggested that:

- NIH shifting was a minor process for fluorinated compounds *or*

- It is a significant process *in vivo* but the intermediates formed are lost to other, competing, biotransformations

Table 1.5: Percentage shifting of substituted fluoro- and chloro-benzenes observed *in vivo*.

X = F	0.7	0.3	0.2	3.3
X = Cl	3.5	9.1	10.0	78.6

Studies of 1,4-difluorobenzene showed markedly greater percentages of NIH-shifted metabolites *in vitro* than *in vivo* (26.8 % and 0.7 % respectively). Moreover, addition

of glutathione to the *in vitro* incubations resulted in a marked decrease in the percentage of observed shifted metabolites, and glutathione depleted rats showed a four-fold increase in NIH shifted metabolites implicating glutathione conjugation as a competing pathway for NIH shifting.[114]

The earlier example of the fluorinated quinoxaline antiviral GW420897X (**figure 1.17c**) was shown to undergo metabolic defluorination, which may have been enhanced by the para relationship with the amine.[102] However, in contrast to para fluorinated acetanilides and anilines, GW420897X has also been shown to form NIH shifted metabolites as highlighted in **figure 1.23**.[117]
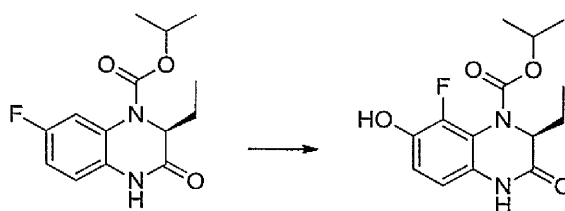

Figure 1.23: NIH shifted metabolite of GW420867X.

1.4 Conclusions

The clinical manifestations of adverse drug reactions are often highly similar to other diseases making their early diagnosis by physicians difficult.[118] Although it is widely believed that the formation and accumulation of reactive drug metabolites are responsible for the cause of many adverse drug reactions the detailed mechanisms behind these effects remain largely unelucidated.[56, 68] While in an ideal world the medicinal chemist would direct the formation of new drug candidates to compounds that did not contain structural features known to be prone to cause adverse effects (so called "structural alerts"). However attempts to do this would be virtually impossible.

Therefore it is important to try to determine the extent a molecule may be metabolized and which metabolites are responsible for adverse drug reactions.[56, 119, 120] Halogens, particularly fluorine,[121, 122] have been routinely incorporated into molecules as a method of preventing oxidative metabolism of drug molecules and so strategic incorporation of fluorine, chlorine, or bromine in the 2- and 2,8- positions of carbamazepine may be postulated to prevent the formation of 2,3-arene oxides. However by virtue of the NIH shift the formation of hydroxylated metabolites may not be completely prevented. Furthermore, if the carboxamide moiety may be removed in sufficient quantities, the para relationship of the halogen substituent and the amide may enhance dehalogenation.

While the incorporation of these atoms may not have a direct effect on oxidations at the 10,11- positions: the increased steric demand of the larger halogens, and their potentially different binding in the P450 active site (fluorine would act as a hydrogen bond donor, bromine and chlorine would act more as acceptors) may reduce the formation of CBZE. Consequently, chemical modification of CBZ resulting in a decrease in oxidative metabolism could be very informative in the assessment of associated ADRs with pathways of bioactivation.

1.5 References

1. Gibson, G. G.; Skett, P., *Introduction to Drug Metabolism*. Third ed.; Nelson Thornes: Cheltenham, 2001.

2. Rang, H. P.; Dale, M. M.; Ritter, J. M., *Pharmacology*. Fourth ed.; Churchill Livingstone: New York; Edinburgh, 1999.

3. Coleman, M. D., *Human Drug Metabolism: An Introduction*. John Wiley: Chichester, 2005; p 274.

4. Brodie, B. B.; Papper, E. M.; Mark, L. C., Fate of procaine in man and properties of its metabolite diethylaminoethanol. *Current researches in anesthesia & analgesia* **1950,** 29, (1), 29-33.

5. Madsen, H.; Rasmussen, B. B.; Brøsen, K., Imipramine demethylation in vivo: Impact of CYP1A2, CYP2C19, and CYP3A4. *Clinical Pharmacology and Therapeutics* **1997,** 61, (3), 319-324.

6. Vevelstad, M.; Pettersen, S.; Tallaksen, C.; Brørs, O., O-demethylation of codeine to morphine inhibited by low-dose levomepromazine. *European Journal of Clinical Pharmacology* **2009,** 65, (8), 795-801.

7. Timbrell, J. A., The role of metabolism in the hepatotoxicity of isoniazid and iproniazid. *Drug Metabolism Reviews* **1979,** 10, (1), 125-147.

8. Guengerich, F. P., Uncommon P450-catalyzed reactions. *Current Drug Metabolism* **2001,** 2, (2), 93-115.

9. Guengerich, F. P., Common and Uncommon Cytochrome P450 Reactions Related to Metabolism and Chemical Toxicity. *Chemical Research in Toxicology* **2001,** 14, (6), 611-650.

10. Zhao, L.; Pickering, G., Paracetamol metabolism and related genetic differences. *Drug Metabolism Reviews* **2011,** 43, (1), 41-52.

11. Genter St. Clair, M. B.; Amarnath, V.; Anthony Moody, M.; Anthony, D. C.; William Anderson, C.; Graham, D. G., Pyrrole oxidation and protein cross-linking as necessary steps in the development of γ-diketone neuropathy. *Chemical Research in Toxicology* **1988,** 1, (3), 179-185.

12. Lock, E. A.; Charbonneau, M.; Strasser, J.; Swenberg, J. A.; Bus, J. S., 2,2,4-Trimethylpentane-induced nephrotoxicity. II. The reversible binding of a TMP metabolite to a renal protein fraction containing $\alpha(2u)$-globulin. *Toxicology and Applied Pharmacology* **1987,** 91, (2), 182-192.

13. Poulos, T. L., Cytochrome P450. *Current Opinion in Structural Biology* **1995,** 5, (6), 767-774.

14. Peterson, J. A.; Graham, S. E., A close family resemblance: The importance of structure in understanding cytochromes P450. *Structure* **1998,** 6, (9), 1079-1085.

15. Denisov, I. G.; Makris, T. M.; Sligar, S. G.; Schlichting, I., Structure and chemistry of cytochrome P450. *Chemical Reviews* **2005,** 105, (6), 2253-2277.

16. Shaik, S.; Kumar, D.; de Visser, S. P.; Altun, A.; Thiel, W., Theoretical perspective on the structure and mechanism of cytochrome P450 enzymes. *Chemical Reviews* **2005,** 105, (6), 2279-2328.

17. Schlichting, I.; Berendzen, J.; Chu, K.; Stock, A. M.; Maves, S. A.; Benson, D. E.; Sweet, R. M.; Ringe, D.; Petsko, G. A.; Sligar, S. G., The catalytic pathway of cytochrome P450cam at atomic resolution. *Science* **2000,** 287, (5458), 1615-1622.

18. Dabrowski, M. J.; Schrag, M. L.; Wienkers, L. C.; Atkins, W. M., Pyrene-pyrene complexes at the active site of cytochrome P450 3A4: Evidence for a multiple substrate binding site. *Journal of the American Chemical Society* **2002,** 124, (40), 11866-11867.

19. Roberts, A. G.; Campbell, A. P.; Atkins, W. M., The thermodynamic landscape of testosterone binding to cytochrome P450 3A4: Ligand binding and spin state equilibria. *Biochemistry* **2005,** 44, (4), 1353-1366.

20. Ortiz De Montellano, P. R., *Cytochrome P450: structure, mechanism, and biochemistry.* Second ed.; Plenum, New York, 1995.

21. Isin, E. M.; Guengerich, F. P., Substrate binding to cytochromes P450. *Analytical and Bioanalytical Chemistry* **2008,** 392, (6), 1019-1030.

22. Vermilion, J. L.; Coon, M. J., Identification of the high and low potential flavins of liver microsomal NADPH-cytochrome P-450 reductase. *Journal of Biological Chemistry* **1978,** 253, (24), 8812-8819.

23. Oprian, D. D.; Coon, M. J., Oxidation-reduction states of FMN and FAD in NADPH-cytochrome P-450 reductase during reduction by NADPH. *Journal of Biological Chemistry* **1982,** 257, (15), 8935-8944.

24. Montellano, P. R. O. d., *Cytochrome P450: Structure, Mechanism, and Biochemistry.* Second ed.; Plenum Press: New York and London, 1995.

25. Guengerich, F. P., Reduction of cytochrome b5 by NADPH-cytochrome P450 reductase. *Archives of Biochemistry and Biophysics* **2005,** 440, (2), 204-211.

26. Beedham, C., The role of non-P450 enzymes in drug oxidation. *Pharmacy World and Science* **1997,** 19, (6), 255-263.

27. Hlavica, P.; Kehl, M., Studies on the mechanism of hepatic microsomal N-oxide formation. The role of cytochrome P-450 and mixed-function amine oxidase in the N-oxidation of NN-dimethylaniline. *Biochemical Journal* **1977,** 164, (3), 487-496.

28. Malle, E.; Furtmüller, P. G.; Sattler, W.; Obinger, C., Myeloperoxidase: A target for new drug development? *British Journal of Pharmacology* **2007**, 152, (6), 838-854.

29. Lu, W.; Uetrecht, J. P., Peroxidase-Mediated Bioactivation of Hydroxylated Metabolites of Carbamazepine and Phenytoin. *Drug Metabolism and Disposition* **2008**, 36, (8), 1624-1636.

30. Klebanoff, S. J., Myeloperoxidase: Friend and foe. *Journal of Leukocyte Biology* **2005**, 77, (5), 598-625.

31. Uetrecht, J. P., Myeloperoxidase as a generator of drug free radicals. *Biochemical Society symposium* **1995**, 61, 163-170.

32. Uetrecht, J.; Zahid, N.; Shear, N. H.; Biggar, W. D., Metabolism of dapsone to a hydroxylamine by human neutrophils and mononuclear cells. *Journal of Pharmacology and Experimental Therapeutics* **1988**, 245, (1), 274-279.

33. Uetrecht, J. P.; Zahid, N., N-chlorination and oxidation of procainamide by myeloperoxidase: Toxicological implications. *Chemical Research in Toxicology* **1991**, 4, (2), 218-222.

34. Gill, H. J.; Tingle, M. D.; Park, B. K., N-Hydroxylation of dapsone by multiple enzymes of cytochrome P450: Implications for inhibition of haemotoxicity. *British Journal of Clinical Pharmacology* **1995**, 40, (6), 531-538.

35. Uetrecht, J. P., Reactivity and possible significance of hydroxylamine and nitroso metabolites of procainamide. *Journal of Pharmacology and Experimental Therapeutics* **1985**, 232, (2), 420-425.

36. Hofstra, A. H.; Uetrecht, J. P., Myeloperoxidase-mediated activation of xenobiotics by human leukocytes. *Toxicology* **1993**, 82, (1-3), 221-242.

37. Nierenberg, A. A., A critical appraisal of treatments for bipolar disorder. *Primary Care Companion to the Journal of Clinical Psychiatry* **2010**, 12, (SUPPL. 1), 23-29.

38. Frye, M. A., Bipolar disorder - A focus on depression. *New England Journal of Medicine* **2011**, 364, (1), 51-59.

39. Ehret, M. J.; Levin, G. M., Long-term use of atypical antipsychotics in bipolar disorder. *Pharmacotherapy* **2006**, 26, (8 I), 1134-1147.

40. Johannessen Landmark, C., Antiepileptic drugs in non-epilepsy disorders: Relations between mechanisms of action and clinical efficacy. *CNS Drugs* **2008**, 22, (1), 27-47.

41. Häßler, F.; Dück, A.; Reis, O.; Buchmann, J., Alternative agents used in ADHD. *Substanzgebundene alternativen in der therapie von ADHS* **2009**, 37, (1), 13-25.

42.   Leucht, S.; Heres, S.; Kissling, W.; Davis, J. M., Evidence-based pharmacotherapy of schizophrenia. *International Journal of Neuropsychopharmacology* **2011**, 14, (2), 269-284.

43.   Hoaken, P. C., Carbamazepine in the treatment of aggressive behavior in schizophrenic patients: a case report. *Canadian journal of psychiatry. Revue canadienne de psychiatrie* **1984**, 29, (3), 282.

44.   Leucht, S.; McGrath, J.; White, P.; Kissling, W., Carbamazepine augmentation for schizophrenia: How good is the evidence? *Journal of Clinical Psychiatry* **2002**, 63, (3), 218-224.

45.   Baron, R.; Binder, A.; Wasner, G., Neuropathic pain: diagnosis, pathophysiological mechanisms, and treatment. *The Lancet Neurology* **2010**, 9, (8), 807-819.

46.   Kaufman, K. R., Antiepileptic drugs in the treatment of psychiatric disorders. *Epilepsy and Behavior* **2011**, 21, (1), 1-11.

47.   Ginsberg, L. D., Carbamazepine extended-release capsules: A retrospective review of its use in children and adolescents. *Annals of Clinical Psychiatry* **2006**, 18, (SUPPL. 1), 3-7.

48.   Cates, M.; Powers, R., Concomitant rash and blood dyscrasias in geriatric psychiatry patients treated with carbamazepine. *Annals of Pharmacotherapy* **1998**, 32, (9), 884-887.

49.   Tohen, M.; Castillo, J.; Baldessarini, R. J.; Zarate Jr, C.; Kando, J. C., Blood dyscrasias with carbamazepine and valproate: A pharmacoepidemiological study of 2,228 patients at risk. *American Journal of Psychiatry* **1995**, 152, (3), 413-418.

50.   Baskar, V.; Kamalakannan, D.; Singh, B. M., Carbamazepine-induced rapid and severe hyponatraemia. *Pharmaceutical Journal* **2002**, 268, (7198), 690.

51.   Salawu, F.; Danburam, A., Hyponatraemia during low-dose carbamazepine therapy. *Annals of African Medicine* **2007**, 6, (4), 207-208.

52.   Kalapos, M. P., Carbamazepine-provoked hepatotoxicity and possible aetiopathological role of glutathione in the events: Retrospective review of old data and call for new investigation. *Adverse Drug Reactions and Toxicological Reviews* **2002**, 21, (3), 123-141.

53.   Morales-Diaz, M.; Pinilla-Roa, E.; Ruiz, I., Suspected carbamazepine-induced hepatotoxicity. *Pharmacotherapy* **1999**, 19, (2), 252-255.

54.   Romero Maldonado, N.; Sendra Tello, J.; Raboso Garcia-Baquero, E.; Harto Castaño, A., Anticonvulsant hypersensitivity syndrome with fatal outcome. *European Journal of Dermatology* **2002**, 12, (5), 503-505.

55. Singh, G., Do no harm-But first we need to know more: The case of adverse drug reactions with antiepileptic drugs. *Neurology India* **2011**, 59, (1), 53-58.

56. Park, B. K.; Boobis, A.; Clarke, S.; Goldring, C. E. P.; Jones, D.; Kenna, J. G.; Lambert, C.; Laverty, H. G.; Naisbitt, D. J.; Nelson, S.; Nicoll-Griffith, D. A.; Obach, R. S.; Routledge, P.; Smith, D. A.; Tweedie, D. J.; Vermeulen, N.; Williams, D. P.; Wilson, I. D.; Baillie, T. A., Managing the challenge of chemically reactive metabolites in drug development. *Nature Reviews Drug Discovery* **2011**, 10, (4), 292-306.

57. Ana Alfirevic; Tracy Mills; Pauline Harrington; Tracy Pinel; James Sherwood; Ansar Jawaid; John C. Smith; Ruth E. March; Bryan J. Barratt; David W. Chadwick; B. Kevin Park; Pirmohamed., M., Serious carbamazepine-induced hypersensitivity reactions associated with the HSP70 gene cluster. *Pharmacogenetics and Genomics* **2006**, 16, 287-296.

58. Pirmohamed, M.; James, S.; Meakin, S.; Green, C.; Scott, A. K.; Walley, T. J.; Farrar, K.; Park, B. K.; Breckenridge, A. M., Adverse drug reactions as cause of admission to hospital: prospective analysis of 18 820 patients. *British Medical Journal* **2004**, 329, 12-19.

59. Maldonado, N. R.; Tello, J. S.; Garcia-Baquero, E. R.; Castaño, A. H., Anticonvulsant Hypersensitivity Syndrome with fatal outcome. *European Journal of Dermatology* **2002**, 12, (5), 503-505.

60. Meyer, U. A., Pharmacogenetics and adverse drug reactions. *The Lancet* **2000**, 356, (9242), 1667-1671.

61. Brain, C.; Mac Ardle, B.; Levin, S., Idiosyncratic reactions to carbamazepine mimicking viral infection in children. *British Medical Journal* **1984**, 289, (6441), 354.

62. Knowles, S. R.; Shapiro, L. E.; Shear, N. H., Anticonvulsant hypersensitivity syndrome. Incidence, prevention and management. *Drug Safety* **1999**, 21, (6), 489-501.

63. Muller, P.; Dubreil, P.; Mahé, A.; Lamaury, I.; Salzer, B.; Deloumeaux, J.; Strobel, M., Drug Hypersensitivity Syndrome in a West-Indian population. *European Journal of Dermatology* **2003**, 13, (5), 478-481.

64. Alfirevic, A.; Jorgensen, A. L.; Williamson, P. R.; Chadwick, D. W.; Park, B. K.; Pirmohamed, M., HLA-B locus in Caucasian patients with carbamazepine hypersensitivity. *Pharmacogenomics* **2006**, 7, (6), 813-818.

65. Green, V. J.; Pirmohamed, M.; Kitteringham, N. R.; Gaedigk, A.; Grant, D. M.; Boxer, M.; Burchell, B.; Park, B. K., Genetic analysis of microsomal epoxide hydrolase in patients with carbamazepine hypersensitivity. *Biochemical Pharmacology* **1995**, 50, (9), 1353-1359.

66. Asconapé, J. J., The selection of antiepileptic drugs for the treatment of epilepsy in children and adults. *Neurologic Clinics* **2010**, 28, (4), 843-852.

67.   Naisbitt, D. J.; Williams, D. P.; Pirmohamed, M.; Kitteringham, N. R.; Park,
        B. K., Reactive metabolites and their role in drug reactions. *Current Opinion*
        in Allergy and Clinical Immunology **2001,** 1, 317-325.

68.   Uetrecht, J., Evaluation of which reactive metabolite, if any, is responsible
        for a specific idiosyncratic reaction. *Drug Metabolism Reviews* **2006,** 38,
        (38).

69.   Seitz, C. S.; Pfeuffer, P.; Raith, P.; Bröcker, E. B.; Trautmann, A.,
        Anticonvulsant hypersensitivity syndrome: Cross-reactivity with tricyclic
        antidepressant agents. *Annals of Allergy, Asthma and Immunology* **2006,** 97,
        (5), 698-702.

70.   Pearce, R. E.; Uetrecht, J. P.; Leeder, J. S., Pathways of carbamazepine
        bioactivation in vitro: II. The role of human cytochrome P450 enzymes in the
        formation of 2-hydroxyiminostilbene. *Drug Metabolism and Disposition*
        2005, 33, (12), 1819-1826.

71.   Lertratanangkoon, K.; Horning, M. G., Metabolism of Carbamazepine. *Drug*
        Metabolism and Disposition **1982,** 10, (1), 1-10.

72.   Madden, S.; Maggs, J. L.; Park, B. K., Bioactivation of carbamazepine in the
        rat *in vivo*: Evidence for the Formation of Reactive Arene Oxide(s). *Drug*
        Metabolism and Disposition **1996,** 24, (4), 469-479.

73.   Lillibridge, J. H.; Amore, B. M.; Slattery, J. T.; Kalhorn, T. F.; Nelson, S. D.;
        Finnell, R. H.; Bennett, G. D., Protein-reactive metabolites of carbamazepine
        in mouse liver microsomes. *Drug Metabolism and Disposition* **1996,** 24, (5),
        509-514.

74.   Robin E. Pearce; Wei Lu; YongQiang Wang; Jack P. Uetrecht; Maria Almira
        Correia; Leeder., J. S., Pathways of Carbamazepine Bioactivation in Vitro.
        III. The Role of Human Cytochrome P450 Enzymes in the Formation of 2,3-
        Dihydroxycarbamazepine. *Drug Metabolism and Disposition* **2008,** 36, (8),
        1637-1649.

75.   Besag, F. M. C.; Berry, D. J.; Pool, F.; Newbery, J. E.; Subel, B.,
        Carbamazepine   toxicity   with   lamotrigine: Pharmacokinetic   or
        pharmacodynamic interaction? *Epilepsia* **1998,** 39, (2), 183-187.

76.   Warner, T.; Patsalos, P. N.; Prevett, M.; Elyas, A. A.; Duncan, J. S.,
        Lamotrigine-induced   carbamazepine   toxicity: An   interaction   with
        carbamazepine-10,11-epoxide. *Epilepsy Research* **1992,** 11, (2), 147-150.

77.   Bu, H. Z.; Kang, P.; Deese, A. J.; Zhao, P.; Pool, W. F., Human in vitro
        glutathionyl and protein adducts of carbamazepine-10,11-epoxide, a stable
        and pharmacologically active metabolite of carbamazepine. *Drug Metabolism*
        and Disposition **2005,** 33, (12), 1920-1924.

78.   Ju, C.; Uetrecht, J. P.; Van Koppen, C. J., Detection of 2-
        hydroxyiminostilbene in the urine of patients taking carbamazepine and its

oxidation to a reactive iminoquinone intermediate. *Journal of Pharmacology and Experimental Therapeutics* **1999**, 288, (1), 51-56.

79. Staines, A. G.; Coughtrie, M. W. H.; Burchell, B., N-glucuronidation of carbamazepine in human tissues is mediated by UGT2B7. *Journal of Pharmacology and Experimental Therapeutics* **2004**, 311, (3), 1131-1137.

80. Maggs, J. L.; Pirmohamed, M.; Kitteringham, N. R.; Park, B. K., Characterization of the metabolites of carbamazepine in patient urine by liquid chromatography/mass spectrometry. *Drug Metabolism and Disposition* **1997**, 25, (3), 275-280.

81. Furst, S. M.; Uetrecht, J. P., Carbamazepine metabolism to a reactive intermediate by the myeloperoxidase system of activated neutrophils. *Biochemical Pharmacology* **1993**, 45, (6), 1267-1275.

82. Kosjek, T.; Andersen, H. R.; Kompare, B.; Ledin, A.; Heath, E., Fate of carbamazepine during water treatment. *Environmental Science and Technology* **2009**, 43, (16), 6256-6261.

83. Leclercq, M.; Mathieu, O.; Gomez, E.; Casellas, C.; Fenet, H.; Hillaire-Buys, D., Presence and fate of carbamazepine, oxcarbazepine, and seven of their metabolites at wastewater treatment plants. *Archives of Environmental Contamination and Toxicology* **2009**, 56, (3), 408-415.

84. Mathieu, O.; Dereure, O.; Hillaire-Buys, D., Presence and ex vivo formation of acridone in blood of patients routinely treated with carbamazepine: Exploration of the 9-acridinecarboxaldehyde pathway. *Xenobiotica* **2011**, 41, (2), 91-100.

85. Hernandes, M. Z.; Cavalcanti, S. M. T.; Moreira, D. R. M.; De Azevedo Jr, W. F.; Leite, A. C. L., Halogen atoms in the modern medicinal chemistry: Hints for the drug design. *Current Drug Targets* **2010**, 11, (3), 303-314.

86. Hardegger, L. A.; Kuhn, B.; Spinnler, B.; Anselm, L.; Ecabert, R.; Stihle, M.; Gsell, B.; Thoma, R.; Diez, J.; Benz, J.; Plancher, J. M.; Hartmann, G.; Banner, D. W.; Haap, W.; Diederich, F., Systematic investigation of halogen bonding in protein-ligand interactions. *Angewandte Chemie - International Edition* **2011**, 50, (1), 314-318.

87. Park, B. K.; Kitteringham, N. R.; O'Neill, P. M., Metabolism of fluorine-containing drugs. In 2001; Vol. 41, pp 443-470.

88. Ojima, I., *Fluorine in Medicinal Chemistry and Chemical Biology*. 1 st ed.; Wiley-Blackwell: Chichester, 2009.

89. O'Hagan, D.; Rzepa, H. S., Some influences of fluorine in bioorganic chemistry. *Chemical Communications* **1997**, (7), 645-652.

90. Bondi, A., van der Waals Volumes and Radii. *The Journal of Physical Chemistry* **1964**, 68, (3), 441-451.

91.   Lima, L. M.; Barreiro, E. J., Bioisosterism: A useful strategy for molecular modification and drug design. *Current Medicinal Chemistry* **2005**, 12, (1), 23-49.

92.   Motta, C. L.; Sartini, S.; Mugnaini, L.; Salerno, S.; Simorini, F.; Taliani, S.; Marini, A. M.; Settimo, F. D.; Lavecchia, A.; Novellino, E.; Antonioli, L.; Fornai, M.; Blandizzi, C.; Tacca, M. D., Exploiting the pyrazolo[3,4-d]pyrimidin-4-one ring system as a useful template to obtain potent adenosine deaminase inhibitors. *Journal of Medicinal Chemistry* **2009**, 52, (6), 1681-1692.

93.   Zou, J. W.; Jiang, Y. J.; Guo, M.; Hu, G. X.; Zhang, B.; Liu, H. C.; Yu, Q. S., Ab initio study of the complexes of halogen-containing molecules RX (X = Cl, Br, and I) and NH3: Towards understanding the nature of halogen bonding and the electron-accepting propensities of covalently bonded halogen atoms. *Chemistry - A European Journal* **2005**, 11, (2), 740-751.

94.   Politzer, P.; Lane, P.; Concha, M. C.; Ma, Y.; Murray, J. S., An overview of halogen bonding. *Journal of Molecular Modeling* **2007**, 13, (2), 305-311.

95.   Lu, Y.; Shi, T.; Wang, Y.; Yang, H.; Yan, X.; Luo, X.; Jiang, H.; Zhu, W., Halogen bonding - A novel interaction for rational drug design? *Journal of Medicinal Chemistry* **2009**, 52, (9), 2854-2862.

96.   Parisini, E.; Metrangolo, P.; Pilati, T.; Resnati, G.; Terraneo, G., Halogen bonding in halocarbon-protein complexes: A structural survey. *Chemical Society Reviews* **2011**, 40, (5), 2267-2278.

97.   Auffinger, P.; Hays, F. A.; Westhof, E.; Ho, P. S., Halogen bonds in biological molecules. *Proceedings of the National Academy of Sciences of the United States of America* **2004**, 101, (48), 16789-16794.

98.   Ahr, H. J.; King, L. J.; Nastainczyk, W.; Ullrich, V., The mechanism of reductive dehalogenation of halothane by liver cytochrome P450. *Biochemical Pharmacology* **1982**, 31, (3), 383-390.

99.   Berkowitz, D. B.; Karukurichi, K. R.; de la Salud-Bea, R.; Nelson, D. L.; McCune, C. D., Use of fluorinated functionality in enzyme inhibitor development: Mechanistic and analytical advantages. *Journal of Fluorine Chemistry* **2008**, 129, (9), 731-742.

100.   Bauer, H.; Fritz-Wolf, K.; Winzer, A.; Kühner, S.; Little, S.; Yardley, V.; Vezin, H.; Palfey, B.; Schirmer, R. H.; Davioud-Charvet, E., A fluoro analogue of the menadione derivative 6-[2'-(3'-methyl) -1',4'-naphthoquinolyl]hexanoic acid is a suicide substrate of glutathione reductase. Crystal structure of the alkylated human enzyme. *Journal of the American Chemical Society* **2006**, 128, (33), 10784-10794.

101.   Cerqueira, N. M. F. S. A.; Fernandes, P. A.; Ramos, M. J., Understanding Ribonucleotide Reductase Inactivation by Gemcitabine. *Chemistry – A European Journal* **2007**, 13, (30), 8507-8515.

102. Mutch, P. J.; Dear, G. J.; Ismail, I. M., Formation of a defluorinated metabolite of a quinoxaline antiviral drug catalysed by human cytochrome P450 1A2. *Journal of Pharmacy and Pharmacology* **2001,** 53, (3), 403-408.

103. O'Neill, P. M.; Harrison, A. C.; Storr, R. C.; Hawley, S. R.; Ward, S. A.; Kevin Park, B., The effect of fluorine substitution on the metabolism and antimalarial activity of amodiaquine. *Journal of Medicinal Chemistry* **1994,** 37, (9), 1362-1370.

104. Cousins, M. J.; Sharp, J. H.; Gourlay, G. K., Hepatotoxicity and halothane metabolism in an animal model with application for human toxicity. *Anaesthesia and Intensive Care* **1979,** 7, (1), 9-24.

105. Larrey, D., Drug-induced liver diseases. *Journal of Hepatology* **2000,** 32, (SUPPL.1), 77-88.

106. Spracklin, D. K.; Hankins, D. C.; Fisher, J. M.; Thummel, K. E.; Kharasch, E. D., Cytochrome P450 2E1 is the principal catalyst of human oxidative halothane metabolism in vitro. *Journal of Pharmacology and Experimental Therapeutics* **1997,** 281, (1), 400-411.

107. Kharasch, E. D.; Hankins, D.; Mautz, D.; Thummel, K. E., Identification of the enzyme responsible for oxidative halothane metabolism: Implications for prevention of halothane hepatitis. *Lancet* **1996,** 347, (9012), 1367-1371.

108. Chow, T.; Imaoka, S.; Hiroi, T.; Funae, Y., Reductive metabolism of halothane by cytochrome P450 isoforms in rats and humans. *Research Communications in Molecular Pathology and Pharmacology* **1996,** 93, (3), 363-374.

109. Goldblum, A.; Loew, G. H., Quantum chemical studies of anaerobic reductive metabolism of halothane by cytochrome P-450. *Chemico-Biological Interactions* **1980,** 32, (1-2), 83-99.

110. Daly, J. W.; Jerina, D. M.; Witkop, B., Arene oxides and the NIH shift: The metabolism, toxicity and carcinogenicity of aromatic compounds. *Experientia* **1972,** 28, (10), 1129-1149.

111. Silverman, I. R.; Daub, G. H.; Vander Jagt, D. L., Methoxybenzo[a]pyrene 4,5-oxides labeled with carbon-13: Electronic effects in the NIH shift. *Journal of Organic Chemistry* **1985,** 50, (26), 5550-5556.

112. Guroff, G.; Daly, J., Quantitative studies on the hydroxylation-induced migration of deuterium and tritium during phenylalanine hydroxylation. *Archives of Biochemistry and Biophysics* **1967,** 122, (1), 212-217.

113. Guroff, G.; Kondo, K.; Daly, J., The production of meta-chlorotyrosine from para-chlorophenylalanine by phenylalanine hydroxylase. *Biochemical and Biophysical Research Communications* **1966,** 25, (6), 622-628.

114. Koerts, J.; Soffers, A. E. M. F.; Vervoort, J.; De Jager, A.; Rietjens, I. M. C. M., Occurrence of the NIH shift upon the cytochrome P450-catalyzed in vivo and in vitro aromatic ring hydroxylation of fluorobenzenes. *Chemical Research in Toxicology* **1998**, 11, (5), 503-512.

115. Cnubben, N. H. P.; Vervoort, J.; Boersma, M. G.; Rietjens, I. M. C. M., The effect of varying halogen substituent patterns on the cytochrome P450 catalysed dehalogenation of 4-halogenated anilines to 4-aminophenol metabolites. *Biochemical Pharmacology* **1995**, 49, (9), 1235-1248.

116. Daly, J., Metabolism of acetanilides and anisoles with rat liver microsomes. *Biochemical Pharmacology* **1970**, 19, (12), 2979-2993.

117. Dear, G. J.; Ismail, I. M.; Mutch, P. J.; Plumb, R. S.; Davies, L. H.; Sweatman, B. C., Urinary metabolites of a novel quinoxaline non-nucleoside reverse transcriptase inhibitor in rabbit, mouse and human: Identification of fluorine NIH shift metabolites using NMR and tandem MS. *Xenobiotica* **2000**, 30, (4), 407-426.

118. Gogtay, N. J.; Bavdekar, S. B.; Kshirsagar, N. A., Anticonvulsant hypersensitivity syndrome: A review. *Expert Opinion on Drug Safety* **2005**, 4, (3), 571-581.

119. Park, B. K.; Kitteringham, N. R.; Kenny, J. R.; Pirmohamed, M., Drug metabolism and drug toxicity. *Inflammopharmacology* **2001**, 9, (1-2), 183-199.

120. Park, B. K.; Naisbitt, D. J.; Gordon, S. F.; Kitteringham, N. R.; Pirmohamed, M., Metabolic activation in drug allergies. *Toxicology* **2001**, 158, (1-2), 11-23.

121. Morgan, P.; Maggs, J. L.; Page, P. C. B.; Park, B. K., Oxidative dehalogenation of 2-fluoro-17α-ethynyloestradiol in vivo. A distal structure-metabolism relationship of 17α-ethynylation. *Biochemical Pharmacology* **1992**, 44, (9), 1717-1724.

122. Barnard, S.; Storr, R. C.; O'Neill, P. M.; Park, B. K., The effect of fluorine substitution on the physicochemical properties and the analgesic activity of paracetamol. *Journal of Pharmacy and Pharmacology* **1993**, 45, (8), 736-744.

Results and Discussion: Synthesis of Halogenated Carbamazepine Analogues

Chapter 2

This chapter details the chemical synthesis of halogenated carbamazepine analogues. It includes a brief introduction to the literature precedent for the synthesis of such molecules, before moving on to a detailed discussion of the synthetic strategies employed in the formation of selectively substituted iminostilbenes and carbamazepine analogues.

Contents

2.   Synthesis of Halogenated Carbamazepine Derivatives

2.1.   Introduction: Dibenz[b,f]azepines and related ring systems

First synthesised in 1899 by Theile and Holzinger,[1] 10,11-dihydrodibenz[b,f]azepine

(iminodibenzyl) was prepared from o,o'-diaminobibenzyl hydrochloride as shown in

scheme 2.1 below. Yet a further 50 years were to elapse before other derivatives of

this ring system were prepared and characterized.[2, 3]
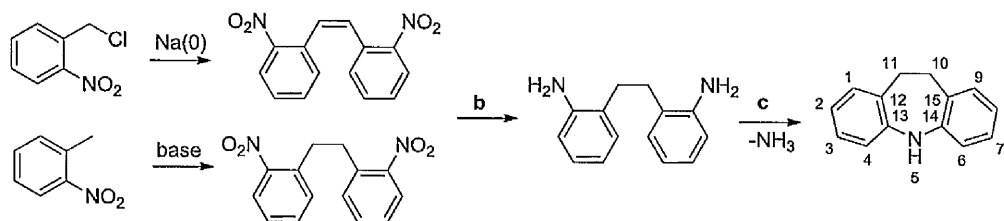
Scheme 2.1: Synthesis of iminodibenzyl[3] Reagents and conditions: (a) sodium ethoxide – isoamyl nitrate, (b) Sn/HCl, (c) heat or Polyphosphoric acid.[3]

Benzodiazapines are a highly significant class of therapeutic agents. 1H-3-

Benzazepine-2-amines (figure 2.1) possess antihypertensive activity, additionally

iminostilbenes possess some limited pharmacological potential such as antimalarial,[4]

and antioxidant[5-8] properties. However, their 5-substituted analogues are generally

more potent and most similar seven-membered ring systems bearing a basic side-

chain will have some effect on the central nervous system.[9] Iminostilbenes (ISB) and

iminodibenzyls (IDB) are present in a variety of pharmaceutical agents besides the

antiepileptic CBZ. Almost all iminostilbenes that bear a γ-dialkylaminopropyl

substituent display antidepressant activity; depramine (iminostilbenes) and

imipramine (iminodibenzyl) are both active anti depressants,[10] similarly opipramol is

an antidepressant[11] but also displays some antipsychotic activity.[12] Quinupramine[13]

displays some anticholinergic and antihistamine character[14] and is a weak serotonin and norepinephrine reuptake inhibitor. [15]
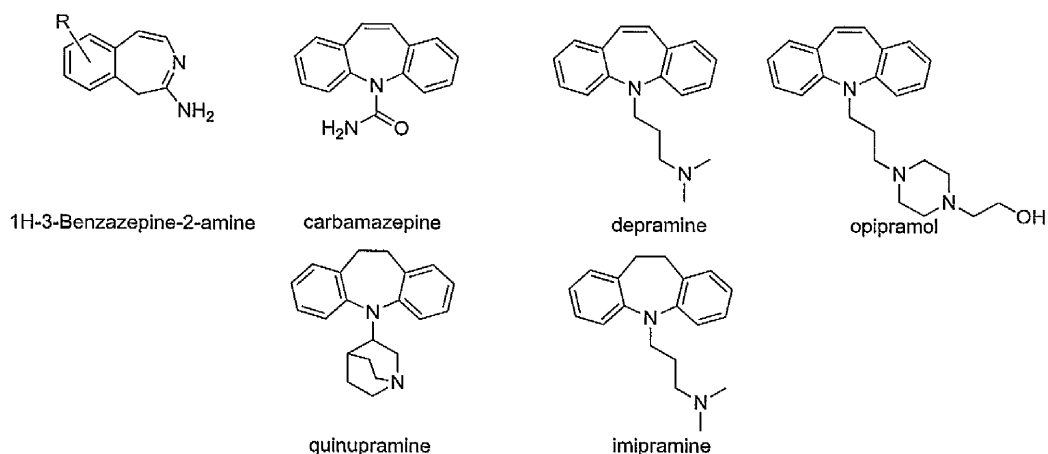
Figure 2.1: Some pharmacologically active dibenzazepines.

Other regio-isomers of the azepine nucleus (figure 2.2) have been shown to possess biological activity: Etazepine retains anticonvulsant activity;[16] 11H-dibenz[b,e]azepines (morphanthridine) derivative perlapine and its 2- fluoro analogue fluperlapine have similar neuroleptic properties to clozapine and are important pharmaceuticals.[17-19] Conversely, other dibenz[b,e]azepines are extreme irritants to both skin and mucous membranes as well as powerful lachrymators and have been examined as chemical defense agents.[20]

etazepine

R= H perlapine
R= F fluperlapine

dibenz[b,f][1,4]oxazepine
a component of tear gas
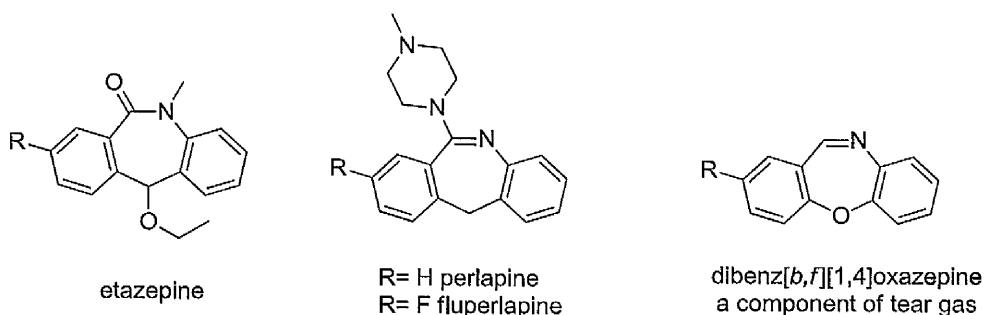
Figure 2.2: Biologically active 11H-dibenz[b,e]azpeines and related compounds.

49

Other benzazepine derivatives are mainly considered from a synthetic standpoint [21-23] as many do not have known pharmacological effects. However dibenz[c,e]azepines have been shown to retain good anticonvulsive activity despite loss of the antidepressant activity.[24] Some derivatives have limited effects as multi-drug resistance reversal agents (R4DPP).[25] Other derivatives retain some limited beneficial pharmacological properties such as antihistamine (epinastine),[26] and hypolipidemic (6,7-dihydro-5H-dibenz[c,e]azepine) as highlighted in **figure 2.3** below.[27, 28]

epinastine

Multi-drug resistance reversal agent
R4DPP

6,7-dihydro-5H-dibenz[c,e]azepine
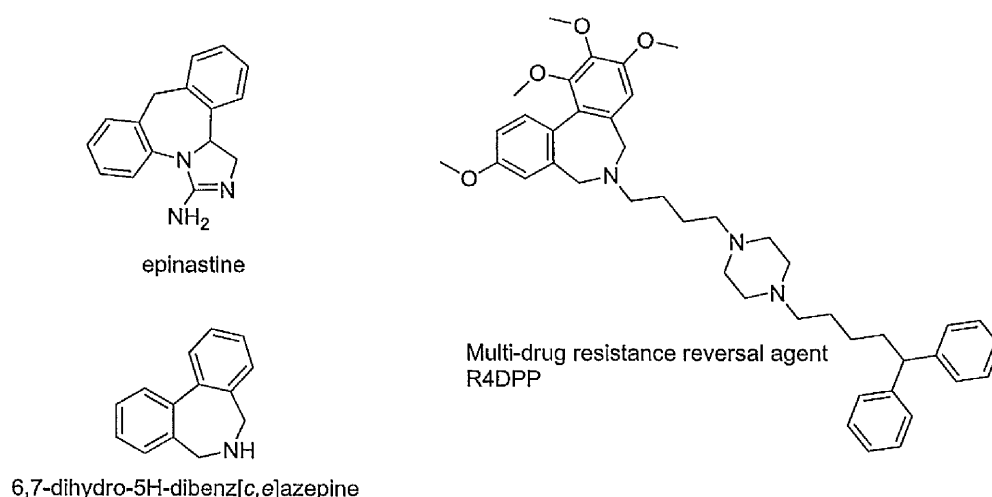
Figure 2.3: Other heteropine derivitaves with pharmacological activity.

2.2 Synthesis of dibenzazepines by ring closing reactions

2.2.1 From bis(2-(bromomethyl)phenyl)amine

Preparation of the fully unsaturated iminostilbene ring system by ring closing reactions is rare. One such example is the treatment of the unstable intermediate, bis(2-(bromomethyl)phenyl)amine *in situ* with an excess of phenyl lithium as shown

in **scheme 2.2**. This forms mainly *N*-acetyl iminodibenzyl (66.5 %)[29] with *N*-acetyl iminostilbene as a minor product (3.5 %).
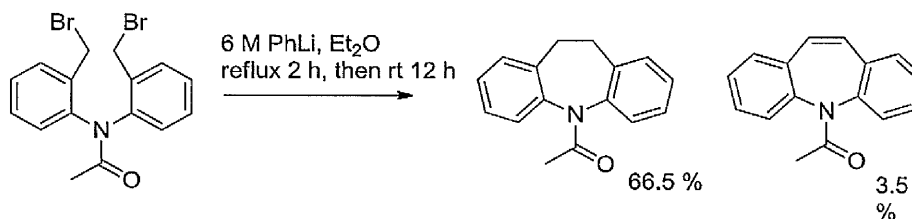
Scheme 2.2: Synthesis of multi substituted iminostilbenes by ring-closing reaction of bis(2-(bromomethyl)phenyl)amine.[29]

Few other alternatives to this reaction exist, however as shown in **scheme 2.3**, refluxing bis(2'-formylphenyl)amine with 60 % hydrazine hydrate in acetic acid yields iminostilbene in excellent yield (98 %). [30]
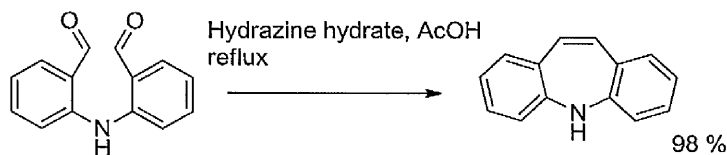
Scheme 2.3: Synthesis of iminostimbene from bis(2'-formylphenyl)amine.[30]

2.2.2 By palladium-ligand controlled ring closure

The most recent method of ring-closing synthesis of iminostilbenes is the palladium-ligand controlled reaction of stable 2-chloro-N-(2-vinyl)aniline derivatives.[31] Selectivity of the ring closing reaction was demonstrated to be highly ligand dependent with 2-dicyclohexylphosphino-2'-(*N*,*N*-dimethylamino)biphenyl (DavePhos) identified as exclusively forming iminostilbene derivatives. Conversely [1,1'-binaphthalen]-2-yldi-tert-butylphosphine (TrixiePhos) was shown to preferentially form 1-vinylcarbazoles and 9-methyl acridine derivatives exclusively.

The conditions and yields of the reactions are highlighted in **scheme 2.4**. Use of other ligands in the reactions tended to give rise to mixtures of the products.[31]
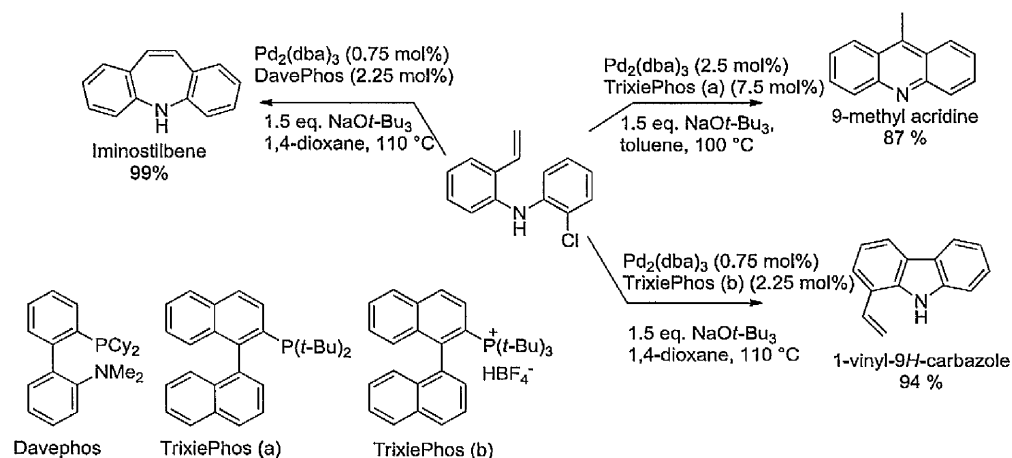
Scheme 2.4: Pd-Ligand controlled stereoselective ring-closing cyclisations.[31]

Direct transformation to iminostilbene was uniquely achieved by tandem reaction of 2-bromo-styrene with 2-chloroaniline, which proceeded in 99 % yield in the presence of $Pd_2(dba)_3$ and NaOt-Bu$_3$ with the DavePhos ligand at 100-110 °C.[31] All other ligands proceeded via the diaryl intermediate shown in the centre of **scheme 2.4**. The reaction was further shown to be reasonably general with a range of mono and di-substituted derivatives formed with a range of functional groups (Cl, OMe, F, CF$_3$, Me) in good yields.[31] However, there are no examples of brominated derivatives or symmetrical substituent patterns.

The currently postulated mechanism of the formation of the iminostilbene is shown in **scheme 2.5**. It is thought to be initiated by the oxidative addition of Pd(0) to the diarylamine intermediate.[31] The carbon-carbon bond formation for iminostilbenes is then suggested to proceed via an eight-membered palladacycle which undergoes reductive elimination to liberate the product.[31]
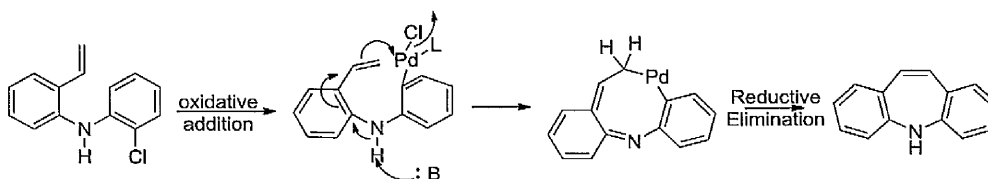
Scheme 2.5: Proposed mechanism for formation of iminostilbenes.[31]

2.2.3 Synthesis from iminodibenzyls

Substituted iminostilbenes may be synthesized from an appropriate iminodibenzyl. While the original synthesis was accomplished by heating o,o'-diaminobibenzyl with o,o'-diaminobibenzyl hydrochloride in 80-85 % yield,[1] it has since been superseded by other methods, such as heating over $AlCl_3$.[32] Though the reported yields are slightly reduced (79 %), the benefit to this is the reduced reaction temperatures (280-290 °C), and shorter reaction times which are more tolerant of substitutions on the aryl rings.[32]

Such ring closing reactions have been exploited in the synthesis of complex binaphthyl derivatives as shown in **scheme 2.6**.[33] Nitration of the binaphthyl derivative occurred in 31 % yield. This product was converted to the diamine and the cyclisation step progressed in 73 % yield in the presence of HCl.
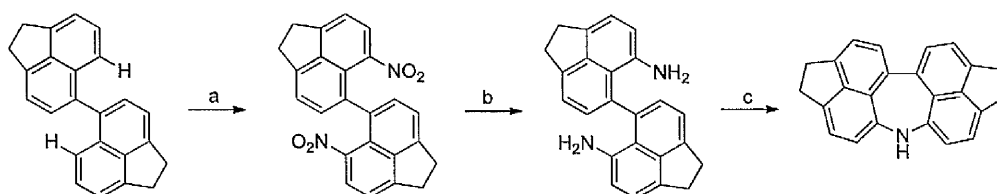
Scheme 2.6: Synthesis of complex binapthyl derivatives. Reagents and Conditions: a) HNO_3/HOAc, 30 %; b) Pd/C, formaldehyde; c) HCl, 73 %. [33]

Fluorinated iminodibenzyls have also similarly been prepared by Li *et al* as the key intermediate in the synthesis of novel analogues of imipramine as highlighted in **scheme 2.7**.[34]
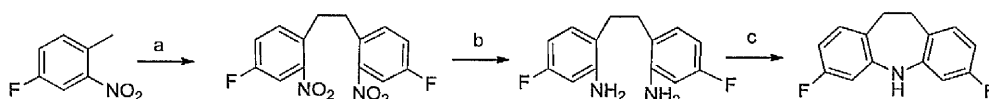
Scheme 2.7: Synthesis of 3,7-difluoro iminodibenzyl. Reagents and Conditions: a) CH_3ONa, 5–15 °C, 4–5 h, 72 %; b) Fe/HCl, 60–70 °C, 3 h, 76 % ; c) 290 °C, 1 h, 5 %.

The condensation of 4-fluoro-2-nitro-toluene in the presence of sodium methoxide progressed in 72 % yields. The dinitrodibenzyl was subsequently reduced to the diaminodibenzyl in 76 % yield. However, thermal condensation, at 290 °C for 1 h, of the diamine to the iminodibenzyl yielded the key iminodibenzyl in only 5 % yield as the reactant was largely carbonized under the reaction conditions.[34]

Jorgensen et al[35] have also reported the synthesis of a range of mono and di-substituted iminodibenzyls, which incorporates much of the chemistry discussed above. Among the final products synthesised was 2,8-difluoro iminodibenzyl as shown in **scheme 2.8**.
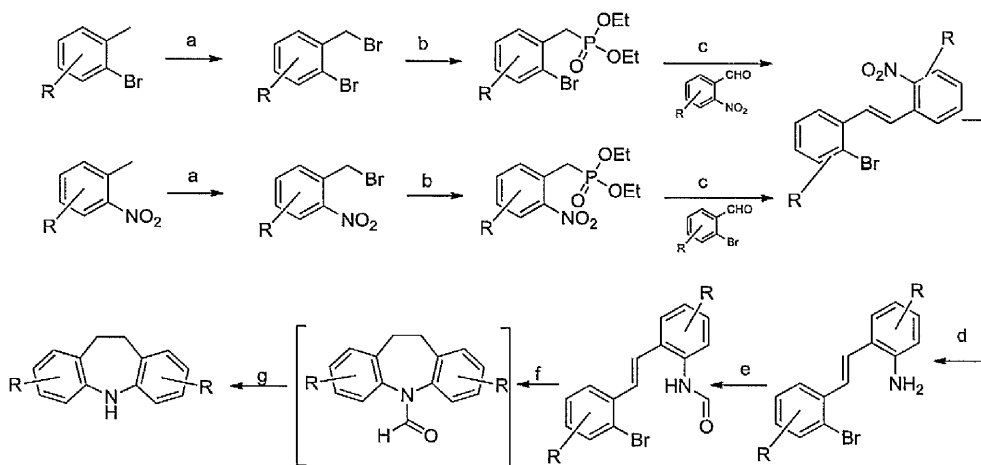
Scheme 2.8: Synthesis of 2 and 2,8-difluoro iminodibenzyls. Reagents and conditions: (a) NBS, dibenzoyl peroxide, CCl_4, 50-100 %; (b) $P(OEt)_3$, quantitative; (c) NaH, dimethoxyethane, 75 %; (d) Pt/C (5 %) or Rh/C, 3:1 EtOH/MeOH, 51-98 %; (e) HCO_2Na, HCO_2H, 79-92 %; (f) K_2CO_3, Cu, CuBr, DMSO; (g) KOH, MeOH, over all yield of steps (f) to (g) 46-75 %.[35]

Modification of either of these methods could be usefully extended to the synthesis of 2- and 2,8- substituted iminostilbenes and thus, carbamazepine derivatives, as introduction of a double bond at C10,11 is plausible. However, the amine nitrogen

must be protected which will result in long and complex reaction sequences: eleven steps in the case of Jorgensen, and eight in the case of Li.

As discussed earlier, the 10,11-double bond may be introduced by dehydrogenation of iminodibenzyls. Dehydrogenation of iminodibenzyls is the principal route to synthesis of iminostilbene derivatives.[3] Palladium on charcoal is the most commonly utilized catalyst;[36, 37] often by sublimation of the iminodibenzyl through an electrically heated glass column that has 20-30 % palladium on charcoal sprinkled on it.[3] Alternative reagents and catalyst systems exist, such as hydrochloric acid,[38] manganese oxides,[39, 40] mixed catalyst systems e.g. ZnO, CaO, and SiO_2[41] and ferric oxide.[42, 43] Furthermore, the iminodibenzyl may be heated with the dehydrogenation catalyst alone,[40] or in the presence of a high-boiling solvent such as diphenyl ether.[44] Industrial production is conducted in the gas-phase, at 500 °C, with a ferric oxide catalyst progressing in 86 % yields. However, the crude product contains acridine and 9-methyl acridine as by-products.[3]

Most of the above chemistry requires complex catalytic mixtures or high temperatures and so are impractical on the laboratory scale. Dehydrobromination of 10-bromo, and 10,11-dibromo iminodibenzyls is a more suitable and practical alternative. It generally affords the desired iminostilbene product in good to excellent yields after protection of the amine and is tolerant of substituents on the aryl ring as shown in **scheme 2.9**.[2] Bromine is typically introduced into the etheno bridge by radical bromination, with N-bromosuccinimide as the most common bromine source.[2] The subsequent elimination of the bromine as hydrogen bromide is accomplished with potassium hydroxide,[2, 45] or occasionally by means of a tertiary

organic base, such as collidine, under more forcing conditions.[46] Effective use of this method will be exemplified later for compounds synthesised for our study.
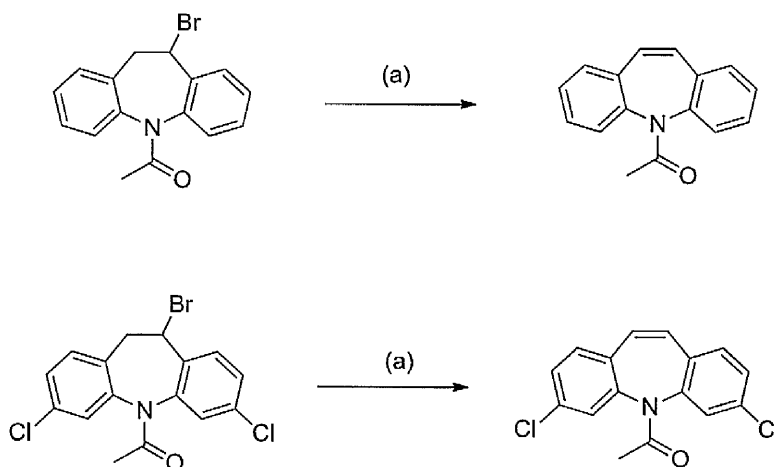
Scheme 2.9: Dehydrobromination of iminodibenzyls. Reagens and conditions (a) KOH (aq), EtOH, 60 °C, 90 %.

## 2.3 Synthesis of dibenzazepines by ring expansion reactions

2.3.1 Acridine-9-methanol expansion

Wagner-Meerwein rearrangement of 9-hydroxymethyl-9,10-dihydroacridine (acridine methanol) is a valuable route to access highly substituted iminostilbenes particularly ring,[4, 47] and etheno bridge derivatives. [48]

Formation of 2-fluoro iminostilbene from 9-chloro acridine has been reported by Varma [4] in 30 % yield as shown below in **scheme 2.10**. Thus addition of the chloroacridine to a solution of NaOEt and diethylmalonate, followed by ester hydrolysis and decarboxylation yielded the carboxylic acid which is further treated with NaOH to give the 9-methylacridine. Treatment of the methyl acridine with 2 equivalents of *N,N*-dimethyl-4-nitrosoaniline and piperidine yielded a nitrone. This sensitive intermediate is then reacted *in situ* with HCl to yield the

acridinecarboxaldehyde. This intermediate may then be esterified and then reduced selectively with lithium aluminium hydride.[4]
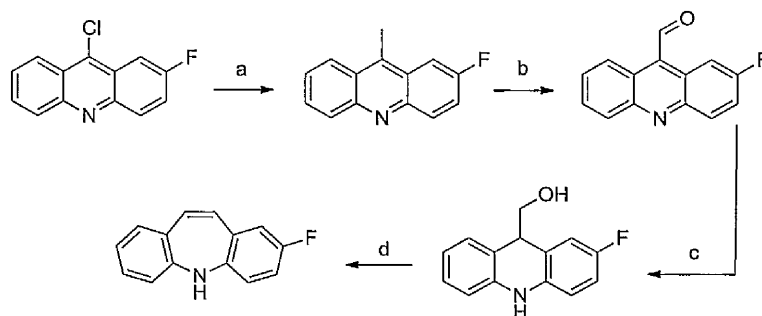
Scheme 2.10: Synthesis of asymmetrically substituted 2-fluoro iminostilbene by the acid catalysed ring expansion of acridine methanol. Reagents and conditions (a) NaOEt, diethylmalonate, EtOH/tol, *then* HCl$_{(aq)}$ (18 %), reflux, *then* NaOH (b) *N,N*-dimethyl-4-nitrosoaniline, piperidine, DMF; (c) LiAlH$_4$; (d) P$_2$O$_5$, xylene, reflux, 2 h, yield 30 %.

The synthesis of iminostilbenes by this method is not without its limitations as acridine methanols are also subject to dehydration reactions forming 9-methylene-9,10-dihydro acridines which can rearrange to 9-methyl acridine. [47]

Work by Bowkett[49] has also further shown the formation of 2-fluoro iminostilbene by ring expansion of the corresponding acridine methanol derived instead from acridine carboxylic acid as shown in **scheme 2.11**.
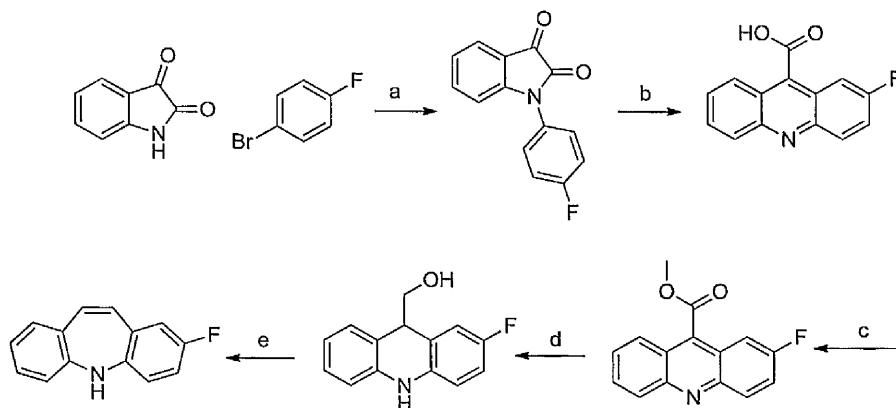
Scheme 2.11: General synthetic route of dibenzazepine formation from isatins. Reagents and Conditions a) CuO, Dimethylacetamide, 150 °C, 18-24 h; b) KOH, EtOH; c) thionylchloride, methanol; d) LiAlH$_4$; e) P$_2$O$_5$, heat.

Here the acridine was formed by cyclisation of an *N*-aryl isatin which was prepared by reacting isatin and bromobenzene in twice stoichiometric quantities of CuO. The reaction progresses well in good yield, although modification of the original Copolla procedure was required to prevent degradation of the product at longer reaction times.[50]

2.3.2 Polyphosphoric acid cyclisation of N-arylindoles

N-aryl indoles, which may be prepared by a variety of methods, undergo ring expansion in hot polyphosphoric acid to give dibenzazepines (**scheme 2.12**)[51]
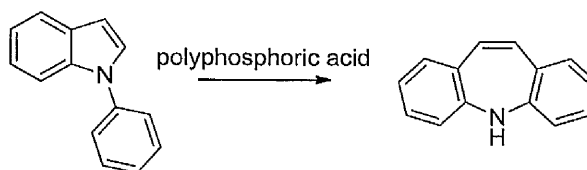
Scheme 2.12: Polyphosphorc acid catalysed cyclisation of N-aryl indoles.

The reaction is particularly sensitive to the position and electronic nature of substituents on the *N*-aryl group and at the 2- and 3-positions of the indole ring.[51] For instance cyclisation of 3-Methyl-1-phenyl-1*H*-indole gave rise to a mixture of products as shown in **scheme 2.13**. However, 2-methyl-1phenyl-1*H*-indole and 2,3-dimethyl-1-phenyl-1*H*-indole both failed to cyclise highlighting the importance of non-substitution at the 2- position for the reaction to proceed.[51]

58

3-Methyl-1-phenyl-1H-indole

37 %

63 %

1-(m-tolyl)-1H-indole

0 %

65 %
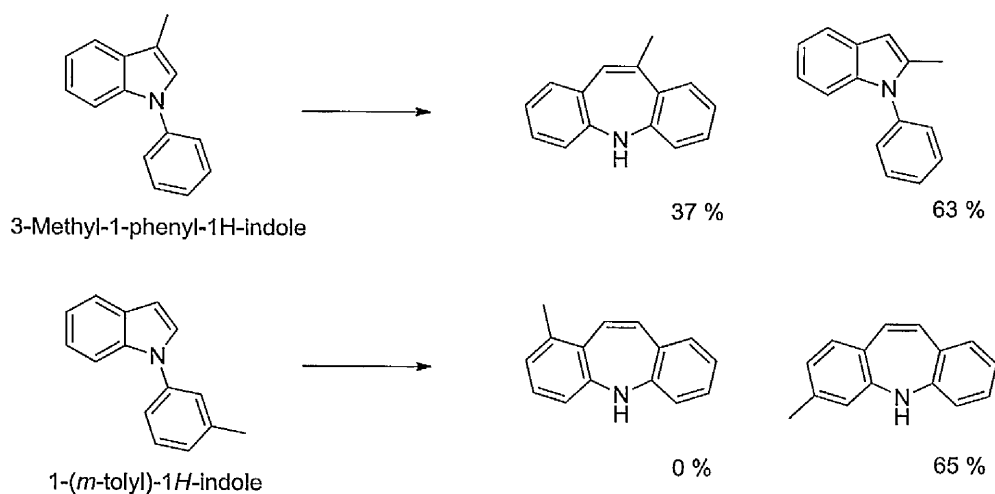
Scheme 2.13: Polyphosphoric acid cyclisation of N-aryl indoles giving rise to mixtures of products.[51]

Furthermore, cyclisation of 1(m-tolyl)-1H-indole may be envisaged to form two potential region isomers, 1-methyl iminostilbene or 3-methyl iminostilbene. However, as highlighted in **scheme 2.13** only one isomer, 3-methyl iminostilbene, was isolated in good yield (65 %).[52] Cyclisation of 1-(p-tolyl)-1H-indole and 5-methyl-1-phenyl-1H-indole both formed the same iminostilbene (2-methyl iminostilbene) as seen in **scheme 2.14**.[51] This allows the reaction to be optimised for the most convenient route of synthesis with the substituent on the indole ring or phenyl substituent. [51]

5-methyl-1-phenyl-1H-indole

1-(p-tolyl)-1H-indole
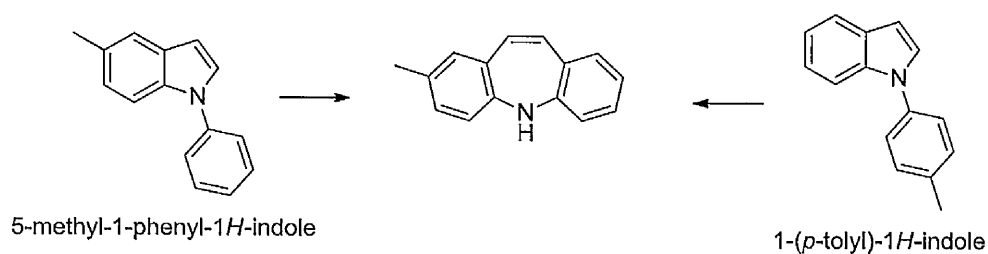
Scheme 2.14: Cyclisation of two different regioisomers of N-aryl indoles forming a single iminostilbene derivative.[51]

59

The nature of the substituents on the aryl ring is also important. Rearrangement was not observed for highly electron withdrawing groups such as NO_2, and CF_3,[51] whereas electron-donating substituents were observed to promote the reaction, with the reaction being most efficient when the aryl group was activated for electrophilic attack at the position *ortho* to nitrogen.[51]

Interestingly, the reaction fails in sulfuric, trifluoroacetic, and trichloroacetic acids: trace yields were observed for *ortho* phosphoric acids. [51]

2.4 Synthetic project aims

The formation of selectively substituted iminostilbenes remains a challenging synthetic goal. While some synthetic routes are high yielding and selective[31] they require highly specific reaction conditions and some halogenated derivatives, e.g. brominated, remain inaccessible. Other routes are long and complex,[4, 35, 49] require high temperatures,[39, 40] or are poor yielding.[34, 53]

A synthetic route to a variety of selectively substituted iminostilbenes, which may be generally applied, is therefore highly desirable. Furthermore, reproducibility of yields, ease of preparation, and safety of reagents are increasingly sought after in synthetic routes.

Our aim therefore was to devise a synthetic route to a variety of substituted iminostilbenes, and hence carbamazepines, that is; general, selective, high yielding, reproducible, easily accomplishable, and forming the carbamazepine in no more than three to four steps. Syntheses of 2-fluoro, 2-chloro, 2-bromo, 2,8-difluoro, 2,8-dichloro, and 2,8-dibromo iminostilbenes were successfully achieved and these intermediates were converted to carbamazepines in reasonable yields. What follows is a discussion of the synthetic approach employed in the synthesis of these compounds.

2.5   Direct Electrophilic Halogenation of Iminodibenzyl

2.5.1   Direct electrophilic bromination with N-halo succinimides

Electrophilic brominaton:

Originally reported by Smith *et al*[52] selective mono- and di-bromination of commercially available iminodibenzyl (1) shown in **scheme 2.15** was successfully achieved by electrophilic substitution. This was accomplished with use of one or two equivalents of *N*-bromo succinimide (NBS) in the presence of silica gel acting as a mild acid catalyst. In an effort to reduce over bromination [52] or uncontrolled bromination in the etheno bridge,[54] light was excluded from the reaction.
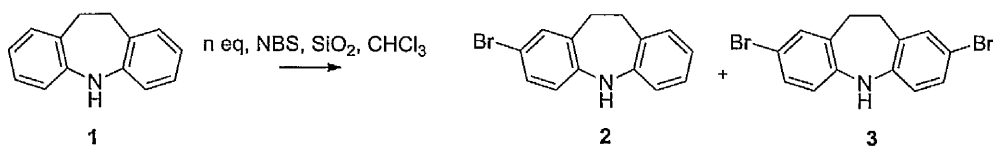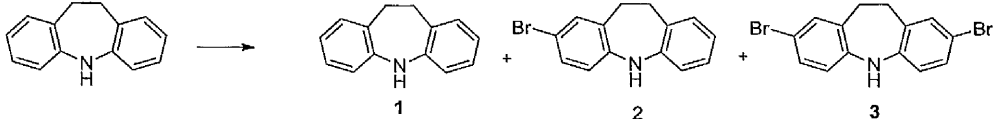
Scheme 2.15: Electrophilic bromination of iminodibenzyls with *N*-bromosuccinimide in the presence of silica gel.[52]

Formation of 2,8-dibromo iminodibenzyl (3) was clean and high yielding, as **table 2.1** shows, although the practicalities of handling the large quantities of silica gel that are required to elicit the reaction on scales above 2 g is difficult. However, use of an overhead stirring mantle was found to be sufficient to stir the reaction efficiently.

Table 2.1: Ratio of products isolated from the reaction of N-Bromosuccinimde and iminodibenzyl in the presence of silica gel.[a]
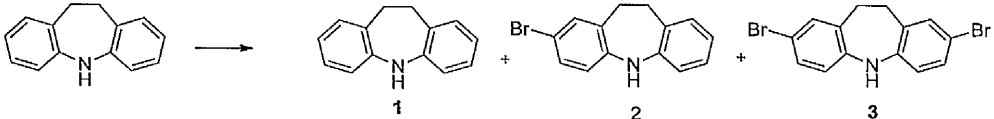
| NBS equivalent	Time to completion (h)	Ratio of 1:2:3*		
		1	2	3
1	0.2	12	78	10
2	0.4	-	-	100

*Percentage of isolated solid from manual chromatography.
[a]Reaction conditions: Iminostilbene (5.0 mmol), N-bromosuccinimide (10.0 mmol), silica gel (2 g per mmol), CHCl₃.

As discussed in the original procedure by Smith,[52] the reaction of iminodibenzyl and N-bromosuccinimide can occur in the absence of silica gel, and the acidity of the reaction solvent, chloroform, appeared to be sufficient for mono- and di- substitution to occur. However, as **table 2.2** shows, the reaction is slower and the requirement for the addition of silica gel becomes greater as the number of substitutions on the aryl ring increases.[52]

Table 2.2: Formation of brominated iminodibenzyls with different catalysts.[a]

Solvent	Acid	Time to completion (h)	Ratio of 1:2:3*		
			1	2	3
CHCl₃	None	6	-	Trace	99+
CHCl₃	SiO₂	0.4	-	-	100

*isolated yields of product after column chromatography.
[a]Reaction conditions: Iminostilbene (5.0 mmol), N-bromosuccinimide (10.0 mmol), silica (2 g per mmol), CHCl₃.

Mono-bromination of iminodibenzyl, with one equivalent of *N*-bromo succinimide was more difficult. Mixtures of mono-, di-, and unsubstituted iminodibenzyls were isolated, in concordance with literature precedent[52] as shown in **table 2.1**. Purification of the crude mixture by column chromatography was difficult as the compounds were similar in polarity but found to be possible and suitable quantities of **2** could be isolated in excellent purity. Previous work by Bowkett[49] has demonstrated that Amberlyst® H⁺ resin is also a suitable catalyst for this reaction, and progresses with similar selectivity and rate to the silica method.

Electrophilic chlorination:

Similar methods of chlorination with *N*-chlorosuccinimide (NCS) are rare in the literature.[55] No specific examples of *N*-chlorination of iminodibenzyls by this method exist. The closest method, outlined in **scheme 2.16**, by Axtell *et al*[56] uses *tert*-butyl hypochlorite as the chlorinating agent. The reaction was performed at -78 °C for 1 h before being gently warmed to room temperature overnight. The reaction was unselective; forming complex mixtures of mono- and di- chlorinated derivatives that were not isolated individually.
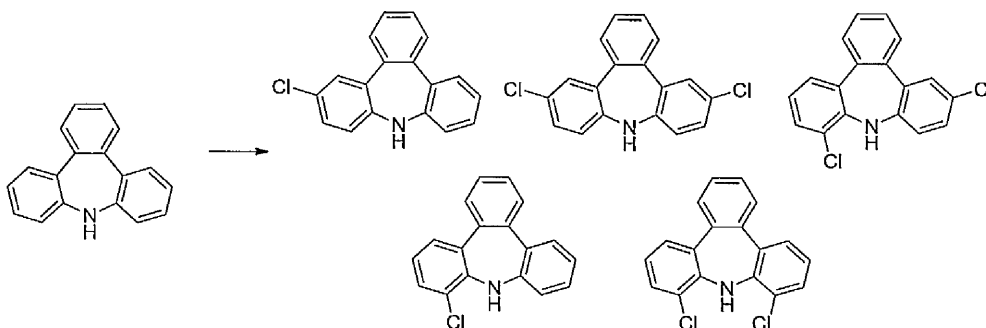
Scheme 2.16: Electrophilic chlorination of 9H-tribenzo[*b,d,f*]azepine. Reagents and conditions: i) -78 °C, 1 h; ii) RT, overnight.[56]

Tert-butyl hypochlorite is highly flammable, and modification of the Smith method[52]

utilizing NCS as the chlorine source was considered to potentially represent a milder

and safer alternative.

Table 2.3: Reaction of *N*-chlorosuccinimide with iminodibenzyl.[a]
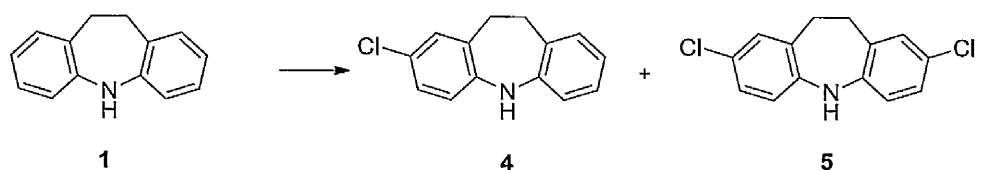
NCS equivalent	Time to completion (h)	Ratio of 1:4:5		
		1	4	5
1	24	23	65	12
2	48	-	20	80

[a] Reaction conditions iminodibenzyl (5.0 mmol), *N*-chlorosuccinimide (5.0-10.0 mmol), silica gel (2 g per 1 mmol NCS), CHCl₃.

As seen in **table 2.3**, compared to NBS the reaction is slower and less selective with

NCS. Complex mixtures of mono- and di-substituted iminodibenzyls as well as

unreacted starting material were obtained. This is partially attributable to the stronger

N-Cl bond in comparison to N-Br.[57] This observation is also in agreement with work

by Duan and co-workers[58] where halogenation of dibenz[*a,c*]anthracene with NBS

was rapid and formed 9-bromo and 9,10-dibromo dibenz[*a,c*]anthracene in a 9:1

ratio. Reaction with NCS was much slower and exclusively formed 9-chloro

dibenz[*a,c*]anthracene.[58]

It was noticed that NCS was only partially soluble in the reaction solvent chloroform,

and so investigations into the effects of solvent were made and are summarized in

table 2.4.

Table 2.4: Effect of solvent on the dichlorination of iminodibenzyl with NCS[a]

Solvent	Time (h)	Ratio of 1:4:5*		
		1	4	5
Acetonitrile	72	-	37	63
CHCl₃	48	trace	20	80
CH₂Cl₂	48	7	55	33
EtOAc	72 +	76	24	-

*Isolated yields determined by manual chromatography. All samples isolated after 5 days regardless of level of completion and their relative percentages determined.
[a] Reaction conditions iminodibenzyl (5.0 mmol), N-chlorosuccinimide (5.0-10.0 mmol), silica gel (2 g per 1 mmol NCS), CHCl₃.

None of the solvents studied led to exclusive formation of **5**. Instead mixtures of varying substitution levels were obtained. As indicated in **table 2.4** acetonitrile, chloroform, and dichloromethane all gave different mixtures of **4** and **5** with no unconverted starting material remaining. Chloroform gave the greatest conversion to **5** with only trace quantities of **1** isolated from the reaction mixture. Dichloromethane reacted at a similar rate, although **1** was isolable from the reaction mixture in greater quantities. Interestingly, the selectivity of the reaction had changed and greater quantities of **4** were isolated in most cases. Acetonitrile gave the greatest conversion, with no isolation of **1**, although still yielding a mixture of **4** and **5**. Ethyl acetate showed only partial conversion of iminodibenzyl after 5 days: here **4** was formed in a mixture with unconverted **1**. This was advantageous as the separation of **4** from **1** was simpler than separating mixtures of the three compounds **1, 4,** and **5**.

The type of acid used in the reaction had a pronounced effect on both the rate of reaction and the ratios of product isolated and the results are summarized in **table 2.5**. In the case of chlorination, reaction in chloroform alone was not sufficient to elicit much reaction between N-chlorosuccinimide and iminodibenzyl with only small quantities of **4** isolated after 3 days. As for bromination, the inclusion of silica gel was important for reducing the reaction time and, although not wholly selective for one product, gave reasonable yields of **4** and **5**.

Table 2.5: Effect of acid on the electrophilic di-chlorination of iminodibenzyl with NCS.[a]

Solvent	Acid	Time (h)	Ratio of 1:4:5		
			1	4	5
CHCl$_3$	None	72	88	12	-
CHCl$_3$	SiO$_2$	48	-	20	80
CHCl$_3$	Amberlyst® H$^+$ resin (10 mol %)	48	13	24	53
CHCl$_3$	10 % TFA	36	-	31	59
CHCl$_3$	10 % HCl (1 M)	36	26	33	41

*isolated yields determined by manual chromatography. All samples isolated after 5 days regardless of level of completion and their relative percentages determined.
a Reaction conditions iminodibenzyl (5.0 mmol), N-chlorosuccinimide (5.0-10.0 mmol), silica gel (2 g per 1 mmol NCS), CHCl$_3$.

The strongly acidic ion exchange resin Amberlyst®, which has a sulfonic acid functional group gave mixtures of **1**, **4**, and **5**. However, relatively small quantities of **1** were isolable after 48 hours. Despite their low selectivity, solid-liquid reaction

systems have significant advantage over other methods as the acid sources are easy to remove from the mixtures at the end of the reaction.[59]

Addition of small quantities of trifluroacetic acid (TFA) increased the rate of reaction, as did 1 M hydrochloric acid. Both were capable of generating the products more rapidly than the solid/liquid systems although the ratios of the isolated products were not always consistent and other, highly polar, components were observed to develop by TLC.
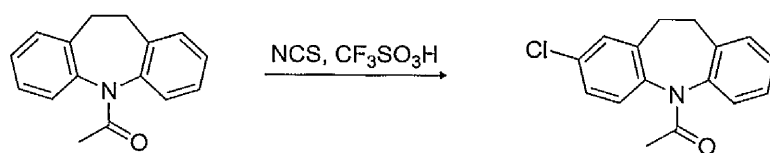

Figure 2.4: Olah-type electrophilic chlorination of iminodibenzyl with NCS. Reaction conditions: N-chlorosuccinimide (3 eq), CF$_3$SO$_3$H.

In an attempt to form selectively the mono-chloro derivative, acyl protection of the amine before reaction with N-chlorosuccinimide was considered. This substantially reduced the reactivity of the amine and the reaction did not readily occur under the same NCS/silica conditions. The use of Olah's strongly acidic conditions,[60] depicted in **figure 2.4**, was found to elicit the reaction. However, the reaction required NCS to be used in excess which was detrimental to the reaction selectivity, forming complex mixtures of products. Mass spectrometry of the product suggested a trisubstituted compound as a major product when three equivalents of NCS were used in the reaction.

2.5.2 Incorporation of the 10,11-double bond

Protection of the iminodibenzyl nitrogen

As discussed earlier, the incorporation of the double bond in the 10,11 position is most suitably conducted by radical bromination followed by elimination. Schindler *et al* first exploited this method in the synthesis of the 3,7-dichloro and 3,7-dibromo carbamazepines as outlined in **scheme 2.17**.[61, 62]
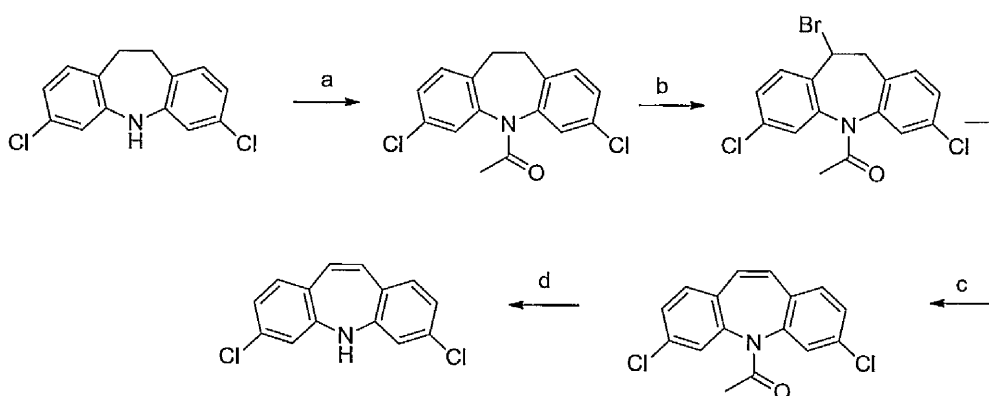
Scheme 2.17: Synthesis of 3,7-dichloro iminostilbene. Reagents and conditions: (a) Acetyl chloride, Benzene, reflux, 90 %; (b) NBS 1.2 eq. hv (200 W UV lamp), CCl$_4$, 60 °C, 90 %; (c) KOH(aq), EtOH, 60 °C, 90 %; (d) KOH (3.5 eq), EtOH, reflux, 95 %.[62]

Protection of the amine nitrogen is an important step, particularly in the case of the mono substituted derivatives. A further equivalent of NBS is used for the radical bromination of the etheno-bridge. The formation of mixtures of products, as illustrated in **figure 2.5**, may be envisioned as the lone pair of the amine nitrogen contributes significantly to reactivity of the aryl rings. The reduction in the capacity of *N*-acyl iminodibenzyl to undergo electrophilic halogenations under mild conditions was described earlier; where protection of the amine nitrogen resulted in no aryl chlorination with NCS except under highly forcing conditions. It was thus presumed that as long as the nitrogen was protected and care was taken with the

stoichiometry of the reaction, over-bromination of the compounds would be less likely to occur.
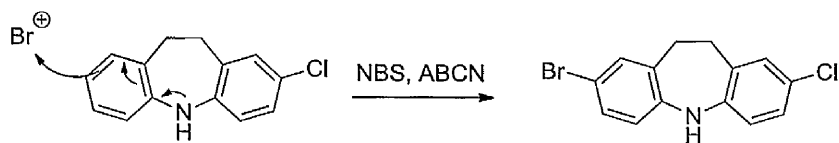
Figure 2.5: Potential formation of mixed halogenated iminostilbenes resulting from unprotected amine.

Protection of the amine with acetic anhydride was considered to be a potentially efficient and high yielding method. However, reaction with 2-, and 2,8- substituted brominated and chlorinated iminodibenzyl analogues were low yielding as summarised in **table 2.6**.

Table 2.6: Formation of N-acylated, halogenated iminodibenzyls.[a]

2 $X_1 = Br, X_2 = H$ 6 $X_1 = Br, X_2 = H$
3 $X_1 = X_2 = Br$ 7 $X_1 = X_2 = Br$
4 $X_1 = Cl, X_2 = H$ 8 $X_1 = Cl, X_2 = H$
5 $X_1 = X_2 = Cl$ 9 $X_1 = X_2 = Cl$
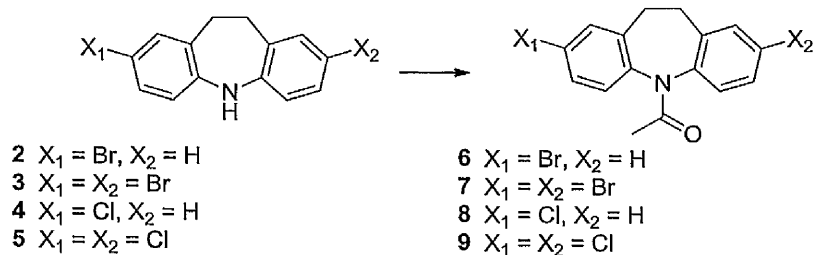
Iminodibenzyl	Time (h)	Temperature (°C)	Yield (%)
2	24	18	12
3	24	18	18
3	24	60	31
4	24	60	trace
5	24	60	9

[a] Reaction conditions: iminodibenzyl (0.6 mmol), Ac$_2$O (2.5 mL).

As the protecting group needed to be inserted into the molecule in high yields, we chose to optimize the reaction conditions for the dibrominated derivative **3** as shown in **table 2.7**.

Table 2.7: Acyl protection of iminodibenzyl 3 under various conditions.
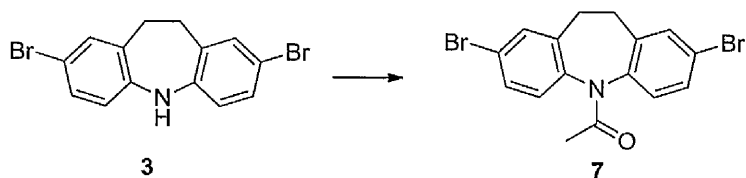
Acylating agent	Solvent	Base/Additive	Time (h)	Temperature (°C)	Yield (%)
Ac$_2$O	Toluene	-	24	100	-
AcCl	Toluene	-	24	r.t.	29
AcCl	Toluene	-	24	100	56
AcCl	Toluene	NEt$_3$	24	r.t.	68
AcCl	Toluene	NEt$_3$	24	100	71
AcCl	Toluene	Imidazole	24	100	50
AcCl	Toluene	DMAP	24	r.t.	69
AcCl	Toluene	DMAP	24	100	92
AcCl*	-	I$_2$	6	r.t.	77

*3.5 equivalents of AcCl in the presence of a 0.1 eq I$_2$.

Of all the transfer catalysts used in **table 2.7** DMAP was the most effective, and when heated to near reflux temperature the yields were near quantitative. Triethylamine and imidazole gave reasonable yields of N-acetyated derivatives when heated.

Phukan et al[63] discovered that molecular iodine was a relatively mild and efficient promoter of N-acylation reactions at room temperature in solvent free conditions with typically one equivalent of acylating agent. The reaction was shown to be reasonably efficient for the protection of relatively deactivated amines such as diphenyl amine which formed the acylated product in 98 % yield.

This method was applied for compound **3**, however I$_2$ was found to be poorly soluble in AcCl and three equivalents of the reagent were required. Although the reaction of AcCl with an iminodibenzyl can occur at room temperature, as shown in **table 2.7**, addition of iodine does appear to increase the rate of the reaction. Monitoring of the reaction by TLC showed that the reaction had progressed to completion within 6

hours. However, while the isolated yield is good, it is significantly lower than for diphenylamine as studied by Phukan.[63] Removal of iodine and excess acyl chloride from the sample was not easily accomplished and column chromatography was required to return the product in high purity.

2.5.3 Radical bromination of the 10-11 bond

Radical bromination at C10 was attempted with NBS and 1,1'-azobis(cyclohexanecarbonitrile) (ACBN) as the radical initiator as illustrated in **scheme 2.18**.

6 X_1 = Br, X_2 = H
7 X_1 = X_2 = Br
8 X_1 = Cl, X_2 = H
9 X_1 = X_2 = Cl

Azobis(cyclohexanecarbonitrile)

10a X_1 = Br, X_2 = H
11a X_1 = X_2 = Br
12a X_1 = Cl, X_2 = H
13a X_1 = X_2 = Cl

10b X_1 = Br, X_2 = H
11b X_1 = X_2 = Br
12b X_1 = Cl, X_2 = H
13b X_1 = X_2 = Cl
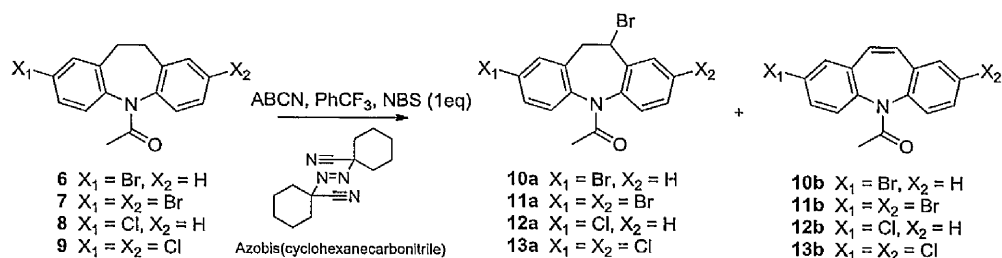
Scheme 2.18: Radical bromination of the etheno bridge of halogenated iminodibenzyls.

As highlighted in **scheme 2.18**, it was observed that as the reaction progressed the starting material was converted to the etheno-bridge brominated products **10-13a**. This intermediate was found to undergo simultaneous elimination to the 10,11-unsaturated products **10-13b** under the reaction conditions in an approximate 3:2 ratio with **10-13a** in agreement with previous work.[49]

Progress of the reaction was difficult to monitor as the starting materials and both products all have similar polarities. Previous work by Bowkett[49] demonstrated that the formation of the products and consumption of the starting material can be monitored by LC-MS. However, the two products tend to co-elute, frustrating their isolation as separate entities.

As the isolation of the materials is difficult it was necessary to develop reaction conditions that entirely converted the starting N-acyl iminodibenzyl to either **10-13a** or **10-13b**. However it is necessary to note here that a crude mixture of **10-13a** and **10-13b** may be transformed to the respective iminostilbene in one step, without the requirement of isolating the N-acyl derivatives, as discussed later, i.e. complete consumption of starting material is most important.

It was discovered that the reaction could be more easily monitored by ^{1}H NMR (**figure 2.6**) of the crude reaction material after a suitable small scale work-up and evaporation of solvent. Although the detection limit for impurities in compounds in ^{1}H NMR[64] are lower than those of LC-MS,[65] monitoring of the reaction by NMR is significantly quicker.
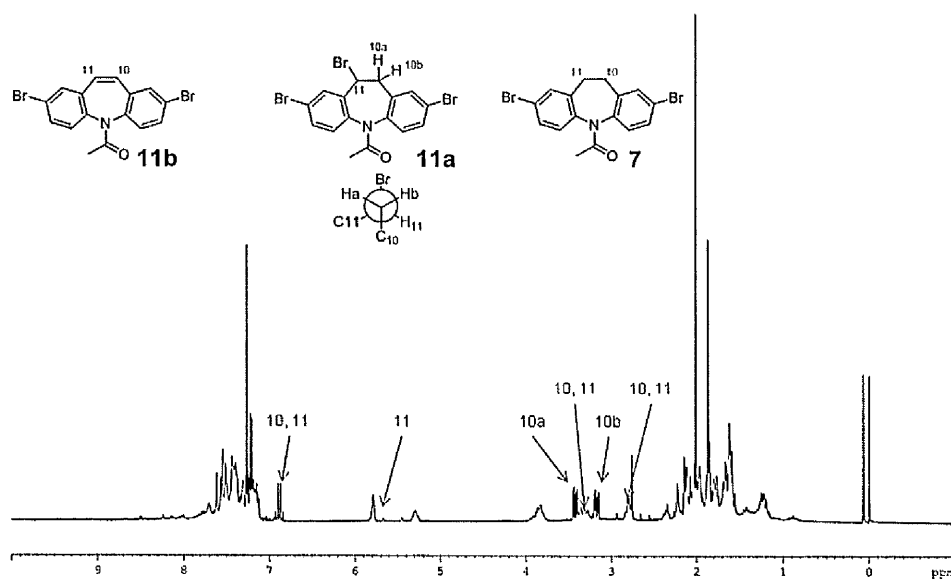
Figure 2.6: Crude reaction mixture taken after 12 h showing the transformation of 7 to 11a and 11b.

It is clearly seen in **figure 2.6** that the 10,11 proton shifts are highly dependent upon their relative substitutions. The unreacted 10,11-N acyl iminodibenzyl, highlighted in green, is visible at 3.38-3.25 ppm and 2.83-2.76 ppm. The protons corresponding to

C10a/10b are also clearly identifiable as doublets of doublets at 3.42 (J = 14.7, 6.3 Hz) ppm and 3.17 (J = 14.8, 5.10 Hz) ppm, as is the proton at C11 as a complex multiplet at 5.79 ppm, indicated in blue. **Figure 2.7**, which shows an expansion of the 2.5-2.6 ppm region, compares the NMR traces at the start of the reaction and at 12 hours where the removal of 7 and emergence of **11a** can be clearly seen.

Figure 2.6 also further highlights the spontaneous elimination of bromine as hydrogen bromide (HBr) from the etheno bridge to form **11b**, as a clear AB quartet ($\Delta v/J$ = 0.5) can be seen developing at 6.9-6.8 ppm and is indicated by the red arrow.
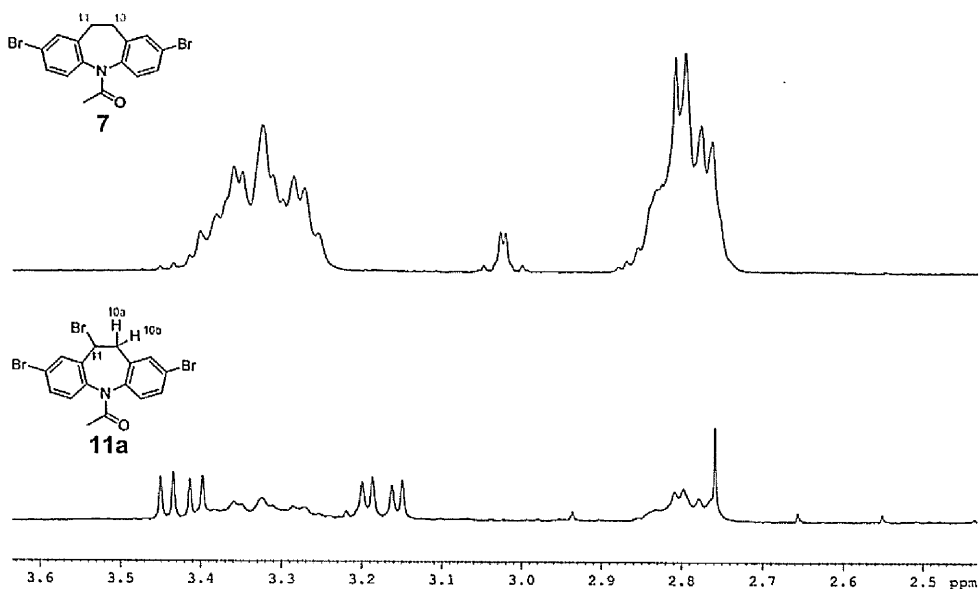
Figure 2.7: ^{1}H NMR comparison of 7 and **11a** at the start of the radical bromination reaction and at 12 hours.

Monitoring of the reaction of monohalo derivatives by ^{1}H NMR is more difficult as bromine was eliminated more rapidly from the etheno-bridge. However, appearance of two distinct AB quartets at 7.05-6.80 ppm associated with formation of **10b** could be observed for the reaction with **6**. Observation of the AB quartets associated with the formation of **12b** was more difficult as the peaks in that region are poorly

dispersed, however, disappearance of the 10,11 protons of **8** could be observed, and their disappearance used to judge an appropriate end-point for the reaction.

Building on previous work by Bowkett[49] the reaction conditions were further optimised for **7** in an effort to form exclusively the *N*-acetlyated product **11b**. The key results are summarised in **table 2.8** with all reactions performed in trifluorotoluene ($PhCF_3$). This solvent is used as a substitute for CCl_4 as it is easier to obtain, and is less damaging to the environment, and it is inert to the reaction conditions.

Table 2.8 Optimisation of the radical bromination of **7** with ABCN to form **11a** and **11b**.
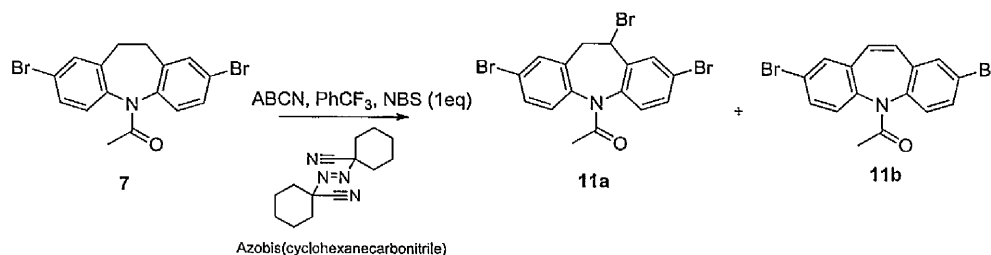
NBS (equiv)	Radical initiator	Temperature (°C)	Time (h)	ratio of 11a to 11b (determined by ¹H NMR)
1.1	hv	60	24	9:1*
1.1	ABCN (10 mol %)	110	24	3:2*
1.2	ABCN (10 mol %)	110	24	3:2*
1.2	ABCN (20 mol %)	110	24	1:1
1.5	ABCN (20 mol %)	110	14	1:1

* Trace amounts of **7** were detectable in the ¹H NMR.

Selective formation of one product was not accomplished; the use of light as the radical initiator was the closest result to selective formation with the products formed in a 9:1 ratio, however some trace amounts of starting material were still observable in agreement with previous work.[49]

There was some concern over increasing the quantity of NBS by a large amount as it could have yielded mixtures of compounds by further nuclear bromination: although

we have demonstrated that *N*-acetylation is effective at reducing the reactivity of iminodibenzyl the potential for mixtures of compounds, as postulated in **figure 2.4**, was still possible.

Increasing the equivalents of NBS in the reaction by small quantities did not result in the formation of mixtures of products with **8**.[49] However, it appears that reaction with **6** is less selective and subject to the formation of isomers. This suggests that *N*-acylation is not sufficient to reduce the reactivity of **6** in the same way as it was for **8**. The additional product from **6** was detected in ^{1}H NMR of the spectra of 2-bromoiminostilbene (**14**) after *N*-deprotection as shown in **figure 2.8** as a singlet at 6.3 ppm. This could suggest the product to be either 3- or 4-bromo iminostilbene as both would be expected to produce a singlet C10-11 peak in ^{1}H NMR. However we were never able to isolate sufficient quantities of the isomer to obtain a clear ^{1}H NMR.
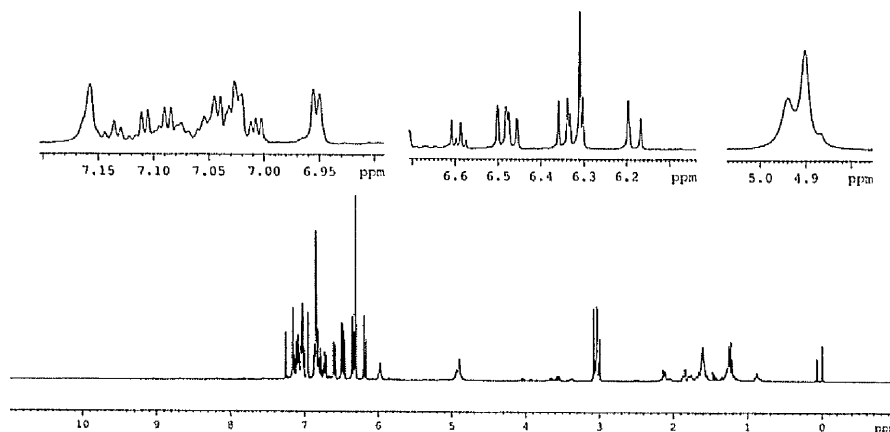
Figure 2.8: Proton NMR of **14** the expansion of the AB quartet at 6.2-6.5 ppm indicates the presence of a large singlet which may correspond to a regioisomer of **14**. This is further supported by the presence of a shoulder on the NH peak at 4.9 ppm which indicates the presence of more than one amine.

Unfortunately, further optimisation of the reaction had little effect on the outcome with similar quantities of the isomeric product still being detectable after several

attempts. These regioisomers could not be separated and so the possibility of separating them after conversion to carbamazepine derivatives (discussed in section 2.3) was considered. The two compounds were highly similar in polarity and their separation was finally achieved on an analytical reverse-phase HPLC column.
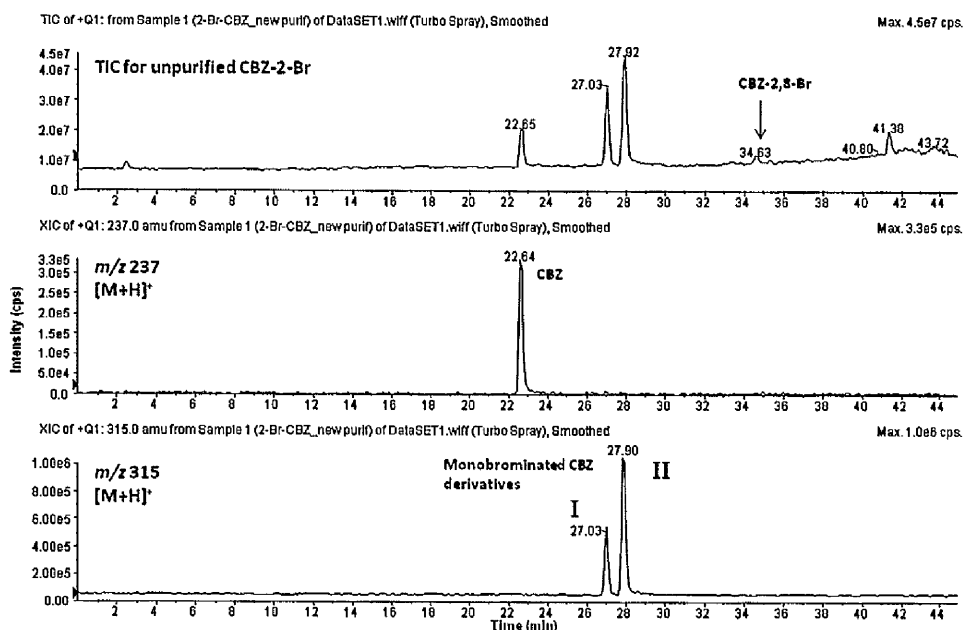
Figure 2.9: LC-MS trace of the product isolated after reaction of the mixture of 10a and 10b is taken through elimination, deprotection, and carbamylation steps to form the carbamazepine analogue **44**.

Figure 2.9 depicts the total ion current (TIC) of the LC-MS analysis of 2-bromo carbamazepine (compound **44**) with extracted ion currents (XIC) for m/z 237 and 315. The LC-MS analysis revealed further impurities in the form of un-halogenated carbamazepine with m/z 236 and some 2,8-dibromo carbamazepine (**45**). The two mono-brominated derivatives I and II at m/z 315 fragment differently in the mass spectra shown in **figure 2.10**. Both compounds show a parent ion at m/z 315 with the corresponding isotope pattern for a molecule containing a single bromine atom. Product II fragmented with a mass loss of 45 amu corresponding to the loss of the carboxamide moiety ($CONH_2$). Bromine was also lost from the molecule leaving iminostilbene with m/z 193. Product I fragmented similarly by loss of bromine to

77

give the iminostilbene ion at *m/z* 193. However, the loss of the carboxamide moiety was more pronounced, although ions were detected at *m/z* 272, which correspond to a mono-brominated iminostilbene.
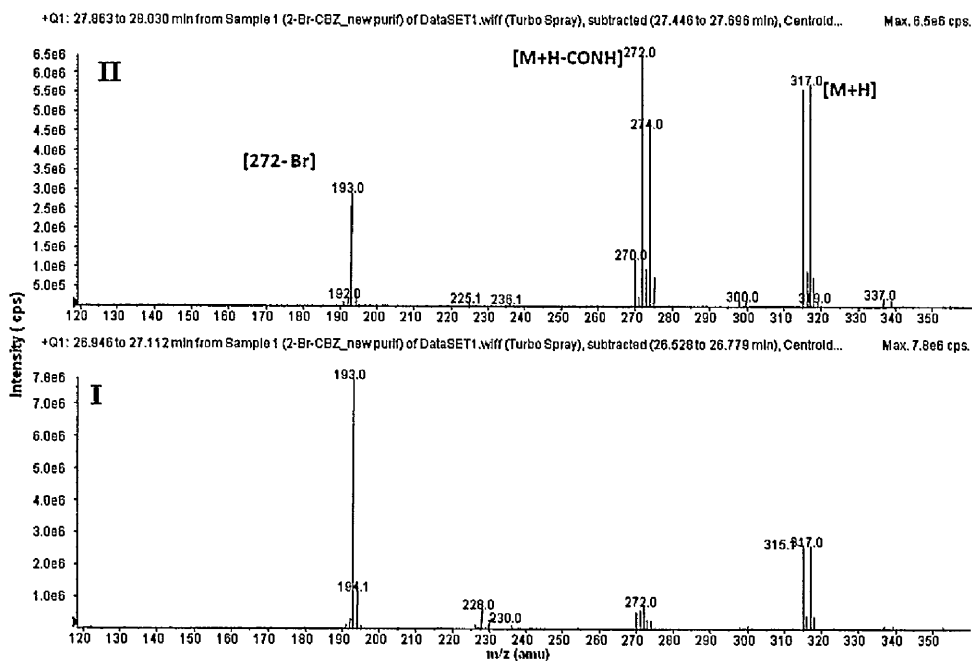
Figure 2.10: Mass spectrometry the isomers I and II identified in figure 2.9.

As seen in **table 2.7** increasing ABCN in the reaction was found to have the most pronounced effect for bromination at the etheno bridge, with increased amounts of the eliminated product forming. The reaction occurred in 24 hours with no trace of starting material detectable by ^{1}H NMR. Increasing the equivalents of NBS further still to 1.5 with a larger concentration of radical initiator was not detrimental to the reaction for either the mono or the di- substituted derivatives **7**, **8**, and **9** and progressed slightly faster with no trace of the starting material after 14 hours.

Elimination of HBr from **10-13a** could be driven to completion in the next step by treatment of the crude mixture with 50 % w/v KOH$_{(aq)}$. This reaction progressed

cleanly and resulted in near qualitative conversions of **10-13a** to **10-13b** in

agreement with previous work[49] as highlighted in **table 2.9**.

Table **2.9**: Elimination of bromine from the etheno bridge of N-acyl iminodibenzyls to form N-acyl iminostilbenes.[a]

10a X$_1$ = Br, X$_2$ = H	10b X$_1$ = Br, X$_2$ = H	10b X$_1$ = Br, X$_2$ = H
11a X$_1$ = X$_2$ = Br	11b X$_1$ = X$_2$ = Br	11b X$_1$ = X$_2$ = Br
12a X$_1$ = Cl, X$_2$ = H	12b X$_1$ = Cl, X$_2$ = H	12b X$_1$ = Cl, X$_2$ = H
13a X$_1$ = X$_2$ = Cl	13b X$_1$ = X$_2$ = Cl	13b X$_1$ = X$_2$ = Cl
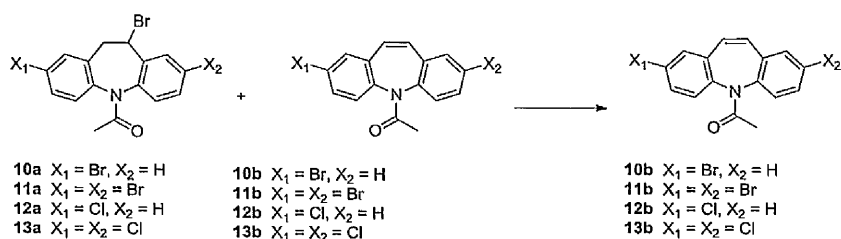
Crude mixture	Temperature (°C)	Yield (%)[b]
10a + 10b	0 then rt	99+
11a + 11b	0 then rt	99+ (a mixture)
12a + 12b	0 then rt	99+
13a +13b	0 then rt	99+

[a]Reaction conditions: 50% w/v KOH$_{(aq)}$, THF:EtOH (1:1), 0 °C (1 h) then 0 °C→r.t. 1 h.
[b]Calculated with respect to the relevant N-acyl iminodibenzyl (compounds 6-9).

Deprotection of the amine was achieved with strongly basic conditions using a 0.4 M

KOH$_{(EtOH)}$ solution and heating to 80 °C. The reaction also progressed extremely

cleanly in near quantitative conversion in each case as shown in **table 2.10**.

Table **2.10**: Deprotection of N-acyl iminostilbenes to iminostilbene.[a]

10b X$_1$ = Br, X$_2$ = H	14 X$_1$ = Br, X$_2$ = H
11b X$_1$ = X$_2$ = Br	15 X$_1$ = X$_2$ = Br
12b X$_1$ = Cl, X$_2$ = H	16 X$_1$ = Cl, X$_2$ = H
13b X$_1$ = X$_2$ = Cl	17 X$_1$ = X$_2$ = Cl
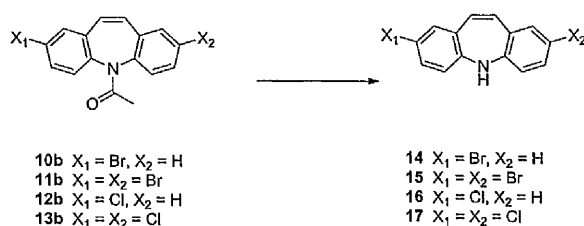
N-acyl iminostilbene	Time (h)	Yield (%)
10b	12	98
11b	12	96 % (although a mixture)
12b	16	95
13b	12	96

[a]Reaction conditions 0.4 mM KOH$_{(EtOH)}$, EtOH/THF (1:1), 80 °C, 12-16 h.

However, as elimination of bromine from **10-13a** and removal of the acyl group from **10-13b** both require KOH at differing concentrations, it was considered that a crude reaction mixture could be used to form the derived iminostilbene directly. Such a transformation would be one-step with the use of an appropriate concentration of KOH and solvent.

Iminostilbenes are generally inert to direct halogenation reactions and to date there has still been no report of effective direct halogenation of iminostilbene.[3, 56] Moreover, it was demonstrated earlier that the addition of the acyl group to the nitrogen reduces the capability of the aryl rings to undergo electrophilic substitution reactions.

One-pot elimination and deprotection was carried out at 80 °C in a 1:1 mixture of EtOH and THF and 50 % w/v $KOH_{(aq)}$. The reaction took 24 hours to progress to completion with the solution rapidly turning dark brown over 1 hour as HBr was evolved. The reaction required chromatography to remove some of the acidic by-products of the crude reaction mixture but the reaction was found to progress cleanly to near quantitative yields for all the iminostilbenes. Clearly then, this one-pot method has a significant advantage over the two-stage procedure as the number of steps in the overall reaction scheme is reduced.

2.6   Synthesis from Halogenated Building Blocks

2.6.1   Synthesis of N-aryl indoles

Ring expansion of a 9-hydroxymethyl acridine was shown to be effective for the synthesis of 2-fluoroiminostilbene.[49] However, the reaction relies upon the availability of a wide variety of fluorinated isatins, which are expensive. Synthesis of

the corresponding N-aryl isatin by the method outlined in **scheme 2.11** was difficult. Furthermore, the N-aryl product was found to have a similar polarity to the starting material making it difficult to isolate.

The difficulty in forming di-substituted precursors and the limitations set by the availability of fluorinated isatins prompted our investigation of N-aryl indoles as precursors for iminostilbenes. N-aryl indoles have significant advantages over isatins; they are more widely available, cheaper, and more literature exists on their preparation.

Because it was aimed to produce a wide variety of substituted N-aryl indoles, building on work already begun on the formation of fluorinated iminostilbenes.[49] A reaction that formed the desired product in high yields and purity was required. Furthermore, it was desirable for the reaction to be scalable to 5 g so that larger quantities of iminostilbene could be generated.

Initially, the palladium catalysed N-arylation of indoles[66, 67] was investigated with the general reaction scheme outlined in **figure 2.11**. Both Old[67] and Watanabe[66] have reported the synthesis of 1-4-(fluorophenyl-)1H-indole in high yields. The reaction uses very low catalyst loadings at 1 mol % and both proceed at reasonably low temperatures (85 °C), in good yields, within 24 hours.

Pd(OAc)$_2$ (1 mol %)
P^{t}Bu$_3$ (3 mol %)
o-xylene, 120 °C
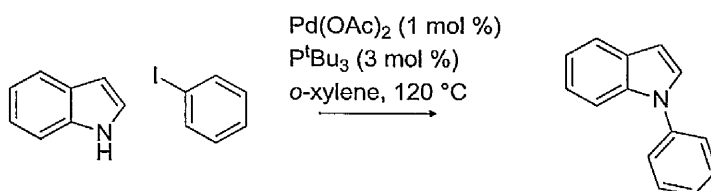
Figure 2.11: Palladium catalysed coupling of N-aryl indoles.[66]

81

The reaction was found to be reasonably general in the formation of fluorinated N-arylindoles, and progressed in good to excellent yields on 1 g scales as shown in **table 2.11**. Initially we discovered that running the reaction at 85 °C resulted in slightly lower yields than those reported in the literature,[66, 67] but increasing the reaction temperature by 25 °C allowed us to obtain N-aryl indoles in reasonable yields.

Table 2.11: Palladium catalysed coupling of N-aryl indoles under a variety of reaction conditions.

Pd(OAc)$_2$ (1 mol %)
P^{t}Bu$_3$ (3 mol %)
o-xylene, 120 °C
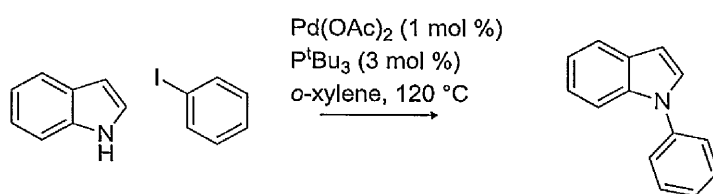
Indole	Aryl halide	Temperature (°C)	Reaction scale (g)	Yield (%)
		110	1	94
		110	1	96
		85	1	53
		110	1	88
		110	1	73
		110^a	5	22
		110^a	5	12

^{a} reaction left a further 24 h with incomplete conversion still observed by TLC.

However, as shown in **table 2.11**, scale-up of the reaction was not as successful. Isolated yields and purity of the product were poor on a 5 g scale. This is largely the result of the difficulty in handling the highly pyrophoric ligand tri-*tert*-butyl phosphine (Pt-Bu$_3$) on this relatively large scale. Exchanging the ligand for the air

stable tri-*tert*-butylphosphonium tetrafluoroborate salt did not aid the reaction, and we consider the possibility that achieving the stringently anhydrous conditions required for the reaction to occur, including the solvent, was difficult on that scale.

Another common method for the formation of *N*-aryl indoles is the use of copper (I) salts. Building on work performed by Bowkett[49] we investigated the method of Chandrasekhar *et al*[68] as outlined in **figure 2.12** as a broad synthetic route to *N*-aryl indoles in a recyclable PEG-400 solvent system.

CuI (5 mol %)
ethylene diamine (20 mol %)
K$_2$CO$_3$, PEG400, 80 °C
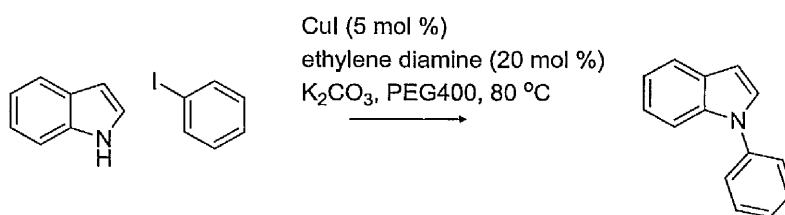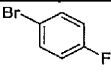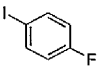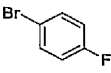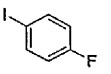
Figure 2.12: Copper catalysed coupling of *N*-aryl indoles in a recyclable PEG-400 solvent system.

The reported reaction,[68] although requiring greater quantities of catalyst (10 mol %), has advantages over the palladium methods[66, 67] as the reaction should be less susceptible to traces of water and air. However, in order to get the reaction to progress in similar yields to those reported in the paper we found that both increased reaction temperatures and catalyst loadings were required to obtain good yields, **table 2.12**.

Table 2.12: Copper catalysed coupling of *N*-aryl indoles in a recyclable solvent system under a variety of conditions.
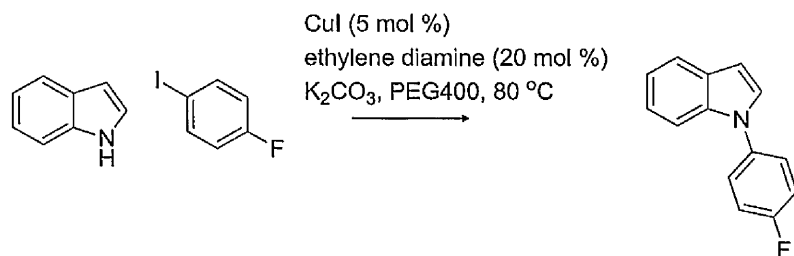
Indole	Aryl halide	Temperature (°C)	Catalyst loading (mol %)	Time (days)	Yield (%)
		80	10	3	NPI
		80	10	3	NPI
		160	10	3	45
		160	20	3	59

Difficulties in isolating the *N*-aryl indole from the reaction medium in significant quantities were encountered. This was because Et_2O and the PEG 400 were found to be fairly miscible even when cooled Et_2O was used. Exchanging the extracting solvent to dichloromethane allowed separation of the phases, but multiple back-washes of the organic phase were required to remove all traces of PEG 400 and copper catalyst.

As we considered the difficulty in isolating the product from the reaction mixture to be the main cause for the low yields other copper catalysed reactions were considered.
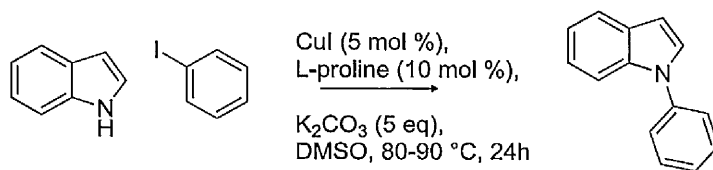
Figure 2.13: CuI-catalysed coupling reaction between indole and iodobenzene. Reaction conditions: Aryl iodide (2.0 mmol), indole (2.4 mmol), K_2CO_3 (5.0 mmol), CuI (0.2 mmol), L-proline (0.4 mmol), 4 mL DMSO.

Figure 2.13 describes the reaction conditions of Ma *et al.*[69] This reaction appeared to be the most general of all the reactions considered forming a wide variety of differently substituted *N*-aryl indoles as shown in **table 2.13**. The reaction uses a relatively low catalyst loading (10 mol %) compared to the other methods and was high yielding on 1 g test scales with the fluorinated derivatives. It was gratifying to discover that the reaction could further be scaled up to 5 g (with respect to indole) and yields remained in the same range as the 1 g scale. Furthermore, the reaction was observed by TLC to progress to completion at the reported temperature ranges of 80-100 °C.

The reactions to form the methoxy- (**26, 27,** and **28**) and hydroxyl- derivatives (**29**) were the most difficult of all the derivatives. This is because emulsions were formed when partitioning the reaction mixture between water and EtOAc. Addition of NH_4Cl to the aqueous phase assisted the separation of the two phases for the methoxy derivatives **26, 27,** and **28**. However, separation of the hydroxyl-derivative **29** only yielded starting materials, the presence of the free phenol possibly contributing to the difficulty in forming and isolating the product.
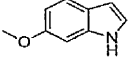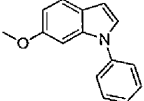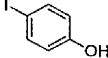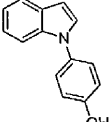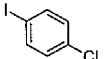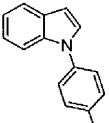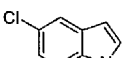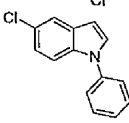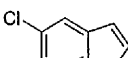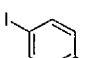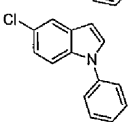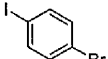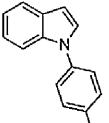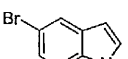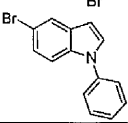
Table 2.13: Copper catalysed synthesis of *N*-aryl indoles with L-proline as an additive.
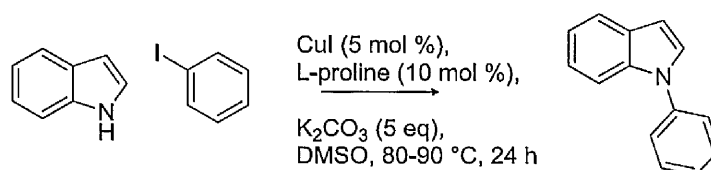
Indole	Aryl iodide	Temp (°C) / Time (h)	Product	Product number	Yield (%)
		90/24		18	97
		100/24		19	81
		100/28		20	78
		100/24		21	70
		100/24		22	76
		100/24		23	83
		100/24		24	75
		100/24		25	85
		90/36		26	68
		90/36		27	71

		90/36		**28**	62
		80/48		**29**	NPI
		80/24		**30**	87
		80/24		**31**	92
		80/24		**32**	85
		90/36		**33**	79
		90/36		**34**	83

All the fluorinated derivatives **19-25** were isolated in excellent yields, and were purified easily from the crude materials by column chromatography.

The reaction was further found to be applicable to the formation of chlorinated *N*-aryl indoles. Furthermore, the reaction was selective for the formation of *N*-aryl indole **34** in excellent yields with virtually no trace of polymeric products formed. Formation of indole **33** was also excellent, and although small traces of what could have been a polymeric product were observed by TLC, none were isolated and the product was obtained in high purity.

2.6.2 Polyphosphoric acid cyclisation

As alluded to in chapter 1, polyphosphoric acid cyclisation of N-aryl indoles with strongly electron-withdrawing substituents (such as NO_2, CF_3, Cl) was reported to give low or zero yields of iminostilbenes.[51] However, cyclisation using polyphosphoric acid was found by Bowkett to be satisfactory for 2-fluoro iminostilbene and 2,8-difluroiminostilbene,[49] although fairly low-yielding as shown in **table 2.14**. That the reaction occurs with fluorine is likely due in part to the unique properties of fluorine, viz. back donation of its lone pairs and stabilization of the cationic intermediates; a process that is less efficient for other groups (e.g. chlorine). Interestingly, it was discovered that the poor yields were, in part, due to the formation of 9-methylacridine;[49] a side-product that was not observed in the work of Tokmakov.[51]

Table 2.14: Cyclisation of N-aryl indoles to iminostilbenes.
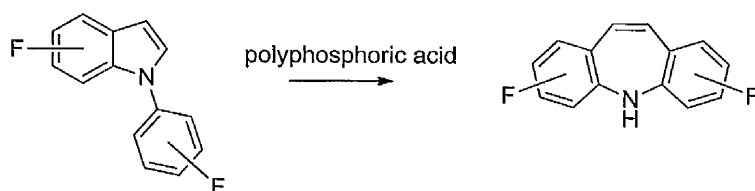
| N-aryl indole	Temperature (°C)	Time (h)	Product	Product	Yield (%)
19	150	36		36	38
24	150	36		41	15

It was observed early on in the study of this reaction that the presence of air or water is detrimental, as it has been shown that oxygen can aid the conversion of iminostilbenes to 9-methylacridines.[3] Anhydrous polyphosphoric acid (PPA) is not

commercially available: we were careful to ensure the PPA was thoroughly degassed by bubbling nitrogen or argon through gently heated PPA in a two-neck flask.

Furthermore, the yields of the 2,8-difluoroiminostilbene were low due to the formation of 9-methyl acridine during the reaction. Iminostilbenes are known to undergo cyclisation to methyl acridines in the presence of a variety of acids.[3] Indeed, when purified 2-fluoroiminostilbene **36** or 2,8-difluoroiminostilbene **41** are added to hot polyphosphoric acid cyclisation to 9-methyl acridine occurs in reasonable yield. However, as cyclisation of *N*-aryl indoles is known not to occur in other acids[51] optimization was instead focused upon time and temperature as outlined in **table 2.15**.

Table 2.15: Effect of temperature on the cyclisation of 24 to 41 and 41(i) in PPA.
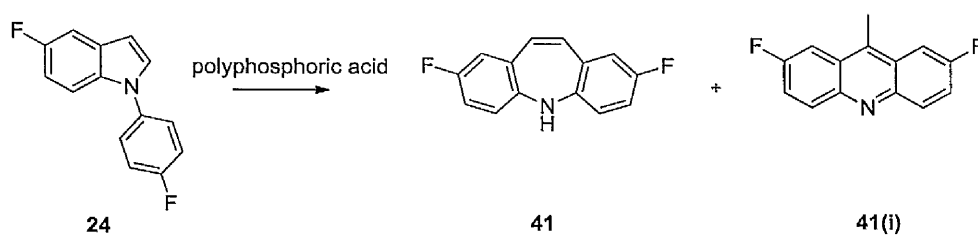
Temperature (°C)	Time (h)	Isolated yield (%)	
		41	**41(i)**
150	72	15	43
130	72	22	30
100	72	66	5
90	> 96	32	0

Reducing the reaction temperature to 100 °C did increase the quantity of iminostilbene and decrease 9-methylacridine. However, the reaction is highly capricious and over several runs the yield of **41** isolated at this temperature is more consistently in the range of 35-55 %.

The reaction still occurs at lower temperatures as can clearly be seen in **table 2.15**. More variable yields are obtained at this temperature, but the reaction occurs with little development of acridine byproducts. This may partially explain the difference in observed products between Bowkett's reactions, performed at 150 °C,[49] and Tokmakov's reactions, performed at 80 °C.[51]

Unsurprisingly, if the reaction at 100 °C is left for longer periods of time more 9-methylacridine is isolable from the reaction mixture as the formed iminostilbene is subject to further reaction with polyphosphoric acid.
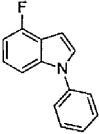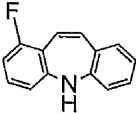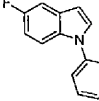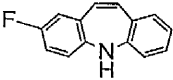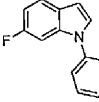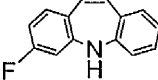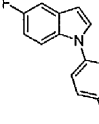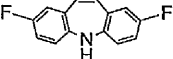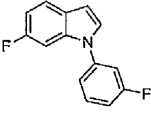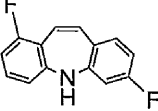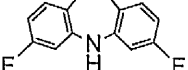
These reaction conditions were found to be reasonably general: a series of six mono- and di-fluorinated iminostilbenes were examined and are summarized in **table 2.16**.

Table 2.16: The cyclisation of various fluorinated *N*-aryl indoles in PPA.
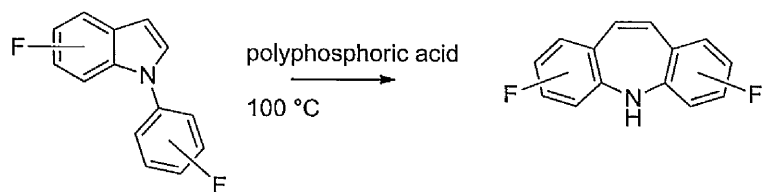
N-aryl indole	Number	Iminostilbene	Product number	Yield (%)
	18		35	67
	19		36	40
	20		37	18
			38	22

90

Structure	No.	Structure	No.	Yield
	21		37	24
	22		36	47
	23		38	48
	24		39	66
	25		40	16
			41	35

As discussed earlier, the cyclisation of 1-(*m*-tolyl)-1*H*-indole only yielded a single isomer.[51] We hoped to exploit this to selectively form the 3,7-difluorinated iminostilbene **41**. Contrary to the literature precedent however, cyclisation of **20** and **25** yielded two distinct regioisomers as shown in **figure 2.14**.
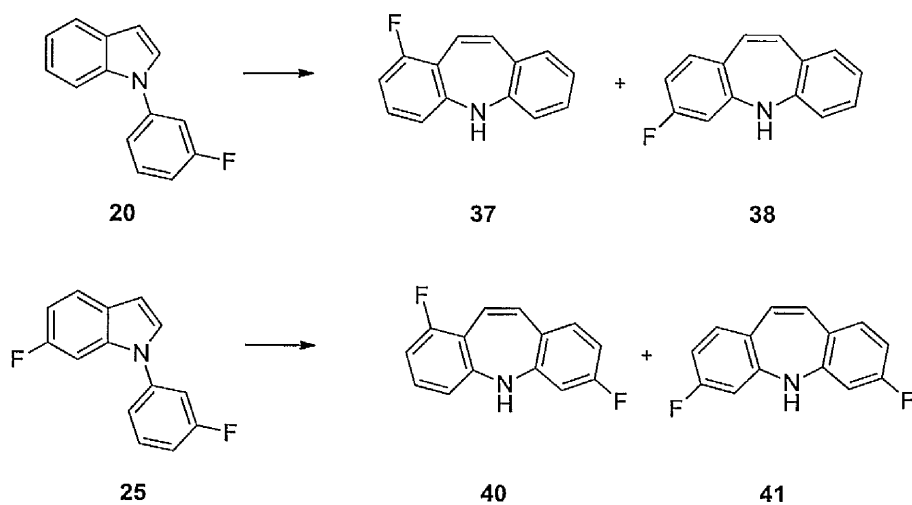
Figure 2.14: Cyclisation of 20 forms two regioisomers.

A subtle combination of steric and electronic effects was found to play some role in the cyclisation as the 3-F isomers **38** and **41** were repeatedly isolated in slightly greater yields than the 1-fluoroiminostilbene in each instance. Pleasingly, the two isomers could be separated by column chromatography by using a silica-to-product ratio of 100:1.

The ^{13}C NMR of 1,7-difluoro iminostilbene aptly demonstrates the non-planar nature of the iminostilbenes as it contains an extra ^{19}F-^{13}C coupling indicated in **figure 2.15**. It is postulated that this is caused by some through-space coupling of the fluorine to C10 as the molecule has taken on more of a bowl shape as indicated in **figure 2.15**.
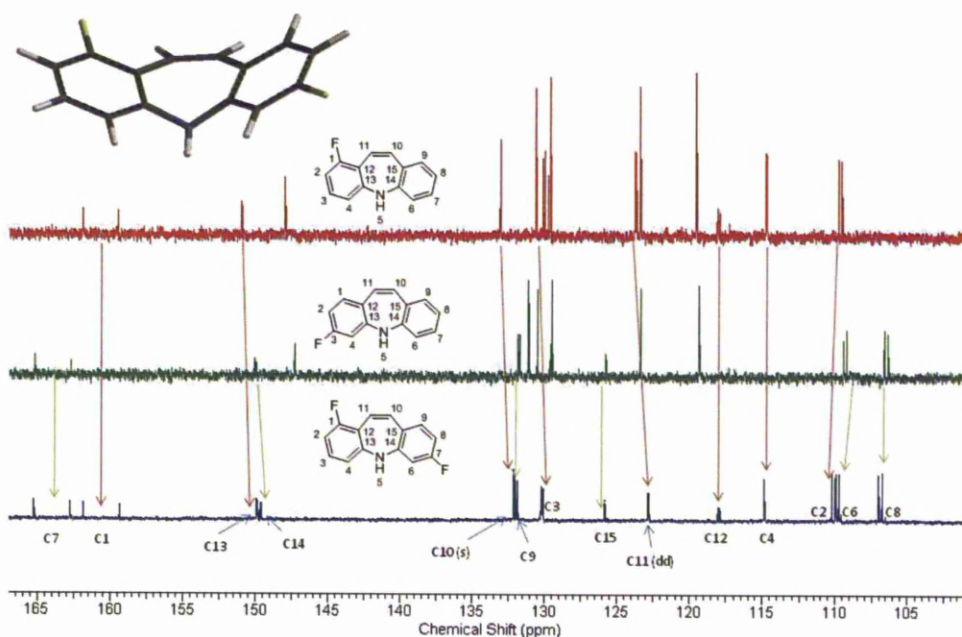
Figure 2.15: Comparison ^{13}C NMR comparing the monosubstituted iminostilbenes **37** and **38** to **40**. Conserved peaks between the spectra are indicated by the arrows in the respective colour of the spectra. The carbon assignments only correspond to **40** to simplify the spectra. Top left of the figure depicts an ab initio molecular modelling structure for **40**, calculated as a single-point energy, Hartree-Fock_3-21G level, (MMFF, AM1) which illustrates the bending in the molecule. The molecule was modeled using Spartan '08, v1.1.1 build 132.

The synthesis of the two methoxy iminostilbene isomers **42** and **43** in **table 2.17** was investigated as they may prove to be useful precursors to hydroxylated derivatives of carbamazepine. Since other methods are multi-step and low yielding.[70]

Reaction of **26** and **27** to yield **42** progressed in good yield. We observed the reaction to be slightly better when the methoxy group was situated on the indole ring. Time precluded further study of these compounds for their potential as precursors to hydroxylated carbamazepine derivatives.

Table 2.17: Reaction of other *N*-aryl indoles to substituted iminostilbenes.
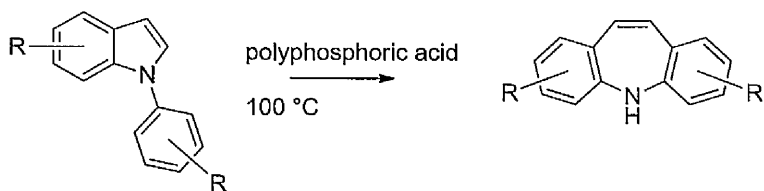
N-aryl indole	Number	Iminostilbene	Number	Yield (%)
	26		42	25
	27		42	37
	28		43	22
	30		16	41 (+5 % 35)
	31		16	60
	32		17	32 (+ 15% 16)
	33		14	NPI*
	34		14	5*

*reaction temperature reduced to 65 °C.

As the synthesis of chlorinated iminostilbenes was difficult by direct electrophilic addition of chlorine to iminodibenzyl, the possibility of extending the reaction to chlorinated derivatives was further examined and are summarised in **table 2.17**. Synthesis of 2-chloro iminostilbene had already been demonstrated by Tokmakov, [51] and cyclisation of the same intermediate progressed in similar yields. However, reaction of the dichlorinated intermediate **32** revealed the occurrence of dehalogenation during the reaction: both **16** and **17** were clearly seen in the ^{1}H NMR, **figure 2.16**.
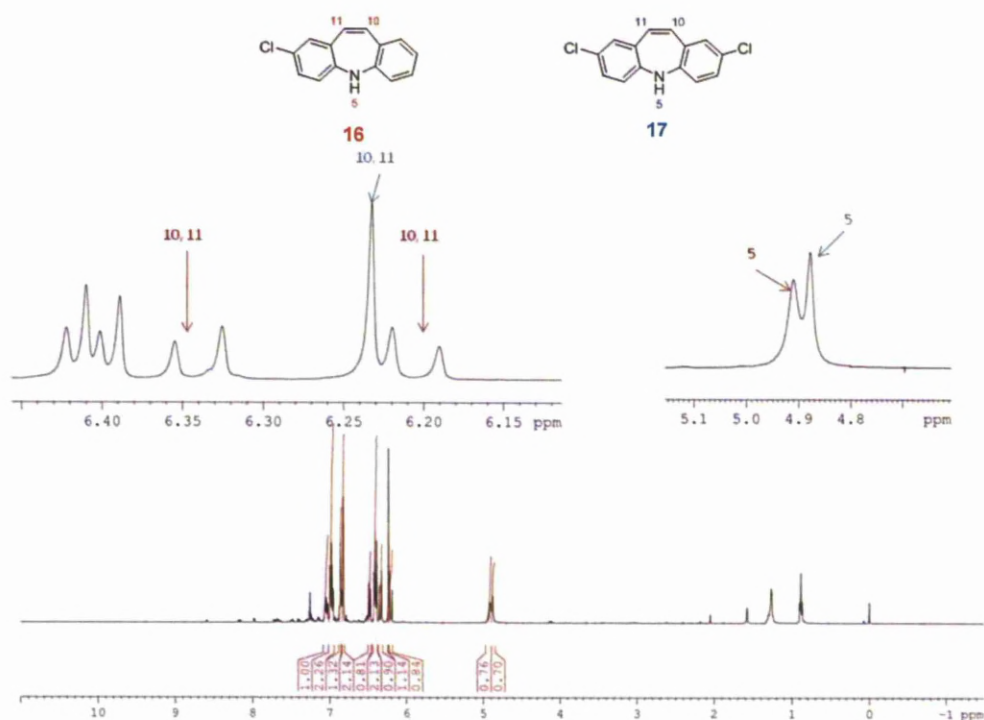
Figure 2.16: Crude ^{1}H NMR of the product isolated from the cyclisation of **32** to **17**.

Comparison of the cyclisation of **30** and **31** revealed that the chlorine substituted on the indole ring was less prone to dehalogenation than on the aryl ring as it was

repeatedly isolated in higher yields and with trace to zero quantities of **35** isolable from the reaction mixture.

Given the difficulty in isolating **14** pure, and without the presence of other isomers, by direct electrophilic substitution (inferred from **figures 2.9 and 2.10**); the reaction conditions were further examined for the brominated *N*-aryl indoles **33** and **34**. Disappointingly, the formation of **14** was not observed in either case when the reaction was performed at 100 °C. However, reduction of the reaction temperature to 65 °C was found to be successful for **34**. Reaction for **33** still failed to yield any quantity of **14** after several attempts, which may be the result of a more labile C-Br bond on the aryl ring.

2.7   Incorporation of the carboxamide moiety

2.7.1   Phosgenation

Industrially the production of carbamazepine is centred around the use of phosgene,[71-74] or a phosgene *source* such as trichloromethylcarbonate (diphosgene)[38] or bis(trichloromethyl)carbonate (triphosgene).[75-81]

The liquid and crystalline phosgene equivalents, diphosgene and triphosgene respectively, have been extensively used as phosgene sources for chemical transformations.[82] They offer an important advantage over gaseous phosgene as they are easier to both store and handle. Triphosgene on the laboratory scale provides the greatest degree of handling convenience, and in particular offers the greater safety advantage. It is much easier to handle and store and exact, stoichiometric quantities can be measured to perform a chemical transformation.[82] As triphosgene can also

liberate three molecules of phosgene, as shown in **figure 2.17**, reactions also typically require a third of an equivalent of triphosgene.[82]
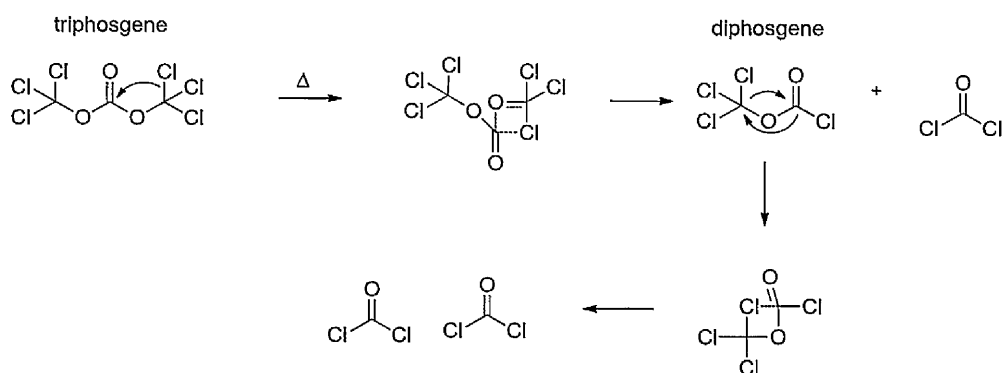
Figure 2.17: Decomposition of triphosgene at high temperatures to form 3 equivalents of phosgene.[82]

Several one-pot procedures for the transformation of iminostilbene, through a phosgene equivalent, exist in patent literature.[75-81] Before attempting to perform similar reactions on the halogenated iminostilbenes the reaction conditions were first optimised for unsubstituted iminostilbene. The results are summarised in **table 2.18**.

All reactions were carried out by adaptation of the procedure of Milanese.[78] The reaction was easily monitored by TLC and when consumption of iminostilbene was complete, as indicated in **table 2.18**, a solution of 30 % (aq) ammonia solution was added and the reaction left overnight.

Table 2.18: Study of the formation of carbamazepine with phosgene under a variety of conditions.

Phosgene source	Stoichiometric equivalents	Solvent	Temperature °C	Time before addition of 30 % NH₃ (Aq)	Yield of carbamazpine
Triphosgene	0.3	THF	10-15	6 h	27 %
Triphosgene	0.3	Toluene	10-15	6 h	92 %
Triphosgene*	0.3	Toluene	10-15 → reflux	6 h	NPI
Diphosgene	0.5	Toluene	10-15	8 h	79%

* no triethylamine added.

Performing the reaction in THF was low yielding for formation of carbamazepine. Monitoring of the reaction by TLC did show the formation of the carbonyl chloride, however on addition of the ammonia solution carbamazepine failed to precipitate out due to its greater solubility in THF. Furthermore, the water added to the reaction mixture enhanced the chances for hydrolysis of the carbonyl chloride to the starting amine. This hypothesis is supported by the quantity of iminostilbene isolated after the reaction.

As observed for other reactions the final product was insoluble in toluene and precipitated out of the reaction, the carbonyl chloride remained in solution. The clear advantage of removing carbamazepine from the reaction is that it was no longer susceptible to competing hydrolysis reactions. Furthermore, the compound was easier to isolate in high purity by vacuum filtration.

The reaction conditions were also usefully extended for the reaction with diphosgene in good yields. The reaction took slightly longer to consume iminostilbene, as monitored by TLC, possibly due to enhanced difficulty liberating phosgene from the molecule.

Triethylamine (0.3 equivalents) was essential for the reactions, acting as a nucleophile to liberate the phosgene. Without triethylamine the reactions failed at the lower temperatures. However, thermal decomposition of both diphosgene and triphosgene is known as discussed earlier in **figure 2.17** and vigorously refluxing the reaction mixture with triphosgene did indicate some reaction with the iminostilbene, but no product was isolated after the addition of aqueous ammonia solution.

As the procedure with triphosgene yielded the best result, and required little optimisation the reaction was then examined with the halogenated iminostilbene derivatives as summarised in **table 2.19**.

Table 2.19: Formation of halogenated carbamazepines with a phosgene source.

14 X_1 = Br X_2 = H
15 X_1 = X_2 = Br
16 X_1 = Cl X_2 = H
17 X_1 = X_2 = Cl
35 X_1 = F X_2 = H
39 X_1 = X_2 = F

44 X_1 = Br X_2 = H
45 X_1 = X_2 = Br
46 X_1 = Cl X_2 = H
47 X_1 = X_2 = Cl
48 X_1 = F X_2 = H
49 X_1 = X_2 = F
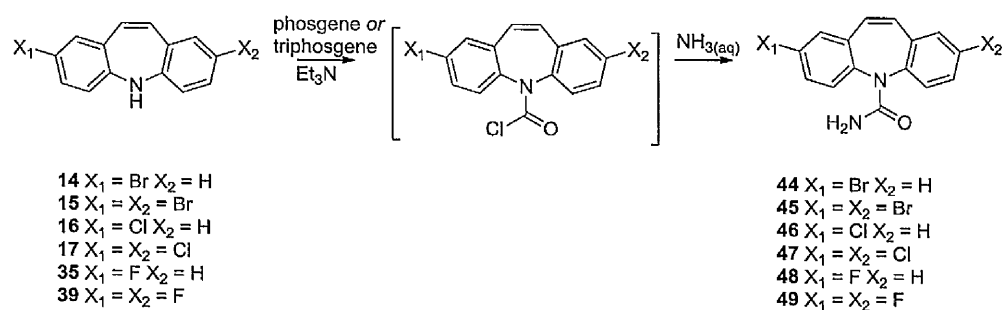
Iminostilbene	14	15	16	17	35	39
Solvent	Toluene	Toluene	Toluene	Toluene	Toluene	Toluene
Temperature (°C)	60	10-15	60	60	110	110
Time before NH$_3$ addition (h)	12	6	12	12	24	24
Yield of carbamazepine	9 %	24 %	8 %	12 %	NPI	NPI

In the reaction of bromo and chloro derivatives **14, 15, 16,** and **17,** the depletion of the iminostilbene and formation of a polar compound was clearly observed TLC. Formation of the carbonyl chloride was also indicated by the change of colour of the reaction mixture from a strong yellow colour to colourless. The reaction to the intermediate carbonyl chloride was also observed to progress within a similar timescale to unsubstituted iminostilbene (**table 2.18**). However, with the exception of the formation of **45** which was low yielding at 24 %, other brominated and chlorinated derivatives were only isolated in trace quantities. Moreover, the fluorinated derivatives **48** and **49** yielded no isolated products although some formation of the carbonyl chloride intermediate was observed by TLC. However, only the starting iminostilbenes **35** and **39** were isolated from the reaction mixture and no precipitation of the corresponding carbamazepine observed.

This could be attributed to a significant change in solubility of the halogenated carbamazepine derivatives. 2,8-Dibromocarbamazepine is the least soluble of all the derivatives and precipitates out of solution rapidly. All the other derivatives were found to be more soluble than carbamazepine. This enhances the possibility of water hydrolysing the intermediate carbonyl chloride to the starting amine on the addition of aqueous ammonia.

2.7.2 Isocyanates

Previously, 2,8-dibromocarbamazepine had been synthesised by reaction with chlorosulfonyl isocyanate and subsequent hydrolysis of the intermediate to yield the product as shown in **figure 2.18**.[49]
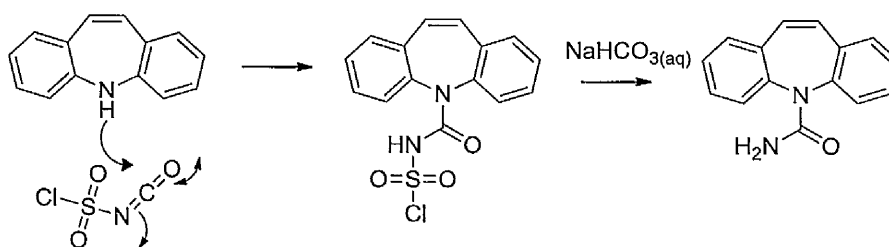
Figure 2.18: Formation of carbamazepine via chlorsulfonyl isocyanate.

The reaction with chlorosulfonyl isocyanate progressed reasonably well but the products of the reaction after hydrolysis with sodium hydrogen carbonate ($NaHCO_3$) were low yielding and difficult to separate,[49] although the reaction appeared to progress in higher yields than for the phosgene series of reactions with 50 % conversion observed by LC-MS.[49]

As the conversion of the iminostilbene with chlorosulfonyl isocyanates was poor,[49] more active isocyanates were sought to effect the transformation.

Excellent results were obtained with trichloroacetyl isocyanate for dibrominated and chlorinated derivatives **15** and **17** as shown in **table 2.20** below. The reaction was observed to be almost instantaneous with the colour of the reaction solvent going from yellow to colourless over a period of seconds after the addition of the isocyanate. Precipitation of the intermediates **15a** and **17a** was observed after 30 minutes and these were easily isolated by vacuum filtration.

Table 2.20: Formation of halogenated carbamazepines via trichloroacetyl isocylanate intermediates.[a]

14 X_1 = Br X_2 = H
15 X_1 = X_2 = Br
16 X_1 = Cl X_2 = H
17 X_1 = X_2 = Cl
36 X_1 = F X_2 = H
39 X_1 = X_2 = F

14a X_1 = Br X_2 = H
15a X_1 = X_2 = Br
16a X_1 = Cl X_2 = H
17a X_1 = X_2 = Cl
36a X_1 = F X_2 = H
39a X_1 = X_2 = F
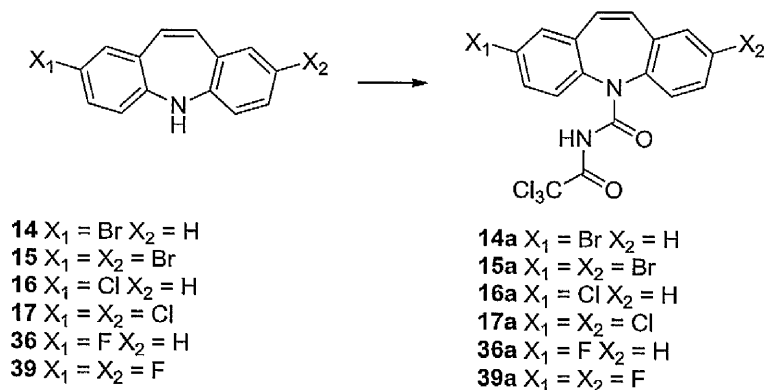
Iminostilbene	Time (h)	Yield
35	6	89
14	24	NPI
15	8	78
16	24	Trace
17	24	75
36	24	NPI
39	24	NPI

[a]reaction conditions: Trichloroacetyl isocyanate 1.2 eq, toluene, rt-0 °C.

Disappointingly, application of the same reaction conditions to the fluorinated analogues **35** and **39** failed to yield the desired product. As observed in the methods previously discussed, the fluorinated derivatives were found to be more soluble in the reaction making their isolation difficult: only starting materials were isolated from the reaction of **35** and **39** with trichloracetyl isocyanate.

The reaction progressed in reasonable yields for **15** and **17**; however the monobrominated derivatives **14** and **16** were very low yielding. Given that this reaction is also dependent on the crystallisation of the intermediate out of the reaction mixture it can be postulated that the asymmetry of **14** and **16** frustrate their crystallisation, allowing them to remain in the reaction solvent for longer and making them more prone to hydrolysis with trace water in the reaction solvent. This could be observed as the reaction mixture turned from bright yellow to colourless almost

immediately as observed earlier. However, instead of precipitation of the intermediates **14a** and **16a** the reaction slowly returned to yellow. The back reaction of the intermediates in the reaction solvent is further supported by the isolation of almost all **14** and **16** used in the reaction.

Once isolated, the question became one of selectively removing the trichloroacetyl group without removing the masked urea moiety entirely. Based on literature precedent[83] the possibility of acid hydrolysis was considered.

However, as listed in **table 2.21**, the reaction was highly unselective for carbamazepine itself and predominately formed the amine. The difference in the chemical reactivity of the two groups is slight and the success or failure of the deprotection is dependent on the relative ease of attack at one or the other carbonyl groups.

Industrially this is done by many methods, although the most common is the use of aqueous sodium carbonate. Mild base hydrolysis was also considered as a possible method for removing the trichloroacetyl protecting group. 0.1 M NaOH was as unselective as acid hydrolysis. However, the use of solid – liquid reaction systems such as sodium or potassium carbonate was more successful with up to 50 % yields of carbamazepine isolated from the model system.

Table 2.21: Deprotection of the trichloroacetyl intermediate to form substituted carbamazepine analogues under various reaction conditions.
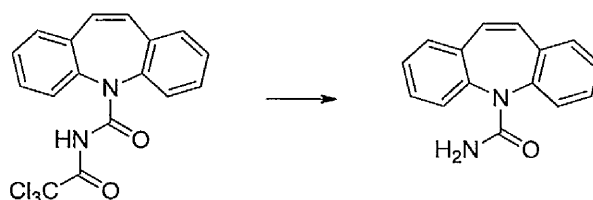
Reagent	percentage of carbamazepine (CBZ) and iminostilbene (ISB) isolated	
	CBZ	ISB
0.1 M HCl	10	90
0.1 M NaOH	12	88
5 % aq Na_2CO_3	57	33
5 % aq KCO_3	34	56

Unfortunately, again when applied to the halogenated carbamazepine derivatives **15a** and **17a** the reaction was not quite as selective, although up to 40-55 % yields of **45** and **47** were isolated from the reaction mixture.

Industrially the use of sodium[84, 85] or potassium[86, 87] isocyanate (NaOCN and KOCN respectively) in acetic acid is used to form carbamazepine derivatives directly from the corresponding iminostilbene. This reaction has the advantage over all other methods of incorporating the urea that carbamazepine is formed in a single step rather than via an intermediate.

Moreover, sodium and potassium isocyanate are easy to handle and store and are less toxic than other reagents. Optimisation of the model reaction between the isocyanate salt and **35** in acetic acid is summarised in **table 2.22**.

Table 2.22: Model reaction between 35 to form carbamazepine with sodium or potassium isocyanate.
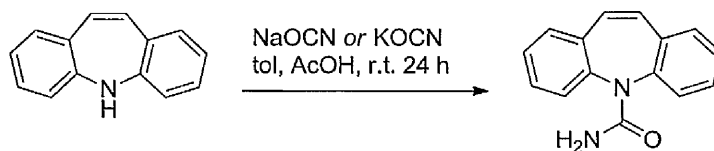
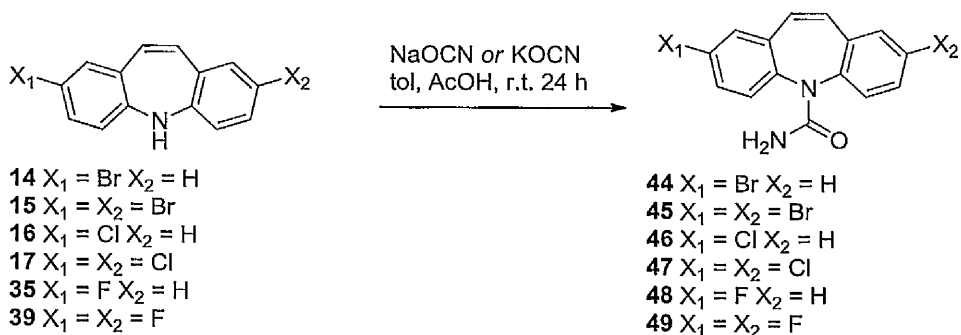| Reagent/equivalents	Temperature (°C)	Time (h)	Yield (%)
NaOCN/1.2	r.t.	6	89
KOCN/1.2	r.t	6	83

The reaction progressed smoothly and in excellent yield and purity for NaOCN. As was the case for trichloroacetyl isocyanate the reaction was almost instantaneous, with precipitation occurring within the first half hour of the reaction. Although KOCN progressed in similar yields, the reaction was not as clean and the formation of several non-polar by-products was observed by TLC.

However, while the reaction progressed in good yields for the model reaction, we were disappointed to observe uniform failure of the reaction with the halogenated derivatives.

Encouragingly, transformation of diphenylamine with sodium isocyanate in the presence of trifluoroacetic acid has been demonstrated for highly deactivated amines.[88] The pK_a of trifluoroacetic acid is 0.3, which makes it nearly 100,000 fold more acidic then acetic acid with a pK_a of 4.8. Given that the reaction appeared to work with some deactivated diphenylamines[88] the possibility of a link between pK_a and the reactivity of the amine suggested this should be a reagent of choice for halo-iminostilbenes.

Table 2.23: Reaction of halogenated iminostilbene analogues with sodium isocyanate in trifluoroacetic acid.[a]

NaOCN *or* KOCN
tol, AcOH, r.t. 24 h

14 X_1 = Br X_2 = H
15 X_1 = X_2 = Br
16 X_1 = Cl X_2 = H
17 X_1 = X_2 = Cl
35 X_1 = F X_2 = H
39 X_1 = X_2 = F

44 X_1 = Br X_2 = H
45 X_1 = X_2 = Br
46 X_1 = Cl X_2 = H
47 X_1 = X_2 = Cl
48 X_1 = F X_2 = H
49 X_1 = X_2 = F

Iminostilbene	Temperature (°C)	Time (h)	Yield (%)
14	r.t	6	89 (50% pure)
15	r.t	6	87
16	r.t.	6	79
17	r.t.	6	91
35	r.t	12	77
39	r.t	12	75

[a]reaction conditions: 1.2 eq NaOCN, toluene, Trifluoroacetic acid (2 eq), r.t.

Table 2.23 shows that the reaction with TFA was general for all the halogenated iminostilbenes. In comparison to all the other methods examined the reaction was high yielding, and the reaction was observed to be almost instantaneous for **14-17**, with precipitation occurring after 30 minutes to form carbamazepines **44-47**. Reaction with **35** and **39** was also observed to be instantaneous, but onset of precipitation of **48** and **49** was a little slower occurring after 1-2 hours. As long as a minimal amount of toluene was present in the reaction mixture the carbamazepine analogues precipitated out of the reaction and were easily isolated by vacuum filtration.

Once isolated each analogue was purified by reverse-phase preparative HPLC (except for **44** as discussed in section 2.1.6) to remove any traces of unsubstituted or monosubstituted derivatives that may not have been detected and removed earlier on

106

in the reaction sequences. As high compound purity is required before the compounds can be incubated with hepatocytes as described in chapter 3.

Once the compounds were found to have greater than 99 % purity as determined by LC-MS and LC-UV analysis they were sent to the department of Pharmacology at the University of Liverpool to examine their structure-activity relationships in freshly isolated rat hepatocytes.

2.8 Conclusions

Robust synthetic methods for the synthesis of halogenated carbamazepine analogues **44-49** were devised.

Direct electrophilic halogenations of iminodibenzyls to form brominated and chlorinated derivatives were reasonably selective, although the formation of the mono-brominated derivative still requires optimization to reduce the formation of isomeric material. This method is particularly good for the production of the di substituted derivatives **15** and **17** as they do not require separation from mono- and unsubstituted materials as is the case for the cyclisation of *N*-aryl indoles.

Polyphosphoric acid cyclisation of *N*-aryl indoles yielded a wide variety of iminostilbenes. The reaction is reasonably general and is tolerant of fluorine, chlorine, and methoxy groups. No reaction was observed to occur for hydroxylated *N*-aryl indoles and the isolated yields for brominated derivatives was poor. Although chlorinated and brominated derivatives were observed to undergo some de-halogenation during the reaction the iminostilbenes were formed in a reasonably efficient one-step process.

A general and efficient method for incorporating the carboxamide moiety has also been developed using alkali metal isocyanates and trifluoroacetic acid. The reaction was found to be general and high yielding in comparison to other methods.

2.9 References

1. Thiele, J.; Holzinger, O., Ueber o - Diamidodibenzyl. *Justus Liebigs Annalen der Chimie* **1899**, 305, 96-102.

2. Schindler, W.; Häfliger, F., Über Derivate des Iminodibenzyls. *Helvetica Chimica Acta* **1954**, 37, (2), 472-483.

3. Kricka, L. J.; Ledwith, A., Dibenz*[b,f]*azepines and related ring systems. *Chemical Reviews* **1974**, 74, (1), 101-123.

4. Varma, R. S.; Whisenant, L. K.; Boykin, D. W., Synthesis of some substituted 5H-dibenz*[b,f]*azepines as potential antimalarials. *Journal of Medicinal Chemistry* **1969**, 12, (5), 913-914.

5. Kumar, H. V.; Gnanendra, C. R.; Naik, N.; Gowda, D. C., In vitro antioxidant activity of dibenz*[b,f]*azepine and its analogues. *E-Journal of Chemistry* **2008**, 5, (SUPPL. 2), 1123-1132.

6. Kumar, H. V.; Kumar, C. K.; Naik, N., Synthesis of novel 3-chloro-1-(5H-dibenz*[b,f]*azepine-5yl) propan-1-one derivatives with antioxidant activity. *Medicinal Chemistry Research* **2011**, 20, (1), 101-108.

7. Vijay Kumar, H.; Gnanendra, C. R.; Naik, N., Synthesis of amino acid analogues of 5H-dibenz*[b,f]*azepine and evaluation of their radical scavenging activity. *E-Journal of Chemistry* **2009**, 6, (1), 125-132.

8. Vijay Kumar, H.; Naik, N., Synthesis and antioxidant properties of some novel 5H-dibenz*[b,f]*azepine derivatives in different in vitro model systems. *European Journal of Medicinal Chemistry* **2010**, 45, (1), 2-10.

9. Meigh, J. P. K., Product subclass 6: benzazepines and their group 15 analogues. *Sci. Synth.* **2004**, 17, 825-927.

10. Dubois, J. P.; Kung, W.; Theobald, W.; Wirz, B., Measurement of clomipramine, N desmethyl clomipramine, imipramine, and dehydroimipramine in biological fluids by selective ion monitoring, and pharmacokinetics of clomipramine. *Clinical Chemistry* **1976**, 22, (6), 892-897.

11. Fun, H. K.; Loh, W. S.; Siddegowda, M. S.; Yathirajan, H. S.; Narayana, B., Opipramol. *Acta Crystallographica Section E: Structure Reports Online* **2011**, 67, (7).

12. Luboch, E.; Wagner-Wysiecka, E.; Jamrógiewicz, M.; Szczygelska-Tao, J.; Magielka, S.; Biernat, J. F., Determination of the chemical structure of potential organic impurities occurring in the drug substance opipramol. *Pharmazie* **2010**, 65, (4), 239-244.

13. Owen, R. T.; Castaner, J., Quinupramine. *Drugs of the Future* **1978**, 3, (7), 548-549.

14. Sakamoto, H.; Yokoyama, N.; Kohno, S.; Ohata, K., Receptor binding profile, of quinupramine, a new tricyclic antidepressant. *Japanese Journal of Pharmacology* **1984**, 36, (4), 455-460.

15. Sakamoto, H.; Yokoyama, N.; Nishimoto, T.; Murai, K.; Tatsumi, H.; Kohno, S.; Ohata, K., Effects of quinupramine on the central monoamine uptake systems and involvement of pharmacokinetics in its pharmacological activities. *Japanese Journal of Pharmacology* **1987**, 45, (2), 169-175.

16. Borsini, F.; Volterra, G.; Cutrufo, C.; Furio, M.; Meli, A., Pharmacological profile of the new anticonvulsant etazepine. *Arzneimittel-Forschung/Drug Research* **1989**, 39, (4), 475-479.

17. Dain, J. G.; Jaffe, J. M., Effect of diet and gavage on the absorption and metabolism of fluperlapine in the rat. *Drug Metabolism and Disposition* **1988**, 16, (2), 238-242.

18. Fischer-Cornelssen, K. A., Fluperlapine in 104 schizophrenic patients. Open multicenter trial. *Arzneimittel-Forschung/Drug Research* **1984**, 34, (1 A), 125-130.

19. Viti, G.; Giannotti, D.; Altamura, m.; Ricci, R.; Volterra, G.; Lecci, A.; Borsini, F.; Pestellini, V., New [dibenzo(b,e)azepin-5-yl]-acetamides with anti-convulsant activity. *European Journal of Medicinal Chemistry* **1993**, 28, (5), 439-445.

20. Gijsen, H. J. M.; Berthelot, D.; Zaja, M.; Brône, B.; Geuens, I.; Mercken, M., Analogues of morphanthridine and the tear gas dibenz[b, f][1,4]oxazepine (CR) as extremely potent activators of the human transient receptor potential ankyrin 1 (TRPA1) channel. *Journal of Medicinal Chemistry* **2010**, 53, (19), 7011-7020.

21. Weitzberg, M.; Abu-Shakra, E.; Azeb, A.; Aizenshtat, Z.; Blum, J., Syntheses and chemistry of some dibenz[c,e]azepines. *Journal of Organic Chemistry* **1987**, 52, (4), 529-536.

22. Pigeon, P.; Decroix, B., Synthesis of dibenz[c,e]azepine and benzo[e]thieno[c]azepine via N-acyliminium ion cyclization. *Tetrahedron Letters* **1997**, 38, (6), 1041-1042.

23. Palma, A.; Galeano, N.; Bahsas, A., A Simple and practical approach to the dibenzo[c,f]thiazolo[3,2- a]azepines: A novel fused tetracyclic azepine system. *Synthesis* **2010**, (8), 1291-1302.

24. Aboul-Enein, H. Y.; Ibrahim, S. E.; Khalifa, M., Synthesis and biological activity of dibenz[c,e]azepines. *Drug Design and Delivery* **1988**, 4, (1), 27-33.

25. Schmidt, M.; Teitge, M.; Castillo, M. E.; Brandt, T.; Dobner, B.; Langner, A., Synthesis and biochemical characterization of new phenothiazines and related drugs as MDR reversal agents. *Archiv der Pharmazie* **2008**, 341, (10), 624-638.

26. Tasaka, K.; Kamei, C.; Kitazumi, K.; Izushi, K.; Mio, M., Pharmacological activities of some metabolite and decomposition products of epinastine. *Japanese Pharmacology and Therapeutics* **1992**, 20, (1), 57-62.

27.   Barakat, S. E. S.; El-Zahabi, M. A.; Radwan, M. F., Synthesis and hypolipidemic activity of some new dibenz[c,e]azepine derivatives. *Saudi Pharmaceutical Journal* **2000**, 8, (2-3), 110-115.

28.   Hall, I. H.; Wong, O. T.; Reynolds, D. J.; Simlot, R., Comparison between 6,7-dihydro-5H-dibenz(c,e)azepine and lovastatin as hypolipidemic agents in rats. *Journal of Pharmaceutical Sciences* **1993**, 82, (6), 565-570.

29.   Bergmann, E. D.; Shahak, I.; Aizenshtat, Z., A new approach to the dibenz*[b,f]*azepine and *[b,f]*oxepine system. *Tetrahedron Lett.* **1968**, (31), 3469-70.

30.   Sinha, A.; Nizamuddin, S. , A New Synthesis of 5H-Dibenz*[b,f]*azepin-5-carboxamide (Carbamazepine) *Indian Journal of Chemistry, Section B: Organic Chemistry Including Medicinal Chemistry* **1982**, 21, (3), 237-238.

31.   Tsvelikhovsky, D.; Buchwald, S. L., Synthesis of Heterocycles via Pd-Ligand Controlled Cyclization of 2-Chloro-N-(2-vinyl)aniline: Preparation of Carbazoles, Indoles, Dibenzazepines, and Acridines. *J. Am. Chem. Soc.* **2010**, 132, 14048-14051.

32.   Wang, H., Improved synthesis of 10,11-dihydro-5H-dibenzo*[b,f]*azepine. *Zhongguo Yiyao Gongye Zazhi* **2001**, 32, 35-36.

33.   Vorozhtsov, G. N.; Dokunikhin, N. S.; Fel'dblyum, N. B.; Alekseeva, E. V., 1,1'-Binaphthyl derivatives. V. Synthesis and reactions of 8,8'-diamino and 8,8'-dinitro derivatives of 1,1'-biacenaphthenyl. *Zh. Org. Khim.* **1977**, 13, 620-4.

34.   Li, W.; You, Q., Synthesis and local anesthetic activity of fluoro-substituted imipramine and its analogues. *Bioorg. Med. Chem. Lett.* **2007**, 17, 3733-3735.

35.   Jorgensen, T. K.; Andersen, K. E.; Lau, J.; Madsen, P.; Huusfeldt, P. O., Synthesis of substituted 10,11-dihydro-5H-dibenz*[b,f]*azepines; key synthons in syntheses of pharmaceutically active compounds. *J. Heterocycl. Chem.* **1999**, 36, 57-64.

36.   Koehegyi, I.; Galamb, V., 5H-Dibenz*[b,f]*azepines. Part 5. Comparative study of 10,11-dihydro-5H-dibenz*[b,f]*azepine and its analogs in the hydrogen-transfer dehydrogenation reaction. *Heterocycles* **1995**, 40, 109-14.

37.   Galamb, V.; Joo, F.; Koehegyi, I., 5H-Dibenz*[b,f]*azepines. Part 6. Kinetics of palladium-catalyzed transfer dehydrogenation of 10,11-dihydro-5H-dibenz*[b,f]*azepine. *J. Chem. Res., Synop.* **1995**, 216-17.

38.   Haasz, F.; Galamb, V.; Hosztafi, S.; Szabo, J. M.; Garadnay, S. New process for producing 10-alkoxy-5H-dibenz*[b,f]*azepines starting from 5-acetyl-5H-dibenzazepine. HU63391A2, 1993.

39.   Hull, J. F.; Balcells, D.; Sauer, E. L. O.; Raynaud, C.; Brudvig, G. W.; Crabtree, R. H.; Eisenstein, O., Manganese Catalysts for C-H Activation: An Experimental/Theoretical Study Identifies the Stereoelectronic Factor That Controls the Switch between Hydroxylation and Desaturation Pathways. *J. Am. Chem. Soc.* **2010**, 132, 7605-7616.

40. Inoue, M.; Itoi, Y.; Enomoto, S.; Ishizuka, N.; Ameniya, H.; Takeuchi, T., Catalytic dehydrogenation of iminodibenzyl to iminostilbene on manganese oxide-stannic oxide. *Chem. Pharm. Bull.* **1982**, 30, 24-7.

41. Su, W.; Liang, X.; Jiang, Z.; Xu, J.; Song, G.; Wang, Q. Method for chemical synthesis of iminostilbene as intermediate for synthesizing carbamazepine. CN101307021A, 2008.

42. Agarwal, A.; Singh, S.; Verma, P. K.; Arugulasait, R. Catalyst and its preparation process and application to production of 5H-dibenz*[b,f]*azepine. CN1754623A, 2006.

43. Yin, W.-p.; Li, R.; Kou, L.; Li, Y.; Ma, J.-t., Catalytic dehydrogenation of iminodibenzyl. *Fenzi Cuihua* **2004**, 18, 248-252.

44. Scholl, T.; Roth, H. J., Synthesis of sulfur-containing carbamazepine derivatives. *Arch. Pharm. (Weinheim, Ger.)* **1985**, 318, 624-30.

45. Pop, E.; Kovacs, B.; Sclifos, M.; Lenta, L.; Bercovici, S. H.; Miloia, R. T. 5-Chlorocarbonyl-5H-dibenzo*[b,f]*azepine. RO80232A2, 1983.

46. Shamshin, V. P.; Voronin, V. G.; Borisov, M. M.; Mufazalova, T. P., Synthesis of carbamazepine and its antialcoholic action. *Khim.-Farm. Zh.* **1987**, 21, 711-16.

47. Bergmann, E. D.; Rabinovitz, M.; Bromberg, A., Some derivatives of 5-dibenz[b.f]azepine. *Tetrahedron* **1968**, 24, (3), 1289-1292.

48. Groth, U.; Richter, L.; Schöllkopf, U., Synthesis of Substituted Dibenzo[a,d]azepines via a Base-Mediated Ring Expansion. *Liebigs Annalen der Chemie* **1992**, 1992, (3), 199-202.

49. Bowkett, E. R. The Synthesis of Chemical Probes for Drug Metabolism and Toxicity. PhD thesis, The University of Liverpool, Liverpool, 2007.

50. Van Quaqebeke, E.; Gentiane, S.; El Yazidi, M.; Tuti, J.; Van Den Hove, L.; Darro, F.; Kiss, R. Preparation of ureidonaphthalimides as anticancer drugs. WO2007128538A1, 2007.

51. Tokmakov, G. P.; Grandberg, I. I., Rearrangement of 1-arylindoles to 5H-dibenz*[b,f]*azepines. *Tetrahedron* **1995**, 51, (7), 2091-2098.

52. Smith, K.; James, D. M.; Mistry, A. G.; Bye, M. R.; Faulkner, D. J., A new method for bromination of carbazoles, [beta]-carbolines and iminodibenzyls by use of N-bromosuccinimide and silica gel. *Tetrahedron* **1992**, 48, (36), 7479-7488.

53. Li, W.; Zhou, Y.; Zhang, Y.-d.; Hu, G.-q.; Li, H., Synthesis of 3,7-difluoro-10,11-dihydro-5H-dibenz*[b,f]*azepine. *Huaxue Shiji* **2007**, 29, 759-760.

54. Chhattise, P. K.; Ramaswamy, A. V.; Waghmode, S. B., Regioselective, photochemical bromination of aromatic compounds using N-bromosuccinimide. *Tetrahedron Letters* **2008**, 49, (1), 189-194.

55. Koval, I. V., N-halo reagents. N-halosuccinimides in organic synthesis and in chemistry of natural compounds. *Russian Journal of Organic Chemistry* **2002**, 38, (3), 301-337.

56. Axtell, H. C.; McHugh, K. B.; Cann, M. C., Reaction of 8H-furo[3,4-d]dibenz*[b,f]*azepine and 9H-tribenz[b,d,f]azepine with t-butyl hypochlorite and silver trifluoroacetate. Attempts to form a long-lived aromatic nitrenium ion. *Heterocycles* **1995**, 41, 431-8.

57. Andrieux, C. P.; Differding, E.; Robert, M.; Saveant, J. M., Controlling factors of stepwise versus concerted reductive cleavages. Illustrative examples in the electrochemical reductive breaking of nitrogen-halogen bonds in aromatic N-halosultams. *J. Am. Chem. Soc.* **1993**, 115, (15), 6592-9.

58. Duan, S.; Turk, J.; Speigle, J.; Corbin, J.; Masnovi, J.; Baker, R. J., Halogenations of anthracenes and dibenz[a,c]anthracene with N-bromosuccinimide and N-chlorosuccinimide. *J. Org. Chem.* **2000**, 65, (10), 3005-3009.

59. Goldberg, Y.; Alper, H., Electrophilic halogenation of aromatics and heteroaromatics with N-halosuccinimides in a solid/liquid system using an H+ ion exchanger or ultrasonic irradiation. *Journal of Molecular Catalysis* **1994**, 88, (3), 377-383.

60. Olah, G. A.; Wang, Q.; Sandford, G.; Surya Prakash, G. K., Synthetic methods and reactions. 181. Iodination of deactivated aromatics with N-iodosuccinimide in trifluoromethanesulfonic acid (NIS-CF3SO3H) via in situ generated superelectrophilic iodine(I) trifluoromethanesulfonate. *The Journal of Organic Chemistry* **1993**, 58, (11), 3194-3195.

61. Schindler, W. 5H-Dibenx*[b,f]*azepines. US2948718, 1960.

62. Schindler, W.; Blattner, H., Über Derivate des Iminodibenzyls Iminostilben-Derivate. *Helvetica Chimica Acta* **1961**, 44, (3), 753-762.

63. Phukan, K.; Ganguly, M.; Devi, N., Mild and Useful Method for N-Acylation of Amines. *Synthetic Communications* **2009**, 39, (15), 2694-2701.

64. Forshed, J.; Erlandsson, B.; Jacobsson, S. P., Quantification of aldehyde impurities in poloxamer by 1H NMR spectrometry. *Analytica Chimica Acta* **2005**, 552, (1-2), 160-165.

65. Kakadiya, P. R.; Reddy, B. P.; Singh, V.; Ganguly, S.; Chandrashekhar, T. G.; Singh, D. K., Low level determinations of methyl methanesulfonate and ethyl methanesulfonate impurities in Lopinavir and Ritonavir Active pharmaceutical ingredients by LC/MS/MS using electrospray ionization. *Journal of Pharmaceutical and Biomedical Analysis* **2011**, 55, (2), 379-384.

66. Watanabe, M.; Nishiyama, M.; Yamamoto, T.; Koie, Y., Palladium/P(t-Bu)3-catalyzed synthesis of N-aryl azoles and application to the synthesis of 4,4',4"-tris(N-azolyl)triphenylamines. *Tetrahedron Letters* **2000**, 41, (4), 481-483.

67.   Old, D. W.; Harris, M. C.; Buchwald, S. L., Efficient palladium-catalyzed N-arylation of indoles. *Organic Letters* **2000**, 2, (10), 1403-1406.

68.   Chandrasekhar, S.; Sultana, S. S.; Yaragorla, S. R.; Reddy, N. R., Copper-catalyzed N-arylation of amines/amides in poly(ethylene glycol) as recyclable solvent medium. *Synthesis* **2006**, (5), 839-842.

69.   Ma, D.; Cai, Q., L-Proline Promoted Ullmann-Type Coupling Reactions of Aryl Iodides with Indoles, Pyrroles, Imidazoles or Pyrazoles. *Synlett* **2004**, (1), 128-130.

70.   Ju, C.; Uetrecht, J. P., Detection of 2-Hydroxyiminostilbene in the Urine of Patients Taking Carbamazepine and Its Oxidation to a Reactive Iminoquinone Intermediate. *Journal of Pharmacology and Experimental Therapeutics* **1999**, 288, (1), 51-56.

71.   Raml, W.; Eichberger, G. Process for the preparation of carbamazepine from 5H-dibenz*[b,f]*azepine and phosgene with subsequent ammonium hydroxide amidation of the carbonyl chloride intermediate. DE4421294A1, 1995.

72.   Raml, W.; Eichberger, G. Preparation of carbamazepine by the phosgenation and amidation of 5H-dibenz*[b,f]*azepine. AT401174B, 1996.

73.   Palitzsch, P.; Czernotzky, K.; Mueller, R.; Richter, E.; Klump, W.; Kolodzeizik, K. Preparative method for carbamazepine. DD298508A5, 1992.

74.   Osowski, A.; Dereszynski, H.; Marzycki, M.; Klecha, U. Preparation of 5H-dibenz*[b,f]*azepine-5-carboxamide. PL147078B1, 1989.

75.   Parenky, C.; Chaturvedi, R. Novel process for preparation of 10-oxo-10,11-dihydro-5H-dibenz*[b,f]*azepine-5-carboxamide (oxcarbazepine) via intermediate, 10-methoxy-5H-dibenz[*b,f*]azepine-5-carbonyl chloride. WO2005066133A2, 2005.

76.   Banfi, A.; Bollini, D.; Serra, M.; Di, L. G. Process for preparing oxcarbazepine via chlorocarbonylation with triphosgene. WO2005092862A1, 2005.

77.   Milanese, A. Preparation of iminostilbene derivatives. IT2004RM0260A1, 2004.

78.   Milanese, A. Process for the preparation of oxcarbazepine. EP1600443A1, 2005.

79.   Mody, P. A.; Motiwala, J. K. Process for preparation of Carbamazepine by reaction of 5H-dibenz[b,f]azepine with triphosgene in the presence of DMF and then with methanolic ammonia. IN179809A1, 1997.

80.   Kumata, K.; Takei, M.; Ogawa, M.; Kato, K.; Suzuki, K.; Zhang, M.-R., One-pot radiosynthesis of [13N]urea and [13N]carbamate using no-carrier-added [13N]NH3. *J. Labelled Compd. Radiopharm.* **2009**, 52, (5), 166-172.

81.   Venkataraman, S.; Eswaraiah, S.; Reddy, K. R.; Satyanarayana, R. A process for the purification of oxcarbazepine. IN2004CH00142A, 2005.

82.   Cotarca, L.; Eckert, H., *Phosgenations - A Handbook*. WIELY-VCH: Weinheim, 2004.

83.   La, D. S.; Belzile, J.; Bready, J. V.; Coxon, A.; DeMelfi, T.; Doerr, N.; Estrada, J.; Flynn, J. C.; Flynn, S. R.; Graceffa, R. F.; Harriman, S. P.; Larrow, J. F.; Long, A. M.; Martin, M. W.; Morrison, M. J.; Patel, V. F.; Roveto, P. M.; Wang, L.; Weiss, M. M.; Whittington, D. A.; Teffera, Y.; Zhao, Z.; Polverino, A. J.; Harmange, J.-C., Novel 2,3-Dihydro-1,4-Benzoxazines as Potent and Orally Bioavailable Inhibitors of Tumor-Driven Angiogenesis‖. *Journal of Medicinal Chemistry* **2008**, 51, (6), 1695-1705.

84.   Karusala, N. R.; Tummalapally, U. S. S.; Talatala, A. R.; Datta, D. An improved process for the preparation of oxcarbazepine. WO2009139001A2, 2009.

85.   Gutman, D.; Baidossi, W. Method of preparing a 5H-dibenz[b,f]azepine-5-carboxamide. WO2003106414A2, 2003.

86.   Eckardt, R.; Jaensch, H.-J. Process for producing carbamazepine. US7015322B1, 2006.

87.   Liu, X.; Li, M.; Xiao, F., Synthesis of oxcarbazepine. *Zhongguo Yiyao Gongye Zazhi* **2006**, 37, (7), 443-445.

88.   Durant, G. J., Improved synthesis of N,N-diarylureas. *Chem. Ind. (London, U. K.)* **1965**, 1428-9.

Results and Discussion: Structure-Metabolism Relationships of Carbamazepine Analogues

Chapter 3

This chapter discusses the results from the incubation of six carbamazepine analogues in freshly isolated rat hepatocyte suspensions. This work was performed by Dr. Sophie L. Regan and Dr. James L. Maggs of the department of pharmacology and summarizes the key observations of the study.

Contents

3 Results and Discussion: Structure-Metabolism Relationships of Halogenated Carbamazepine Analogues

Note: Dr. S. L. Regan and Dr. J. L. Maggs performed work on the structure-metabolism

relationships of the carbamazepine analogues. LC-MS identification of the metabolites

was performed by Dr. J. L. Maggs. Isolation of hepatocytes and incubation of the

compounds was performed by Dr. S. L. Regan. Dr. Regan further quantified all the

metabolites by LC-UV. All metabolic work was performed at the MRC Centre for Drug

Safety Science, School of Biomedical Science, University of Liverpool, Liverpool, L69

3BX.

All the figures shown below are the results from incubation 50 μM substrate after 6 h,

because it is at this concentration that substrate turnover is greatest and metabolites are

detected most consistently in the present investigation.

3.1 Introduction

As discussed in chapter 1 (section 1.2) the clinical use of carbamazepine has been

frequently associated with the development of ADRs, including hepatotoxicity.[1]

Metabolism of carbamazepine is complex, with the identification of over 30 metabolites

in vivo as discussed in chapter 1 (section 1.3).[2] Consequently, the bioactivation of CBZ

has been implicated in the pathogenesis of ADRs.[3, 4]

Exploration of the structure-metabolism relationships of xenobiotics with reference to

the mechanism and prediction of toxicity is typically performed *in vitro*.[5-7] The

homeostatic role of hepatocytes, and their ability to detoxify xenobiotics make them an attractive tool for *in vitro* investigation of pharmacotoxicology of xenobiotics.[8, 9] Hepatocytes in culture are widely agreed to be a suitable model for toxicological investigations.[10, 11] However, the method is not without its limitations as the loss of specific liver functions, by a method known as cell dedifferentiation has been observed.[12-14] Freshly isolated hepatocyte suspensions have been demonstrated to have a higher metabolic capacity when compared to cells in culture,[15] and hence represent an appropriate model for the investigation of the relevance of drug bioactivation in the cytotoxic outcome of a xenobiotic.[15] This is because suspensions may be immediately incubated with a drug, whereas cells in culture must be allowed to adhere for 1-2 hours before dosing. Furthermore, hepatocytes in culture have been demonstrated to lose CYP activities.[14]

3.2   Project Aims

As discussed in chapter 1 section 1.2.1, CBZ metabolism is complex with over 30 metabolites identified in animal and man. This extensive bioactivation of carbamazepine has led to the hypothetical linking of several reactive metabolites to the casuse of ADRs. However, to date no metabolite has been clearly identified as the cause of a specific ADR.

Characterisation of the metabolites formed in hepatocyte suspensions with the mono- and di- halo carbamazepine analogues, particularly hydroxylated arenes and 10,11-epoxidation, will enable greater understanding of the bioactivation of carbamazepine analogues. This knowledge could be further used to aid the development of safer drugs if

drug efficacy can be retained and makes a contribution to our wider understanding of

structure-reactivity effects in oxidative metabolic pathways.

3.3 Identification of CBZ Metabolites in freshly isolated hepatocyte suspensions
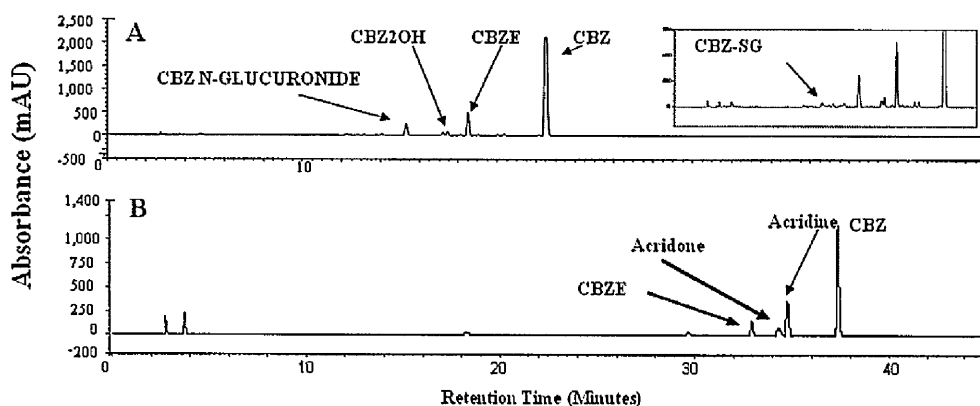
3.3.1 Rat vs. Mouse metabolism

Figure 3.1: LC_UV chromatogram showing the metabolites identified in rat (A) and mouse (B) models with 50 µM substrate.[16]

Before the CBZ analogues may be assessed the most appropriate rodent model for CBZ

metabolism was determined. The metabolism of CBZ was first investigated in both rat

and mouse fresh hepatocyte suspensions, LC-UV analysis in **figure 3.1** reveals a clear

distinction between the two profiles. Rat hepatocytes (**figure 3.1A**) had a decreased

turnover at higher concentrations, ranging from 64.37 ± 17.54 % (50 µM) to 17.79 ±

4.03 % (1000 µM). Saturation of metabolic pathways may be the cause of the observed

reduction in turnover at higher concentrations.

The major metabolite identified from the rat hepatocytes is the 10,11 epoxide (CBZE).

Co-elution with an authentic standard confirmed the identity of CBZE and its diagnostic

fragmentation pathway (**figure 3.2**). Identification of CBZE as the major metabolite is in

agreement with previous observations in rodent and man.[2, 17, 18]
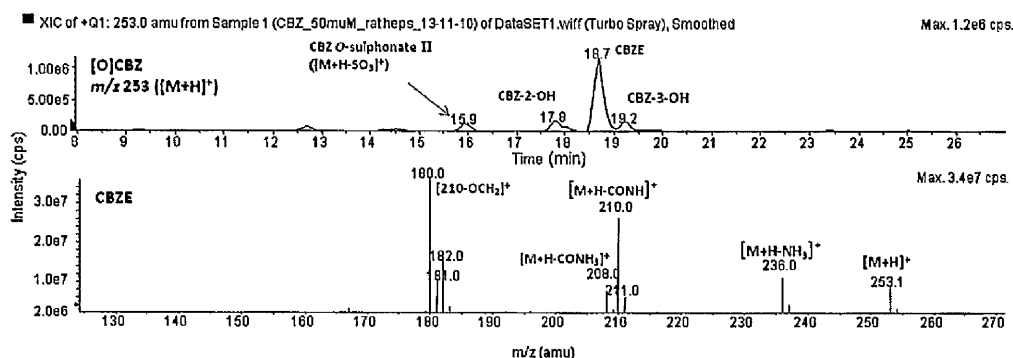
Figure 3.2: Identification of oxygenated CBZ metabolites by LC-MS. Extracted Ion Current (XIC) chromatogram (top) m/z 253 revealing mono-oxygenated carbamazepine metabolites and fragments of metabolites that contain a mono-oxygenated species. Mass Spectroscopic analysis (bottom) of the peak eluting at 18.7 min reveals the characteristic fragmentation of CBZE. Isolated from rat hepatocytes (50 μM substrate).

Detection of *N*-glucuronide (CBZ-*N*-gluc), in **figure 3.3**, as another major metabolite in

freshly isolated hepatocyte suspensions was also in agreement with observations in

rodent models [19] and in man.[2, 18] Furthermore the *N*-glucuronide of CBZE (**figure 3.3**)

was also detected by LC-MS.[19] However, its inconsistent appearance in the current

investigations may be due to saturation of the glucuronidation pathway with the parent

compound. Fragments in the MS that have a star above them in **figure 3.3** are fragments

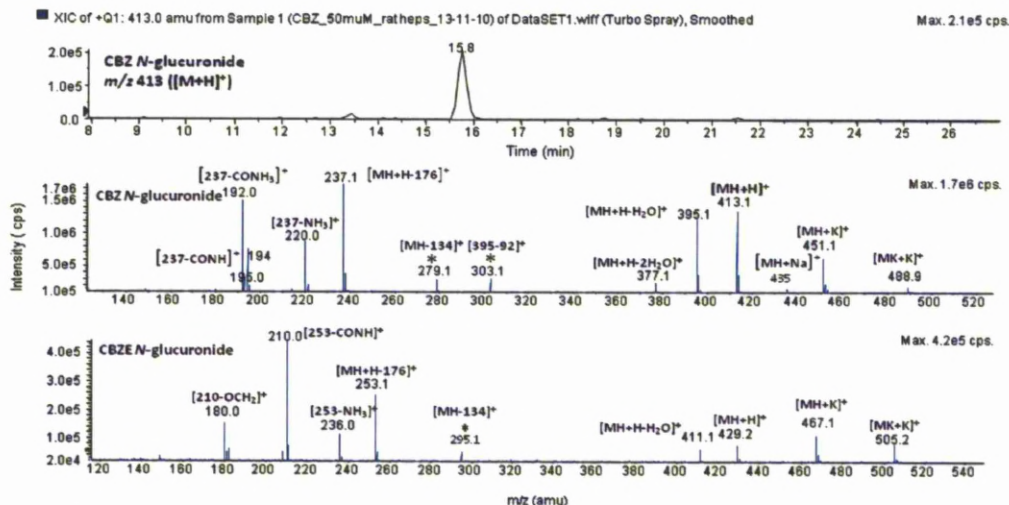observed as a result of fragmentation of the glucuronosyl side chain.

Figure 3.3: XIC for *N*-glucuronides of CBZ (top) with the mass spectra for CBZ-*N*-glucuronide (middle) and CBZE-*N*-glucuronide (bottom) in rat hepatocytes (50 μM substrate).

Two other mono-oxygenated derivatives were found and identified by their retention times (**figure 3.2**). They were further identified as oxygenated metabolites distinct from CBZE by their different fragmentation pathway as seen in **figure 3.4**. Such biotransformations of the aromatic rings are known but less defined, as phenols, and the derivatives thereof (catechols, methyl thioethers, sulfates) have been previously identified in the urine of rats and humans.[2]
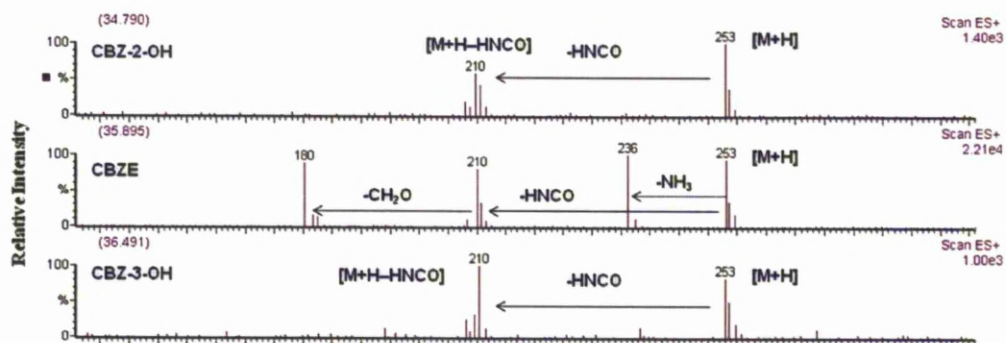
Figure 3.4: Comparison of the mass spectra of mono-oxygenated carbamazepine metabolites: CBZE, CBZ-2-OH, and CBZ-3-OH detected in rat hepatocytes at 50 μM CBZ.

121

The presence of CBZ-2-OH and CBZ-3-OH has been postulated to be an indicator of the arene-oxide pathway[20] as dicussed in chapter 1 (section 1.3), which has been implicated in the development of ADRs.[4, 21] However, as discussed, the formation of such metabolites does not necessarily implicate epoxide intermediates, and DHDs or DHOH metabolites represent stronger evidence for the presence of arene oxide intermediates.[22] As discussed earlier, two DHDs of CBZ have been observed in the urinary metabolites of rat and man but no DHOH.[4] Only one CBZ-GSH adduct was detected (m/z 512) in the present investigation. It is observable in the XIC of **figure 3.3** for detection of the *N*-glucuronide corresponding to a pyroglutamate fragment of the CBZ-GSH adduct. This is further indicated in **figure 3.5** by a red arrow.
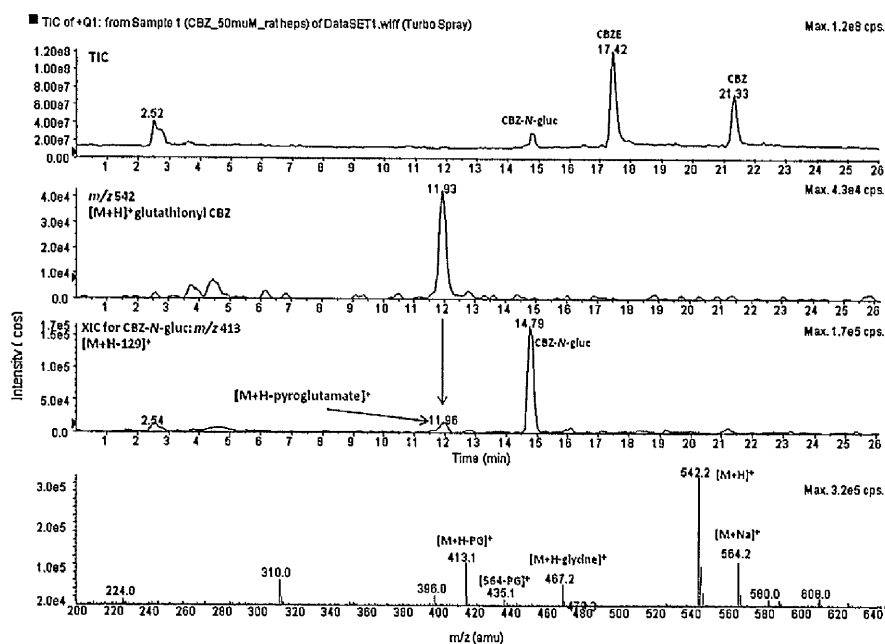
Figure 3.5: Detection of glutathione conjugates of CBZ in rat hepatocytes at 50 μM CBZ. The glutathione conjugate cannot be observed in the TIC but a fragment corresponding to a diagnostic pyroglutamate ion is observable in the XIC for CBZ-*N*-gluc (indicated by the red arrow). Mass spectrometry of this peak (bottom) highlights two diagnostic fragments of a CBZ-GSH adduct: m/z 467 and m/z 413.

This observation contrasts with the observation of Mahajan *et al* where four GSH
conjugates of CBZ were observed at lower concentrations of CBZ.[23] However, the
milder work-up procedure of Mahajan, and the use of a more sensitive mass
spectrometer may have compensated for the low concentration of CBZ in the study.
Furthermore, this metabolite is only observed at 50 μM CBZ and was not observed at
higher concentrations.

Finally, two sulfates of carbamazepine were detected in the hepatocyte suspensions
(**figure 3.6**). These two metabolites showed similar fragmentation and may be
considered to be structurally related. However, the limitations of mass spectrometry
means that the structure cannot be more firmly assigned as it would be by other methods
(such as NMR). However, given their similarity, the two compounds are postulated to be
sulfonated derivatives of CBZ-2-OH and CBZ-3-OH.
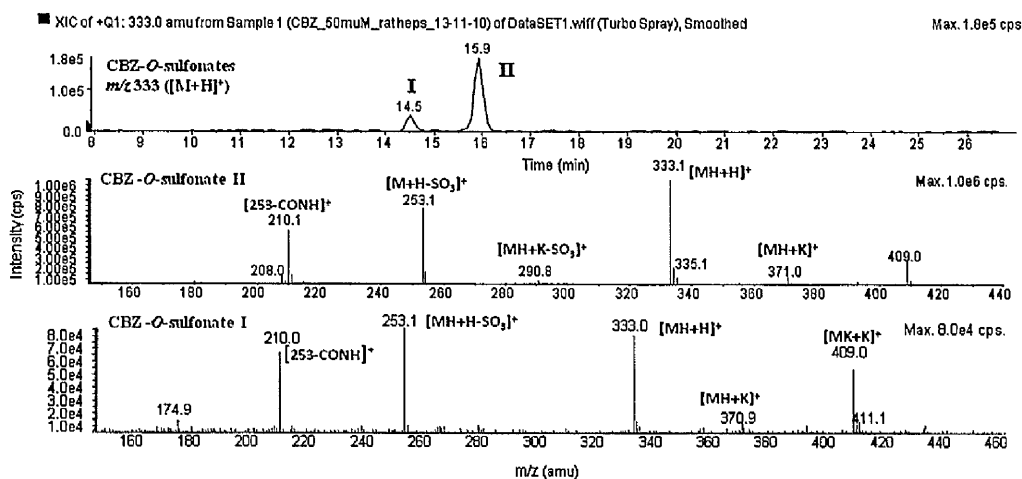
Figure 3.6: XIC of sulfonated metabolites of CBZ at *m/z* 333 (top) and the mass spectrum for each sulfonate in rat
hepatocytes 50 μM substrate.

Metabolism of CBZ in mouse hepatocyte suspensions (**figure 3.1B**) yielded a metabolic profile distinct from that of the rat. However, it only partly replicates the metabolism observed *in vivo*.[24] Metabolism of CBZ *in vivo* and *in vitro* is not directly comparable as the *in vitro* study uses both a highly in-bred strain and the mice were pre-treated with CBZ.[24] As CBZ is a known inducer of P450s in humans[16] the same response may be expected in mouse models. The formation of CBZE *in vitro* was observed in mice as it was for rats, yet it was not the principal metabolite identified. Acridine (AI) was instead identified as the major metabolite, Formation of AI in mouse has not previously been reported, although, as discussed in section 1.3, the metabolite has been reported in a myeloperoxidase system of activated human neutrophils[25, 26] and is considered to be a minor metabolite of human CBZ metabolism.[27] However no evidence of the formation of the carboxaldehyde intermediate (9-AC)[26] was observed in mouse hepatocyte suspensions.[28] The only metabolites detected in the mouse hepatocyte suspensions were CBZE, AI, and acridone (AO), which could implicate CBZE as an intermediate in the formation of AI. However, incubation of CBZE in mouse hepatocytes at 50 μM[28] did not show the formation of any metabolite. Because CBZE has been substantially altered by metabolism to a more polar compound it is feasible that the structural and electronic changes make CBZE a poor substrate for further oxidative metabolism and saturation of metabolic pathways may occur. However, that CBZE was not observed to be turned over in the incubations is a reasonable indication that CBZE is not responsible for the formation of these metabolites, and indeed it may be turned over by other enzymes such as aldehyde oxidase.

No evidence of GSH conjugation was found in mouse hepatocyte suspensions: this conflicts with previous findings in mouse liver microsomes, as protein and thiol reactive metabolites were identified.[29] However, these studies used mice pre-treated with phenobarbital (PB), an inducer of P450s. Lack of induction of P450s in our chosen model may explain the apparent lack of GSH conjugates formed in mouse metabolites.
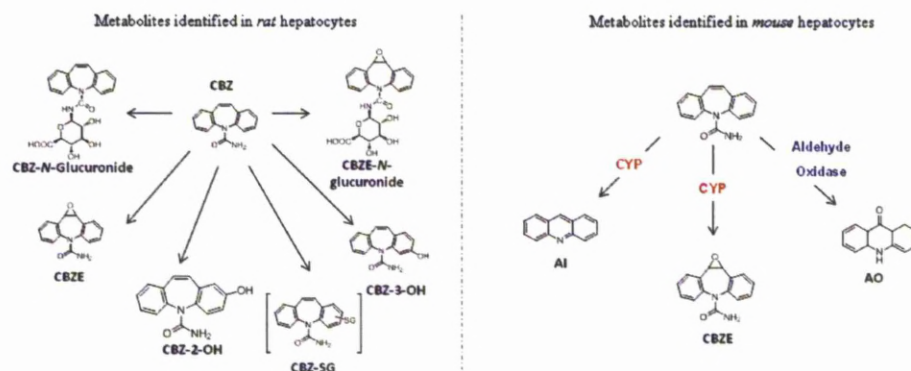

Figure 3.7: Summary and comparison of metabolites of carbamazepine identified in rat and mouse hepatocytes. CBZ-SG is a postulated structure.

Figure 3.7 highlights the key metabolites identified in freshly isolated rat and mouse hepatocytes. Because CBZ was found to be metabolised to GSH conjugates, *N*-glucuronide, and several mono-oxygenated species and were more representative of human metabolism of CBZ overall the rat was chosen for subsequent investigation of the structure-metabolism relationships of CBZ analogues.

3.3.2 Role of Cytochromes P450 in CBZ metabolism in hepatocyte suspensions

As the project is directed towards preventing formation of oxidative metabolism by P450 enzymes through appropriate substitution, the role of cytochrome P450

metabolism in rat was investigated. This was accomplished by pre-incubation of the

hepatocytes with two non-specific P450 inhibitors 1-aminobenzotriazole (ABT 1 mM)

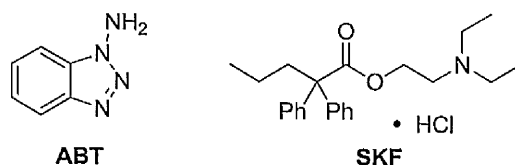and Proadifen hydrochloride (SKF-525A 50 μM), which are shown in **figure 3.8** below.

ABT   **SKF**

Figure 3.8: Non-specific P450 inhibitors used to assess the role of P450 metabolism in rat and mouse hepatocyte
suspensions.

In rat hepatocyte suspensions metabolism was found to be inhibited by both ABT and

SKF (**table 3.1**), although the latter inhibited to a lesser degree. Formation of the

oxygenated metabolites; CBZE, CBZ-2-OH, and CBZ-3-OH was found to be inhibited

or showed significantly decreased formation. When formed, this was also found to apply

to the GSH conjugate, indicating a P450-mediated pathway of bioactivation to be a

necessary step in the formation of the GSH conjugate. Glucuronidation was observed to

be slightly decreased in the presence of ABT and SKF. In the case of ABT this may be

attributed to ABT undergoing *N*-glucuronidation itself, and although the data is not

shown here ABT was observed to undergo significant *N*-glucuronidaton and *N*-

acetylation in the incubations in agreement with previous observations. [28]

Table 3.1: The effect of P450 inhibitors on CBZ turnover and identified metabolites in rat hepatocytes. *Values are the mean ±SEM of four independent isolations.* [28]

Conditions		CBZ (%)	3-OH CBZ (%)	CBZE (%)	2-OH CBZ (%)	CBZ-N-Glucuronide (%)	CBZ-SG (%)	Total % Turnover
500 CBZ	µM	82.96 (±4.08)	1.96 (±0.87)	5.24 (±1.70)	0.28 (±0.07)	0.84 (±0.519)	0.96 (±0.66)	17.04 (±2.41)
500 CBZ ABT	µM +	98.42 (±0.6)	0.02 (±0.02)	0.04 (±0.03)	0.02 (±0.02)	0.35 (±0.24)	0 (±0)	1.59 (±0.7)
500 CBZ SKF	µM +	94.01 (±1.24)	0.135 (±0.04)	1.09 (±0.39)	0.04 (±0.04)	0.38 (±0.26)	0.395 (±0.235)	5.99 (±1.3)

3.3.3 Structure-metabolism relationships of CBZ analogues

As discussed in chapter 1, investigation of structure-metabolism relationships is predominantly focused upon the effects of fluorine substitution upon the xenobiotics.[30,] [31] However, discussion of the heavier halogens is typically restricted to their steric influences at receptor sites. In the following section, the comparative behavior of all six mono- and di-halogenated CBZ analogues in rat hepatocytes is discussed.

Metabolism of 2,8-difluorocarbamazepine (CBZ-2,8-F) showed a significant decrease in the overall turnover of substrate between CBZ 22.63 % (± 6.23) and CBZ-2,8-F at 8.67 % (± 3.76) at 1000 µM (other concentrations are highlighted in **table 3.2**).

Table 3.2: Total percentage turnover of CBZ and CBZ-2,8-F in rat hepatocytes after 6 h. *Values are the mean ±SEM of three independent isolations.*

Concentration (μM)	CBZ	CBZ-2,8-F
50	63.55 (±3.08)	25.35 (±1.52)
200	35.08 (±3.11)	11.24 (±3.87)
500	24.75 (±5.63)	10.73 (±4.29)
1000	22.63 (±6.23)	8.67 (±3.76)

Figure 3.9 shows the LC-UV analysis comparing the metabolites found for CBZ and CBZ-2,8-F at 50 μM concentrations. The principal metabolites formed were the *N*-glucuronide and CBZ-2,8-F-*N*-glucuronide with small quantities of the 10,11 epoxide (CBZ2,8FE) and epoxide-*N*-glucuronide (CBZ-2,8-FE-*N*-glucuronide) detected.
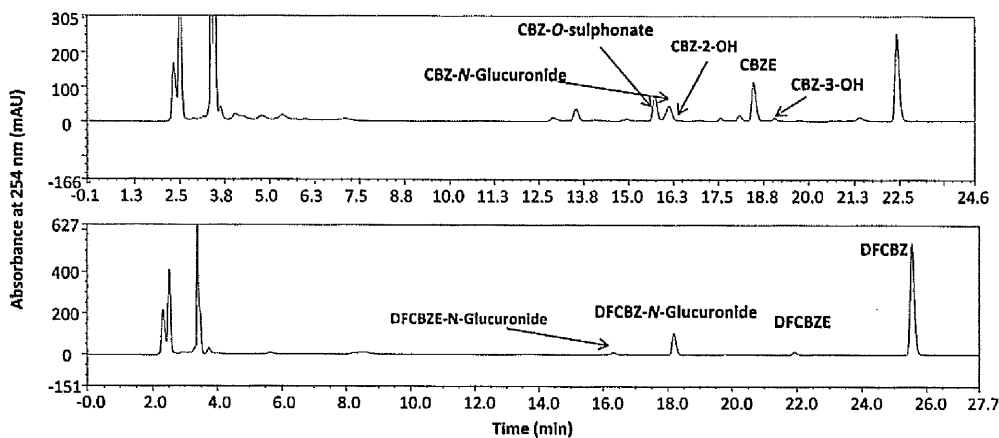
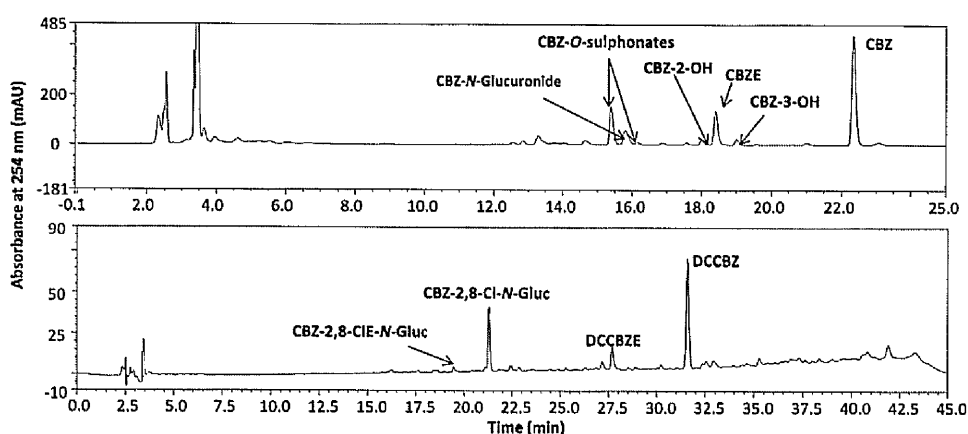Figure 3.9: LC-UV analysis of CBZ (upper) and CBZ-2,8-F (lower) metabolites identified in rat at 50 μM concentrations after incubation for 6 h.

As seen in **figure 3.9** the latter two metabolites were barely detectable by LC-UV but

could be more accurately detected and identified by LC-MS analysis as shown in **figure**

3.10. When searching for m/z 289, which corresponds to a mono-oxygenated CBZ-2,8-F

metabolite, two peaks are identified. The first peak at a retention time of 22.00 min was

identified by its characteristic fragmentation pathway (illustrated in **figure 3.2** and

figure 3.4) as the 10,11-epoxide CBZ-2,8-FE. However searching for m/z 289 further

revealed a peak corresponding to the mono-oxygenated CBZ-2,8-FE fragment of CBZ-

2,8-FE-*N*-glucuronide at 15.49 min. The presence of the CBZ-2,8-FE-*N*-glucuronide

could be further confirmed by searching the TIC for m/z 465 ([M+H] for CBZ-2,8-FE-

N-glucuronide): this revealed a co-incident peak for the XIC at 15.49 min. No other

mono-oxygenated species that may correspond to an arene-oxide derived metabolite

(e.g. CBZ-2-OH) were observed, nor was metabolic de-fluorination or NIH shifting of

the fluorine atom.
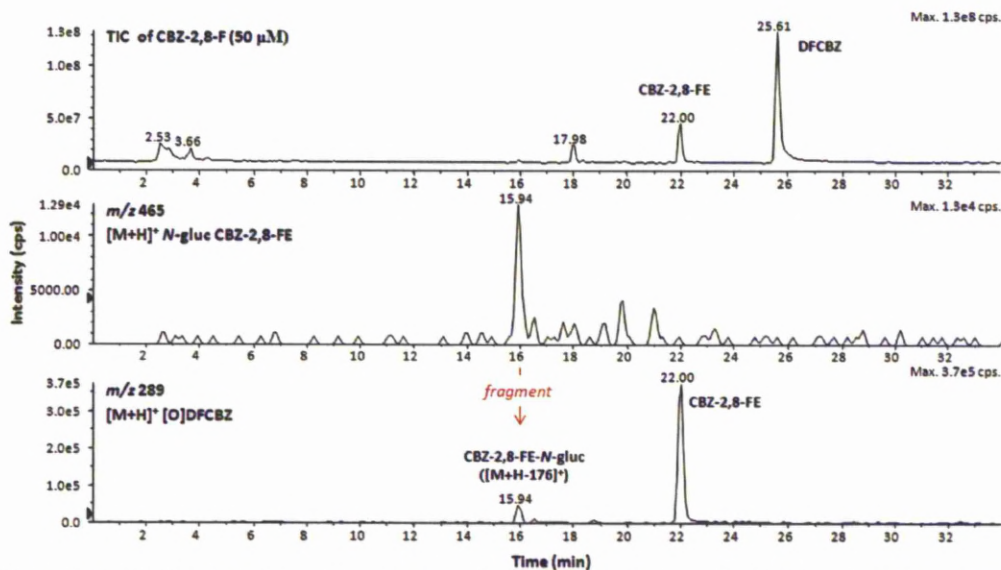
Figure 3.10: Identification of mono-oxygenated metabolites and fragments of CBZ-2,8-F by LC-MS after 6 h incubation in rat hepatocytes.

Incubation of 2,8-dichlorocarbamazepine (CBZ-2,8-Cl) revealed a similar turnover of the analogue to that of CBZ as highlighted in **table 3.3**. The difference at lower concentrations was more pronounced than at higher concentrations of CBZ and CBZ-2,8-Cl.

Table 3.3: Total percentage turnover of CBZ and CBZ-2,8-Cl in rat hepatocytes after 6 h, *values are the mean ±SEM of three independent isolations.*

Concentration (µM)	CBZ	CBZ-2,8-Cl
50	66.46 (±6.59)	41.37 (±1.54)
200	37.50 (±4.12)	23.38 (±4.9)
500	24.06 (±5.43)	23.31 (±7.3)
1000	20.17 (±6.60)	20.43 (±3.67)

As was observed for CBZ-2,8-F the principal metabolites detected were the 10,11-epoxide (CBZ-2,8-ClE), the *N*-glucuronide (CBZ-2,8-Cl-*N*-gluc), and the 10,11-epoxide-*N*-glucuronide (CBZ-2,8-ClE-*N*-gluc): these are shown in the LC-UV trace in **figure 3.11**.

Figure 3.11: LC-UV analysis of CBZ and CBZ-2,8-Cl metabolites identified in rat at 50 µM concentrations after incubation for 6 h.

Examination of the LC-MS TIC in **figure 3.12** for other mono-oxygenated species of CBZ-2,8-Cl at *m/z* 321 revealed CBZ-2,8-ClE at 27.80 min and CBZ-2,8-ClE-*N*-gluc at 19.54 min. However, in contrast to CBZ-2,8-F it also revealed a small amount of a mono-oxygenated species that eluted at 4.01 min, although the exact identity of the metabolite is to be determined, this does not appear to correspond to either CBZ-2-OH or CBZ-3-OH derivatives which could be expected to have retention times of ~8 min. Further examination of the TIC at *m/z* 497 revealed the CBZ-2,8-Cl-*N*-gluc at 19.53 min which was detectable by LC-UV. Further revealed was CBZ-2,8-ClE-*N*-gluc at 6. 00 min.
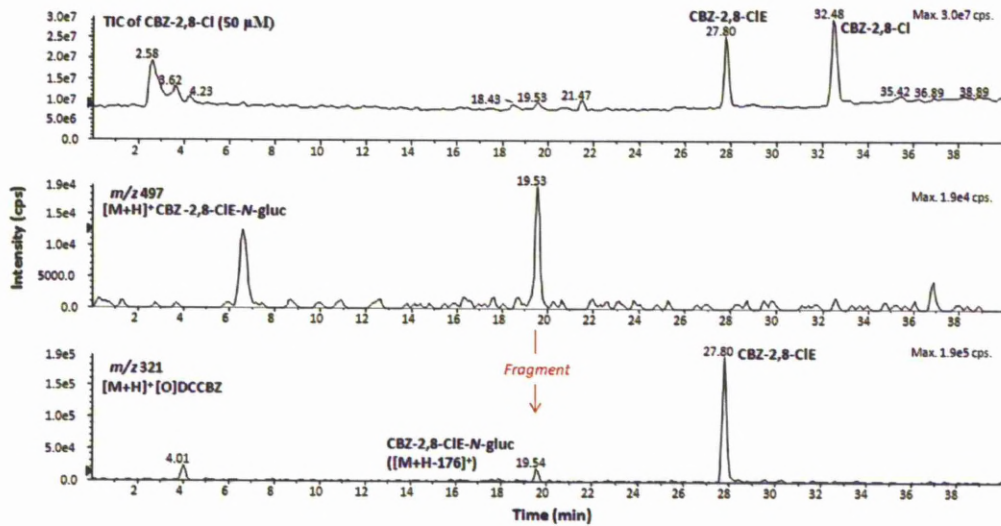
131

Figure 3.12: Identification of mono-oxygenated metabolites and fragments of CBZ-2,8-Cl by LC-MS after 6 h incubation in rat hepatocytes.

2,8-Dibromocarbamazepine (CBZ-2,8-Br) also underwent a significant change in substrate turnover compared to CBZ as shown in **table 3.4**. As was the case for CBZ-2,8-F and CBZ-2,8-Cl this difference in turnover was found to be less pronounced at higher concentrations.

Table 3.4: Total percentage turnover of CBZ and CBZ-2,8-Br in rat hepatocytes after 6 h. *Values are the mean ±SEM of three independent isolations.*

Concentration (µM)	CBZ	CBZ-2,8-Br
50	62.92 (±25.69)	32.36 (±6.32)
200	47.61 (±19.36)	12.11 (±2.07)
500	25.67 (±9.17)	14.00 (±3.28)

As shown in the LC-UV trace in **figure 3.13** the predominant metabolites were again the

10,11 epoxide (CBZ-2,8-BrE) and the *N*-glucuronide (CBZ-2,8-Br-*N*-gluc).
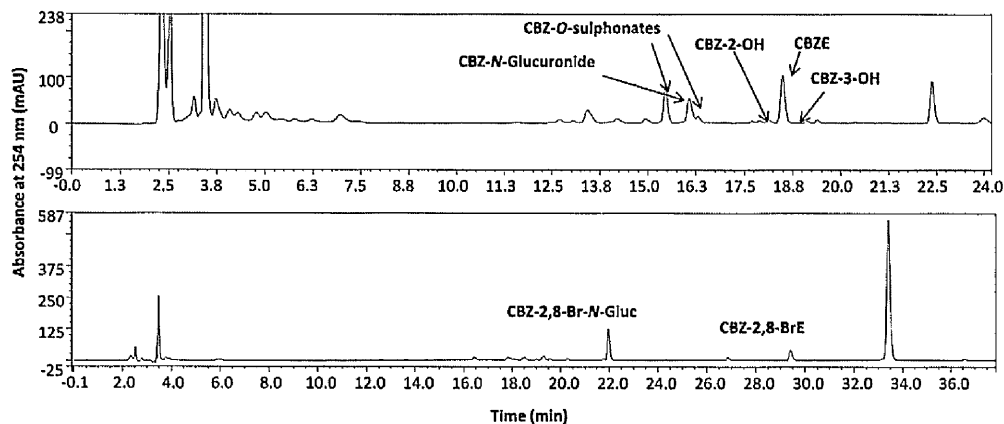
Figure 3.13: LC-UV analysis of CBZ and CBZ-2,8-Br metabolites identified in rat at 50 µM concentrations after incubation for 6 h.

Presence of these metabolites was confirmed by LC-MS analysis shown in **figure 3.14**.

Searching at *m/z* 571 confirmed the *N*-glucuronide at 23.00 min. Searching at *m/z* 395

($[M+H]^+$ for CBZ-2,8-Br), identified all compounds that contained CBZ-2,8-Br as the

parent ion or a fragment. This identified the peak at 34.60 min to be CBZ-2,8-Br, and

further identified the CBZ-2, 8-Br fragment of CBZ-2,8-Br-*N*-gluc. Searching at *m/z* 411

revealed a peak at 29.40 min which was identified by its fragmentation to be CBZ-2,8-
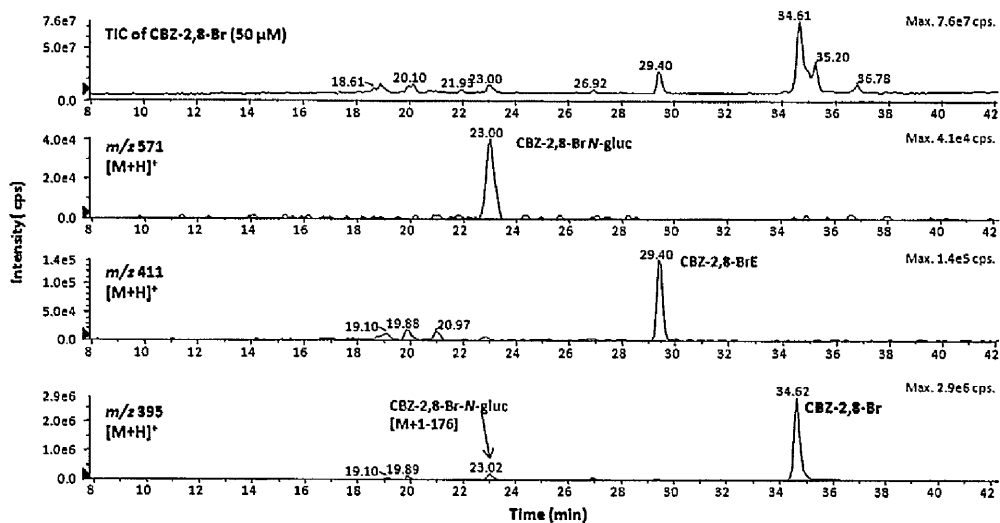
BrE.

Figure 3.14: Identification of mono-oxygenated metabolites and fragments of CBZ-2,8-Br by LC-MS after 6 h incubation of 50 μM substrate in rat hepatocytes.

In summary, for the dihalo carbamazepines the general trend for turnover of the substrate was CBZ > CBZ-2,8-Cl > CBZ-2,8-F > CBZ-2,8-Br. Reduction in the turnover of the substrate may further be ascribed to the reduction in the number of different metabolites observed in the assays with the predominant metabolic pathways being N-glucuronidation and 10,11-epoxidation. Furthermore, the differences in substrate turnover at low concentrations were found to be greater than at higher concentrations which may be the result of saturation of epoxidation and glucuronidation pathways.

In all cases there was an interesting shift in dominance between N-glucuronidation and 10,11-epoxidation for the di-halo analogues where N-glucuronidation can be seen to become the principal route of dihalo CBZ metabolism. This switch in dominance is more prominent from fluorine to bromine which suggests that the steric as well as

electronic influences of the halogen atoms in the 2,8-positions have a pronounced effect

on the ability of the molecule to undergo epoxidation. Conversely *N*-glucuronidation

becomes the prominent pathway as the amide nitrogen may be considered too distant to

be affected greatly by either the steric or electronic effects of halogen substitution in the

2,8-position.

Formation of derivatives of the other mono-oxygenated metabolites CBZ-2-OH and

CBZ-3-OH was not observed for any of the di-halo analogues. This indicates that the

inhibition of the pathways was direct for CBZ-2-OH. This could be due to the high

relative strength of the C-F bond in CBZ-2,8-F and possibly an alternative binding mode

in P450s active sites for CBZ-2,8-Cl and CBZ-2,8-Br by virtue of their σ-holes as

discussed in chapter 1. Blockade of the formation of CBZ-3-OH is more indirect as there

is no direct substitution in these positions. If CBZ-2-OH and CBZ-3-OH are formed *via*

the postulated arene oxide intermediate then it may be argued that prevention of the

formation of the products is linked structurally to the interference with oxygen

attachment in the 2 and 8 positions. Importantly, the formation of the GSH conjugates

observed for the metabolism of CBZ was not observed in the di-halo incubations

indicating that their formation is derived from oxidation of the arene ring rather than the

10,11-bond.

Considering now the mono-halo derivatives, 2-fluoro carbamazepine (CBZ-2-F) was

turned over slightly less than carbamazepine by the hepatocyte suspensions (**table 3.5**),

although this reduction was less marked than for any of the dihalogenated

carbamazepine derivatives.

Table 3.5: Total percentage turnover of CBZ and CBZ-2-F in rat hepatocytes after 6 h. *Values are the mean ±SEM of three independent isolations.*

Concentration (µM)	CBZ	CBZ-2-F
50	81.48 (±2.03)	69.77 (±4.57)
200	36.30 (±3.99)	22.46 (±5.61)
500	32.71 (±3.51)	21.22 (±4.45)
1000	31.40 (±5.86)	20.98 (±4.12)

As **figure 3.15** shows, several more metabolites were identified by LC-UV (and LC-MS. **Figure 3.16**), than were identified in the di-halo incubations The principal metabolites were found to be the ubiquitous 10,11 epoxide (CBZ-2-FE), the N-glucuronide (CBZ-2-F-N-gluc), and the glucuronide of the 10,11-epoxide (CBZ-2-FE-N-gluc).
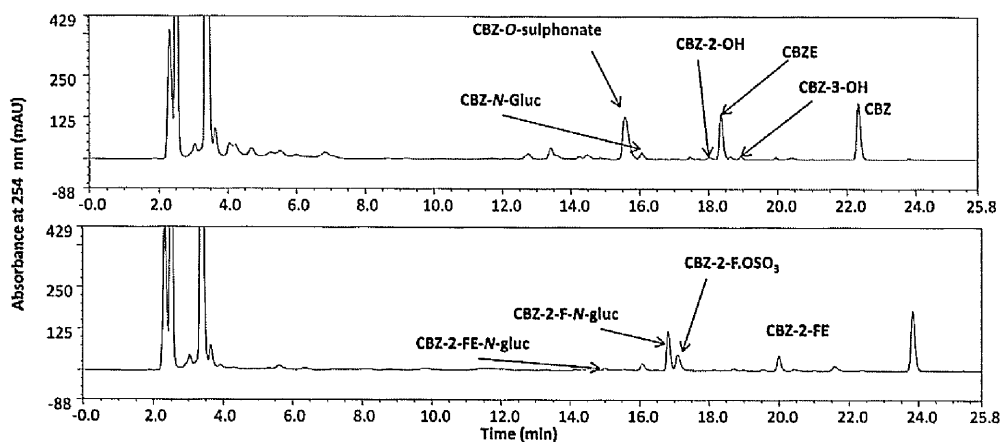
Figure 3.15: LC-UV analysis of CBZ and CBZ-2-F metabolites identified in rat at 50 µM after incubation for 6 h.

Interestingly when searching the TIC for mono-oxygenated 2-F-CBZ metabolites at m/z 271, as shown in **figure 3.16**, it was discovered that 2-F-CBZ formed an O-sulfonate

derivative that eluted at 17.36 min. Although no CBZ-2-OH or CBZ-3-OH type
metabolites were identified by either LC-MS or LC-UV this compound may still be
formed from the conjugation of a ring hydroxylated CBZ derivative.

Searching for m/z corresponding to $[M+H]^+$ for CBZ-2-F (255) in LC-MS analysis did
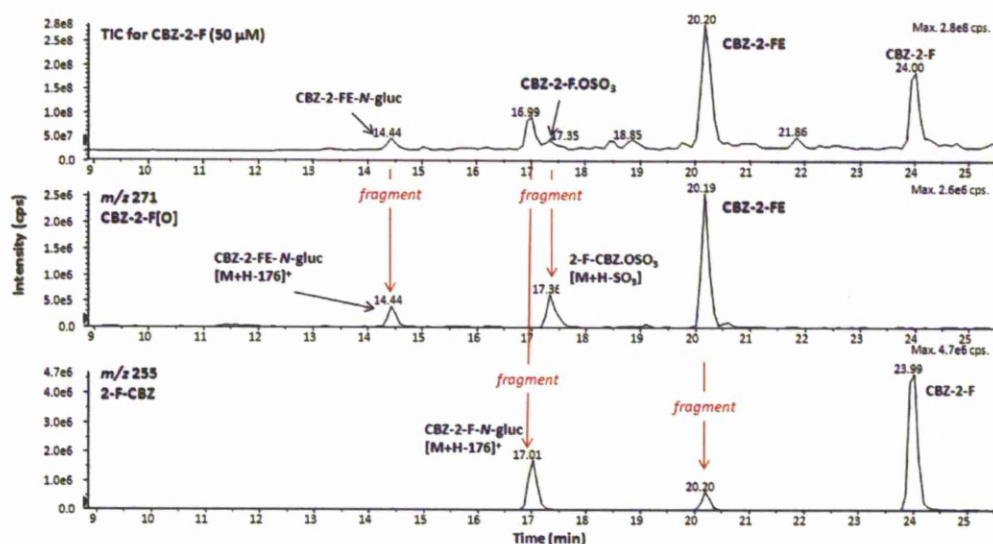not further highlight any other metabolites of the analogue (**figure 3.16**).

Figure 3.16: Identification of mono-oxygenated metabolites and fragments of 2-F-CBZ in rat hepatocytes after 6 h
incubation with 50 μM substrate by LC-MS.

At the time of writing, analysis of CBZ-2-Cl and CBZ-2-Br are not yet complete.
However, at 50 μM both CBZ-2-Cl (**table 3.6**) and CBZ-2-Br (**table 3.7**) are observed to
undergo greater turnover than CBZ. At slightly higher concentrations (200 to 1000 μM),
metabolic pathways begin to be saturated: the turnovers of CBZ-2-Cl and CBZ-2-Br are
slightly reduced when compared to CBZ.

Table 3.6: Total percentage turnover of CBZ and CBZ-2-Cl in rat hepatocytes after 6 h with 50 μM substrate. *Values are the mean ±SEM of two independent isolations.*

Concentration (μM)	CBZ	CBZ-2-Cl
50	64.85 (±15.26)	75.58 (±4.52)
200	31.50 (±1.50)	35.44 (±4.73)
500	27.22 (±1.89)	34.92 (±8.55)
1000	25.36 (±2.20)	19.46 (±9.73)

Table 3.7: Total percentage turnover of CBZ and CBZ-2-Br in rat hepatocytes after 6 h with 50 μM substrate. *Value is the mean ±SEM of one independent isolation.*

Concentration (μM)	CBZ	2-Br-CBZ
50	81.09	93
200	40.48	62.12

The LC-UV traces shown in **figures 3.17** and **3.18** both highlight the high turn-over of CBZ-2-Cl and -2-Br at 50 μM. As in all other assays the *N*-glucuronide and 10,11-epoxide of each derivative were observed and characterised by LC-MS. Yet interestingly these two derivatives represent the greatest turnover of any of the analogues to the *N*-glucuronide. This contrasts vastly with the observations for CBZ and CBZ-2-F where the substrates were observed to undergo similar amounts of 10,11-epoxidation and *N*-glucuronidation. Furthermore, the formation of 2/3-OH derivatives also seems to be completely blocked.
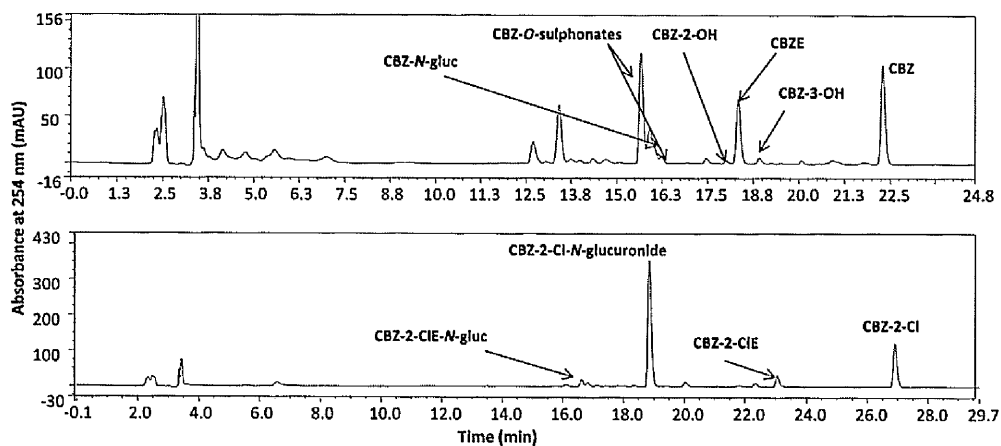
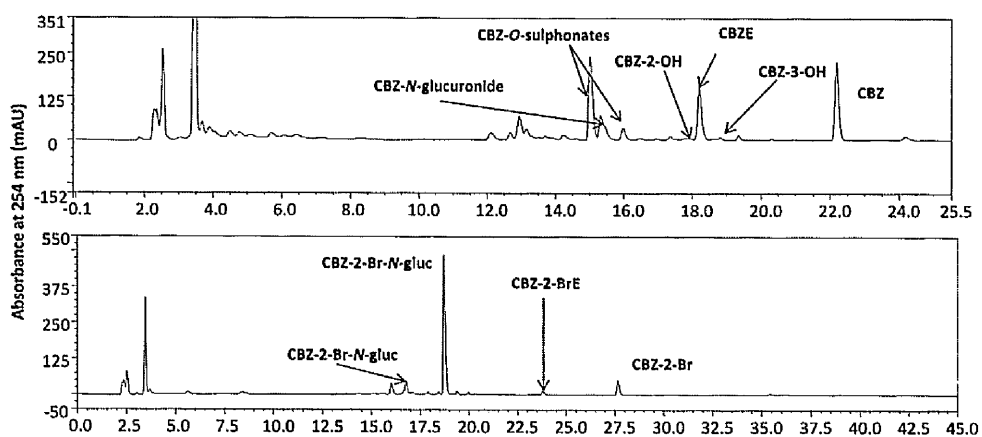Figure 3.17: LC-UV analysis of CBZ and CBZ-2-Cl metabolites identified in rat at 50 µM after incubation for 6 h.

Figure 3.18: LC-UV analysis of CBZ and CBZ-2-Br metabolites identified in rat at 50 µM after incubation for 6 h.

Such an observation for CBZ-2-Cl is in agreement with what is known about the metabolism of imipramine, thus the 3-chloro analogue clomipramine (figure 1.1(b), see chapter 1) exhibits a marked decrease in the degree of oxidative metabolism. By contrast, clomipramine is able to undergo oxidative metabolism on the unsubstituted ring in several animal models, including rat.[32] CBZ-2-Cl was consequently expected to undergo some oxidative metabolism on the unsubstituted ring in hepatocyte suspensions. However no oxidative metabolism of CBZ-2-Cl was observed and while the difference

139

in the position of the chlorine atom could more fully explain the differences in oxidative metabolism if both of the molecules were di-substituted (since both rings would be blocked), it does not explain why clomipramine is able to undergo oxidative metabolism and CBZ-2-Cl is not. Examination of the global minimum conformers for the two molecules (**figure 3.19**) shows that the two molecules adopt different conformations. Of the two, clomipramine shows the greater ring-puckering by virtue of the lack of substitution at the 10-11 position. The lack of substitution means the two arene rings are able to rotate away from each other, minimizing steric and electronic interactions with the halogen and residues in the P450 active site. Although CBZ-2-Cl is also non-planar, it does not show the same distortion of the 7-membered ring as clomipramine and is unable to adopt a variety of different conformers, indicating that it may be a poor substrate for oxidative metabolism.
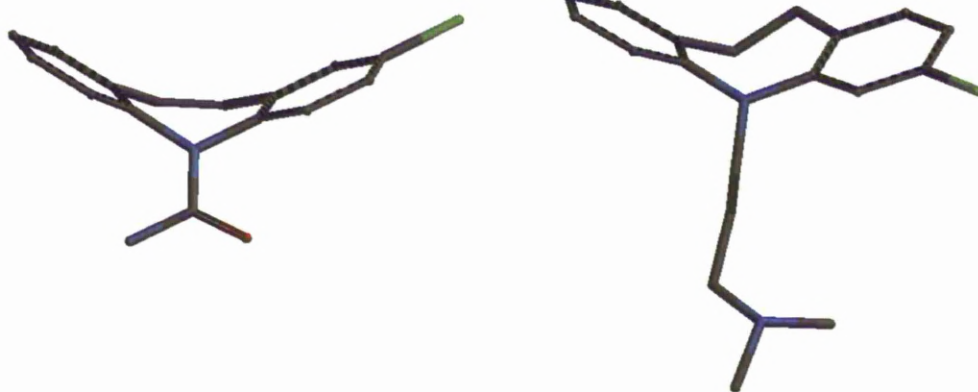

Figure 3.19: Models showing the different preffered conformations of CBZ-2-Cl (left) and clomipramine (right). The geometry was optimised at the Hartree-Fock/3-21G level with a MMFF-AM1 calculation using Spartan '08 v1.2.0 build 132. Hydrogens have been omitted for clarity.

3.3.4 Investigation of the role of oxidative defluorination in CBZ-2-F

In order to investigate what may be the structural determinant of oxidative

defluorination in the hepatocytes (*viz.* *N*-substitution) 2-fluoro iminostilbene (compound

36) was incubated in the freshly isolated suspensions.

Although glutathione has been shown to add to ring systems such as quinones, resulting

in a structure with glutathione directly attached to an aromatic system,[33] the Michael

addition of the glutathione in these cases results in direct formation of an aromatic

system and does not require the loss of a small molecule to restore aromaticity.[34]

However, oxidatative defluorination of fluorobenzenes can occur *via* initial epoxidation,

followed by conjugate addition of gluathione, rearrangement, and defluorination;

yielding a phenoxyl *S*-glutathione adduct after rearomatisation rather than a simple

phenol derivative.[34] This type of rearrangement may be considered to be initiated or

assisted by *N*-oxidation in para-imine structures yielding quinone-imine intermediate

and then a phenolic end product.[35] However, the incorporation of a bulky carboxamide

group, as is the case for CBZ, would be expected to block the quinone-imine pathway of

oxidative defluorination.

It is clear in **figure 3.9** that CBZ-2,8-F does not undergo oxidative defluorination to an

intermediate such as CBZ-2-F-8-OH. This implies that the C-2 substitution prevents

formation of the theoretical 2,3-epoxide precursor of CBZ-2-OH and CBZ-3-OH.

Oxidative defluorination of CBZ-2,8-F or CBZ-2-F could occur by formation of a 1,2 or

2,3 epoxide, but no evidence of a phenoxyl-*S*-glutathione adduct was detected. CBZ-3-

OH has been shown to undergo rapid metabolic activation by human P450 mono-

oxygenases,[20, 36] so the possibility of the loss of the intermediate to another metabolic pathway must be considered.

Metabolic excision of the carboxamide side chain of CBZ yielding 2-hydroxyiminostilbene (ISB-2-OH) was discussed in chapter 1 (section 1.2.1),[37] and both iminostilbene and ISB-2-OH have been identified as minor metabolites of CBZ in humans.[38] Formation of ISB-2-OH from carbamazepine may be oxidative, and dependent upon the introduction of a C-2 hydroxyl function in CBZ, and enzyme assisted excision of the carboxamide group[38] (shown in **figure 1.9** of chapter 1). Rather than by direct oxidation of iminostilbene.
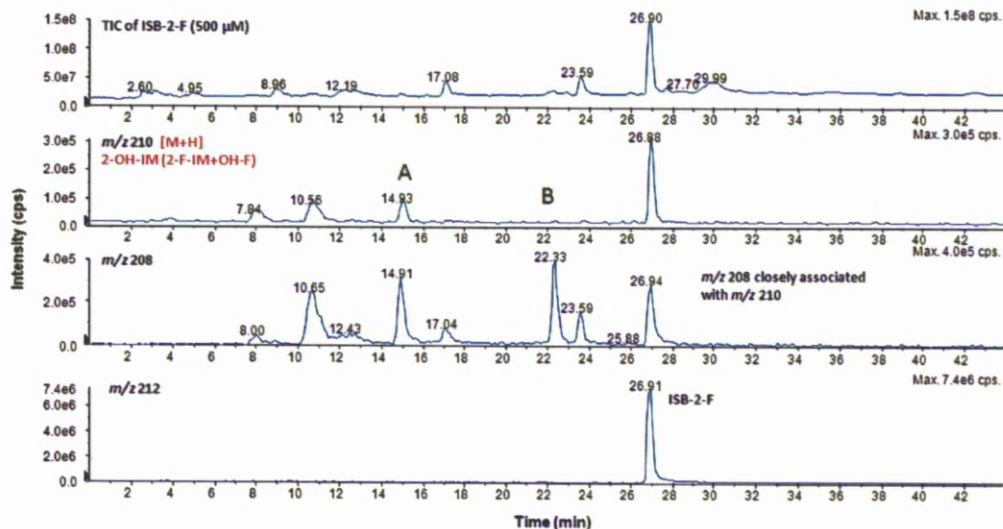
Figure 3.20: Identification of metabolites formed from ISB-2-F after incubation in rat hepatocytes with 500 μM substrate.

Metabolism of ISB-2-F was much more complex than for the CBZ analogues. **Figure 3.20** shows the LC-MS data on the metabolism of ISB-2-F at 500 μM. This

concentration was used for the identification of the metabolites rather than 50 μM as it
was the least complex, and most consistent of all the data.

Oxidative defluorination of ISB-2-F to ISB-2-OH *via* a quinone-imine intermediate
would be expected to yield an [M+H]$^+$ ion of *m/z* 210. Three candidate peaks were
identified by LC-MS in **figure 3.20**. However, each of these peaks was also associated
with abundant *m/z* 208 ions. We speculate that one of these peaks may be associated
with ISB-2-OH, but that it undergoes near quantitative oxidation in the MS source
shown for peaks **A** and **B** in figure **3.21**.
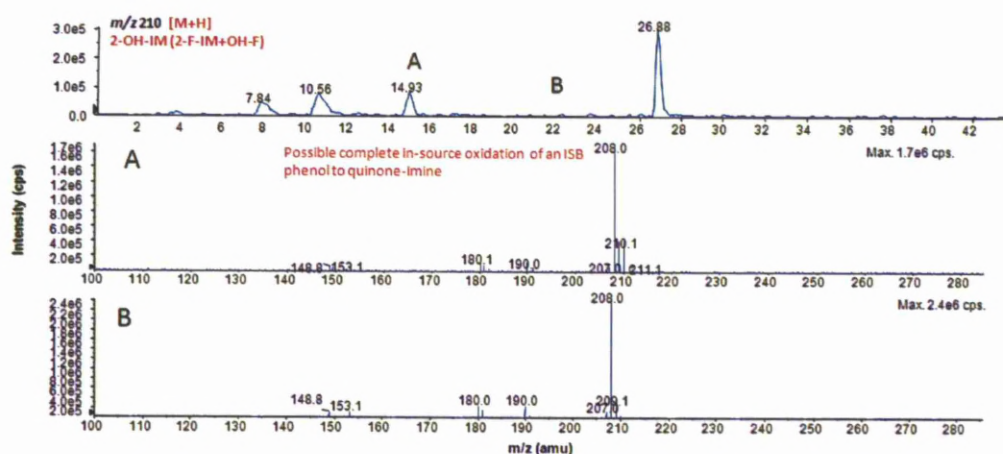
Figure 3.21: XIC chromatogram for *m/z* 210 (top) and mass spectra for two of the candidate peaks showing possible
oxidation of the iminostilbene to a quinone-imine after incubation for 6 h in rat hepatocyte suspensions with 500 μM
substrate.

One other plausible pathway of oxidative defluorination is phenolic hydroxylation or
epoxidation: Pantarotto *et al*[39] identified both the 10,11 epoxide of iminostilbene and
10,11-dihydro-10,11-dihydroxy iminostilbene following intraperitoneal administration
of iminostilbene. The dihydrodiol was also found as a glucuronide. The epoxide-diol
pathway of iminostilbene metabolism was also catalysed by rat liver microsomes.

143

However, no ISB-2-F diol or diol glucuronide was identified in the hepatocyte
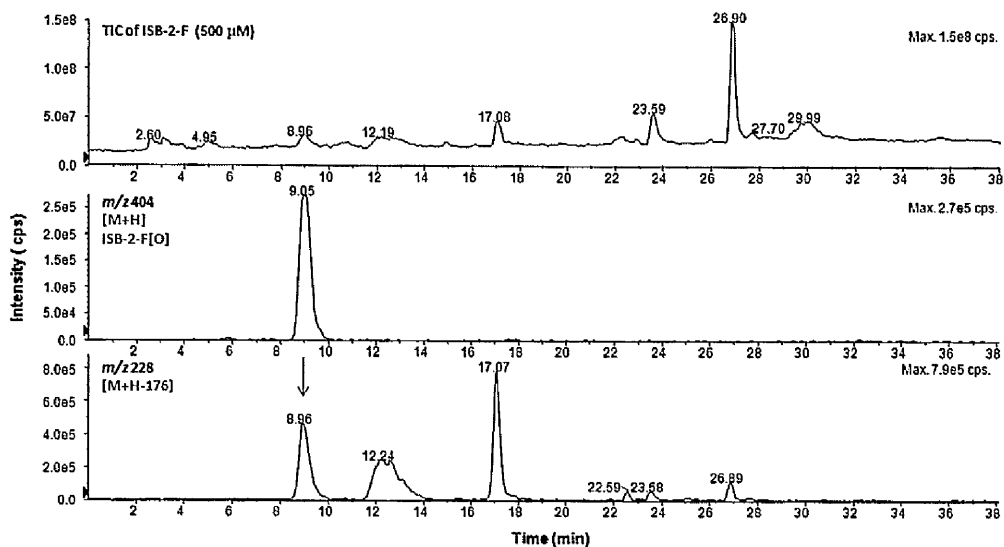incubations and the XIC for m/z 228 (**figure 3.22**).

Figure 3. 22: TIC and XIC chromatograms of ISB-2-F after incubation of 500 μM substrate in rat hepatocytes for 6 h,
showing the O-glucuronide and for formation of a diol m/z 228.

Again, as was the case for **figure 3.20** these ions ([M+H]$^+$) were associated closely with
abundant -2H ions (m/z 226) which is suggestive of in-source oxidation of the
metabolites in the MS. Formation of the N-glucuronide of 2-F-ISB was not observed, but
the oxygenated iminostilbene does appear to undergo glucuronidation (**figure 3.22**).

3.4 Conclusions

Metabolism of CBZ in freshly isolated rat and mouse hepatocyte suspensions was examined to determine which animal would be a more appropriate model of CBZ metabolism in man. The two metabolic profiles were distinct from one another and, because rat hepatocytes yielded the more representative metabolites this was selected as the model for metabolism of the CBZ analogues.

CBZ analogues CBZ-2-F, CBZ-2,8-F, CBZ-2-Cl, CBZ-2,8-Cl, CBZ-2-Br, and CBZ-2,8-Br, were examined for changes in metabolic profile compared to unsubstituted CBZ in rat hepatocytes. All of the analogues displayed a pronounced switch of dominance of the primary metabolic route, from 10,11-epoxidation, to N-glucuronidation.

All the analogues except CBZ-2-F also showed no formation of 2- or 3- hydroxylated derivatives, by either direct hydroxylation or by prevention of formation of an arene oxide.

CBZ-2-F was the only derivative to undergo hydroxylation in the hepatocytes. The location of the sulfonated hydroxyl could not be determined by these methods, and thus the possibility of an NIH-shift type fluorine migration mediated by a 2,3-epoxide intermediate cannot be excluded.

As all of the derivatives formed the 10,11-epoxide to some extent the inhibition of arene oxidation was highly selective, as not even 2,8-dibromination significantly blocked either 10,11-epoxidation or N-glucuronidation.

3.5   References

1.   Björnsson, E., Hepatotoxicity associated with antiepileptic drugs. *Acta Neurologica Scandinavica* **2008**, 118, (5), 281-290.

2.   Lertratanangkoon, K.; Horning, M. G., Metabolism of Carbamazepine. *Drug Metabolism and Disposition* **1982**, 10, (1), 1-10.

3.   Wang, X. Q.; Shi, X. B.; Au, R.; Chen, F. S.; Wang, F.; Lang, S. Y., Influence of chemical structure on skin reactions induced by antiepileptic drugs-The role of the aromatic ring. *Epilepsy Research* **2011**, 94, (3), 213-217.

4.   Madden, S.; Maggs, J. L.; Park, B. K., Bioactivation of carbamazepine in the rat *in vivo*: Evidence for the Formation of Reactive Arene Oxide(s). *Drug Metabolism and Disposition* **1996**, 24, (4), 469-479.

5.   Ahr, H. J.; King, L. J.; Nastainczyk, W.; Ullrich, V., The mechanism of reductive dehalogenation of halothane by liver cytochrome P450. *Biochemical Pharmacology* **1982**, 31, (3), 383-390.

6.   Gómez-Lechón, M. J.; Donato, M. T., In vitro investigation of drug metabolism and toxicity in man. *Anales de la Real Academia Nacional de Farmacia* **2007**, 73, (1), 5-26.

7.   Oesch, F.; Diener, B., Cell systems for use in studies on the relationship between foreign compound metabolism and toxicity. *Pharmacology and Toxicology* **1995**, 76, (5), 325-327.

8.   Tichý, M.; Pokorná, A.; Hanzlíková, I.; Nerudová, J.; Tumová, J.; Uzlová, R., Primary rat hepatocytes in chemical testing and QSAR predictive applicability. *Toxicology in Vitro* **2010**, 24, (1), 240-244.

9.   Piron, F.; Vanthuyne, N.; Joulin, B.; Naubron, J. V.; Cismas, C.; Terec, A.; Varga, R. A.; Roussel, C.; Roncali, J.; Grosu, I., Synthesis, structural analysis, and chiral investigations of some atropisomers with EE-tetrahalogeno-1,3-butadiene core. *Journal of Organic Chemistry* **2009**, 74, (23), 9062-9070.

10. Rogiers, V.; Vercruysse, A., Rat hepatocyte cultures and co-cultures in biotransformation studies of xenobiotics. *Toxicology* **1993**, 82, (1-3), 193-208.

11. Wrighton, S. A.; Ring, B. J.; VandenBranden, M., The use of in vitro metabolism techniques in the planning and interpretation of drug safety studies. *Toxicologic Pathology* **1995**, 23, (2), 199-208.

12. Silverman, I. R.; Daub, G. H.; Vander Jagt, D. L., Methoxybenzo[a]pyrene 4,5-oxides labeled with carbon-13: Electronic effects in the NIH shift. *Journal of Organic Chemistry* **1985,** 50, (26), 5550-5556.

13. Cerqueira, N. M. F. S. A.; Fernandes, P. A.; Ramos, M. J., Understanding Ribonucleotide Reductase Inactivation by Gemcitabine. *Chemistry – A European Journal* **2007,** 13, (30), 8507-8515.

14. Berkowitz, D. B.; Karukurichi, K. R.; de la Salud-Bea, R.; Nelson, D. L.; McCune, C. D., Use of fluorinated functionality in enzyme inhibitor development: Mechanistic and analytical advantages. *Journal of Fluorine Chemistry* **2008,** 129, (9), 731-742.

15. Reboud-Ravaux, M.; Vergely, I.; Maillard, J.; Favreau, C.; Kobaiter, R.; Joyeau, R.; Wakselman, M., Prevention of some types of inflammatory damage using AA 231-1, a fluorinated β-lactam. *Drugs under Experimental and Clinical Research* **1992,** 18, (5), 159-162.

16. Regan, S. L.; Maggs, J. L.; Hammond, T. G.; Lambert, C.; Williams, D. P.; Park, B. K., Acyl glucuronides: The good, the bad and the ugly. *Biopharmaceutics and Drug Disposition* **2010,** 31, (7), 367-395.

17. Maggs, J. L.; Pirmohamed, M.; Kitteringham, N. R.; Park, B. K., Characterization of the metabolites of carbamazepine in patient urine by liquid chromatography/mass spectrometry. *Drug Metabolism and Disposition* **1997,** 25, (3), 275-280.

18. Cnubben, N. H. P.; Vervoort, J.; Boersma, M. G.; Rietjens, I. M. C. M., The effect of varying halogen substituent patterns on the cytochrome P450 catalysed dehalogenation of 4-halogenated anilines to 4-aminophenol metabolites. *Biochemical Pharmacology* **1995,** 49, (9), 1235-1248.

19. Madden, S.; Maggs, J. L.; Kitteringham, N. R.; Pirmohamed, M.; Park, B. K., Bioactivation of carbamazepine in the rat in vivo. *British Journal of Clinical Pharmacology* **1996,** 41, (5).

20. Bu, H. Z.; Zhao, P.; Dalvie, D. K.; Pool, W. F., Identification of primary and sequential bioactivation pathways of carbamazepine in human liver microsomes using liquid chromatography/tandem mass spectrometry. *Rapid Communications in Mass Spectrometry* **2007,** 21, (20), 3317-3322.

21. Pirmohamed, M.; Kitteringham, N. R.; Park, B. K., Idiosyncratic reactions to antidepressants: A review of the possible mechanisms and predisposing factors. *Pharmacology and Therapeutics* **1992,** 53, (1), 105-125.

22. Guroff, G.; Kondo, K.; Daly, J., The production of meta-chlorotyrosine from para-chlorophenylalanine by phenylalanine hydroxylase. *Biochemical and Biophysical Research Communications* **1966**, 25, (6), 622-628.

23. Mutch, P. J.; Dear, G. J.; Ismail, I. M., Formation of a defluorinated metabolite of a quinoxaline antiviral drug catalysed by human cytochrome P450 1A2. *Journal of Pharmacy and Pharmacology* **2001**, 53, (3), 403-408.

24. Van, Q. E.; Simon, G.; El, Y. M.; Tuti, J.; Van, D. H. L.; Darro, F.; Kiss, R. Compositions and methods using ureyl-substituted naphthalimide derivatives for the treatment of esophageal cancer. US20090232907A1, 2009.

25. Furst, S. M.; Uetrecht, J. P., Carbamazepine metabolism to a reactive intermediate by the myeloperoxidase system of activated neutrophils. *Biochemical Pharmacology* **1993**, 45, (6), 1267-1275.

26. Furst, S. M.; Uetrecht, J. P., The effect of carbamazepine and its reactive metabolite, 9-acridine carboxaldehyde, on immune cell function in vitro. *International Journal of Immunopharmacology* **1995**, 17, (5), 445-452.

27. Mathieu, O.; Dereure, O.; Hillaire-Buys, D., Presence and ex vivo formation of acridone in blood of patients routinely treated with carbamazepine: Exploration of the 9-acridinecarboxaldehyde pathway. *Xenobiotica* **2011**, 41, (2), 91-100.

28. Regan, S. L. In vitro and in vivo models for the investigation of drug bioactivation and drug-induced liver injury. University of Liverpool, Liverpool, 2009.

29. Lillibridge, J. H.; Amore, B. M.; Slattery, J. T.; Kalhorn, T. F.; Nelson, S. D.; Finnell, R. H.; Bennett, G. D., Protein-reactive metabolites of carbamazepine in mouse liver microsomes. *Drug Metabolism and Disposition* **1996**, 24, (5), 509-514.

30. Park, B. K.; Kitteringham, N. R.; O'Neill, P. M., Metabolism of fluorine-containing drugs. In 2001; Vol. 41, pp 443-470.

31. O'Hagan, D.; Rzepa, H. S., Some influences of fluorine in bioorganic chemistry. *Chemical Communications* **1997**, (7), 645-652.

32. Janetka, J. W.; Almeida, L.; Ashwell, S.; Brassil, P. J.; Daly, K.; Deng, C.; Gero, T.; Glynn, R. E.; Horn, C. L.; Ioannidis, S.; Lyne, P.; Newcombe, N. J.; Oza, V. B.; Pass, M.; Springer, S. K.; Su, M.; Toader, D.; Vasbinder, M. M.; Yu, D.; Yu, Y.; Zabludoff, S. D., Discovery of a novel class of 2-ureido thiophene carboxamide checkpoint kinase inhibitors. *Bioorg. Med. Chem. Lett.* **2008**, 18, 4242-4248.

33. Nelson, S. D.; Vaishnav, Y.; Kambara, H.; Baillie, T. A., Comparative electron impact, chemical ionization and field desorption mass spectra of some thioether metabolites of acetaminophen. *Biological Mass Spectrometry* **1981**, 8, (6), 244-251.

34. Yergey, J. A.; Trimble, L. A.; Silva, J.; Chauret, N.; Li, C.; Therien, M.; Grimm, E.; Nicoll-Griffith, D. A., In Vitro Metabolism of the COX-2 Inhibitor DFU, Including a Novel Glutathione Adduct Rearomatization. *Drug Metabolism and Disposition* **2001**, 29, (5), 638-644.

35. Chen, W.; Shockcor, J. P.; Tonge, R.; Hunter, A.; Gartner, C.; Nelson, S. D., Protein and Nonprotein Cysteinyl Thiol Modification by N-Acetyl-p-benzoquinone Imine via a Novel Ipso Adduct†. *Biochemistry* **1999**, 38, (25), 8159-8166.

36. Pearce, R. E.; Lu, W.; Wang, Y.; Uetrecht, J. P.; Correia, M. A.; Leeder, J. S., Pathways of Carbamazepine Bioactivation in Vitro. III. The Role of Human Cytochrome P450 Enzymes in the Formation of 2,3-Dihydroxycarbamazepine. *Drug Metabolism and Disposition* **2008**, 36, (8), 1637-1649.

37. Pearce, R. E.; Uetrecht, J. P.; Leeder, J. S., Pathways of carbamazepine bioactivation in vitro: II. The role of human cytochrome P450 enzymes in the formation of 2-hydroxyiminostilbene. *Drug Metabolism and Disposition* **2005**, 33, (12), 1819-1826.

38. Ju, C.; Uetrecht, J. P.; Van Koppen, C. J., Detection of 2-hydroxyiminostilbene in the urine of patients taking carbamazepine and its oxidation to a reactive iminoquinone intermediate. *Journal of Pharmacology and Experimental Therapeutics* **1999**, 288, (1), 51-56.

39. Pantarotto, C.; Martini, A.; Belvedere, G.; Bossi, A.; Donnelli, M. C.; Frigerio, A., Application of gas chromatography—chemical ionization mass fragmentography in thed evaluation of bases and nucleoside analogues used in cancer chemotherapy. *Journal of Chromatography A* **1974**, 99, (0), 519-527.

Conclusions

Chapter 4

This chapter summarises the key findings of chapter 2 and chapter 3 and discusses where the project could go in the future.

Contents

4. Conclusions

A range of 2- and 2,8-di substituted CBZ analogues were prepared from the appropriate iminostilbenes. Two different strategies were employed in the synthesis of these analogues: Direct electrophilic halogenations of iminodibenzyl or efficient ring expansions of an appropriate *N*-aryl indole with polyphosphoric acid. The strategy used to form each derivative is largely dependent upon what halogen is being incorporated into the molecule.

While direct electrophilic bromination of iminodibenzyl was efficient for formation of the di-brominated derivative, it was not so for the synthesis of the monobrominated derivative. Where synthesis of 2-bromo iminostilbene was subject to the formation of mixtures of isomers during the radical bromination step used to incorporate the 10,11-double bond. While time precludes further optimization of this procedure, the use of a more deactivating protecting group at *N*-5 may be more suitable to attenuate formation of the isomers. Nonetheless, electrophilic chlorination was found to be a reasonable, if slow, procedure for the synthesis of both the 2- and 2,8-dichloro derivatives. In the case of 2-chloro the formation of isomers in a manner analogues to 2-bromo was not observed, and greater deactivation of the arene rings by chlorine is considered to be a contributing factor.[1]

The cyclisation of *N*-aryl indoles to iminostilbenes has previously been described.[2] However, it was noted that the cyclisation of electrophilic derivatives was poor. That fluorine substituted *N*-aryl indoles were able to undergo efficient cyclisation to iminostilbenes highlights the unique electronic properties of fluorine.

This reaction was usefully extended to a wide range of differently substituted fluorinated iminostilbenes and separation of regioisomers, formed by some *N*-aryl indoles, by column chromatography was found to be possible.

The reaction was also found to be usefully extended to the formation of both 2- and 2,8- chlorine substituted derivatives; and although dehalogenation is thought to occur during the reaction, the mixtures are easily separated. Furthermore the method is exceptionally high yielding for both derivatives and represents the more efficient method for formation of these analogues.

Given the success of the chlorinated analogues the extension of the reaction to form mono and di-brominated derivatives was examined. However, the reaction was very difficult to control leading to complex mixtures of products that were not easily separated. However isolation of a small quantity of 2-bromo iminostilbene was achieved with a small amount of optimization of the reaction conditions.

Incorporation of the carboxamide side-chain was not a trivial transformation. Several methods of incorporating this side chain into the derivatives were attempted. However, additional deactivation of *N*-5 by the incorporation of the halogens in the arene rings and increased solubility of the compounds reduced the suitability of commonly employed strategies, such as phosgenation to incorporate the side chain.

Transformation was finally achieved with alkali metal isocyanates and trifluoroacetic acid. This reaction was both high yielding and convenient for isolation of the carbamazepines for all of the derivatives. This is interesting in light of the failure of trichloroacetyl isocyanate to react with certain derivatives. On-balance the possibility of traces of trichloroacetic acid auto catalyzing the transformation and rapid

decomposition of the reagent once exposed to air are considered to be additional contributing factors for the failure of this reagent to react with certain derivatives.

The compounds utilized in the structure metabolism study were designed to identify the minimum aryl substitution, in respect of steric bulk, required to completely inhibit the aromatic hydroxylation of carbamazepine, and thus the formation of electrophilic arene oxide precursors that have been hypothetically linked to the formation of ADRs.[3-5]

This objective was efficiently achieved with the 2-chloro and 2,8-difluoro derivatives without significantly affecting formation of the 10,11 epoxide. The substituent effect compares well with the reduction of oxidative metabolism observed by substitution of Cl at C-3 of imipramine. Although oxidative dehalogenation is known for many halogenated aromatics, both chlorinated,[6] and fluorinated,[7] none of the analogues were observed to undergo this reaction in rat hepatocytes. Remarkably, the steric hindrance of the 2-chloro and 2-bromo derivatives was observed to be sufficient to block the hydroxylation of both the unsubstituted ring and the functionalized one. Monohalogenation of an aromatic ring is capable of blocking hydroxylation entirely, yet it is not consistent across a variety of halogenated aromatic rings.[8] Arene oxidation can occur, and in some cases extensively,[7] at ring carbons adjacent to and more distant from fluorine- and chlorine- substituted carbons. Thus the C-3 chlorine of clomipramine (3-chloroimipramine) fails to prevent hydroxylation at C-2 as well as hydroxylation of the unsubstituted ring.[9] However, only CBZ-2-F was the only derivative to undergo detectable hydroxylation in the hepatocytes. The exact structure of this metabolite could not be determined, and NIH-shifting of the fluorine intermediate may occur[7,10, 11] *via* a 2,3-arene oxide cannot be excluded. The chemical

shift of fluorine in ^{19}F NMR is highly sensitive to its chemical environment,[12] this coupled with the high sensitivity of ^{19}F NMR[12] could allow indentification of an NIH shifted metabolite of CBZ-2-F, or and oxidatitive de-fluorination yielding fluoride ions. Formation of the 10,11-epoxide is the major metabolic fate of CBZ in man[5] however even incorporation of two bromine atoms into the parent structure was not enough to significantly block formation of this metabolite. Indicating that the blockade of the ring-oxygenated metabolites is selective.

Formation of the *N*-glucuronide was not significantly reduced; indeed in some cases the formation of the *N*-glucuronide was increased. That such compounds are more effectively conjugated to glucuronic acid is not necessarily an indicator of an inherently toxic compound. Indeed, the fact that they are efficiently transformed to the *N*-glucuronide suggests that they may be more efficiently cleared from the host and would thus be safer pharmaceuticals, although this would be expected to have an adverse effect on pharmacological activity of the compound. Consequently, it is CBZ-2,8-F and CBZ-2-Cl that may be expected to have the minimum effect on the pharmacological properties compared to CBZ.

4.1 References

1. Duan, S.; Turk, J.; Speigle, J.; Corbin, J.; Masnovi, J.; Baker, R. J., Halogenations of anthracenes and dibenz[a,c]anthracene with N-bromosuccinimide and N-chlorosuccinimide. *J. Org. Chem.* **2000**, 65, (10), 3005-3009.

2. Tokmakov, G. P.; Grandberg, I. I., Rearrangement of 1-arylindoles to 5H-dibenz[b,f]azepines. *Tetrahedron* **1995**, 51, (7), 2091-2098.

3. Madden, S.; Maggs, J. L.; Park, B. K., Bioactivation of carbamazepine in the rat *in vivo*: Evidence for the Formation of Reactive Arene Oxide(s). *Drug Metabolism and Disposition* **1996**, 24, (4), 469-479.

4. Madden, S.; Maggs, J. L.; Kitteringham, N. R.; Pirmohamed, M.; Park, B. K., Bioactivation of carbamazepine in the rat in vivo. *British Journal of Clinical Pharmacology* **1996**, 41, (5).

5. Maggs, J. L.; Pirmohamed, M.; Kitteringham, N. R.; Park, B. K., Characterization of the metabolites of carbamazepine in patient urine by liquid chromatography/mass spectrometry. *Drug Metabolism and Disposition* **1997**, 25, (3), 275-280.

6. Wen, B.; Ma, L.; Nelson, S. D.; Zhu, M., High-Throughput Screening and Characterization of Reactive Metabolites Using Polarity Switching of Hybrid Triple Quadrupole Linear Ion Trap Mass Spectrometry. *Analytical Chemistry* **2008**, 80, (5), 1788-1799.

7. Dear, G. J.; Ismail, I. M.; Mutch, P. J.; Plumb, R. S.; Davies, L. H.; Sweatman, B. C., Urinary metabolites of a novel quinoxaline non-nucleoside reverse transcriptase inhibitor in rabbit, mouse and human: Identification of fluorine NIH shift metabolites using NMR and tandem MS. *Xenobiotica* **2000**, 30, (4), 407-426.

8. Li, C.; Chauret, N.; Trimble, L. A.; Nicoll-Griffith, D. A.; Silva, J. M.; MacDonald, D.; Perrier, H.; Yergey, J. A.; Parton, T.; Alexander, R. P.; Warrellow, G. J., Investigation of the in Vitro Metabolism Profile of a Phosphodiesterase-IV Inhibitor, CDP-840: Leading to Structural Optimization. *Drug Metabolism and Disposition* **2001**, 29, (3), 232-241.

9. Nielsen, K. K.; Flinois, J. P.; Beaune, P.; Brøsen, K., The biotransformation of clomipramine in vitro, identification of the cytochrome P450s responsible for the separate metabolic pathways. *Journal of Pharmacology and Experimental Therapeutics* **1996**, 277, (3), 1659-1664.

10. Park, B. K.; Kitteringham, N. R.; O'Neill, P. M., Metabolism of fluorine-containing drugs. In 2001; Vol. 41, pp 443-470.

11. Koerts, J.; Soffers, A. E. M. F.; Vervoort, J.; De Jager, A.; Rietjens, I. M. C. M., Occurrence of the NIH shift upon the cytochrome P450-catalyzed in vivo

and in vitro aromatic ring hydroxylation of fluorobenzenes. *Chemical Research in Toxicology* **1998,** 11, (5), 503-512.

12.   Vervoort, J.; De Jager, P. A.; Steenbergen, J.; Rietjens, I. M. C. M., Development of a 19F-n.m.r. method for studies on the in vivo and in vitro metabolism of 2-fluoroaniline. *Xenobiotica* **1990,** 20, (7), 657-670.

Experimental Methods and Techniques: Chemistry

Chapter 5

This chapter describes the synthetic methods and physical data of the compounds discussed in chapter 2

Contents

5. *Experimental Methods and Techniques: Chemistry*

5.1 *General Experimental*

Moisture sensitive reactions were carried out in anhydrous organic solvents (purchased from Sigma-Aldrich™ or Fluka) under Nitrogen or Argon atmosphere using oven dried glassware and a vacuum manifold to maintain the atmosphere.

Halogenated indoles and benzenes were purchased from fluorochem and used as received. All other reagents were purchased from Sigma-Aldrich™ and used as received.

Thin Layer Chromatography (TLC) and Flash Chromatography

Reactions were monitored by comparative thin layer chromatography using Merck aluminium-backed Kieselgel 60 F_{254} silica plates, and were viewed with a UV lamp (λ 254 nm) or by staining with anisaldehyde, vanillin, $KMnO_4$, iodine, or bromocresol green.

Preparative column chromatography was performed on VWR PROLABO® silica gel for flash chromatography or Sigma-Aldrich™ silica gel for flash chromatography particle size 40-63 Å. Unless specifically stated in the text separation of compounds was achieved with a product to silica ratio of 1:25.

Analytical and Preparative HPLC methods

Purity analysis of carbamazepine analogues was performed by LC-MS and LC-UV (HPLC) methods.

LC-MS Method

For LC-MS analysis, aliquots (10 μL) of acetonitrile solutions (0.5 mg/mL) of the carbamazepine derivative were injected onto the HPLC column without further treatment. The solutions were chromatographed at room temperature on a Phenominex Gemini-NX 5-μm C18 110 Å column (250 × 4.6 mm i.d.) by gradient elution with acetonitrile/0.1 % formic acid (15 %, 5 min; 15→50 %, 20 min; 50→75 %, 3 min; 15 %, 5 min) in 25 mM ammonium acetate, pH 3.8. The eluent flow rate was 1.0 mL/min

The LC system consisted of a PerkinElmer Series 200 pump and a PerkinElmer Series 200 autosampler.

The flow rate of eluate to the LC-MS interface was *ca.* 160 μL/min. An AB Sciex API 2000 mass spectrometer was operated with a TurboIonSpray electrospray source. The interface temperature was 400 °C; electrospray capillary voltage, 5.0 kV; heater gas (Gas2) setting, 75. The instrument was set up for full scanning (Q1) acquisitions in the positive-ion mode as follows: scan range *m/z* 100-1000, with a scan time of 5 s. Instrument management and data processing was accomplished through Analyst 1.4 software.

Preparative HPLC

For purification of samples by preparative HPLC, aliquots (800 μL) of acetonitrile solutions (10 mg/mL) of the carbamazepine derivative were injected onto the HPLC column without further treatment. The solutions were chromatographed at room temperature on a Knauer erurosphere 100-5 Si column (250 × 20 mm i.d.) by gradient

elution with acetonitrile (34 %, 10 min; 34→66 %, 15 min; 66→75 %, 40 min; 75-34 %, 45 min) in 25 mM ammonium acetate, pH 3.8. The eluent flow rate was 10.0 mL/min. UV detection was set at λ 254 nm. Instrument management and data processing was accomplished through Clarity software.

Analytical HPLC

For analytical HPLC analysis, aliquots (10 μL) of acetonitrile solutions (0.5 mg/mL) of the carbamazepine derivative were injected onto the HPLC column without further treatment. The solutions were chromatographed at room temperature on a Phenominex Gemini-NX 5-μm C18 110 Å column (250 × 4.6 mm i.d.) by gradient elution with acetonitrile (15 %, 5 min; 15→50 %, 20 min; 50→75 %, 3 min; 15 %, 5 min) in 25 mM ammonium acetate. The gradient was delivered with a Dionex Summit HPLC System at a flow rate of 1ml/min through a UVD170S UV detector set at 254 nm (Dionex). Instrument management and data processing were accomplished through Chromeleon software.

IR spectroscopy

Infra red spectra were recorded on a Jasco FTIR ATR spectrometer and are recorded as a neat liquid, or a ground solid, except where stated in the text.

Melting points

Melting points were recorded using Bibby-Sterlin Stuart SMP3 melting point apparatus and are uncorrected.

Mass Spectrometry

High resolution mass spectrometry for the N-aryl indoles and fluorinated iminostilbenes were performed by the National Mass Spectrometry Service based in Swansea. Analysis of carbamazepine analogues below molecular weight 300 were performed by the Mass Spectrometry Service at the University of Oxford. All other samples were obtained in electrospray mode (ES) with a micromass LCT mass spectrometer or a trio 1000 mass spectrometer in chemical ionization mode (CI) with ammonia as the CI gas. Mass spectra were recorded in the positive or negative mode as indicated in the text.

CHN Microanalysis

Elemental analyses for fluorinated N-aryl indoles and iminostilbenes were performed by Mr. Stephen Boyer of London Metropolitan University. Non-fluorinated samples were analysed by Mr. Steve Apter of the University of Liverpool.

NMR spectroscopy

^{1}H, ^{13}C and ^{19}F NMR Spectra were obtained using a Bruker Avance or a bruker DPX 400 instrument operating at 400, 100 and 376 MHz respectively. spectral data are reported in ppm (δ) relative to their residual solvent peaks.[1] Coupling constants (J) are reported in Hz.

5.2 Direct electrophilic halogenation:

The methods outlined below record the highest yielding large-scale preparations of coumpounds **2-5**. Reaction conditions for the reactions to generate the tables in chapter 2 are listed under each table.

2-bromo-10,11-dihydro-5H-dibenz[b,f]azepine 2: Iminodibenzyl (3.624 g, 18.54 mmol) were dissolved in $CHCl_3$ (100 mL) pre-dried silica gel (~2.000 g per 1.0 mmol of NBS) added. The mixture was stirred gently with overhead stirring and the reaction vessel covered with foil to exclude light from the reaction. NBS (3.021 g, 16.86 mmol) as solution in $CHCl_3$ (15 mL) was then added dropwise over 20 min at room temperature. Once addition of NBS was complete the reaction was left to stir for a further 10 min before vacuum filtration to remove the silica. The silica cake was then washed with $CHCl_3$ (2 × 20 mL). The filtrate was washed with water (2 × 150 mL) and dried over Na_2SO_4, filtered and concentrated *in vacuo*. The crude product was purified by column chromatography, with neat hexane as eluent, to return the product a white powder. 2.871 g, 62 %; mp 102.0-103.1 °C (lit[2] 100-101 °C); ^{1}H NMR (400 MHz, $CDCl_3$) δ 7.12 - 7.17 (m, 1 H, H-C^1), 7.01 - 7.11 (m, 3 H), 6.68 - 6.84 (m, 3 H), 5.96 (br. s., 1 H, H-N), 3.00 - 3.10 (m, 4 H$_2$-C^{10,11}); ^{13}C NMR (101 MHz, $CDCl_3$) δ 142.4, 141.6, 133.0, 130.7, 129.5, 128.6, 128.5, 126.9, 119.9, 119.4, 117.9, 111.2, 34.7, 34.6; IR (cm^{-1}) 3386.39 (w, secondary amine stretch), 1484 (s), 1457 (m, aromatic CH stretch), 802 (m); MS (CI+, m/z) 274 (100), 276 (97) [MH]$^+$.
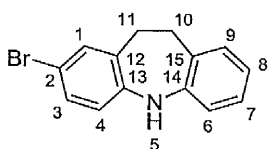
Spectral data in agreement with those published in [2]
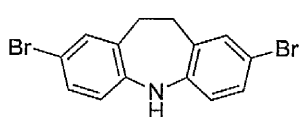
2,8-dibromo-10,11-dihydro-5H-dibenz[b,f]azepine   **3:**

Iminodibenzyl (5.018 g, 25.70 mmol) were dissolved in CHCl₃ (300 mL) pre-dried silica gel (~2.000 g per 1.0 mmol of NBS) added. The mixture was stirred gently with overhead stirring and the reaction vessel covered with foil to exclude light from the reaction. NBS (9.152 g, 51.04 mmol) as solution in CHCl₃ (200 mL) was then added dropwise over 1 h at room temperature. Once addition of NBS was complete the reaction was left to stir for a further 20 min before vacuum filtration to remove the silica. The silica cake was then washed with CHCl₃ (2 × 150 mL). The filtrate was washed with water (2 × 350 mL) and dried over Na₂SO₄, filtered and concentrated *in vacuo*. The crude product was purified by column chromatography hexane → 1:9 ethyl acetate/hexane to return the product as pale blue needles. 7.214 g, 78 %, mp 153.7-154.9 °C (lit[2] 177-178 °C); ^{1}H NMR (400 MHz, CDCl₃) δ 7.14 - 7.18 (dd, J = 9.1, 2.4 Hz, 2 H, H-C^{3,7}) 7.13 (d, J = 2.4 Hz, 1 H, H-C^{1,9}) 6.60 (d, J = 9.1 Hz, 1 H, H-C^{4,6}) 5.95 (br. s., 1 H, H-N^5) 3.01 (s, 4 H, H-C^{10,11}); ^{13}C NMR (101 MHz, CDCl₃) δ 141.0, 133.1, 130.4, 129.6, 119.6, 111.7, 34.3; IR (cm^{-1}) 3402 (w, secondary amine stretch), 1485 (m), 1342 (m), 802 (m); MS (ES-, *m/z*) 350 (51), 351 (100), 353 (49) [M-H]⁻.

Spectral data in agreement with those published in [2]
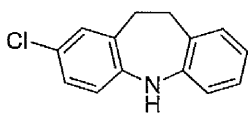
2-chloro-10,11-dihydro-5H-dibenz[b,f]azepine 4: Iminodibenzyl (4.024 g, 20.59 mmol) was dissolved in EtOAc (300 mL), pre-dried silica gel (~2.000 g per 1.0 mmol of NCS) added. The mixture was stirred gently with overhead stirring and the reaction vessel covered with foil to exclude light from the reaction. NCS (3.021 g, 16.86 mmol) was added portion-wise over 40 min at

room temperature. Once addition of NCS was complete the reaction was left to stir for 72 h before vacuum filtration to remove the silica. The silica cake was then washed with EtOAc (2 × 150 mL). The filtrate was washed with water (2 × 250 mL) and dried over Na_2SO_4, filtered and concentrated *in vacuo*. The crude product was purified by column chromatography, hexane → 1:4 ethyl acetate/hexane to return the product as a pale green powder, 1.013 g, 24 %, mp 89.0-89.8 °C, ^{1}H NMR (400 MHz, Acetone-d_6) δ 7.73 (br. s., 1 H, H-N^5) 6.99 - 7.07 (m, 4 H,) 6.90 - 6.97 (m, 2 H) 6.65 - 6.75 (m, 1 H, H-C^1) 3.03 (s, 4 H, H-C^{10,11}); ^{13}C NMR (101 MHz, Acetone-d_6) δ 144.5, 142.9, 131.4, 131.3, 131.1, 129.6, 129.5, 127.9, 127.8, 120.9, 120.1, 119.3, 36.3, 35.6; IR (cm^{-1}) 3379 (w, secondary amine stretch); 1481 (s); 813 (m); MS (CI+, *m/z*) 230 (100), 232 (34) [M+H]$^+$, HRMS: found, *m/z* 230.0734; $C_{14}H_{13}^{35}ClN$ (MH$^+$) requires *m/z* 230.0707.
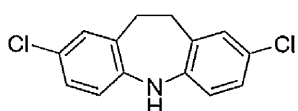
2,8-dichloro-10,11-dihydro-5H-dibenz[*b,f*]azepine

5: Iminodibenzyl (2.496 g, 12.80 mmol) was dissolved in CHCl$_3$ (350 mL) pre-dried silica gel (~2.000 g per 1.0 mmol of NCS) added. The mixture was stirred gently with overhead stirring and the reaction vessel covered with foil to exclude light from the reaction. NCS (3.421 g, 25.61 mmol) was then added portion-wise over 1 h at room temperature. Once addition of NCS was complete the reaction was left to stir for a further 48 h before vacuum filtration to remove the silica. The silica cake was then washed with CHCl$_3$ (2 × 250 mL). The filtrate was washed with water (2 × 500 mL) and dried over Na$_2$SO$_4$, filtered and concentrated *in vacuo*. The crude product was purified by column chromatography hexane → 1:9 ethyl acetate/hexane to return the product as pale a beige powder, 2.712 g, 80%. mp 113.7-114.8 °C, 1H NMR (400 MHz, Acetone-d_6) δ 7.93 (s, 1H, H-N^5); 7.08-7.07 (d, 2H, *J*=

2.4 Hz, $\underline{H}$-C^{1,9}); 7.06-7.04 (dd, 2H, J = 8.4, 2.5 Hz, $\underline{H}$-C^{3,7}); 6.97-6.95 (d, 2H, J = 8.48

Hz, $\underline{H}$-C^{4,6}); 2.89 (s, 4H, $\underline{H}$-C^{10,11}); ^{13}C NMR (400 MHz, Acetone-d_6) δ 141.0, 129.4,

130.1, 125.4, 120.9, 123.6, 32.5; IR (cm^{-1}); 3399.9 (m, secondary amine stretch), 1484

(s), 1330(m), 802.2 (m); MS (ES+, m/z) 263 (100), 265 (64), 266 (12) [M+H]$^+$; HRMS:

found, m/z 264.0341; C$_{14}$H$_{12}$^{35}Cl$_2$N (MH$^+$) requires m/z 264.0347.

5.3 General Reaction Procedure for N-acyl protection of iminodibenzyls

Iminodibenzyl derivatives (5.00 mmol) and DMAP (5.00 mmol) were dissolved in

toluene (25 mL), and gently heated to reflux. AcCl (6.00 mmol) was then added

dropwise and the reaction left at reflux for 24 h. Once reaction was judged to have

progressed to completion by TLC (1:9 EtOAc/hexane; KMnO$_4$ stains the N-acyl product

yellow) the reaction was cooled to room temperature and partitioned between EtOAc

and water. The aqueous phase was washed with EtOAc (2 × 50 ml) and the combined

organic extracts backwashed with water (1 × 50 mL) saturated NaHCO$_{3(aq)}$ (1 × 50 ml)

and brine (1 × 50 ml) then dried over Na$_2$SO$_4$, filtered and concentrated *in vacuo* to yield

the crude material. Crude products were then purified by column chromatography 1:7

EtOAc/Hexane to yield the purified products as colourless oils.

1-(2-bromo-10,11-dihydro-5H-dibenz[b,f]azepin-5-yl)ethanone 6: compound 2 (1.35
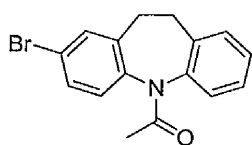
g, 4.98 mmol) was treated according to the general method

described above to yield the product as a colourless oil, 1.224 g,

78 %; ^{1}H NMR (400 MHz, CDCl$_3$) δ 7.46 - 6.94 (m, 7 H),

3.52 - 3.18 (m, 2 H, $\underline{H}_2$-C^{10}), 2.93 - 2.70 (m, 2 H, $\underline{H}_2$-C^{11}), 2.13 - 1.82 (s, 3 H, COC$\underline{H}_3$);

The ^{13}C NMR of this compound is complex and does not account for the different

conformers present in the solution: ^{13}C NMR (101 MHz, CDCl$_3$) δ = 170.5, 142.5,

142.2, 139.9, 138.8, 137.7, 137.4, 137.1, 136.6, 134.4, 133.3, 132.8, 130.5, 130.3, 129.8,

129.5, 129.2, 128.9, 128.7, 128.5, 128.4, 128.1, 127.6, 127.5, 127.4, 127.4, 127.2, 126.7,

126.4, 125.2, 30.9, 30.1, 22.6; IR (cm^{-1}) 3032 (w, aromatic CH stretch), 1678 (s, tertiaty

amide C=O stretch). 1550 (m), 1485 (s); MS (CI+, m/z) 346 (100), 318 (88) [MH]$^+$.

1-(2,8-dibromo-10,11-dihydro-5H-dibenz[b,f]azepin-5-yl)ethanone 7: Compound **3**
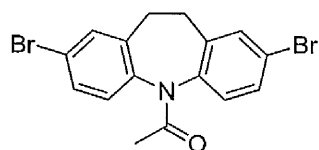
(1.781 g, 5.04 mmol) was treated according to the general

method described above to yield the product as a

colourless oil (occasionally returning as a white solid, mp

147.9-148.6 °C) 1.834 g, 92 %; 1H NMR (400 MHz, CDCl$_3$) δ ppm 7.28 - 7.46 (m, 4 H,

H-C^{1,3,7,9}) 7.10 - 7.22 (m, 2 H, H-C^{4,6}) 3.32 (m, 2 H, H-C^{10}) 2.69 - 2.92 (m, 2 H, H-C^{11})

2.01 (s, 3 H, H$_3$CCO); ^{13}C NMR (101 MHz, CDCl$_3$) δ ppm 170.3, 141.3, 139.4, 138.6,

136.3, 133.4, 132.9, 130.7, 130.3, 129.9, 129.2, 122.3, 121.2, 30.5, 29.8, 22.6; IR (cm^{-1})

3032 (w, aromatic CH stretch), 1678 (s, tertiary amide C=O stretch). 1550 (m), 1485 (s);

MS (ES+, m/z) 394 (51), 396 (100), 398 (49) [MH]$^+$.

1-(2-chloro-10,11-dihydro-5H-dibenzo[b,f]azepin-5-yl)ethanone 8: Compound **4**
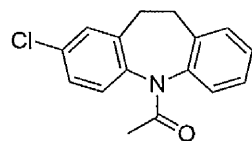
(1.218 g, 5.30 mmol) was treated according to the general

method outlined above to yield the product as a pale yellow oil

1.018 g, 78 %; ^{1}H NMR (400 MHz, CDCl$_3$) δ 6.93 - 7.38 (m, 7

H) 3.09 - 3.54 (m, 2 H, H$_2$-C^{10}) 2.68 - 2.87 (m, 2 H, H$_2$-C^{11}) 1.99 - 2.04 (m, 3 H,

H$_3$CC=O); ^{13}C NMR of this compound is complex and does not account for the different

conformers present in the solution: ^{13}C NMR (101 MHz, CDCl$_3$) δ 170.8, 170.5, 142.4,

139.7, 139.2, 138.4, 137.3, 136.2, 132.9, 130.6, 130.5, 130.1, 129.9, 129.0, 129.0, 128.8, 128.5, 128.2, 127.7, 127.5, 126.8, 125.3, 31.0, 30.6, 30.2, 29.8, 22.7, 22.6; IR (cm^{-1}) 3034 (w, aromatic CH stretch), 1680 (s, tertiary amide C=O stretch). 1554 (m), 1485 (s); MS (CI+, m/z) 272 (100), 274 (31) [MH]$^+$

1-(2,8-dichloro-10,11-dihydro-5H-dibenzo[b,f]azepin-5-yl)ethanone 9: Compound **5**
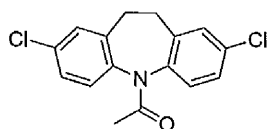
(1.289 g, 4.88 mmol) was treated according to the general method outlined above to yield the product as a colourless oil (occasionally returning as a white solid, mp 136.9-138.5 °C)

1.176 g, 79 %; ^{1}H NMR (400 MHz, CDCl$_3$) δ 7.18 - 7.23 (m, 2 H, H-C^{1,3,7,9}), 7.15 (d, J=7.9 Hz, 2 H, H^{4,6}), 3.25 - 3.41 (m, 2 H, H$_2$-C^{10}), 2.75 - 2.85 (m, 2 H, H$_2$-C^{11}), 2.01 (s, 3 H, H$_3$CC=O); ^{13}C NMR (101 MHz, CDCl$_3$) δ = 170.6, 138.8, 138.6, 135.9, 134.7, 133.9, 133.3, 131.6, 129.8, 129.6, 129.1, 129.1, 129.1, 31.6, 29.7; IR (cm^{-1}) 3033 (w, aromatic CH stretch), 1671 (s, tertiary amide C=O stretch). 1550 (m), 1483 (s); MS (CI+, m/z) 306 (100), 308 (64), 310 (11) [MH]$^+$.

5.4 General reaction procedures for incorporation of the 10,11 double bond:

Radical bromination of the etheno bridge (C^{10,11})

ABCN (0.1 mmol) was dissolved in PhCF$_3$ (10 mL) and added dropwise to a stirred solution of *N*-acyliminodibenzyl **5-9** (5.0 mmol) and NBS (6.0 mmol) in PhCF$_3$ (50 mL). The reaction was then heated to 110 °C and stirred for 14-24 hours with reaction monitoring by ^{1}H NMR spectroscopy to ensure complete conversion of the *N*-acyl iminodibenzyl **5-9**. Once judged to have completed the reaction was cooled to room

temperature, and partitioned between Et_2O and water. The organic phase was washed with water (2 × 50 mL) and saturated $NaHCO_{3(aq)}$ (1 × 50 mL), dried over Na_2SO_4, filtered and concentrated *in vacuo* to yield mixtures of eliminated and brominated products **10-13 a/b** as observed by ^1H NMR (discussed in chapter 2 (2.5.2.1)).

In each case the crude mixture generated from this reaction was transformed to the corresponding iminostilbene by either method A or method B as outlined below in section **5.5**.

Bromine Elimination from the Etheno Bridge

The crude reaction mixture of **10-13a/b** was dissolved in a 1:1 mixture of EtOH and THF (150 mL). With ice cooling and vigorous stirring, 50 % w/v $KOH_{(aq)}$ (50 mL) was added dropwise to the mixture slowly turning the solution from orange to dark brown. The reaction was left at 0 °C for 1 hour and then warmed to room temperature and left for a further 2 hours. The reaction was then quenched by addition of water (150 mL) and the product extracted with CH_2Cl_2 (2 × 100 mL). The combined organic extracts were dried over Na_2SO_4, filtered and evaporated to yield the eliminated products as colourless to orange oils.
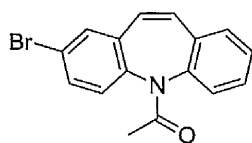
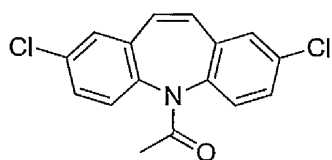**1-(2-bromo-5H-dibenz[*b,f*]azepin-5-yl)ethanone 10b:** Crude reaction mixture of **10a/b** was treated according to the general method for bromine elimination as outlined above to yield the product as a pale yellow oil 1.528 g, 99 %; *50 % pure* (calculated from quantity of compound **5** used in the radical bromination step; 1.546 g, 4.89 mmol); ^1H NMR (400 MHz, $CDCl_3$) δ = 7.57 - 7.48 (m, 1 H, H-C^1), 7.47 - 7.28 (m, 6 H), 7.05 - 6.91 (m, 1 H,

H̲-C^{10}), 6.91 - 6.79 (m, 1 H, H̲-C^{11}), 1.88 - 1.85 (m, 3 H, H̲$_3$CC=O); ^{13}C NMR (101

MHz, CDCl$_3$) δ 170.3, 136.7, 135.4, 132.2, 132.0, 131.5, 130.1, 129.7, 129.5, 128.5,

128.2, 127.9, 127.7, 77.3, 76.7, 22.0; IR (cm^{-1}) 3010 (m, aromatic CH stretch), 1675 (s,

tertiary amide C=O stretch), 1489 (m), 1346 (m), 1327 (m); MS (CI+, *m/z*) 314 (100),

316 (96) [MH]$^+$.

1-(2,8-dibromo-5H-dibenzo[*b,f*]azepin-5-yl)ethanone 11b: Crude reaction mixture of
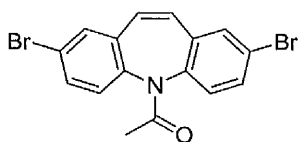
11a/b was treated according to the general method for

bromine elimination as outlined above to yield the product

as a pale yellow oil 1.977 g, 99 % (calculated from quantity

of compound **6** used in the radical bromination step; 2.008 g, 5.08 mmol); ^{1}H NMR (400

MHz, CDCl$_3$) δ ppm 7.37 - 7.66 (m, 4 H, H̲-C^{1,3,7,9}), 7.25 (dd, *J* = 11.0, 8.2 Hz, 2 H, H̲-

C^{4,6}), 6.91 (d, *A of AB*, *J*=12.1 Hz, 1 H. H̲-C^{10}) 6.85 (d, *B of AB*, *J* = 10.9 Hz, 1 H, H̲-

C^{11}), 1.83 - 1.92 (m, 3 H, H̲$_3$CC=O); ^{13}C NMR (101 MHz, CDCl$_3$) δ 170.5, 139.2, 139.0,

136.2, 135.0, 132.5, 132.5, 132.1, 132.1, 131.4, 130.1, 129.4, 129.0, 121.8, 121.3; 22.0;

IR (cm^{-1}) 2989 (m, aromatic CH stretch), 1673 (s, tertiary amide C=O stretch), 1488 (m),

1346 (m), 1326 (m); MS (ES-, *m/z*) 348 (51), 350 (100), 352 (49) [M-H]$^-$.

1-(2-chloro-5H-dibenz[*b,f*]azepin-5-yl)ethanone 12b: Crude reaction mixture of **12a/b**
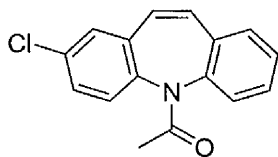
was treated according to the general method for bromine

elimination as outlined above to yield the product as a pale

yellow oil 1.393 g, 99 % (calculated from quantity of

compound **6** used in the radical bromination step; 1.421 g, 5.23 mmol); ^{1}H NMR (400

MHz, CDCl$_3$) δ7.49 - 7.28 (m, 7 H, H̲-C^{1,3,4,6,7,8,9}), 7.04 - 6.80 (m, 2 H, H̲-C^{10,11}), 1.88 -

1.85 (m, 3 H, $\underline{H}_3$C-CO). ^{13}C NMR for this compound is complex and does not account

for the different conformers present in solution. ^{13}C NMR (101 MHz, CDCl$_3$) δ 171.2,

170.9, 140.4, 140.2, 138.9, 138.7, 136.3, 135.0, 134.4, 133.6, 133.2, 133.1, 132.9, 130.4,

130.2, 129.8, 129.7, 129.6, 129.5, 129.2, 129.1, 128.9, 128.5, 128.1, 127.8, 127.8, 127.6,

22.1, 22.0; IR (cm^{-1}) 2989 (m, aromatic CH stretch), 1673 (s, tertiary amide C=O

stretch), 1488 (m), 1346 (m), 1326 (m); MS (CI+, m/z) 270 (100), 272 (34) [MH]$^+$.

1-(2,8-dichloro-5H-dibenz[b,f]azepin-5-yl)ethanone 13b: Crude reaction mixture of

13a/b **(13a/13b, g)** was treated according to the general

method for bromine elimination as outlined above to

yield the product as a pale yellow oil 1.496 g, 99 %

(calculated from quantity of compound **6** used in the radical bromination step; 1.511 g,

4.93 mmol) ^{1}H NMR (CDCl$_3$,400MHz) δ 7.40 - 7.44 (m, 2 H, $\underline{H}$-C^{1,8}), 7.37 (dd, J=10.9,

2.3 Hz, 2 H, $\underline{H}$-C^{4,6}), 7.29 - 7.35 (m, 2 H, $\underline{H}$-C^{3,7}), 6.93 (d, A of AB J = 11.6 Hz, 1 H,

$\underline{H}_2$C^{10}), 6.87 (d, B of AB J = 11.9 Hz, 1 H, $\underline{H}_2$C^{10}), 1.88 ppm (s, 3 H, $\underline{H}_3$CC=O); ^{13}C

NMR (101 MHz, CDCl$_3$) δ 170.7, 138.9, 138.6, 136.0, 134.7, 134.0, 133.4, 131.6,

130.0, 129.9, 129.6, 129.2, 129.2, 129.1, 129.0, 22.0; IR (cm^{-1}) 2990 (m, aromatic CH

stretch), 1673 (s, tertiary amide C=O stretch), 1487 (m), 1345 (m), 1326 (m); MS (CI+,

$m/$) [M+H]$^+$ 304 (100), 306 (67), 307 (12) [MH]$^+$.

5.5 Elimination and deprotection to form iminostilbenes

Method A: Deprotection of the amine

To a solution of KOH$_{(EtOH)}$ (50 mL, 0.4 M) at 80 °C was added a solution of compounds

10-13b (1.000 g) in 1:1 EtOH/THF (150 mL). The mixture was then left to stir for 12-16

h with reaction monitoring by TLC (1:9 EtOAc/Hexane). Once complete, water (250 mL) was added to the reaction mixture and the reaction neutralized to pH 7 by treatment with 1M HCl. The aqueous mixture was then extracted with EtOAc (3 × 150 mL) and the combined organic extracts back washed with water (1 × 250 mL) and saturated sodium thiosulfate$_{(aq)}$. The combined organic extract was dried over Na_2SO_4, filtered, and evaporated to yield the product as a yellow or orange solid after column chromatography with 1:9 EtOAc/Hexane.

Method B: One-pot Elimination and deprotection

Crude reaction mixture of **10-13a/b** was dissolved in a 1:1 mixture of THF/EtOH (100 mL) and cooled to 0 °C in an ice bath. 50 % (w/v) KOH$_{(aq)}$ (50 mL) was then added dropwise over an hour and the reaction left at 0 °C for a further hour. During this time the reaction was observed to change from orange to brown/black. The reaction was then gently heated to 80 °C and left for a further 12 hours with reaction monitoring by TLC (1:9 EtOAc/Hexane). Once complete, water (100 mL) was added to the reaction mixture and the reaction neutralised to pH 7 by treatment with 1M HCl. The aqueous mixture was then extracted with EtOAc (2 × 150 mL) and the combined organic extracts back washed with water (1 × 150 mL) and saturated sodium thiosulfate$_{(aq)}$ (1 × 50 mL). The combined organic extract was dried over Na_2SO_4, filtered, and concentrated *in vacuo* to yield the crude product. In each case purification was performed by column chromatography with 1:9 EtOAc/Hexane to isolate the iminostilbene as a yellow or orange solid.
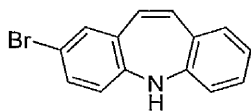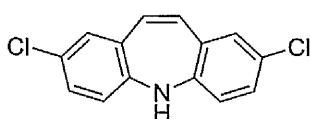
2-bromo-5H-dibenz[*b,f*]azepine 14: 10b (1.116 g, 3.67 mmol) was treated according to **method A** to yield the product as an orange solid, 0.925 g (95 % yield; *50 % purity*). Treatment of the crude mixture **10a/b** was accomplished by **method B**, to yield the product as an orange solid in near quantitative yields after purification by column chromatography. *N-aryl indole cyclisation* (discussed below): Cyclisation of **34** (2.010 g, 7.39 mmol) at the reduced temperature of 65 °C yielded the product as an orange solid after column chromatography (1:9 EtOAc/Hexane). 0.098 g, 5 %; mp 152.1-153.7; ^{1}H NMR (400 MHz, CDCl$_3$) δ 7.09 (dd, J = 8.3, 2.3 Hz, 1 H, H-C^4), 7.03 (ddd, J = 7.9, 5.9, 3.1 Hz, 1 H, H-C^3), 6.95 (d, J = 2.3 Hz, 1 H, H-C^1), 6.82 - 6.86 (m, 3 H, H-C^{6,7,8}), 6.46 (d, J = 7.6 Hz, 1 H, H-C^9), 6.30 (d, *A of AB*, J = 12.0 Hz, 1 H, H-C^{10}), 6.17 (d, *B of AB*, J = 11.6 Hz, 1 H, H-C^{11}), 4.89 (br. s., 1 H, H-N^5); ^{13}C NMR (CDCl$_3$, 101 MHz) δ 148.3, 147.4, 133.4, 132.8, 131.8, 131.7, 130.7, 130.6, 129.8, 129.3, 123.3, 120.7, 119.3, 115.3 ppm; MS (CI+, *m/z*) 272 (97), 274 (100) [MH]$^+$; found 270.9991; C$_{14}$H$_{10}$N^{79}Br req 270.9997.
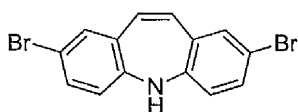
2,8-dibromo-5H-dibenz[*b,f*]azepine 15: 11b (1.010 g, 2.57 mmol) was treated according to **method A** to yield **15** as an orange solid, 0.856 g, 95 %. Crude mixture **11a/b** was treated according to **method B** to yield the product as an orange solid in near quantitative yields after purification by column chromatography. ^{1}H NMR (400 MHz, CDCl$_3$) δ 7.12 (dd, J = 8.3, 2.3 Hz, 2 H, H-C^{3,7}), 6.96 (d, J = 2.3 Hz, 2 H, H-C^{1,9}), 6.34 (d, J = 8.4 Hz, 2 H, H-C^{4,6}), 6.21 (s, 2 H, H-C^{10,11}), 4.88 (br. s., 1 H, HN^5); ^{13}C NMR (CDCl$_3$, 101 MHz) δ 147.5, 133.5, 132.6, 132.4, 131.8, 121.2, 116.1; MS (EI$^-$, *m/z*) 348 (51), 350 (100), 351 (49) [M-H]$^-$; found 347.9031: C$_{14}$H$_8$N^{79}Br$_2$ req 347.9023.
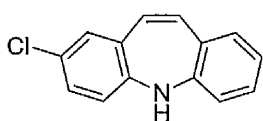
2-chloro-5*H*-dibenz[*b,f*]azepine 16: 12b (1.021 g, 3.78 mmol) was treated according to **method A** to yield the product as an orange solid, 0.0.814 g, 95 %. Crude mixture **12a/b** was reated according to **method B** to yield the product as an orange solid, in near quantitative yields after purification by column chromatography. *N-aryl indole cyclisation* (discussed below): Cyclisation of **30** (2.004 g, 8.80 mmol) yielded the product **16** as a mixture with **35**. **16** was isolated as a pale yellow solid after column chromatography 1:9 EtOAc/Hexane; 0.814 g, 41 %. Cyclisaton of **31** (1.498 g, 6.58 mmol) yielding the product as an orange solid after column chromatography (1:9 EtOAc/Hexane) to yield the product as an orange solid 0.903 g, 60 %; ^{1}H NMR (400 MHz ,CDCl$_3$) δ 7.09 - 6.94 (m, 1 H, $\underline{H}$-C^4), 6.98 (dd, J = 2.3, 8.3 Hz, 1 H, $\underline{H}$-C^3), 6.92 - 6.78 (m, 2 H, $\underline{H}$-C^{7,8}), 6.83 (d, J = 2.1 Hz, 1 H, $\underline{H}$-C^1), 6.43 (d, J = 8.4 Hz, 1 H, $\underline{H}$-C^6), 6.49 (d, J = 7.8 Hz, 1 H $\underline{H}$-C^4), 6.35 (d, A of AB, J = 12.0 Hz, 1 H, $\underline{H}$-C^{10}), 6.22 (d, B of AB, J = 11.7 Hz, 1 H, $\underline{H}$-C^{11}), 4.91 (br. s., 1 H, $\underline{H}$-N^5); ^{13}C NMR (101 MHz, CDCl$_3$) δ 148.0, 146.8, 133.4, 132.1, 131.3, 130.7, 129.9, 129.7, 129.3, 128.9, 127.9, 123.2, 120.3, 119.3; MS (CI+, *m/z*) 228 (100), 230 (39) [MH]$^+$; Found [MH]$^+$ 228.0575 *m/z* C$_{14}$H$_{11}$N^{35}Cl req 228.0575.

2,8-dichloro-5*H*-dibenz[*b,f*]azepine 17: 12b (1.081 g, 3.67 mmol) was treated according to **method A** to yield the product as an orange solid, 0.892 g, 96 % yield. Treatment of the crude mixture **12a/b** **method B** yielded the product as an orange solid in near quantitative yield after purification by column chromatography. *N-aryl indole cyclisation* (discussed below): Cyclisation of **32** (2.508 g, 9.57 mmol) yielded the product **17** as a mixture with **16**. The product was isolated a yellow solid after column

chromatography (1:9 EtOAc/Hexane) 0.797 g, 32 %; mp, ; ^{1}H NMR (400 MHz, CDCl$_3$)

δ ppm 6.99 (dd, J=8.4, 2.4 Hz, 2 H, $\underline{H}$-C^{3,7}), 6.84 (d, J = 2.5 Hz, 2 H, $\underline{H}$-C^{1,9}), 6.42 (d, J

= 8.4 Hz, 2 H, $\underline{H}$-C^{4,6}), 6.25 (s, 2 H, $\underline{H}$-C^{10,11}), 4.89 (br. s., 1 H, $\underline{H}$-N^5); ^{13}C NMR (101

MHz, CDCl$_3$) δ 146.6, 132.0, 131.0, 130.1, 129.2, 128.3, 120.4; MS Found [M+Na]$^+$

262.0186; C$_{14}$H$_{10}$N^{35}Cl$_2$ req 262.0190.

5.6   General experimental procedure for the synthesis of N-aryl Indoles.

N-Aryl indoles were prepared with modification of the procedure reported by Ma *et al*[3] as follows:

The appropriate indole (2.2 mmol), K_2CO_3 (5.0 mmol), CuI (0.1 mmol) and L-proline (0.2 mmol) were dissolved in DMSO (4 mL). The mixture was heated gently to 100 °C (± 5 °C) under an inert atmosphere for 10 min, then iodobenzene (2.0 mmol) was added dropwise over 20 min and the reaction left to stir for 24 h. Upon completion the cooled solution was partitioned between EtOAc and H_2O and the aqueous layer extracted with EtOAc (2× 50 mL); the combined organic phases were washed with brine and dried over Na_2SO_4, filtered and concentrated. The crude material was subsequently purified by column chromatography to give the pure product.
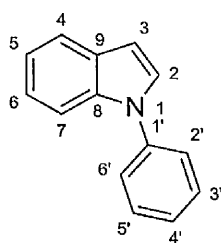
1-phenyl-1H-indole 18: colourless oil, 97 %; ^1H NMR (400 MHz, CDCl$_3$) δ 7.67-7.64 (m, 1H, H-C^7), 7.53-7.51 (m, 1H, H-C^4), 7.40-7.34 (m, 4H, H-C$^{2',3',5',6'}$), 7.25-7.20 (m, 2H, H-C$^{4',2}$), 7.19- 7.11 (m, 2H, H-C^{5,6}), 6.62 (dd, J = 3.3, 0.7 Hz, 1H, H-C^3); ^{13}C NMR (101 MHz, CDCl$_3$) δ 140.0, 136.1, 129.8, 129.6, 128.2, 126.6, 124.5, 122.6, 121.4, 120.7, 110.8, 103.9; Found: m/z 194.0963, $C_{14}H_{12}N$ [MH$^+$]req. m/z 194.0964.

Spectral data in agreement with those reported in [4]
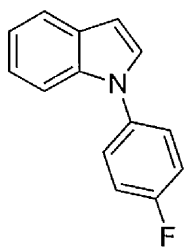
1-(4-fluorophenyl)-1H-indole 19: Colourless oil, (occasionally returns as a white solid, m.p. 36.1-36.7 °C); ^{1}H NMR (400 MHz, CDCl$_3$) δ 7.63 - 7.70 (m, 1 H, $\underline{\text{H}}$-C^7), 7.41 - 7.45 (m, 1 H, $\underline{\text{H}}$-C^6), 7.33 - 7.40 (m, 2 H, $\underline{\text{H}}$-C$^{2',6'}$), 7.21 (d, J=3.2 Hz, 1 H, $\underline{\text{H}}$-C^2), 7.19 (d, J=1.3 Hz, 1 H, $\underline{\text{H}}$-C^5), 7.17 (dd, J=2.6, 1.6 Hz, 1 H, $\underline{\text{H}}$-C^6), 7.10 - 7.16 (m, 2 H, $\underline{\text{H}}$-C$^{3'5'}$), 6.64 (dd, J=3.3, 0.8 Hz, 1 H, $\underline{\text{H}}$-C^3); ^{13}C NMR (101 MHz, CDCl$_3$) δ 161.3 (d, $^1J_{CF}$ = 246.2 Hz, C$^{4'}$), 136.4, 136.2 (d, $^4J_{CF}$ = 3.0 Hz, C$^{1'}$), 129.5, 128.3, 126.4 (d, $^3J_{CF}$ = 8.4 Hz), 122.8, 121.5, 120.7, 116.7 (d, $^2J_{CF}$ = 22.7 Hz), 110.5, 103.9; ^{19}F NMR (376 MHz, CDCl$_3$) δ -115.59 (s); Found: C, 79.73; H, 4.91; N, 6.14; C$_{14}$H$_{10}$FN req. C, 79.60; H, 4.77; N, 6.63 %; Found: m/z, 212.0873; C$_{14}$H$_{11}$FN [MH$^+$] req. m/z, 212.0870.

Spectral data consistent with those reported by[5-7] and the references therin
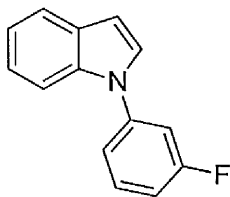
1-(3-fluorophenyl)-1H-indole 20: Pale yellow oil, 78 %; (400 MHz, CDCl$_3$) δ 7.69-7.67 (m, 1H, $\underline{\text{H}}$-C^7), 7.59-7.57 (m, 1H, $\underline{\text{H}}$-C^4), 7.42 (dt, J=8.2, 6.2 Hz, 1H, $\underline{\text{H}}$-C$^{5'}$), 7.31 (d, J=3.3 Hz, 1H, $\underline{\text{H}}$-C^2), 7.30-7.15 (m, 4H, $\underline{\text{H}}$-C$^{5,6,4',6'}$), 7.03 (tdd, J = 8.3, 2.5, 0.9 Hz, 1H, $\underline{\text{H}}$-C$^{2'}$), 6.69 (dd, J= 3.3, 0.8 Hz, 1H, $\underline{\text{H}}$-C^3); ^{13}C NMR (101 MHz, CDCl$_3$) δ 163.5 (d, $^1J_{CF}$ = 247.5 Hz), 141.6 (d, $^3J_{CF}$ = 10.0 Hz), 135.9, 131.2 (d, $^3J_{CF}$ = 9.3 Hz), 129.8, 127.9, 123.0, 121.6, 121.0, 120.0 (d, $^4J_{CF}$ = 3.1 Hz), 113.5 (d, $^2J_{CF}$ = 21.1 Hz), 111.8 (d, $^2J_{CF}$ = 23.8 Hz), 110.7, 104.6; ^{19}F NMR (376.46 MHz, CDCl$_3$) δ -111.22 (s); Found: C, 79.69; H, 4.81; N, 6.52; C$_{14}$H$_{10}$FN req. C, 79.60; H, 4.77; N, 6.63 %; Found: m/z, 212.0872; C$_{14}$H$_{11}$FN [MH]$^+$ req. m/z, 212.0870.
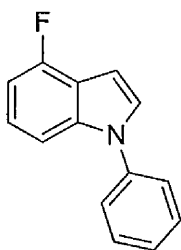
4-Fluoro-1-phenyl-1H-indole 21: Pale yellow oil, (occasionally returns as a white solid, mp) 70 %; 1H NMR (400 MHz, CDCl$_3$) δ ppm 7.42 - 7.51 (m, 4 H, H-C$^{2',3',5',6'}$), 7.32 - 7.38 (m, 1 H, H-C$^{4'}$), 7.29 (dd, J=8.3, 0.4 Hz, 1 H, H-C^5), 7.26 (d, J=3.3 Hz, 1 H, H-C^2), 7.10 (td, J=8.1, 5.2 Hz, 1 H, H-C^6), 6.82 (ddd, J=10.2, 7.9, 0.5 Hz, 1 H, H-C^7), 6.75 (dd, J=3.3, 0.8 Hz, 1 H, H-C^3); ^{13}C NMR (101 MHz, CDCl$_3$) δ 156.4 (d, $^1J_{CF}$ = 248.8 Hz), 139.4, 138.4 (d, $^3J_{CF}$ = 11.1 Hz), 129.6, 127.9, 126.8, 124.4, 122.8 (d, $^3J_{CF}$ = 7.7 Hz), 118.3 (d, $^2J_{CF}$ = 24.5 Hz), 106.6 (d, $^4J_{CF}$ = 3.5 Hz), 105.2, 105.0, 99.5, 99.4; ^{19}F NMR (376 MHz, CDCl$_3$) δ -122.2 (s); Found: C, 79.73; H, 4.91; N, 6.14; C$_{14}$H$_{10}$FN req. C, 79.60; H, 4.77; N, 6.63 %. Found: m/z, 211.0798; C$_{14}$H$_{11}$FN [MH]$^+$ req. m/z, 211.0797.
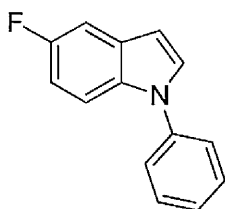
5-Fluoro-1-phenyl-1H-indole 22: Pale yellow oil, 76 %; ^{1}H NMR (400 MHz, CDCl$_3$) δ = 7.54- 7.43 (m, 5 H), 7.38 - 7.30 (m, 3 H), 6.95 (dt, J = 2.5, 9.1 Hz, 1 H) and 6.63 (dd, J = 0.6, 3.2 Hz, 1 H, H-C^3); ^{13}C NMR (101 MHz, CDCl$_3$) δ 158.1 (d, $^1J_{CF}$ = 234.6 Hz), 139.6, 132.5, 129.7, 129.6 (d, $^3J_{CF}$ = 13.8 Hz), 129.4, 126.7, 124.3, 111.2 (d, $^3J_{CF}$= 9.6 Hz), 110.6 (d, $^2J_{CF}$ = 26.1 Hz), 105.8 (d, $^2J_{CF}$=23.4 Hz) and 103.4 (d, $^4J_{CF}$= 4.6 Hz); ^{19}F NMR (376 MHz, CDCl$_3$) δ -122.40; Found: C, 79.70; H, 4.82; N, 6.72; C$_{14}$H$_{10}$FN req. C, 79.60; H, 4.77; N, 6.63 %; Found: m/z, 212.0868; C$_{14}$H$_{11}$FN [MH$^+$] req. m/z, 212.0870.

Spectral data consistent with those reported in [8]
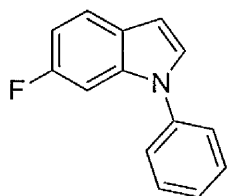
6-Fluoro-1-phenyl-1H-indole 23: Pale yellow oil, 83 %; ^{1}H NMR (400 MHz, CDCl$_3$) δ 7.58 (dd, J = 5.4, 8.7 Hz, 1 H, H-C^5), 7.55 - 7.45 (m, 4 H, H-C$^{2',3',5',6'}$), 7.37 (t, J = 7.4 Hz, 1 H, H-C$^{4'}$), 7.31 (d, J = 3.3 Hz, 1 H, H-C^2), 7.25 - 7.21 (m, 1 H, H-C^7), 6.93 (dt, J = 2.3, 9.0 Hz, 1 H, H-C^4) 6.65 (d, J = 3.3 Hz, 1 H, H-C^3); ^{13}C NMR (101 MHz, CDCl$_3$) δ 160.2 (d, $^1J_{CF}$ = 236.5 Hz), 139.4, 135.8 (d, $^3J_{CF}$ = 12.3 Hz), 129.7, 128.4 (d, $^4J_{CF}$ = 3.8 Hz), 126.7, 125.6, 124.2, 121.8 (d, $^3J_{CF}$ = 10.0 Hz), 109.1 (d, $^2J_{CF}$ = 24.9 Hz), 103.6 and 97.0 (d, $^2J_{CF}$ = 26.5 Hz); ^{19}F NMR (376 MHz, CDCl$_3$) δ -120.65; Found: C, 79.48; H, 4.85; N, 6.7; C$_{14}$H$_{10}$FN req. C, 79.60; H, 4.77; N, 6.63 %; Found: m/z, 212.0869; C$_{14}$H$_{11}$FN [MH$^+$] req. m/z, 212.0870.
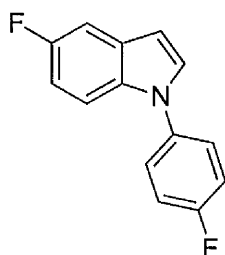
5-Fluoro-1-(4-fluorophenyl)-1H-indole 24: Pale yellow oil, (occasionally returns as a white solid m.p. 53.4-54.2 °C, 85% ; ^{1}H NMR (400 MHz, CDCl$_3$) δ 7.38- 7.43 (m, 2H, H-C), 7.27 - 7.36 (m, 3H), 7.15 - 7.22 (m, 2H, H-C$^{3',5'}$), 6.94 (td, J=9.1, 2.6 Hz, 1H, H-C^7), 6.61 (dd, J=3.2, 0.7 Hz, 1H, H-C^3); ^{13}C NMR (101 MHz, CDCl$_3$) δ 159.9 (d, $^1J_{CF}$ = 247.7 Hz), 157.7 (d, $^1J_{CF}$ = 235.4 Hz), 135.6 (d, $^4J_{CF}$ = 2.7 Hz), 132.7, 129.5, 129.4, 126.1 (d, $^3J_{CF}$ = 8.4 Hz), 116.5 (d, $^2J_{CF}$ = 23.4 Hz), 110.9 (d, $^4J_{CF}$ = 6.5 Hz), 110.7 (d, $^2J_{CF}$ = 23.0 Hz), 105.9 (d, $^2J_{CF}$ = 23.4 Hz) and 103.4 (d, $^4J_{CF}$ = 4.6 Hz); ^{19}F NMR (376 MHz, CDCl$_3$) δ -115.3, -124.5; C$_{14}$H$_9$F$_2$N req. C, 73.36; H, 3.96; N 6.11 %; Found: m/z, 230.0777; C$_{14}$H$_{10}$F$_2$N [MH$^+$] req. m/z, 230.0776.

Spectral data consistent with those reported in[5]
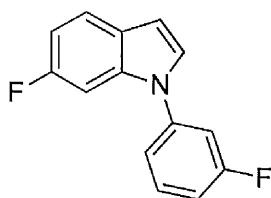
6-Fluoro-1-(3-fluorophenyl)-1H-indole 25: Pale yellow oil, 75 %; ^{1}H NMR (400 MHz, CDCl$_3$) δ 7.56 (dd, J = 8.7, 5.4 Hz, 1 H, $\underline{H}$-C$^{2'}$), 7.45 (dt, J = 8.2, 6.3 Hz, 1 H, $\underline{H}$-C$^{5'}$), 7.29 - 7.20 (m, 3 H, $\underline{H}$-C$^{4',6',2}$), 7.17 (td, J = 2.3, 9.7 Hz, 1 H, $\underline{H}$-C^4), 7.05 (ddt, J = 8.3, 2.5, 0.9 Hz, 1 H, $\underline{H}$-C$^{2'}$), 6.94 (ddd, J = 9.3, 8.8, 2.3 Hz, 1 H, $\underline{H}$-C^5), 6.64 (dd, J = 3.3, 0.8 Hz, 1 H, $\underline{H}$-C^3); ^{13}C NMR (101 MHz, CDCl$_3$) δ 163.2 (d, $^1J_{CF}$ = 248.1 Hz), 160.3 (d, $^1J_{CF}$ = 238.5 Hz), 140.9 (d, $^3J_{CF}$ = 10.0 Hz), 135.6 (d, $^3J_{CF}$ = 12.3 Hz), 131.0 (d, $^3J_{CF}$ = 9.2 Hz), 128.0 (d, $^4J_{CF}$ = 3.5 Hz), 125.8, 122.0 (d, $^3J_{CF}$ = 10.0 Hz), 119.5 (d, $^4J_{CF}$ = 3.1 Hz), 113.5 (d, $^2J_{CF}$ = 21.1 Hz), 111.3 (d, $^2J_{CF}$ = 23.8 Hz), 109.4 (d, $^2J_{CF}$ = 24.5 Hz), 104.3, 97.0 (d, $^2J_{CF}$ = 27.2 Hz); ^{19}F NMR (376 MHz, CDCl$_3$) δ -110.8, -119.9; Found: C, 73.37; H, 4.03; N, 5.94 ; C$_{14}$H$_9$F$_2$N req. C, 73.36; H, 3.96; N, 6.11 %; Found: m/z, 230.0772; C$_{14}$H$_{10}$F$_2$N [MH$^+$] req. m/z, 230.0776.
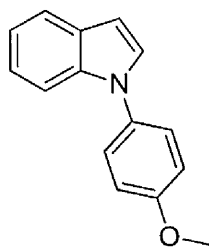
1-(4-methoxyphenyl)-1H-indole 26: Pale pink solid, 68%, mp 71-72 °C ^{1}H NMR (400 MHz, CDCl$_3$) δ 7.65 - 7.70 (m, 1 H, $\underline{H}$-C^7), 7.45 (dd, J=8.1, 0.7 Hz, 1 H, $\underline{H}$-C^4), 7.37 - 7.42 (m, 2 H, $\underline{H}$-C$^{2',6'}$), 7.27 (d, J=3.2 Hz, 1 H, $\underline{H}$-C^2), 7.12 - 7.23 (m, 2 H, H-C^{5,6}), 7.00 - 7.04 (m, 2 H, $\underline{H}$-C$^{3',5'}$), 6.65 (dd, J=3.2, 0.7 Hz, 1 H, $\underline{H}$-C^3), 3.86 (s, 3 H, $\underline{H}_3$C-O); ^{13}C NMR (101 MHz, CDCl$_3$) δ 158.2, 136.3, 132.8, 128.9, 128.2, 125.9, 122.1, 121.0, 120.0, 114.7, 110.3, 102.8, 77.3, 76.7, 55.6; Found: m/z 224.0173; C$_{15}$H$_{14}$ON [MH+] req. m/z 224.1070.

Spectral data in agreement with those reported in [6] and the references therin
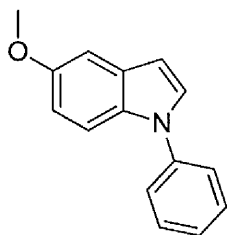
**5-methoxy-1-phenyl-1H-indole 27:** Colourless oil, 71 %; ^{1}H NMR (400 MHz, CDCl$_3$) δ 7.70 (dd, J = 8.3, 1.1 Hz, 1 H, H̲-C^7) 7.44 - 7.53 (m, 3 H) 7.30 - 7.37 (m, 2 H) 7.07 - 7.16 (m, 1 H, H̲-C^4) 6.88 (dd, J = 9.0, 2.5 Hz, H̲-C^6) 6.60 (dd, J = 3.2, 0.7 Hz, 1 H), 3.87 (s, 3 H,. CH̲$_3$-O); ^{13}C NMR (101 MHz, CDCl$_3$) δ ppm 154.5, 139.9, 137.5, 130.2, 129.8, 129.6, 128.3, 127.4, 126.2, 124.0, 112.5, 111.3, 103.2, 102.6, 55.8; Found: m/z 224.1076; C$_{15}$H$_{14}$ON [MH]$^+$ req. m/z 224.1070

Spectral data consistent with those reported in [9]
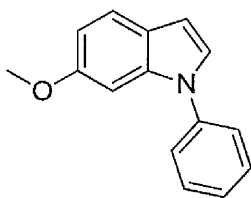
6-methoxy-1-phenyl-1H-indole 28: colourless oil, 62 %; ^{1}H NMR (400 MHz, CDCl$_3$) δ 7.48 - 7.57 (m, 5 H) 7.33 - 7.39 (m, 1 H) 7.23 (d, J=3.3 Hz, 1 H, H̲-C^2) 7.05 (d, J = 2.2 Hz, 1 H, H̲-C^7) 6.84 (dd, J=8.6, 2.3 Hz, 1 H, H̲-C^5) 6.61 (dd, J = 3.3, 0.8 Hz, 1 H, H̲-C^3) 3.82 (s, 3 H, H̲$_3$CO); ^{13}C NMR (101 MHz, CDCl-3) δ ppm 156.7, 139.9, 136.5, 129.6, 127.0, 126.4, 124.3, 123.4, 121.6, 110.2, 103.4, 94.1, 55.7; Found: m/z 224.1074; C$_{15}$H$_{14}$ON [MH]$^+$ req. m/z 224.1070.
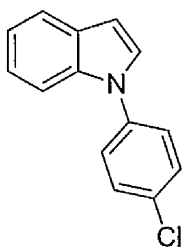
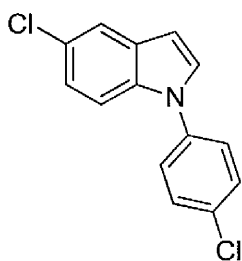**1-(4-chlorophenyl)-1H-indole 30:** Pale yellow oil, 87 %; ^{1}H NMR (400 MHz, CDCl-3) δ ppm ^{1}H NMR (400 MHz, CDCl$_3$) δ ppm 7.65 - 7.70 (m, 1 H, H̲-C^7), 7.51 (dd, J=8.1, 0.8 Hz, 2 H, H̲-C^4), 7.46 - 7.47 (m, 2 H, H̲-C$^{3',5'}$), 7.43 - 7.45 (m, 2 H, H̲-C$^{2',6'}$), 7.28 (d, J = 3.3 Hz, 1 H, H̲-C^2), 7.15 - 7.25 (m, 2 H, H̲-C^{5,6}), 6.69 (dd, J = 3.3, 0.7 Hz, 2 H, H̲-C^3); ^{13}C NMR (101 MHz, CDCl$_3$) δ ppm 138.3, 135.7, 131.9, 129.7, 129.3, 127.7, 125.5, 122.6, 121.2, 120.6, 110.2, 104.0; Found: m/z 228.0572; C$_{14}$H$_{11}$N Cl [M+H]$^+$ req. m/z 228.0575.

180

Spectral data in agreement with those reported in [6] and the references therein.
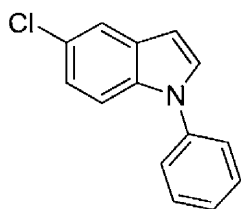
5-chloro-1-phenyl-1H-indole 31: Colourless oil, 92 %; ^{1}H NMR (400 MHz, CDCl$_3$) δ ppm 7.62 (d, J = 2.1 Hz, 1 H, H̲-C^4) 7.44 - 7.50 (m, 2 H) 7.38 - 7.43 (m, 3 H) 7.30 - 7.35 (m, 1 H) 7.29 (d, J = 3.3 Hz, 1 H, H̲-C^2) 7.13 (dd, J = 8.8, 2.1 Hz, 1 H, H-C^6) 6.58 (dd, J = 3.2, 0.6 Hz, 1 H, H̲-C^3); ^{13}C NMR (101 MHz, CDCl$_3$) δ 139.3, 134.2, 130.3, 129.6, 129.2, 126.7, 125.9, 124.2, 122.5, 120.4, 111.5, 103.0; m/z 228.0573; C$_{14}$H$_{11}$NCl [MH]$^+$ req. m/z 228.0575.

5-chloro-1-(4-chlorophenyl)-1H-indole 32: white solid, 85 %, mp 65.8-66.5; ^{1}H NMR (400 MHz, CDCl$_3$) δ ppm 7.63 (d, J = 2.0 Hz, 1 H, H̲-C^4) 7.44 - 7.52 (m, 2 H) 7.36 - 7.42 (m, 3 H) 7.29 (d, J = 3.3 Hz, 1 H, H̲-C^2) 7.17 (dd, J = 8.8, 2.0 Hz, 1 H, H̲-C^7) 6.62 (dd, J = 3.2, 0.6 Hz, 1 H, H̲-C^3); ^{13}C NMR (101 MHz, CDCl$_3$) δ ppm 138.3, 134.6, 132.8, 130.8, 130.3, 129.4, 126.6, 125.9, 123.3, 121.0, 111.7, 104.0; m/z 262.0183; C$_{14}$H$_{10}$N Cl$_2$ [MH]$^+$ req. m/z 232.0185.
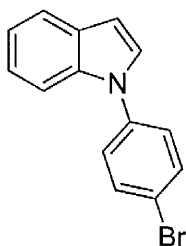
1-(4-bromophenyl)-1H-indole 33: Pale yellow oil, 79 %; ^{1}H NMR (400 MHz, CDCl$_3$) δ ppm 7.66 - 7.70 (m, 1 H, H̲-C^7), 7.59 - 7.65 (m, 2 H, H̲-C$^{3',5'}$), 7.51 (dd, J = 8.1, 0.7 Hz, 1 H, H̲-C^4), 7.34 - 7.39 (m, 2 H, H̲-C^{2,6}), 7.27 (d, J = 3.3 Hz, 1 H, H̲-C^2), 7.14 - 7.26 (m, 2 H, H̲-C^{5,6}), 6.68 (dd, J = 3.3, 0.7 Hz, 1 H, H̲-C^3); ^{13}C NMR (101 MHz, CDCl$_3$) δ 138.8, 135.6, 132.7, 129.4, 127.6, 125.8, 122.6, 121.2, 120.6, 119.7, 110.2, 104.1; Found: 272.0071; C$_{45}$H$_{11}$NBr [MH]$^+$ req. m/z 272.069.

Spectral data consistent with those reported in[9]
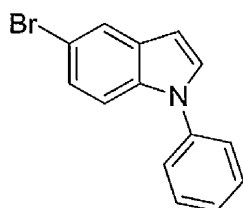
5-bromo-1-phenyl-1H-indole   34: Colourless oil, 83 %; ^{1}H NMR (400 MHz, CDCl$_3$) δ 7.80 (d, J = 1.9 Hz, 1 H, $\underline{H}$-C^4) 7.25 - 7.54 (m, 8 H) 6.60 (d, J = 3.2 Hz, 1 H, $\underline{H}$-C^3); ^{13}C NMR (101 MHz, CDCl$_3$) δ 139.3, 134.5, 130.9, 129.7, 129.1, 126.8, 125.1, 124.3, 123.5, 113.5, 111.9, 102.9; Found: m/z 272.0065; C$_{45}$H$_{11}$NBr [MH]$^+$ req. m/z 272.06.

Spectral data consistent with those reported in [9]

5.7   General experimental for iminostilbene by Polyphosphoric acid cyclisation[10, 11]

Polyphosphoric acid (1 mL per 100 mg aryl indole) was purged with argon and heated to 100 °C for 30 min. The N-aryl indole was then added to the gently stirring reaction mixture via a syringe and the reaction mixture left to stir at 110 °C (± 5 °C) for 36 to 72 h, with monitoring of reaction progress by partition TLC. Once judged to have reached completion the reaction mixture was allowed to cool slowly to room temperature, then poured cautiously into an ice-cold, saturated, aqueous NaHCO$_3$ solution and vigorously stirred for 1 h. The crude product was extracted with dichloromethane (2×100 mL), the combined organic phases were washed with water, NaHCO$_3$ and brine. After concentration *in vacuo*, the combined crude material was purified by column chromatography using EtOAc/hexane 1:9.
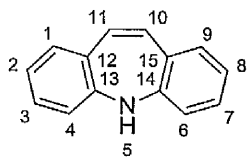
Iminostilbene 35: Compound **18** (2.712 g, 14.03 mmol) was added portionwise to hot polyphosphoric as outlined above to yield the product as an orange solid after column chromatography 1:9 EtOAc/Hexane, 1.810 g, 67 %; ^{1}H NMR (400 MHz, CDCl$_3$) δ 7.00 - 7.06 (m, 2 H) 6.86 (dd, J = 7.5, 1.7 Hz, 2 H) 6.80 - 6.85 (m, 2 H) 6.50 (d, J = 7.9 Hz, 2 H) 6.31 (s, 2 H) 4.94 (br. s., 1 H); ^{13}C NMR (101 MHz, CDCl$_3$): δ 148.3, 132.1, 130.5, 129.7, 129.4, 123.0, 119.3.

Compound consistent with an authentic standard.
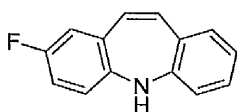
2-Fluoro-5H-dibenz[b,f]azepine 36: Compound **19** (2.018 g, 9.56 mmol) was treated as above to yield **36** after purification by column chromatography 1:9 EtOAc/Hexane (0.810 g, 40.1 %); Treatment of **22** (1.144 g, 5.42 mmol) yielded **36** as a yellow/orange solid after purification by column chromatography 1:9 EtOAc/Hexane (0.534 g, 47 %); ^{1}H NMR (400 MHz, CDCl$_3$) δ 7.08 (dt, J = 1.9, 7.4 Hz, 1 H, H-C^7), 6.95 - 6.86 (m, 2 H, H-C^{8,9}), 6.76 (dt, J = 2.8, 8.3 Hz, 1 H, H-C^3), 6.62 (dd, J = 2.9, 9.2 Hz, 1 H, H-C^1), 6.55 (dd, J = 0.4, 7.8 Hz, 1 H, H-C^6), 6.49 (dd, J = 4.8, 8.6 Hz, 1 H, H-C^4), 6.44 (d, A of AB J = 11.8 Hz, 1 H, H-C^{10}), 6.30 (d, B of AB, J = 11.8 Hz, 1H, H-C^{11}) and 4.94 (br s, 1 H, HN^5); ^{13}C NMR (100 MHz, CDCl$_3$) δ 240.2 (d, $^1J_{CF}$ = 240.2 Hz), 148.8, 144.5 (d, $^4J_{CF}$ = 2.3 Hz), 133.8, 131.9 (d, $^3J_{CF}$ =7.6), 131.2 (d, $^4J_{CF}$ = 1.7), 130.9, 130.1, 129.9, 123.6, 120.6 (d, $^3J_{CF}$ = 8.2 Hz), 119.7, 116.7 (d, $^2J_{CF}$ = 22.8 Hz) and 115.8 (d, $^2J_{CF}$ = 22.5 Hz); ^{19}F NMR (376 MHz, CDCl$_3$) δ = -122.78; Found: C, 79.73; H, 4.81; N, 6.60; C$_{14}$H$_{10}$FN requires C, 79.60; H 4.77; N, 6.63 %; Found: m/z, 212.0879; C$_{14}$H$_{11}$FN [MH]$^+$ requires m/z, 212.0876.

Spectral data consistent with those reported in [12]
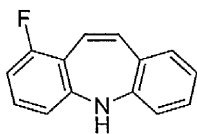
1-Fluoro-5*H*-dibenz[*b,f*]azepine 37: Prepared by the general method outlined using compound **21** (1.012 g, 4.77 mmol). The product was isolated as orange/yellow solid (0.245 g, 24 %) after column chromatography 1:9 EtOAc hexane; when starting from **20** (1.219 g, 5.59 mmol), the product was formed as a mixture with **38** and was separated by gradient elution with hexane → 1:4 EtOAc/hexane with a 1:50 product to silica ratio, to yield the product as a yellow solid, 0.223 g, 18 %; ^{1}H NMR (400 MHz, CDCl$_3$) δ 7.03 - 7.10 (m, 1 H, $\underline{H}$-C^6), 6.98 (td, J = 8.1, 6.1 Hz, 1 H, $\underline{H}$-C^4), 6.84 - 6.93 (m, 2 H, $\underline{H}$-C^{3,9}), 6.48 - 6.60 (m, 3 H, $\underline{H}$-C$^{5, 6, 7}$), 6.43 (d, J = 1.0 Hz, 1 H, $\underline{H}$-C^8), 6.31 (d, J = 7.4 Hz, 1 H, $\underline{H}$-C^2) and 5.03 (br s, 1 H, $\underline{H}$N^5); ^{13}C NMR (101 MHz, CDCl$_3$) δ 160.7 (d, $^1J_{CF}$ = 248.4 Hz), 151.0 (d, $^3J_{CF}$ = 5.4 Hz), 148.0, 133.1 (d, $^4J_{CF}$ = 1.5 Hz), 130.6, 130.1 (d, $^3J_{CF}$ = 10.7 Hz), 129.8, 129.6, 123.7 (d, $^3J_{CF}$ = 8.4 Hz), 123.4, 119.6, 118.0 (d, $^2J_{CF}$ = 14.6 Hz), 114.8 (d, $^4J_{CF}$ = 2.7 Hz) 109.7 (d, $^2J_{CF}$ = 23.0 Hz); ^{19}F NMR (376 MHz, CDCl$_3$) δ -116.99; Found: m/z, 211.0807; C$_{14}$H$_{10}$FN [M$^+$] requires m/z, 211.0797. Combined yield with **38**, 42%.

3-Fluoro-5*H*-dibenz[*b,f*]azepine 38: Compound **23** (1.311 g, 6.01 mmol) yielded the product as an orange oil after purification by column chromatography (1:9 EtOAc/Hexane) 0.624 g, 48 %. Cyclisation of **20** by the method outlined yielded the product as a mixture with **37**. Compound **38** was separated by gradient elution with hexane → 1:4 EtOAc/hexane (1:50 silica to product ratio), 0.271 g (22 %); ^{1}H NMR (400 MHz, CDCl$_3$) δ 7.00 (ddt, J=11.4, 7.9, 4.5, Hz, 1 H), 6.80 (d, J=4.2 Hz, 2 H), 6.80 (dd, J=8.4, 6.5 Hz, 1 H), 6.50 (td, J=8.3, 2.4 Hz, 1 H), 6.50 (d, J=7.8 Hz, 1 H), 6.20 (s, 2 H), 6.20 (dd, J=9.7, 2.5 Hz, 1 H) and 4.9 (br s, 1

H); ^{13}C NMR (101 MHz, CDCl$_3$) δ 163.9 (d, $^1J_{CF}$ = 247.7 Hz), 150.0 (d, $^3J_{CF}$ = 9.2 Hz), 147.3, 131.8 (d, $^3J_{CF}$ = 9.6 Hz), 131.2, 131.1, 130.5, 129.6, 129.5, 125.8 (d, $^4J_{CF}$ = 3.5 Hz), 123.4, 119.3, 109.3 (d, $^2J_{CF}$ = 21.1 Hz) and 106.5 (d, $^2J_{CF}$ = 24.5 Hz); ^{19}F NMR (376 MHz, CDCl$_3$) δ ppm -114.32; Found: m/z, 211.0793; C$_{14}$H$_{10}$FN [M$^+$] requires m/z, 211.0797. The combined yield with **37**, when starting from **20**, was 40%.

Spectral data consistent with those reported in [13]
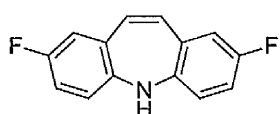
2,8-Difluoro-5*H*-dibenz[*b,f*]azepine 39: Cyclisation of compound **24** (1.214 g, 5.34 mmol) yielded the product as an orange solid after column chromatography (1:9 EtOAc/hexane); 0.797 g, 66 %; ^{1}H NMR (400 MHz, CDCl$_3$) δ 6.77 (ddd, J = 8.5, 8.0, 2.9 Hz, 2 H, H-C^{3,7}), 6.63 (dd, J = 9.1, 2.9 Hz, 2 H, H-C^{1,9}), 6.49 (dd, J = 8.6, 4.8 Hz, 2 H, H-C^{4,6}), 6.38 (s, 2 H, H-C^{10,1}) and 4.86 (br s, 1 H, HN^5); ^{13}C NMR (400 MHz, CDCl$_3$) δ 159.2 (d, $^1J_{CF}$ = 240.8 Hz), 144.2 (d, $^4J_{CF}$ = 2.4 Hz) 132.1 (d, $^4J_{CF}$ = 1.9 Hz), 131.2 (d, $^3J_{CF}$ = 7.7 Hz), 120.3 (d, $^2J_{CF}$ = 8.1 Hz), 116.4 (d, $^2J_{CF}$ = 22.9 Hz) and 115.8 (d, $^2J_{CF}$ = 22.5 Hz); ^{19}F NMR (376 MHz, CDCl$_3$) δ -122.31; Found: C, 73.25; H, 3.9; N, 6.0; C$_{14}$H$_9$F$_2$N requires C, 73.40; H, 3.9; N, 6.1%; Found: m/z, 230.0779; C$_{14}$H$_{10}$F$_2$N [MH]$^+$ requires m/z, 230.0781.

Spectral data are consistent with those reported in [12]
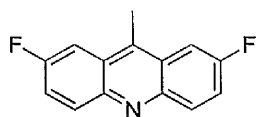
2,7-Difluoro-9-methylacridine: Isolated as a by-product from the preparation of **39**; yield variable, as demonstrated in chapter 2; ^{1}H NMR (400 MHz, CDCl$_3$) δ 8.21 (dd, J = 5.7, 9.7 Hz, 2 H, H-C^{4,5}), 7.76 (dd, J = 2.8, 10.6 Hz, 2 H H-C^{1,8}), 7.56 (ddd, J = 9.6, 7.3, 2.7 Hz, 2 H, H-C^{3,6}) and 2.98 (s, 3 H, CH$_3$); ^{13}C NMR (101 MHz, CDCl$_3$) δ = 160.1 (d, $^1J_{CF}$ = 257.6

Hz), 145.4, 140.5, 133.2 (d, $^3J_{CF}$ = 8.4 Hz), 125.9 (d, $^3J_{CF}$ =10.0 Hz), 121.3 (d, $^2J_{CF}$ = 28.4 Hz), 106.5 (d, $^2J_{CF}$ = 23.0 Hz) and 14.1; ^{19}F NMR (376 MHz, CDCl$_3$) δ = -111.72; Found: m/z, 230.0777; C$_{14}$H$_{10}$F$_2$N [MH]$^+$ requires m/z, 230.0781.

Spectral data consistent with those reported in [12]
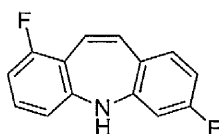
1,7-Difluoro-5H-dibenz[b,f]azepine 40: Cyclisation of **25** (1.008 g, 4.4 mmol) yielded the product as a mixture with **41** and yielded, after isolation by column chromatography with 1:9 EtOAc/Hexane (1:50 silica to product ratio), **40** (0.166 g, 16 %) together with **41** (35%, v. i.); ^{1}H NMR (400 MHz, CDCl$_3$) δ 6.98 (td, J=8.1, 6.1 Hz, 1 H) 6.82 (dd, J=8.4, 6.4 Hz, 1 H) 6.52 - 6.62 (m, 2 H) 6.48 (d, J=1.0 Hz, 1 H) 6.34 (d, J=1.0 Hz, 1 H) 6.21 - 6.29 (m, 2 H) and 5.01 (br s, 1 H); ^{13}C NMR (100 MHz, CDCl$_3$) δ164.0 (d, $^1J_{CF}$ = 248.7 Hz), 160.60 (d, $^1J_{CF}$ = 248.4), 149.9 (d, $^4J_{CF}$ = 5.2 Hz), 149.6 (d, $^3J_{CF}$= 9.1 Hz), 132.11 (s), 131.9 (d, $^3J_{CF}$ = 9.7 Hz), 130.2 (d, $^3J_{CF}$ = 10.8 Hz), 125.8 (d, $^4J_{CF}$ = 3.3 Hz), 122.8 (d, $^3J_{CF}$ = 8.2 Hz), 122.8 (d, $^3J_{CF}$ = 8.8 Hz), 118.0 (d, $^2J_{CF}$ = 14.7 Hz), 114.8 (d, $^4J_{CF}$ = 2.8 Hz), 110.1 (d, $^2J_{CF}$ = 23.1 Hz), 109.9 (d, $^2J_{CF}$ = 21.2 Hz) and 106.9 (d, $^2J_{CF}$ = 24.0 Hz); ^{19}F NMR (376 MHz, CDCl$_3$) δ ppm -113.87, -116.84; Found: C, 73.25; H, 3.9; N, 6.0; C$_{14}$H$_9$F$_2$N requires C, 73.40; H, 3.9; N, 6.1%; Found: m/z, 229.0709; C$_{14}$H$_9$F$_2$N [M$^+$] requires m/z, 229.0703.
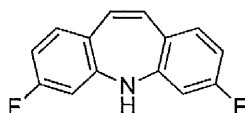
.3,7-Difluoro-5H-dibenz[b,f]azepine 41: Cyclisation of **25** (1.008 g, 4.4 mmol) yielded the product as a mixture with **40**; after isolation by column chromatography (1:9 EtOAc/Hexane with a 1:50 silica to product ratio), there was obtained **41** (0.351 g (35 %); ^{1}H NMR (400 MHz, CDCl$_3$) δ

6.77 (dd, J=8.4, 6.4 Hz, 2 H, H-C^{2,8}), 6.53 (dd, J=8.9, 2.5 Hz, 2 H, H-C^{1,9}), 6.21 (dd, J=9.7, 2.5 Hz, 2 H, H-C^{4,6}), 6.16 (s, 2 H, H-C^{10,11}) and 4.89 (br s, 1 H, HN^5); ^{13}C NMR (101 MHz, CDCl$_3$) δ 163.9 (d, $^1J_{CF}$ = 248.1 Hz), 152.2 (d, $^4J_{CF}$ = 3.0 Hz), 149.0 (d, $^3J_{CF}$ = 10.0 Hz), 131.8 (d, $^3J_{CF}$ = 9.6 Hz), 130.2 (s), 109.7 (d, $^2J_{CF}$ = 21.1 Hz) and 106.7 (d, $^2J_{CF}$ = 24.2 Hz); ^{19}F NMR (376 MHz, CDCl$_3$) δ = -114.06; Found: C, 73.30; H, 3.8; N, 5.95; C$_{14}$H$_9$F$_2$N requires C, 73.40; H, 3.9; N, 6.1%; combined yield with **25**, 51%.
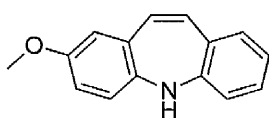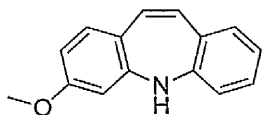
2-methoxy-5*H*-dibenz[*b,f*]azepine 42: Cyclisation of **26** (2.514 g, 11.25 mmol) yielded **42** as a dark orange solid after column chromatography in 2:7 EtOAc/Hexane, 0.618 g, 25 %. Cyclisation of **27** also yielded **42** as a dark orange solid after column chromatography, 0.420, 37 %;

^{1}H NMR (CDCl$_3$,400 MHz) δ 7.05 (t, J = 7.5 Hz, 1 H), 6.83 - 6.94 (m, 1 H), 6.62 (dd, J=8.1, 1.8 Hz, 1 H), 6.41 (br. s., 4 H), 6.47 (br. s., 2 H), 4.87 (br. s., 1 H), 3.73 ppm (br. s., 3 H);

^{1}H NMR (400 MHz, DMSO-d_6) δ 6.97 (t, J = 7.2 Hz, 1 H, H-C^7), 6.74 - 6.79 (m, 2 H, H-C^{1,3}), 6.69 (t, J = 7.2 Hz, 1 H, H-C^8), 6.62 (d, J = 7.6 Hz, 1 H, H-C^4), 6.59 (d, J = 2.6 Hz, 1 H, H-C^9), 6.41 (d, J = 2.1 Hz, 1 H, H-C^6), 6.18 (d, *A of AB*, J=11.5 Hz, 1 H, H-C^{10}), 6.13 (d, *B of AB*, J=12.1 Hz, 1H, H-C^{11}), NH unobserved, 3.63 (s, 3 H, OCH$_3$); ^{13}C NMR (DMSO-d$_6$,101MHz): δ = 154.7, 150.3, 142.4, 134.1, 132.7, 131.6, 130.4, 129.5, 128.9, 121.6, 120.0, 118.9, 115.3, 114.4, 55.1 ppm; (CI+, *m/z*) 224 (100), 225.4 (17) [MH]$^+$.

^{1}H NMR spectrum in CDCl$_3$ consistent with that reported in [2]

3-methoxy-5*H*-dibenz[*b,f*]azepine 43: Cyclisation of **28** (1.984, 8.89 mmol) yielded the product as a pale yellow sold after column chromatograpy in 2:7 EtOAc/Hexane 0.430 g, 22 %; ^{1}H NMR (400 MHz, CDCl$_3$): δ 7.00 (ddd, J = 7.8, 6.1, 2.8 Hz, 1 H, H-C^1), 6.79 - 6.85 (m, 2 H H-C^{7,8}), 6.76 (d, J = 8.4 Hz, 1 H, H-C^9), 6.47 (d, J = 7.6 Hz, 1 H, H-C^6), 6.36 (dd, J = 8.4, 2.4 Hz, 1 H, H-C^2), 6.24 (d, *A* of *AB*, J = 11.9 Hz, 1 H, H-C^{10}), 6.17 (d, *B* of *AB*, J = 11.5 Hz, 1 H, H-C^{11}), 6.06 (d, J = 2.4 Hz, 1 H, H-C^4), 4.91 (br. s., 1 H, H-N^5), 3.75 ppm (s, 3 H, CH$_3$O); ^{13}C NMR (101 MHz, CDCl$_3$) δ 161.2, 152.9, 149.6, 147.5, 131.7, 130.3, 129.9, 129.6, 129.1, 123.0, 119.2, 107.4, 105.6, 103.3, 55.3 ppm; (CI+, *m/z*) 224 (100), 225.4 (17) [MH]$^+$

Spectral data consistent with those reported in [14]

5.8 Incorporation of the carbamoyl functional group.

General Reaction Procedure for Trichloroacetyl Isocyanates: Iminostilbene analogues (12.50 mmol) were dissolved in toluene (25 mL) and trichloroacetyl isocyanate (15.00 mmol) added portion wise via syringe below the solvent level. The solution turned from yellow/orange to colourless within minutes and precipitation of a white solid (the product) is observed within an hour. The reaction is left for 24 hours with gentle stirring to allow precipitation to occur. If no precipitation occurs after 24 hours a small quantity of hexane may be added to the reaction mixture to encourage precipitation. The product is then isolated by vacuum filtration, and the filter cake washed with ice cold water (2 × 15 mL) and left to dry.

Note: obtaining good ^1H and ^{13}C NMRs for these compounds is not trivial, the compound is very unstable in solution and hydrolysis to carbamazepine and iminostilbene mixtures can be observed; by transformation of a colourless solution to yellow and within the NMR itself. Samples must be run immediately if significant quantities of the product are to be observed by ^1H and ^{13}C NMR.
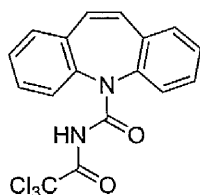
N-(2,2,2-trichloroacetyl)-5H-dibenzo[b,f]azepine-5-carboxamide

35a: White powder, 89 %; ^1H NMR (400 MHz, DMSO-d_6) δ 10.85 (br. s., 1 H, N-H) 7.06 - 7.21 (m, 4 H) 6.88 - 6.98 (m, 2 H) 6.52 (d, J=8.4 Hz, 2 H) 6.05 (s, 2 H); ^{13}C NMR (101 MHz, DMSO-d$_6$) δ 162.9, 148.4, 132.7, 132.2, 131.9, 131.1, 121.0, 113.6, 93.1; (ES+) m/z [MNa]$^+$ 403 (100), 405 (88), 407 (30); Found 402.9784, [MNa]$^+$ C$_{17}$H$_{11}$N$_2$O$_2$^{23}Na^{35}Cl$_3$ req 402.9784.

**N-(2,2,2-trichloroacetyl)2,8-dibromo-5H-dibenz[b,f]azepine-5-carboxamide   15a:**
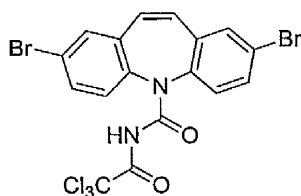
white powder, 78 %; ^1H NMR (400 MHz, DMSO-d_6) δ ppm 10.46 (br.s., 1 H, NH) 7.35 - 7.60 (m, 6 H) 7.08 (s, 2 H); ^{13}C NMR (101 MHz, DMSO-d$_6$) δ 162.9, 158.4, 150.3, 149.5, 140.5, 138.2, 135.1, 133.8, 132.1, 130.4, 129.5, 129.3, 129.3, 127.1, 121.9, 119.1, 91.8; IR (cm^{-1}) 3386.4 (m, NH), 3091.3, 3027.7 (w, CH (sp^3)), 1778.1 (s, C=ONH), 1708.6 (m, CCl$_3$C=O), 1481.06 (s, NH); (EI$^+$, m/z) 559(23), 561(100), 563(90), 565(39), 566(10) [MNa]$^+$; Found 558.8021, [MNa]$^+$ C$_{17}$H$_9$N$_2$O$_2$^{23}Na^{79}Br$_2$^{35}Cl$_3$ req 558.7994.

## General Reaction Procedure for Alkali Metal Isocyanates:

Iminostilbene analogues (200 μmol) were dissolved in toluene (2.5 mL) and NaNCO (240 μmol) added to the solution. Trifluoroacetic acid (240 μmol) was then added, the NaNCO-iminostilbene suspension becomes clear yellow and then colourless and precipitation of a white solid is observed after 30-60 minutes. The reaction was then left for 6-12 hours to allow completion of the precipitation and the product collected by vacuum filtration and the filter cake washed with ice-cold water (2 × 30 mL) yielding the product as a white solid.

All carbamazepine analogues were purified by the preparative HPLC method described in the general experimental to remove any trace impurities.. Compound purity of greater than 98 % is required for metabolite assays.
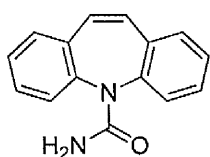
Carbamazepine: ^{1}H NMR (400 MHz, CDCl$_3$): δ 7.26 - 7.50 (m, 8 H), 6.95 (s, 2 H, H-C^{10,11}), 4.53 (br. s., 2 H, HN); ^{13}C NMR (101 MHz, CDCl$_3$): δ 156.9, 140.0, 135.0, 130.4, 129.6, 129.5, 128.7, 127.8 ppm.

NMR data consistent with an authentic sample.
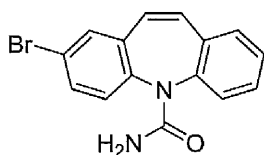
2-Bromo-carbamazepine 44: Compound **14** (0.051 g, 187.40 μmol) was treated according to the general method to yield the product as a white powder as a 1:1 mixture of isomers (determined by LC-MS), as discussed in chapter 2, 0.051 g, 89 %. The mixture was purified by the *preparative* HPLC method to remove most of the impurity, followed

by separation by the *analytical* HPLC method outlined in the general experimental to remove the closely eluting impurity, yielding the final compound as a white powder 0.024 g. ^{1}H NMR (400 MHz, CDCl$_3$): δ 7.54 (dd, J = 8.3, 2.4 Hz, 1 H), 7.50 (d, J=2.2 Hz, 1 H), 7.44 - 7.49 (m, 1 H), 7.33 - 7.40 (m, 1 H), 7.23 - 7.28 (m, 2 H), 7.12 - 7.21 (m, 1 H), 6.97 (d, *A of AB*, J=11.4 Hz, 1 H), 6.95 (s, 1 H), 6.85 (d, *B of AB, J* =11.5 Hz, 1 H), 4.46 (br. s., 2 H); ^{13}C NMR (101 MHz, CDCl$_3$) δ157.8, 156.6, 139.8, 139.0, 136.7, 134.8, 132.3, 132.1, 130.5, 129.9, 129.8, 128.5, 128.1, 121.3; IR (cm^{-1}) 3359 (NH stretch), 1671 (C=O stretch), 1489 (NH$_2$ δ), 1469, 1400; MS (CI+, *m/z*) 315 (94), 317 (100) [MH]$^+$; Found 314.0058, C$_{15}$H$_{11}$^{79}BrN$_2$O req 314.0055
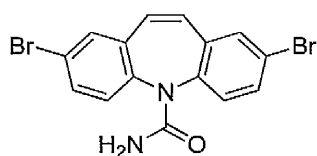
2,8- dibromo-carbamazepine 45: Compound **15** (0.080 g, 225.05 μmol) was reacted according to the general method to yield the product as a white solid after purification by the *preparative* HPLC method outlined above, 0.076 g, 87 %; ^{1}H NMR (400 MHz, CDCl$_3$) δ ppm 7.55 (dd, J = 8.4, 2.2 Hz, 2 H, H-C^{3,7}), 7.51 (d, J = 2.3 Hz, 2 H, H-C^{1,9}), 7.32 (d, J = 8.4 Hz, 2 H, H-C^{4,6}), 6.87 (s, 2 H, H-C^{10,11}), 4.58 (br. s., 2 H, NCONH$_2$); ^{13}C NMR (101 MHz, CDCl$_3$): δ 156.3, 138.8, 136.5, 132.7, 132.4, 130.4, 130.3, 121.7; IR (cm$^-$1) 3491, 3452 (NH stretch), 1682 (C=O stretch), 1597, 1485, 1462, 1400; (ES+, *m/z*) 415 (51), 417 (100), 419 (49) [MNa]$^+$; Found 414.9045, C$_{15}$H$_{10}$^{23}Na^{79}Br$_2$ N$_2$O req 414.9058.

Data consistent with those reported in [12]

191
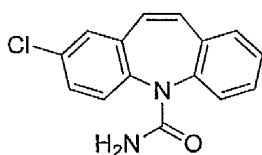
2-chloro-carbamazepine 46: Compound **16** (0.051, 223.99 µmol) was treated according to the general method to yield the product as a white powder after purification, 0.048 g, 79 %. ^{1}H NMR (400 MHz, CDCl$_3$): δ 7.43 - 7.47 (m, 2 H), 7.30 - 7.42 (m, 5 H), 6.96 (d, *A of AB* J=11.6 Hz, 1 H), 6.84 (d, *B of AB* J=11.5 Hz, 1 H), 4.66 ppm (br. s., 2 H); ^{13}C NMR (101 MHz, CDCl$_3$) δ 156.8, 142.4, 139.8, 138.5, 136.3, 134.8, 133.3, 131.4, 130.2, 129.8, 129.8, 129.3, 129.1, 128.5, 128.1; IR 3475, 3421 (NH stretch), 1651 (C=O stretch); 1562, 1485, 1408, 1088, 829, 795, 633; MS found 270.0563 C$_{15}$H$_{11}$^{35}ClN$_2$O [M]$^+$ req 270.0560
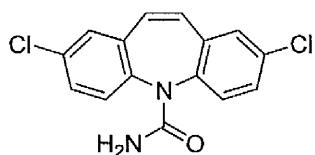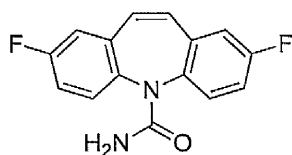
2,8-dichloro-carbamazepine 47: Compound **17** (0.052 g, 198.37 µmol) was treated according to the general method outlined above to yield the product as a white powder after purification 0.055 g, 91 %, ^{1}H NMR (400 MHz. CDCl$_3$): δ 7.40 - 7.42 (d, J=2.3 Hz, 2 H, H-C^{3,7}), 7.36 (d, J = 1.8 Hz, 2 H, H-C^{1,9}), 7.26 (s, 2 H, H-C^{4,6}), 6.89 (s, 2 H, H-C^{10,11}), 4.46 ppm (br. s., 2 H, CONH$_2$); ^{13}C NMR (101MHz, CDCl$_3$) δ 156.3, 138.8, 136.5, 132.7, 132.4, 130.3, 121.7; IR (cm^{-1}) 3483 (amine stretch), 1689 (C=O stretch), 1593, 1485, 1396, 787; MS (ES+, *m/z*) 327 (100), 329 (97), 331(25) [MNa]$^+$; Found: 327.0056 (100) C$_{15}$H$_{10}$N^{35}Cl$_2$ [MNa]$^+$ req 327.0068
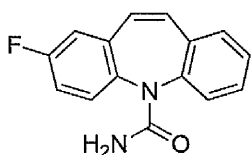
2-fluoro-carbamazepine 48: Compound **36** (0.038 mg, 179.90 µmol) was treated according to the general method to yield the

product as a white powder after purification. 0.035 mg, 78 %; ^{1}H NMR (400 MHz, CDCl$_3$) δ 7.35 (dd, J=3.5, 1.4 Hz, 1 H, H-C^7), 7.22 - 7.34 (m, 4 H), 7.01 (td, J=8.3, 2.9 Hz, 1 H), 6.93 (dd, J = 9.1, 2.8 Hz, 1 H), 6.84 - 6.88 (d, A of AB, J 11.6 Hz, 1 H, H-C^{10}), 6.72 - 6.77 (d, B of AB J = 1.6 Hz, 1 H, H-C^{11}), 4.95 (br. s., 2 H, N^{5}CONH$_2$); ^{13}C NMR (101 MHz, CDCl$_3$) δ ppm 161.46 (d, $^1J_{CF}$ = 246.9 Hz), 157.39, 139.83, 137.83, 135.89 (br. s.), 134.74, 130.39 (d, $^3J_{CF}$ = 8.1 Hz,), 129.81 (d, $^4J_{CF}$ = 4.2 Hz), 128.99, 128.42 (br. s), 128.19, 128.04, 125.2, 116.41 (d, $^2J_{CF}$ = 22.6 Hz), 115.40 (d, $^2J_{CF}$ = 22.2 Hz); IR (cm^{-1}) 3345, 1674, 1581, 1493, 1396, 1211; MS found 254.0847, C$_{15}$H$_{11}$N$_2$OF [M]$^+$ req 254.0855

2,8- difluoro-carbamazepine 49: Compound **39** (0.047 g, 205.04 μmol) was treated according to the general method to yield the product as a white solid after purification, 0.042 g, 75 % ; ^{1}H NMR (400 MHz, CDCl$_3$) δ 7.40 (dd, J = 8.7, 5.2 Hz, 2 H, H-C^{3,7}), 7.08 - 7.14 (m, 2 H, H-C^{1,9}), 7.03 (dd, J = 9.0, 2.8 Hz, 2 H, H-C^{4,6}), 6.86 (s, 2 H, H-C^{10,11}), 4.98 (br. s., 2 H , NCONH$_2$); ^{13}C NMR (101 MHz, CDCl$_3$) δ ppm 161.47 (d, $^1J_{CF}$ = 247.3 Hz), 157.44, 137.80, 136.46 (d, J = 7.7 Hz), 135.95 (br. s.), 130.23 (d, J = 8.4 Hz), 128.96, 128.15, 125.23, 116.70 (d, $^2J_{CF}$ = 23.0 Hz) 115.61 (d, J = 22.6 Hz); IR (cm^{-1}) 3495 (NH stretch), 1693 (C=O stretch), 1604, 1493, 1385, 1257, 879, 818, 795; MS found 272.0764, C$_{15}$H$_{10}$N$_2$OF$_2$ [M]$^+$ req 272.0761.

5.9 References

1. Pretsch, E.; Bühlmann, P.; Affolter, C., *Structure Determination of Organic Compounds: Tables of Spectral Data*. Third Completely Revised and Enlarged English Edition ed.; Springer: Berlin, Heidelberg, New York, HongKong, London, Mailand, Paris, Tokyo, 2000; p 421.

2. Smith, K.; James, D. M.; Mistry, A. G.; Bye, M. R.; Faulkner, D. J., A new method for bromination of carbazoles, [beta]-carbolines and iminodibenzyls by use of N-bromosuccinimide and silica gel. *Tetrahedron* **1992,** 48, (36), 7479-7488.

3. Ma, D.; Cai, Q., L-proline promoted Ullmann-Type Coupling Reactions of Aryl Iodides with Indoles, Pyrroles, Imidazoles or Pyrazoles. *SYNLETT* **2004,** (1), 0128-0130.

4. Nishio, T., Photodesulfurization of indoline-2-thiones: a facile synthesis of indoles. *The Journal of Organic Chemistry* **1988,** 53, (6), 1323-1326.

5. Old, D. W.; Harris, M. C.; Buchwald, S. L., Efficient palladium-catalyzed N-arylation of indoles. *Organic Letters* **2000,** 2, (10), 1403-1406.

6. Yong, F.-F.; Teo, Y.-C.; Tay, S.-H.; Tan, B. Y.-H.; Lim, K.-H., A ligand-free copper(I) oxide catalyzed strategy for the N-arylation of azoles in water. *Tetrahedron Letters* **2011,** 52, (11), 1161-1164.

7. Watanabe, M.; Nishiyama, M.; Yamamoto, T.; Koie, Y., Palladium/P(t-Bu)3-catalyzed synthesis of N-aryl azoles and application to the synthesis of 4,4',4"-tris(N-azolyl)triphenylamines. *Tetrahedron Letters* **2000,** 41, (4), 481-483.

8. Willis, M. C.; Brace, G. N.; Findlay, T. J. K.; Holmes, I. P., 2-(2-Haloalkenyl)-aryl Halides as Substrates for Palladium-Catalysed Tandem CN Bond Formation: Efficient Synthesis of 1-Substituted Indoles. *Advanced Synthesis & Catalysis* **2006,** 348, (7-8), 851-856.

9. Rao, R. K.; Naidu, A. B.; Jaseer, E. A.; Sekar, G., An efficient, mild, and selective Ullmann-type N-arylation of indoles catalyzed by copper(I) complex. *Tetrahedron* **2009,** 65, (23), 4619-4624.

10. Varma, R. S.; Whisenant, L. K.; Boykin, D. W., Synthesis of Some Substituted 5H-Dibenz[*b,f*]azepine as Potent Antimalarials. *Journal of Medicinal Chemistry* **1969,** (12), 913-914.

11. Tomakov, G. P.; Grandberg, I. I., Rearrangement of 1-Aryl indoles to 5H-Dibenz[*b,f*]azepines. *Tetrahedron* **1995,** 51, (7), 2091-2098.

12. Bowkett, E. R. The Synthesis of Chemical Probes for Drug Metabolism and Toxicity. PhD thesis, The University of Liverpool, Liverpool, 2007.

13.   Tsvelikhovsky, D.; Buchwald, S. L., Synthesis of Heterocycles via Pd-Ligand Controlled Cyclization of 2-Chloro-N-(2-vinyl)aniline: Preparation of Carbazoles, Indoles, Dibenzazepines, and Acridines. *J. Am. Chem. Soc.* **2010**, 132, , 14048-14051.

14.   Lucini, V.; Pannacci, M.; Scaglione, F.; Fraschini, F.; Rivara, S.; Mor, M.; Bordi, F.; Plazzi, P. V.; Spadoni, G.; Bedini, A.; Piersanti, G.; Diamantini, G.; Tarzia, G., Tricyclic Alkylamides as Melatonin Receptor Ligands with Antagonist or Inverse Agonist Activity. *Journal of Medicinal Chemistry* **2004**, 47, (17), 4202-4212.

Experimental Methods and Techniques: Pharmacology

Chapter 6

This chapter describes the experimental methods and techniques used by Dr. Sophie L. Regan to isolate the rat hepatocytes and how the cells were incubated with the carbamazepine analogues.

Contents

6. Experimental Methods and Techniques: Pharmacology

6.1 Animals

Male CD1 mice (20-40 g) and male Wistar rats (150-300 g) were obtained from Charles River Laboratories (Margate, Kent). Experiments undertaken were in accordance with the criteria outlined in a license granted under the Animals (Scientific Procedures) Act of 1986 and approved by the Animal Ethics Committee of the University of Liverpool.

6.2 Hepatocyte isolation procedure used for metabolic characterisation

Hepatocytes were isolated from male Wistar rats (150-300 g) by a modified two-step collagenase perfusion method [1]. The animal was anaesthetised with sodium pentobarbital (1 μL/g). The abdomen was opened by a V-shaped transverse incision and the small intestines moved to the left to reveal the hepatic portal vein. A loose ligature was placed around the hepatic portal vein. The rib cage was opened up with incisions up either side of the rib cage to reveal the heart. The vein was cannulated with a 20G catheter. The catheter was secured in place with the already in place ligature and the heart removed. The perfusate (Ca^{2+} free) flow was then started at 40 mL/min. The liver was first perfused with Wash buffer (10x Ca^{2+}-free Hanks Balanced Salt Solution, 5.8 mM HEPES, 4.5 mM $NaHCO_3$) for 9 minutes. After perfusion with wash buffer, the liver was perfused with digestion buffer (wash buffer; 0.05 % collagenase (w/v), 0.0068 % trypsin inhibitor (w/v), 5 mM $CaCl_2$) the time of which was variable from animal to animal. When cracks began to appear throughout the liver lobes, it was an indication of digestion and perfusion was terminated. The liver was removed from the animal and initially rinsed with wash buffer, containing DNase (200 mL wash buffer, 20

mg DNase I). The liver was then transferred to a Petri dish containing approximately 50 mL of Buffer C and cells were liberated from the connective vasculature tissue by gentle combing with sharp forceps. The cell suspension was filtered through nylon mesh (125 μm) to remove the vasculature, resulting in a mixture of both parenchymal and non parenchymal cells.

Further purification of the initial cell suspension was required. This was achieved through three centrifugation steps (50 g, 2 min). For the first stage, cells were washed in wash buffer (containing DNase I) and for the final two stages subsequent washes were in wash buffer before being resuspended in incubation buffer (wash buffer, 1 mM MgSO$_4$.7H$_2$O) to be counted. Cell count and viability were assessed with a haemocytometer. Viability was assessed through trypan blue exclusion (20 μL: 100 μL cells) and only cells of a viability of ≥80 % were used for experiments.

6.3 Metabolic assessment of CBZ and haloarene derivatives in rat hepatocyte suspensions

Rat hepatocytes were incubated in suspension (2x10^6 cells/mL, 6 ml total incubation volume) at 37 °C in an orbital incubator with CBZ and the haloarene analogues (0-1000 μM; MeOH, 1 %) for 6 h. CBZ-2-Br (50 μM and 200 μM; ACN, 1%) CBZ-2-Cl were also incubated (50 μM and 500 μM) in rat hepatocytes as a result of limited stock of the synthetic analogue. Following the 6 h incubation 6 mL of ACN was added to cells to terminate reaction and stored at -20 °C until analysis. After centrifugation (2200 rpm, 10 min) of samples, ACN in the supernatant was evaporated off under a steady stream of N$_2$ at room temperature. The remaining supernatants were loaded onto Sep-Pak C18 solid phase extraction cartridges (Waters Ltd, Herts, U.K.). Cartridges were then washed with 3 mL of distilled water and eluted with 3 mL MeOH. The MeOH fractions were evaporated to dryness under a steady stream of N$_2$ at room temperature. Samples were then reconstituted in MeOH: dH$_2$0 (50:50,

250 µL: 250 µL). Aliquots (50 µL) of the reconstituted samples were injected onto HPLC and LC/MS systems.

Hepatocyte suspension metabolites were resolved on a Gemini NX 5-µm C-18 110 Å column (250 x 4.60 mm; Phenomenex, Macclesfield, Cheshire, U.K.) on a gradient of ACN (15 % for 5 min, increasing to 50 % from 5 to 25 min, and from there a further increase to 75 % over 15 min) in ammonium acetate (10 mM; pH 3.8). The gradient was delivered with a Dionex Summit HPLC System at a flow rate of 1 mL/min through a UVD170S UV detector set at 254 nm (Dionex). Authentic standards of CBZ, and CBZE were used additionally to identify metabolites.

6.4 LC/MS for metabolite identification.

The 50-µM incubations – the only ones that contained all of the drug metabolites that were identified – were taken for metabolite identification by LC/MS. This concentration falls within the therapeutic range of CBZ (17-51 µM). The LC/MS system consisted of a PerkinElmer series 200 pump and autosampler (Norwalk, CT) connected to an API 2000 mass spectrometer (AB Sciex, Foster City, CA) equipped with a TurboIonSpray electrospray ionization source. Separation of parent compounds and their metabolites was achieved at room temperature on a Gemini-NX 110 Å C18 column (5 µm, 4.6 × 250 mm; Phenomenex, Macclesfield, Cheshire, U.K.) using solvent A (10 mM ammonium acetate, pH 3.8) and solvent B (acetonitrile). At a flow rate of 1.0 mL/min, the initial eluent composition (15 % solvent B) was held constant for 5 min followed by an increase to 50 % solvent B over 15 min and a further increase to 75 % over 15 min. The eluent composition was returned to its initial proportions over 3 min and finally held for a 2-min re-equilibration period. The column eluate was split, and approximately 15 % was routed to the LC/MS interface. The mass spectrometer was set for full scanning (m/z 100-1000; 5 s) and was operated in positive-

ion mode. The source temperature was 400 $^{\circ}$C; electrospray capillary voltage, 5.0 kV; desolvation potential, 60 V; source gas, 15 (arbitrary unit); and heater gas, 75 (arbitrary unit). The mass spectrometry data were acquired and analyzed using Analyst software version 1.4 (AB Sciex). Metabolites of CBZ and its derivatives were identified preliminarily by comparing total and extracted ion chromatograms of control (substrate free) and test hepatocyte incubations. They were subsequently characterised from their diagnostic in-source fragmentation.

6.5 References

1.   Seglen, P. O., Preparation of isolated rat liver cells. Methods in Cell Biology 1976, Vol. 13, 29-83.